Vibration, Buckling and Dynamic Stability of Stepped Beams with Multiple Transverse Cracks

A thesis submitted to

National Institute of Technology, Rourkela

for the award of the degree of

Doctor of Philosophy

in

Engineering

by

Uttam Kumar Mishra

Roll No. 50501001

Under the supervision of

Prof. Shishir Kumar Sahu

Department of Civil Engineering

National Institute of Technology, Rourkela-769008, Odisha

November 2014

With dedication to

My Parents

&

With loves to my princesses

Renee and ***Romaa***

Who endured all the sufferings silently

And looked for this day patiently

National Institute of Technology, Rourkela, Odisha, India

Department of Civil Engineering

Prof. Shishir Kumar Sahu
Professor and Head

24th Nov 2014

Certificate

This is to certify that the thesis entitled "Vibration, Buckling and Dynamic Stability of Stepped Beams with Multiple Transverse Cracks" being submitted to the National Institute of Technology, Rourkela (India) by Uttam Kumar Mishra for the award of the degree of Doctor of Philosophy in Engineering is a record of bonafide research work carried out by him under my supervision and guidance. Mr Mishra has worked for more than the minimum stipulated number of years and the thesis fulfills the requirements of the regulations of the degree. The results embodied in this thesis have not been submitted to any other university or institute for the award of any degree or diploma.

(Prof. Shishir Kumar Sahu)
Supervisor, Professor and Head
Department of Civil Engineering
National Institute of Technology
Rourkela, Odisha, India

Acknowledgements

The author expresses deep sense of gratitude to his *advisor* and *supervisor* **Prof. Shishir Kumar Sahu**, Professor and Head, Department of Civil Engineering, National Institute of Technology, Rourkela for his guidance, constant encouragement and invaluable suggestions in all phases of this study. The author adores him for his excellent qualities and working with him was a great pleasure, the moments of which will be carried along throughout his life's journey.

The author expresses sincere gratitude to **Prof. S. K. Das,** Department of Civil Engineering, National Institute of Technology, Rourkela for his valuable help, support, suggestions and inspirations during this Ph.D. program.

The author expresses sincere regards to **Prof. N. Roy, Prof. A. K. Sahoo, Prof. K. C. Patra** and **Prof. M. Panda**, Ex. Heads of Civil Engineering Department for their kind support and advice during this Ph. D. program.

The author expresses deep sense of gratitude to **Prof. A. Kumar, Prof. A. V. Asha, Prof. M. R. Barik, Prof. K. C. Biswal, Prof. A. Patel, Prof. S. P. Singh** and all others for their moral support and kind cooperation during the course of work.

With all humbleness, the author owes a lot to **Prof. P. K. Ray, Prof. D. R. K. Parhi and Prof. R. K. Behera** of Mechanical Engineering Department for their moral support and valuable suggestions during course of the work.

The author expresses sincere thanks to friends like **Komal, Satyabrata, Purna, Prafulla, Pranaya, Bichi and Jala** for their moral support and constant inspiration during the course of the investigation.

The author expresses deep sense of gratitude to **Bhaganani** and **Titu Mamu** for their moral support and constant inspiration for the completion of the work.

Very special appreciation is extended to author's sweet spouse, **Rajashree** whose love and encouragement throughout the period helped him to complete the work.

Last but not the least I bow my head before the Almighty who had shown a beam of spiritual light in the darkness.

Date: 24th Nov 2014 **(Uttam Kumar Mishra)**

Abstract

The present study deals with the vibration, buckling and parametric instability behavior of both uniform and stepped beams with single and multiple transverse cracks. The variation of natural frequency, buckling load and dynamic stability regions with different parameters including relative crack depth, position of cracks, static and dynamic load factors are analyzed using finite element method (FEM) through Bolotin's approach. Experiments are also conducted to determine the natural frequencies of vibration of aluminum and steel beams with open cracks and compared with numerical predictions. The computation of natural frequencies and plotting of mode shapes of the vibration of cracked beams are done using ANSYS. Besides this, the extent of cracks in a beam are predicted using vibration data by ANN technique. The loading on the beam is considered as axial with a simple harmonic fluctuation with respect to time. During the instability, the equation of motion represents a system of second order differential equations with periodic coefficients of the Mathieu-Hill type. The development of the regions of instability arises from Floquet's theory and the periodic solution is obtained by Bolotin's approach using finite element method. Stiffness matrix of the cracked beam element is obtained from the flexibility matrix of the intact beam and the additional flexibility matrix due to crack. The frequencies of vibration and buckling loads of cracked cantilever beams reduce for both uniform and stepped beams with increase in crack depth and number of cracks. However the crack near the step reduces natural frequency and buckling load more than other locations. The onset of instability occurs earlier with introduction of more number of cracks due to reduction of stiffness. The instability region for the beam with crack located nearer to the fixed end occurs at lower excitation frequency than near free end of a cantilever beam. The vibration and instability results can be used as a technique for structural health monitoring or testing of structural integrity, performance and safety. It is observed that the extent of damage can be detected using ANN models with reasonable accuracy considering only frequencies as input. Out of the three models used, BRNN model is found to be the best model as compared to DENN and LMNN considering regression values, root mean square error values and over fitting ratios for simply supported beams.

The thesis has been presented in seven chapters. The **Chapter 1** includes the general introduction and the importance of the present study.

The review of literature relevant to the scope of the study is presented in the **Chapter 2**. The various works done and the methods and conclusions out of the studies on dynamics of uniform and stepped beams are discussed in this chapter. The objective and scope of present investigation have been presented in the **Chapter 2** after critical discussions of the lacunae of studies.

The **Chapter 3** comprises of the mathematical formulation of the problem. The method of solution of the problems is to first reduce the equations of motion to a system of Mathieu-Hill equations with periodic coefficients and the parametric resonance characteristics are then studied using Floquet's principle. Finite Element Method (FEM) has been used for the development of the problem and computation of the dynamic instability regions.

The experimental procedure adopted for free vibration analysis of intact and cracked aluminum and steel beams subjected to single and multiple cracks has been discussed in **Chapter 4**.

Chapter 5 comprises of development of Artificial Neural Network (ANN) models for crack detection in beams using available data in literature and experimental data generated as a part of this research. The methodology adopted for artificial neural network model and generation of experimental data is also presented.

Several numerical examples of free vibration, static stability (buckling) and dynamic stability analysis of structural elements are presented in the **Chapter 6** to validate the formulation of the proposed method. Several problems are solved and results discussed to study the effects of various crack parameters on dynamics of cracked uniform and stepped beams.

The **Chapter 7** sums up and concludes the present investigation. An account of future scope of study has been appended to the concluding remarks.

At the end, some important publications and books referred during the present investigation have been listed in the **References** section.

Key words: Stepped beam, in-plane periodic loading, natural frequency, critical buckling load, parametric resonance, dynamic instability region, excitation frequency.

Contents

1	**INTRODUCTION**		1
	1.1	Introduction	1
	1.2	Research Significance	1
	1.3	Summary	4
2	**REVIEW OF LITERATURE**		5
	2.1	Introduction	5
	2.2	Vibration of Cracked Beams	6
		2.2.1 Vibration of cracked uniform beams	6
		2.2.2 Vibration of cracked stepped beams	13
	2.3	Buckling of Cracked Beams	14
		2.3.1 Buckling of cracked uniform beams	14
		2.3.2 Buckling of cracked stepped beams	15
	2.4	Dynamic Stability of Cracked Beams	16
		2.4.1 Dynamic stability of cracked uniform beams	16
		2.4.2 Dynamic stability of cracked stepped beams	18
	2.5	Crack Detection in Beams	18
		2.5.1 Detection of crack in uniform beams	18
		2.5.2 Detection of crack in stepped beams	20
	2.6	Critical Discussion	21
	2.7	Objective and Scope of the Present Investigation	21
	2.8	Summary	22
3	**MATHEMATICAL FORMULATION**		23
	3.1	Introduction	23
	3.2	The Basic Problem	23
	3.3	Proposed Analysis	24
		3.3.1 Assumptions of the analysis	24
	3.4	Governing Equations	24
	3.5	Finite Element Analysis	27
		3.5.1 Intact beam element	28
		3.5.2 Cracked beam element	29

3.6 Computational Procedure 33
3.7 Numerical Simulation Using ANSYS 34
3.8 Summary 34

4 **EXPERIMENTAL PROGRAMME** 37
4.1 Introduction 37
4.2 Specimen Details 37
4.3 Equipment Required for Vibration Test 37
4.3.1 Modal hammer 38
4.3.2 Accelerometer 38
4.3.3 Portable FFT analyzer 39
4.3.4 Display unit 39
4.4 Setup and Test Procedure for Free Vibration Test 40
4.5 Summary 41
5 **DAMAGE DETECTION BY ANN** 43
5.1 Introduction 43
5.2 Biological Model of a Neuron 43
5.3 Model of an Artificial Neuron 44
5.4 Architecture of an Artificial Neural Network 44
5.5 Learning / Training Process 46
5.6 Testing of Network 48
5.7 Selection of Model Inputs 49
5.8 Division of Data and Preprocessing 49
5.9 Generalization 50
5.10 Artificial Neural Network Model 50
5.10.1 Levenberg-Marquardt Neural Network 51
5.10.2 Bayesian Regularization Neural Network 51
5.10.3 Differential Evolution Neural Network 52
5.11 Rationale behind the ANN models 54
5.12 Prediction of Damage Extent in Beam Using ANN 56
5.12.1 Data base and preprocessing 56
5.13 Summary 56

6 **RESULTS AND DISCUSSION** 57
6.1 Introduction 57
6.2 Convergence Study 57
6.2.1 Vibration of cracked uniform cantilever beam 57
6.2.2 Vibration of cracked stepped cantilever beam 58
6.2.3 Buckling of cracked uniform cantilever beam 59
6.3 Comparison with Previous Studies 60
6.3.1 Free vibration of cracked uniform cantilever beam 60
6.3.2 Buckling of cracked uniform beams 61
6.4 New Examples 62
6.5 Vibration of Beam Subjected to a Single Crack 63
6.5.1 Uniform fixed-free beam 63
6.5.2 Uniform hinged-hinged beam 69
6.5.3 Uniform fixed-hinged beam 73
6.5.4 Uniform fixed-fixed beam 76
6.5.5 Stepped fixed-free beam 79
6.6 Vibration of Beam Subjected to Multiple Cracks 83
6.6.1 Uniform fixed-free beam 83
6.6.2 Stepped fixed-free beam 92
6.7 ANSYS and Experimental Results 98
6.7.1 Single cracked uniform beam 99
6.7.2 Double cracked uniform beam 102
6.8 Experimental Results on Cracked Beam 104
6.8.1 Single cracked beam 106
6.8.2 Double cracked beam 112
6.9 Buckling of Beam Subjected to a Single Crack 117
6.9.1 Uniform fixed-free beam 118
6.9.2 Uniform hinged-hinged beam 119
6.9.3 Uniform fixed-hinged beam 120
6.9.4 Uniform fixed-fixed beam 121
6.9.5 Stepped fixed-free beam 121
6.10 Buckling of Beam Subjected to Multiple Cracks 123
6.10.1 Uniform fixed-free beam 123

6.10.2 Stepped fixed-free beam 125
6.11 Parametric Resonance Characteristics for Single Cracked Beams 127
6.11.1 Uniform fixed-free beam 127
6.11.2 Uniform hinged-hinged beam 129
6.11.3 Uniform fixed-hinged beam 132
6.11.4 Uniform fixed-fixed beam 134
6.11.5 Stepped fixed-free beam 138
6.12 Parametric Resonance Characteristics for Multiple Cracks 141
6.12.1 Uniform fixed-free beam 141
6.12.2 Stepped fixed-free beam 146
6.13 Crack Detection Using ANN 149
6.13.1 Data base and preprocessing 149
6.13.2 Design of ANNs 151
6.13.3 ANN results and discussions 152
6.14 Critical Analysis of Result 156
6.15 Summary 157
7 **CONCLUSIONS** 159
7.1 Introduction 159
7.2 Conclusions 159
7.3 Novelty of the present study 161
Future scope of work 162
REFERENCES 163

List of Symbols

The principal symbols used in this thesis are presented for easy reference.

English

A	cross sectional area of the beam
a	depth of the crack
A_c	effective cracked area
b	breadth of the beam
C	shear modulus
C_{ij}	coefficients of overall flexibility matrix
$[C_{intact}]$	flexibility matrix of intact beam element
$[C_{ovl}]$	overall additional flexibility matrix due to presence of crack
$[C_{total}]$	total flexibility matrix of cracked beam element
E	young's modulus of elasticity
F_I and F_{II}	correction factors for stress intensity factors
G	strain energy release rate
h	depth of the beam
I	moment of inertia of the beam
J	polar moment of inertia of the section
$[k_c]$	stiffness matrix of cracked beam element
$[k_e]$	elemental bending stiffness matrix
$[k_g]$	elemental geometric stiffness matrix
$[K_e]$	bending stiffness matrix of the beam
$[K_g]$	geometric stiffness matrix of the beam
K_I, K_{II} and K_{III}	stress intensity factor for opening, sliding and tearing mode of the crack
L	span of the beam
L_c	distance between crack and right node of the beam element

L_e	length of beam element
L_s	length of beam segment in stepped beam
$[m]$	elemental mass matrix
$[M]$	consistent mass matrix of the beam
$P(t)$	harmonic load
P_{cr}	critical buckling load
q_1	transverse deflection of the beam section
q_2	rotation of the beam section
T	kinetic energy of the beam
U	potential energy of the beam

Greek

κ	shear correction factor
ρ	mass density of the beam material
α	static load factor
β	dynamic load factor

Mathematical Operators

$[\,]^{-1}$	inverse of the matrix
$[\,]^{T}$	transpose of the matrix

List of Figures

3.1	Schematic diagram of a cantilever stepped beam with multiple cracks subjected to harmonic in-plane load	23
3.2	Stepped beam discretized into elements and free body diagrams of intact and cracked beam element with 2 degrees of freedom per node	28
3.3	Flow chart of the present Finite Element Formulation	35
3.4	Modeling of a cracked beam with six-nodded triangular elements	36
4.1	Modal Impact Hammer (B&K 2302-5)	38
4.2	Accelerometer (Model: B&K 4507)	38
4.3	FFT Analyzer (Model: B&K3560 B)	38
4.4	Display unit (Laptop)	39
4.5	Typical Auto spectrum window of a vibration test	40
4.6	Vibration test setup, beam suspended by two strings like free-free beam, accelerometer and modal hammer in position	41
5.1	Simplified configuration of an organic neuron	43
5.2	Artificial (Mathematical) model of a neuron	44
5.3	Typical architecture of a neural network	45
5.4	Different transfer functions (a) stepped (b) linear (c) logistic sigmoid and (d) hyperbolic tangent sigmoid	45
5.5	Typical back propagation neural network	48
6.1	Variation of first four modes of non-dimensional free vibration frequencies with no of elements of discretization of the cantilever beam	58
6.2	Variation of non-dimensional frequencies of a cracked stepped cantilever beam with respect to number of elements per segment for a crack of relative depth 0.5 at 0.05*L* from fixed end	59
6.3	Variation of non-dimensional buckling load of a cracked uniform cantilever beam subjected to a crack of relative depth 0.5 at 0.1L from fixed end with no of elements	60
6.4	Cracked uniform Aluminum cantilever beam	62
6.5	Three stepped cracked cantilever beam	62
6.6	Variation of non-dimensional fundamental frequency (ω_c/ω_i) with relative crack location (L_1/L) for different relative crack depths of the uniform fixed-free beam	63

6.7	Variation of non-dimensional frequency (ω_c/ω_i), Mode II, with relative crack location (L_1/L) for different relative crack depths of the uniform fixed-free beam	64
6.8	Variation of non-dimensional frequency (ω_c/ω_i), Mode III, with relative crack location (L_1/L) for different relative crack depths of the uniform fixed-free beam	65
6.9	Variation of non-dimensional frequency (ω_c/ω_i), Mode IV, with relative crack location (L_1/L) for different relative crack depths of the uniform fixed-free beam	66
6.10	Fundamental mode shape of vibration for different location of a crack of relative depth 0.5 of the uniform fixed-free beam	67
6.11	Second mode shape of vibration for different location of a crack of relative depth 0.5 of the uniform fixed-free beam	67
6.12	Third mode shape of vibration for different location of a crack of relative depth 0.5 of the uniform fixed-free beam	68
6.13	Fourth mode shape of vibration for different location of a crack of relative depth 0.5 of the uniform fixed-free beam	68
6.14	Fundamental mode shape of free vibration for different depth of a crack at 0.05L from fixed end of the uniform fixed-free beam	69
6.15	Variation of non-dimensional fundamental frequency (ω_c/ω_i) with relative crack location (L_1/L) for different relative crack depths of the uniform hinged-hinged beam	70
6.16	Variation of non-dimensional frequency (ω_c/ω_i), Mode II, with relative crack location (L_1/L) for different relative crack depths of the uniform hinged-hinged beam	71
6.17	Variation of non-dimensional frequency (ω_c/ω_i), Mode III, with relative crack location (L_1/L) for different relative crack depths of the uniform hinged-hinged beam	71
6.18	Variation of non-dimensional frequency (ω_c/ω_i), Mode IV, with relative crack location (L_1/L) for different relative crack depths of the uniform hinged-hinged beam	72
6.19	Variation of non-dimensional fundamental frequency (ω_c/ω_i) with relative crack location (L_1/L) for different relative crack depths of the uniform fixed-hinged beam	73
6.20	Variation of non-dimensional frequency (ω_c/ω_i), Mode II, with relative crack location (L_1/L) for different relative crack depths of the uniform fixed-hinged beam	74
6.21	Variation of non-dimensional frequency (ω_c/ω_i), Mode III, with relative crack location (L_1/L) for different relative crack depths of the uniform fixed-hinged beam	75

6.22 Variation of non-dimensional frequency (ω_c/ω_i), Mode IV, with relative crack location (L_1/L) for different relative crack depths of the uniform fixed-hinged beam 75

6.23 Variation of non-dimensional fundamental frequency (ω_c/ω_i) with relative crack location (L_1/L) for different relative crack depths of the uniform fixed-fixed beam 77

6.24 Variation of non-dimensional frequency (ω_c/ω_i), Mode II with relative crack location (L_1/L) for different relative crack depths of the uniform fixed-fixed beam 77

6.25 Variation of non-dimensional frequency (ω_c/ω_i), Mode III, with relative crack location (L_1/L) for different relative crack depths of the uniform fixed-fixed beam 78

6.26 Variation of non-dimensional frequency (ω_c/ω_i), Mode IV, with relative crack location (L_1/L) for different relative crack depths of the uniform fixed-fixed beam 79

6.27 Variation of non-dimensional fundamental frequency (ω_c/ω_i) with relative crack location (L_1/L) for different relative crack depths of the stepped fixed-free beam 80

6.28 Variation of non-dimensional frequency (ω_c/ω_i), Mode II, with relative crack location (L_1/L) for different relative crack depths of the stepped fixed-free beam 81

6.29 Variation of non-dimensional frequency (ω_c/ω_i), Mode III, with relative crack location (L_1/L) for different relative crack depths of the stepped fixed-free beam 82

6.30 Variation of non-dimensional frequency (ω_c/ω_i), Mode IV, with relative crack location (L_1/L) for different relative crack depths of the stepped fixed-free beam 83

6.31 Variation of non-dimensional fundamental frequency (ω_c/ω_i) with relative location of the second crack (L_2/L) for different relative crack depths of the fixed-free beam (L_1= 0.1L, rcd_1 = 0.3) 84

6.32 Variation of non-dimensional fundamental frequency (ω_c/ω_i) with relative location of the third crack (L_3/L) for different relative crack depths of the fixed-free beam (L_1=*0.1L*, L_2=0.2L, rcd_1=0.3, rcd_2=0.2) 85

6.33 Variation of non-dimensional frequency (ω_c/ω_i), Mode II, with relative location of the second crack (L_2/L) for different relative crack depths of the fixed-free beam (L_1= 0.1L, rcd_1 = 0.3) 86

6.34 Variation of non-dimensional frequency (ω_c/ω_i), Mode II, with relative location of the third crack (L_3/L) for different relative crack depths of the fixed-free beam (L_1=*0.1L*, L_2=0.2L, rcd_1=0.3, rcd_2=0.2) 87

6.35 Variation of non-dimensional frequency (ω_c/ω_i), Mode III, with relative location of the second crack (L_2/L) for different relative crack depths of the fixed-free beam (L_1= 0.1L, rcd_1 = 0.3) 88

6.36 Variation of non-dimensional frequency (ω_c/ω_i), Mode III, with relative location of the third crack (L_3/L) for different relative crack depths of the fixed-free beam ($L_1=0.1L$, $L_2=0.2L$, $rcd_1=0.3$, $rcd_2=0.2$) 89

6.37 Variation of non-dimensional frequency (ω_c/ω_i), Mode IV, with relative location of the second crack (L_2/L) for different relative crack depths of the fixed-free beam ($L_1= 0.1L$, $rcd_1 = 0.3$) 90

6.38 Variation of non-dimensional frequency (ω_c/ω_i), Mode IV, with relative location of the third crack (L_3/L) for different relative crack depths of the fixed-free beam ($L_1=0.1L$, $L_2=0.2L$, $rcd_1=0.3$, $rcd_2=0.2$) 91

6.39 Variation of non-dimensional fundamental frequency (ω_c/ω_i) with relative crack depth (a/h) for different relative crack locations of two cracks the stepped fixed-free beam 92

6.40 Variation of non-dimensional fundamental frequency (ω_c/ω_i) with relative crack depth (a/h) for different relative locations of three cracks in the stepped fixed-free beam 92

6.41 Variation of non-dimensional frequency (ω_c/ω_i), Mode II, with relative crack depth (a/h) for different relative crack locations of two cracks the stepped fixed-free beam 93

6.42 Variation of non-dimensional frequency (ω_c/ω_i), Mode II, with relative crack depth (a/h) for different relative locations of three cracks in the stepped fixed-free beam 94

6.43 Variation of non-dimensional frequency (ω_c/ω_i), Mode III, with relative crack depth (a/h) for different relative crack locations of two cracks the stepped fixed-free beam 95

6.44 Variation of non-dimensional frequency (ω_c/ω_i), Mode III, with relative crack depth (a/h) for different relative locations of three cracks in the stepped fixed-free beam 96

6.45 Variation of non-dimensional frequency (ω_c/ω_i), Mode IV, with relative crack depth (a/h) for different relative crack locations of two cracks the stepped fixed-free beam 97

6.46 Variation of non-dimensional frequency (ω_c/ω_i), Mode IV, with relative crack depth (a/h) for different relative locations of three cracks in the stepped fixed-free beam 98

6.47 Mode shapes of single cracked free-free Aluminum beam for a 8 mm depth crack at 0. 25L from right end 101

6.48 Mode shapes of single cracked Steel free-free beam with a 7 mm deep crack at 0.5L from either end 101

6.49 Mode shapes of double cracked free-free Aluminum beam subjected to 8 mm deep crack at 0. 25L from each end 103

6.50 Autospectrum of the free-free Aluminum beam subjected to a 6mm deep crack at 0.33L 104

6.51 FRF response and Coherence of the free-free Aluminum beam with a 2 mm deep single crack at 0.33*L* 105

6.52 FRF response and Coherence of the double cracked free-free Aluminum beam with a 4 mm deep crack at 0.33*L* from both ends 106

6.53 Variation of non-dimensional fundamental frequency (ω_c/ω_i) of single cracked free-free Aluminum beam for different location and depth of the crack in numerically and experimentally 107

6.54 Variation of non-dimensional fundamental frequency (ω_c/ω_i) of single cracked free-free Steel beam for different location and depth of the crack in numerically and experimentally 107

6.55 Variation of 2^{nd} mode non-dimensional frequency (ω_c/ω_i) of single cracked free-free Aluminum beam for different location and depth of the crack in numerically and experimentally 108

6.56 Variation of 2^{nd} mode non-dimensional frequency (ω_c/ω_i) of single cracked free-free Steel beam for different location and depth of the crack in numerically and experimentally 109

6.57 Variation of 3^{rd} mode non-dimensional frequency (ω_c/ω_i) of single cracked free-free Aluminum beam for different location and depth of the crack in numerically and experimentally 110

6.58 Variation of 3^{rd} mode non-dimensional frequency (ω_c/ω_i) of single cracked free-free Steel beam for different location and depth of the crack in numerically and experimentally 110

6.59 Variation of 4^{th} mode non-dimensional frequency (ω_c/ω_i) of single cracked free-free Aluminum beam for different location and depth of the crack in numerically and experimentally 111

6.60 Variation of 4^{th} mode non-dimensional frequency (ω_c/ω_i) of single cracked free-free Steel beam for different location and depth of the crack in numerically and experimentally 111

6.61 Variation of non-dimensional fundamental frequency (ω_c/ω_i) of double cracked free-free Aluminum beam for different location and depth of the crack in numerically and experimentally 112

6.62 Variation of non-dimensional fundamental frequency (ω_c/ω_i) of double cracked free-free Steel beam for different location and depth of the crack in numerically and experimentally 113

6.63 Variation of 2^{nd} mode non-dimensional frequency (ω_c/ω_i) of double cracked free-free Aluminum beam for different location and depth of the crack in numerically and experimentally 114

6.64 Variation of 2^{nd} mode non-dimensional frequency (ω_c/ω_i) of double cracked free-free Steel beam for different location and depth of the crack in numerically and experimentally 114

6.65	Variation of 3rd mode non-dimensional frequency (ω_c/ω_i) of double cracked free-free Aluminum beam for different location and depth of the crack in numerically and experimentally	115
6.66	Variation of 3rd mode non-dimensional frequency (ω_c/ω_i) of double cracked free-free Steel beam for different location and depth of the crack in numerically and experimentally	116
6.67	Variation of 4th mode non-dimensional frequency (ω_c/ω_i) of double cracked free-free Aluminum beam for different location and depth of the crack in numerically and experimentally	116
6.68	Variation of 4th mode non-dimensional frequency (ω_c/ω_i) of double cracked free-free Steel beam for different location and depth of the crack in numerically and experimentally	117
6.69	Variation of non-dimensional buckling load with respect to relative location of crack (L_1/L) for different relative crack depths for Fixed-Free beam	118
6.70	Variation of non-dimensional buckling load (P_c/P_i) with respect to relative location of crack (L_1/L) for different relative crack depths for hinged-hinged beam	119
6.71	Variation of non-dimensional buckling load (P_c/P_i) with respect to relative location of crack (L_1/L) for different relative crack depths for fixed-hinged beam	120
6.72	Variation of non-dimensional buckling load (P_c/P_i) with respect to relative location of crack (L_1/L) for different relative crack depths for fixed-fixed beam	121
6.73	Variation of non-dimensional buckling load with relative location of crack for various relative crack depths of a stepped beam	122
6.74	Variation of non-dimensional buckling load (P_c/P_i) with relative location of the second crack (L_2/L) for different relative crack depths of the fixed-free beam (L_1= 0.1L, rcd_1= 0.3)	123
6.75	Variation of non-dimensional buckling load (P_c/P_i) with relative location of the third crack (L_3/L) for different relative crack depths of the fixed-free beam (L_1=0.1L, L_2=0.2L, rcd_1=0.3, rcd_2=0.2)	124
6.76	Variation of non-dimensional buckling load (P_c/P_i) with relative crack depth for various location of two cracks of the double cracked stepped fixed-free beam	125
6.77	Variation of non-dimensional buckling load (P_c/P_i) with relative crack depth for various location of crack of the triple cracked stepped fixed-free beam	126
6.78	Variation of excitation frequencies with dynamic load factors (β) for different values of static load factor (α) of the fixed-free beam subjected to a single crack at L_1 = 0.1L of relative crack depth = 0.4	127

6.79 Variation of excitation frequencies with dynamic load factors (β) for different values of relative crack depth of the fixed-free beam subjected to a single crack at $L_1 = 0.1L$ and static load factor α = 0.2 128

6.80 Variation of excitation frequencies with dynamic load factor (β) for different relative location of crack of the fixed-free beam subjected to a single crack of relative depth = 0.4 and static load factor α = 0.4 128

6.81 Variation of excitation frequencies with dynamic load factor (β) for different values of static load factor (α) of the hinged-hinged beam subjected to a single crack at $L_1 = 0.1L$ of relative crack depth = 0.4 130

6.82 Variation of excitation frequency with dynamic load factor (β) for different values of relative crack depth of the hinged-hinged beam subjected to a single crack at $L_1 = 0.5L$ and static load factor α = 0 130

6.83 Variation of excitation frequencies with dynamic load factor (β) for different relative location of crack of the hinged-hinged beam subjected to a single crack of relative depth = 0.4 and static load factor α = 0.2 131

6.84 Variation of excitation frequencies with dynamic load factor (β) for different values of static load factor (α) of the fixed-hinged beam subjected to a single crack at $L_1 = 0.6L$ of relative crack depth = 0.6 132

6.85 Variation of excitation frequency with dynamic load factor (β) for different values of relative crack depth of the fixed-hinged beam subjected to a single crack at $L_1 = 0.6L$ and static load factor α = 0.2 133

6.86 Variation of excitation frequencies with dynamic load factor (β) for different relative location of crack of the fixed-hinged beam subjected to a single crack of relative depth = 0.6 and static load factor α = 0.4 134

6.87 Variation of excitation frequencies with dynamic load factor (β) for different values of static load factor (α) of the fixed-fixed beam subjected to a single crack at $L_1 = 0.5L$ of relative crack depth = 0.4 135

6.88 Variation of excitation frequencies with dynamic load factors (β) for different values of relative crack depth of the fixed-fixed beam subjected to a single crack at $L_1 = 0.5L$ and static load factor α = 0.4 135

6.89 Variation of excitation frequencies with dynamic load factor (β) for different relative location of crack of the fixed-free beam subjected to a single crack of relative depth = 0.6and static load factor α = 0.4 136

6.90 Variation of excitation frequencies with dynamic load factor (β) for different end conditions of the beam subjected to a single crack at 0.1L of relative depth = 0.4 and static load factor α = 0.2 137

6.91 Variation of excitation frequencies with dynamic load factor (β) for different end conditions of the beam subjected to a single crack at critical region of the beam of relative depth = 0.4 and static load factor α = 0.2 138

6.92 Effect of dynamic load factor (β) on dynamic instability regions of the Stepped cantilever beam subjected to a single crack at $L_1 = 0.1L$ from fixed end of 4 mm crack depth for different values of static load factor (α) 139

6.93	Effect of dynamic load factor (β) on dynamic instability regions of the Stepped cantilever beam subjected to a single crack at $L_1 = 0.05L$ from fixed end for different values of crack depths and static load factor $\alpha = 0.2$	139
6.94	Effect of dynamic load factor (β) on dynamic instability regions of the Stepped beam subjected to a 4 mm deep single transverse open crack at different locations from fixed end and static load factor $\alpha = 0.4$	140
6.95	Effect of Static load factor (α) on dynamic instability regions of the fixed-free beam subjected to two cracks at $L_1 = 0.1L$, $rcd_1 = 0.2$ and $L_2 = 0.05L$ and $rcd_2 = 0.2$	141
6.96	Effect of second crack depth on dynamic instability regions of the cantilever beam subjected to two cracks at L_1=0.1L, $rcd_1 = 0.2$ and $L_2 = 0.05L$ for static load factor 0.2	142
6.97	Effect of dynamic load factor (β) on dynamic instability regions of a cantilever beam for different locations of the second crack with two cracks, $L_1 = 0.1L$, $rcd_1 = 0.4$, $L_2 = 0.05L$ to $0.9L$, $rcd_2 = 0.4$ for $\alpha = 0.4$	143
6.98	Effect of Static load factor (α) on dynamic instability regions of the cantilever beam with three cracks, $L_1 = 0.1L$, $rcd_1 = 0.2$, $L_2 = 0.2L$ and $rcd_2 = 0.2$ and $L_3 = 0.05L$, $rcd_3 = 0.2$	144
6.99	Variation of dynamic instability regions of the cantilever beam subjected to three cracks at $L_1 = 0.1L$, $rcd_1 = 0.2$, $L_2 = 0.2L$, $rcd_2 = 0.2$ and $L_3 = 0.05L$ with dynamic load factors for different relative depths of third crack and static load factor, $\alpha = 0.2$	145
6.100	Variation of instability regions with dynamic load factor (β) for cantilever intact beam, single cracked beam, double cracked beam and triple cracked beam for different position of third crack of relative depth 0.2	146
6.101	Variation of dynamic instability regions with dynamic load factors of the stepped cantilever beam subjected to two cracks at 0.05L and 0.15L of crack depth 6 mm each for static load factor, $\alpha = 0.2$	147
6.102	Variation of dynamic instability regions with dynamic load factors of the stepped cantilever beam subjected to two cracks at varous locations for static load factor, $\alpha = 0.2$ and crack depth 4 mm each	147
6.103	Variation of dynamic instability regions with dynamic load factors of the stepped cantilever beam subjected to three cracks at 0.05L, 0.15L and 0.25L of different crack depths for static load factor, $\alpha = 0.2$	148
6.104	Variation of dynamic instability regions with dynamic load factors of the stepped cantilever beam subjected to three cracks at varous locations for static load factor, $\alpha = 0.2$ and crack depth 4 mm each	149
6.105	Comparison between predicted relative crack depth and measured relative crack depth showing correlation coefficient (R) during training of LMNN model.	153
6.106	Comparison between predicted relative crack depth and measured relative crack depth showing correlation coefficient (R) during testing of LMNN model.	153

6.107	Comparison between predicted relative crack depth and measured relative crack depth showing correlation coefficient (R) during training of BRNN model.	153
6.108	Comparison between predicted relative crack depth and measured relative crack depth showing correlation coefficient (R) during testing of BRNN model.	154
6.109	Comparison between predicted relative crack depth and measured relative crack depth showing correlation coefficient (R) during training of DENN model.	154
6.110	Comparison between predicted relative crack depth and measured relative crack depth showing correlation coefficient (R) during testing of DENN model.	154
6.111	Comparison of the three models between measured and predicted value of relative crack depth (rcd) of the beam	155

List of Tables

6.1	Comparison of free vibration frequencies (rad/sec) of cracked beam for a crack at L_1=0.2L for different relative crack depths (a/h)	61
6.2	Comparison of non-dimensional buckling load (P_c/P_i) of cracked beam	61
6.3	Free vibration frequencies of single cracked free-free Aluminum beam by ANSYS	99
6.4	Free vibration frequencies of single cracked free-free Steel beam by ANSYS	99
6.5	Free vibration frequencies of double cracked free-free Aluminum beam by ANSYS	102
6.6	Free vibration frequencies of double cracked free-free Steel beam by ANSYS	103
6.7	Natural frequencies for simply supported Aluminum beam with or without cracks	150
6.8	Performance of different neural network models for simply supported Aluminum beam	155

List of Publications

International Journal

1. **Mishra, U. K.** and **Sahu, S. K.**, (2013), "On parametric response characteristics of Beams with multiple Transverse cracks", International Journal of Acoustics and Vibration, 18 (4), 155-162.
2. **Mishra, U. K.** and **Sahu, S. K.**, (2015)(In Press), "Parametric instability of beams with transverse cracks subjected to harmonic in-plane loading", *International Journal of Structural Stability and Dynamics*,15 (1), DOI-1540006
3. **Mishra, U. K.** and **Sahu, S. K.** (Communicated), "Parametric instability of stepped beams with transverse cracks subjected to harmonic in-plane loading".

International Conference

1. **Mishra, U. K.** and **Sahu, S. K.**, 2009, "Vibration and buckling of cantilever beam with crack", ICoVP-2009, IIT Kharagpur,19th – 22 Jan, 2009
2. **Mishra, U. K.** and **Sahu, S. K.**, 2012, "Parametric resonance characteristics of cantilever beam with an open transverse crack subjected to in-plane periodic loading, ICSSD, MNIT Jaipur, 4 – 6 Jun, 2012

Chapter 1

INTRODUCTION

1.1 Introduction

Beams are one of the most fundamental structural components in many structures and are frequently used in Aeronautical, Mechanical and Civil engineering structures. Most of the members of modern structures operate under different loading conditions, which may cause damages like cracks in overstressed zones. The occurrence of cracks or local defects in a structural member induces local variations in stiffness, the magnitude of which depends mainly on the location and the depth of the cracks. These variations, in turn, affect the static and dynamic behavior of the whole structure considerably. In some cases, this can lead to failure unless cracks are detected early enough. To ensure the safe, reliable and operational life of structures, it is of tremendous technical importance to study the static, dynamic and stability behavior of cracked structural components and its detection for structural health monitoring of structures as a whole.

1.2 Research Significance

The environmental mechanical action on a beam may be due to forces, which are in motion and/or time dependent. When these external excitations are parametric with respect to certain form of deformation of the body, they appear as one of the coefficients in the homogeneous governing differential equation of motion of the system. Such systems are said to be parametrically excited and the associated instability of the system is called parametric resonance. Whereas in case of forced vibration of the systems, the equation of motion of the system is inhomogeneous, and the disturbing forces appear as inhomogeneity. In parametric instability, the rate of increase in amplitude is generally exponential and thus potentially dangerous, while in typical resonance due to external excitation the rate of increase in response is linear. Moreover, damping reduces the severity of typical resonance due to transverse load, but may only reduce the rate of increase during parametric resonance. Parametric instability occurs over a region of parameter space and not at discrete points. It may occur due to excitation at frequencies remote from the natural frequencies. Several ways of combating parametric

resonance such as vibration isolation may be inadequate and sometimes dangerous with reverse results. A number of catastrophic incidents can be traced to parametric instability or dynamic instability.

In practice, parametric excitation can occur in structural systems subjected to vertical ground motion, aircraft structures subjected to turbulent flow, and in machine components and mechanisms. Other examples are longitudinal excitation of rocket tanks and their liquid propellant by the combustion chambers during powered flight, helicopter blades in forward flight in a free-stream that varies periodically, and spinning satellites in elliptic orbits passing through a periodically varying gravitational field. In industrial machines and mechanisms, their components and instruments are frequently subjected to periodic or random excitation transmitted through elastic coupling elements. A few examples include those associated with electromagnetic and aeronautical instruments, vibratory conveyers, saw blades, belt drives and robot manipulators etc. One of the main objectives of the analysis of parametrically excited systems is to establish the regions in the parameter space in which the system becomes unstable. These regions are known as dynamic instability regions (DIR). The boundary separating a stable region from an unstable one is called a stability boundary. The plot of these boundaries on the parameter space is called a stability diagram.

Parametric resonance of structures subjected to axial periodic loads has received considerable attention in the literature. Of particular concern are many problems in the structural dynamics of slender structures under dynamic loads such as winds, waves or earthquakes. It is well known that relatively slender structures begin to exhibit instability when subjected to a static compressive load. When these structures are subjected to dynamic axial load, such instability becomes more serious.

The dynamic stability of mechanical systems according to Bolotin (1964), represents a specific aspect of the stability of motion. Several works were presented along the lines of Bolotin's early studies. The object of these works has been to give a quantitative description of the phenomenon, but if one tries to solve the problem with continuum models, it becomes particularly difficult even for quite simple mechanical systems. If one considers Euler's beam subjected to a compressive dynamic force, starting with the equations of motion, the so-called Mathieu Hill equation which governs the dynamic stability problems is obtained. The theory of systems of Mathieu Hill deferential equations with periodic coefficients is useful to distinguish the regions of dynamic stability from those where instability occurs.

A surface crack on a beam section is an area of local flexibility of the structural member, and is caused by the strain energy concentration near the crack tip when the structural member is under load. The crack results in the deviation of frequencies and mode shapes for the vibration. Changes in vibration characteristics may result in changes in stability characteristics.

The dynamic characteristics of beam with crack is studied by various researchers analytically, numerically and experimentally. The emergence of the digital computers with their high speed and core memory capacity has changed the outlook of the structural analyst and caused tremendous advances in the dynamic analysis of cracked beams and allows the researcher to model the beam in a more realistic way.

When the instability is in the form of flutter (oscillations with increasing amplitudes), the system loses stability at eigenvalues that are different from zero. In fact, the instability of the system manifests itself in oscillations with unboundedly increasing amplitudes when the two lowest eigenvalues become complex conjugate. The buckling load of these systems cannot be calculated by means of the static criterion, but only using the kinetic criterion, i.e. through the dynamic analysis. Owing to the action of the forces, the system undergoes a deformation, mathematically described by a deflection vector that in this case has one predominant component: the lateral deflection of a beam. The instability of the system occurs for the critical values of the loads under which the deflection vector may become unbounded. Since the transition of the beam from the state of equilibrium to the state of instability is always related to a motion, it is appropriate to use the dynamic analysis for the investigation of this transition and to discuss in which way the stability is lost. Therefore the study of the stability of the cracked system is reduced to an eigen value problem. The parametric instability characteristics of a beam are often studied in the spectrum of vibration and buckling studies. The computation of natural frequencies and critical buckling loads are used for investigation of dynamic instabilities. Thus the vibration, buckling and dynamic stability of beams with transverse cracks poses a tremendous challenge and must be properly understood in the structural design of dynamic systems.

Besides this, the detection of cracks in the members and its extent are important. The crack detection procedures that are often used are called direct procedures such as ultrasonic, X-rays, etc. However, these methods have proven to be inoperative and unsuitable in some particular cases, since they require expensive and minutely detailed inspections. To avoid these disadvantages, researchers have focused on more efficient procedures in crack detection based

on the changes of modal parameters (natural frequencies, mode shapes and modal damping values) that the crack introduces.

A thorough review of previous literature done in this field is an important requirement to arrive at the objective and scope of the present investigation. The detail reviews of literature along with the author's critical discussion are presented in next chapter.

1.3 Summary

The beams often get cracked during the service life of structures. Cracks may appear due to overstressing or during dynamic loading like wind or earthquake. The whole structure or the structural components either has to be disposed or strengthened or used as it is if the loading condition still supports. So, the dynamic behavior of cracked beams is of tremendous technical importance for safe use of these components.

Chapter 2

REVIEW OF LITERATURE

2.1 Introduction

Many engineering structures may have structural defects such as cracks due to mechanical vibrations, environmental attack, corrosion, long term service and cyclic load etc. The presence of transverse crack in beams may carry potential risk of destruction and produces high costs of maintenance. A crack on a beam element introduces local flexibility due to strain energy concentrations in the vicinity of the crack tip under the load. This flexibility changes the dynamic behavior of the structural member. Besides this, now-a-days direct crack detection procedures such as ultrasonic, X-rays proved to be inoperative and unsuitable in many industrial situations due to detailed periodic inspections. So, crack detection through vibration analysis is of tremendous technical importance. One of the most investigated approaches in detecting damage is the use of vibration data as a basis for structural health monitoring. Many considerations can contribute to the formation of a crack and subsequently the potentially catastrophic consequences, has made structural integrity testing an extremely active area of research. So, the dynamic characteristics of cracked beams are of considerable importance in many designs.

Though the investigation is mainly focused on the dynamic stability of stepped beams with multiple transverse cracks, some relevant researches on free vibration, static stability or buckling of cracked uniform and stepped beams with single and multiple cracks are also studied for the sake of its relevance and completeness. Some recent relevant studies are reviewed elaborately and critically discussed to identify the lacunae in existing literature. The studies in this chapter are grouped into four major parts for beam with crack as follows.

- Vibration
- Buckling
- Dynamic stability
- Crack detection techniques

The studies involving beams made from isotropic and orthotropic materials are discussed separately within the sections.

2.2 Vibration of Cracked Beams

The dynamic behavior of a cracked beam is of significant importance in engineering for which, the effect of crack upon dynamic characteristics of uniform and stepped beams is studied by many researchers.

2.2.1 Vibration of cracked uniform beams

The fact that a crack or local defect affects the dynamic response of a structural member was known long ago. The previous studies on dynamics/vibration behavior of beams/shafts with cracks are reviewed by Waur [1991], Dimarogonas [1996] and recently by Jassim *et al*. [2013]. According to Dimarogonas [1996], the first attempts to quantify local defects were by Thomson [1943] and Kirmsher [1944]. The effect of a notch on the structure flexibility was simulated by a local bending moment or reduced section, with magnitudes which were estimated by experimentation. Later during 1950s, analysis of the local flexibility of a cracked region of structural element was quantified by Irwin [1957], Bueckner [1958], Westmann and Yang [1967] by relating local flexibility to the crack stress intensity factor (SIF). Based on this principle, an experimental method was developed for the computation of the SIF based on the local bending stiffness of a cracked prismatic beam. Several investigators computed the SIF and local flexibility for a variety of geometries of the crack and associated structural member. Liebowitz and co-workers [1967, 1968 and 1969] utilized existing results from fracture mechanics to calculate the local flexibility of beams of rectangular cross-section with transverse surface crack of uniform depth. Cawley and Adams [1979] successfully tested the frequency measurement principle on composite structures made in the presence of damage.

With advent of computers, fine-mesh finite element techniques were used during 1980s to compute local flexibilities by Gudmundson [1983], Rauch [1985] and Chen and Wang [1986]. Papadopoulos and Dimarogonas [1987] investigated the coupling of longitudinal and bending vibrations of a rotating shaft due to an open transverse surface crack analytically. The study assumed the open crack in a beam leads to a system with behavior similar to that of a rotor with dissimilar moment of inertia along two perpendicular directions. Gounaris and Dimarogonas [1988] developed a finite element model to analyze a beam with a surface crack. The

investigators evaluated the dynamic response of a cracked cantilever beam to harmonic point force excitation. It is found that the resonant frequencies and vibration amplitudes are considerably affected by the existence of moderate cracks. Nikpur and Dimarogonas [1988] studied the variation properties of a laminated composite beam containing a central crack on the basis of changes in local compliance. The effect of cracks upon the buckling of an edge-notched column for isotropic and anisotropic composites has been studied by Nikpour [1990]. The study indicated that the instability increases with the column slenderness and the crack length. The author obtained that the material anisotropy conspicuously reduces the load carrying capacity of an externally cracked member.

Ostachowicz and Krawczuk [1990] studied the forced vibration of the beams and the effects of the crack locations and sizes on the vibrational behavior of the structure by finite element method (FEM). They modeled the beam by triangular disk finite elements and also discussed the basis for crack identification. Qian *et al.*, [1991], investigated vibration behavior of cracked plates by finite element method. They derived the element stiffness matrix of plate with a thorough crack from integration of SIFs, estimated under bending, twisting and shearing. Ostachowicz and Krawczuk [1991] presented the effect of two open cracks upon natural vibrations of a beam using analytical method. They assumed both single sided and double-sided cracks which occur due to load fluctuation and cyclic loading respectively. Gounaris and Papazoglou [1992] presented finite element method for computation of the vertical natural vibrations of a Timoshenko beam in water. The method was based on one-dimensional beam finite element for structural part and on fluid boundary elements for fluid part both in coupled and uncoupled versions. Manivasagam and Chandrasekaran [1992] presented the results of experimental investigations upon the reduction effect of the fundamental frequency of layered composite materials with damage in form of cracks.

Kikidis and Papadopoulos [1992] presented bending vibrations of non-rotating cracked shaft (beam) according to Euler-Bernoulli theory and Timoshenko theory for different crack depth and slenderness ratio by analytical method. They found the bending resonant frequencies decreasing with increase in depth and the effect of shear deformation on resonant frequency decreases with increase in slenderness ratio. Krawczuk and Ostachowicz [1992] presented a mathematical model of transverse vibrations of a Bernoulli-Euler beam with a closing crack. Making use of this analytical model the effect of magnitude and position of the crack upon the basic instability area of the beam was carried out. Krawczuk and Ostachowicz [1993] analyzed

the influence of transverse one-edge open cracks on the natural frequencies of the cantilever beam subjected to vertical loads by finite element method. They obtained that the change of the natural frequencies corresponding to the mode of vibration is largest when the crack is located at the point at which an amplitude of the mode of vibration is equal to zero. On the other hand, when the crack is located at points for which the amplitude of the mode of vibration is maximal, the change of the natural frequencies is negligible. Shen and Pierre [1994] used both analytical and finite element approach to study the free vibrations of a uniform Bernoulli-Euler beam containing one single-edge crack. The equation of motion for simply supported and cantilever beam were solved by Galerkin and local Ritz method respectively.

Krawczuk [1994] formulated a new beam finite element with a single non-propagating one-edge open crack located in its mid-length for static and dynamic analysis of cracked composite beams. They considered a three noded beam element with two degrees of freedom per node. Krawczuk and Ostachowicz [1995] investigated eigen-frequencies of a cantilever beam made of graphite-fiber reinforced polyimide with a transverse one-edge non-propagating open crack. They used two both analytical and FEM models and studied the effect of crack parameters, volume fraction of fibers on the natural frequencies. Krawczuk *et al.* [1997] developed models of finite cracked beam element and delaminated beam element. They developed models of the finite cracked beam element for the analysis of the influence of the fatigue cracks and delamination on the dynamic characteristics of the constructions made of composite materials. Ruotolo *et al.* [1996] analysed the vibrational response of a cracked cantilever beam to harmonic forcing function by finite element method. Chati *et al.* [1997] investigated the problem of vibration of cracked beam using finite element method. The study conducted modal analysis of ~~a~~ cantilever beam with transverse edge crack. The non-linearity involved was modeled as a piecewise-linear system. Corn *et al.*, [1997] proposed a new finite element method for vibration characteristics of short beams considering the effect of rotary inertia and transverse shear. Kisa *et al.* [1998] analysed the free vibration characteristics of cracked Timoshenko beam by finite element and component mode synthesis method. The beam was divided into two components related by a flexibility matrix which incorporated the inter action forces obtained from fracture mechanics theory. Yokoyama and Chen [1998] studied the vibration characteristics of a uniform Bernoulli-Euler beam with a single edge crack using a modified line-spring model in finite element method. Chondros and Dimarogonas [1998] developed a continuous beam vibration theory for the lateral vibration of cracked Euler-Bernoulli beams with single-edge or double-edge open cracks. The differential equation used

for the analysis was derived from Hu-Washizu-Barr variational formulation. Shifrin and Ruotolo [1999] proposed a new technique for calculation of natural frequencies of a vibrating beam with an arbitrary number of transverse open cracks. The analytical method involved matrices of reduced sizes taking less time for computation.

Chondros *et al.* [2001] used continuous beam vibration theory for the prediction of changes in transverse vibration of a simply supported beam with a breathing crack. They observed the changes in vibration frequencies for a fatigue-breathing crack are smaller than the ones caused by open cracks. Carneiro and Inman [2001] reviewed the continuous model for the vibrations of a beam with a single-edge crack developed by Shen and Pierre [1994]. They proposed some modifications in order to overcome the lack of self-adjointness of the resulting stiffness operator and presented a new version of the equation of motion. Zheng and Fan [2001] using modified Fourier series also computed the natural frequencies of a Timoshenko beam with an arbitrary number of transverse open cracks. Using modified Fourier series the problem was reduced to a simple one which involved solving some standard linear eigenvalue equations. Khiem and Lien [2001] developed an analytical method based on transfer matrix method and rotational spring model for natural frequency analysis of beam with an arbitrary number of cracks. Carneiro and Inman [2002] derived a continuous model for the transverse vibration of cracked beams considering the effect of shear deformation. The effectiveness of the derived model was validated by comparing the results with 2-D finite element model.

Khiem and Lien [2002] studied the dynamic behavior of a beam with numerous cracks. They developed the dynamic stiffness method for spectral analysis of forced vibration of a multiple cracked beam. Fernandez-Saez and Navarro [2002] presented an analytical approach to the fundamental frequency of cracked Euler-Bernoulli beams in bending vibrations. The investigation used flexibility influence function method to solve the problem which leads to an eigenvalue problem formulated in integral form. Lin *et al.* [2002] presented a hybrid analytical/numerical method for efficient computation of eigen solutions of a vibrating beam with arbitrary number of transverse open cracks for various boundary conditions. Dado and Abuzeid [2003] investigated vibrational behavior of a cracked cantilever beam carrying end mass and rotary inertia by finite element method. End mass ensured their assumption of open cracks during vibration.

Krawczuk *et al.* [2003] introduced a new finite spectral element for a cracked Timoshenko beam for modal and wave propagation analysis and studied the responses of crack parameters on wave propagation. Zheng and Kessissoglou [2004] obtained the natural frequencies and mode shapes of a cracked beam using finite element method. In their investigation an 'overall additional flexibility matrix' was added to the flexibility matrix of the intact beam element to obtain the total flexibility matrix and therefrom the stiffness matrix of the cracked beam element. Kisa [2004] investigated the effect of cracks on dynamical characteristics of a cantilever composite beam, made of graphite fiber-reinforced polyamide. Finite element and the component mode synthesis methods were used to model the problem. Effect of crack parameters, volume fraction and orientation of fibers on natural frequencies and mode shapes of the beam for non-propagating open cracks are studied. Kisa and Gurel [2006] proposed a model that combines FEM and component mode synthesis method for modal analysis of beams with circular cross section containing multiple non-propagating open cracks. They presented natural frequencies and mode shapes of a beam with an arbitrary number of cracks for different boundary conditions. Binici [2005] investigated the vibration of beams with multiple open cracks subjected to axial force using a new analytical approach. A parametric study was conducted to investigate the effect of crack and axial force on eigen frequencies. The study concluded that the eigen frequencies were strongly affected by crack location, severities and axial force level. The method is illustrated to be used to find the critical load of the cracked beam using eigen frequencies. Hsu [2005] by using the differential quadrature method (DQM) formulated the eigenvalue problems of fixed-free and hinged-hinged Bernoulli-Euler cracked beams on elastic foundation with axial force. Lu and Li [2005] discussed the cracked-beam problem as a variant of Motz's problem and its very accurate solution in double precision is explicitly provided by the boundary approximation. Al-Said *et al.* [2006] proposed a three dimensional model to describe the flexural vibration characteristics of a rotating cracked Timoshenko beam. They studied the effect of crack depth, shear deformation and rotation speed on the dynamic characteristics of the beam using three dimensional finite element analysis.

Behera *et al.* [2006] presented an analytical method for the dynamic characteristics of a cantilever beam with two transverse open cracks. They presented the technique of utilization of the dynamic response of a cracked beam for fault diagnosis. Loya *et al.* [2006] obtained natural frequencies for bending vibrations of Timoshenko cracked beams with simple boundary conditions by analytical method. They solved a simply supported beam problem by solving differential equations for free bending vibrations and also by perturbation method. It was found

that perturbation method provides simple expressions for natural frequencies of cracked beams and gives good result for shallow depth of cracks. Fang *et al*. [2006] studied the effect of a crack on the vibratory response of a simplified aero-engine bladed-disk model, which consists of cantilevered beams (blades) coupled with springs (inter-blade internal coupling). Mei *et al.* [2006] presented wave vibration analysis of an axially loaded cracked Timoshenko beam considering axial loading, shear deformation and rotary inertia using analytical method. Mendelsohn [2006] presented a theoretical investigation of the effect of crack-plane plasticity on the vibration of a transversely edge-cracked beam. Viola *et al.* [2007] investigated free vibration analysis of axially loaded cracked Timoshenko beam using dynamic stiffness method. They introduced a new analytical procedure based on the coupling of dynamic stiffness matrix and line-spring element to model the cracked beam. They studied the effect of axial load, shear deformation and rotary inertia on the natural frequencies of beam with transverse cracks.

Arboleda-Monsalve *et al.* [2007] investigated the stability and free vibration analyses of a Timoshenko beam-column with generalised end conditions subjected to constant axial load and weakened by a cracked section along its span. They included the detrimental effects of a single weakened section and the beneficial effects of a lateral bracing located at the discontinuity. Aydin [2008] presented a simple and efficient analytical approach to determine the vibratory characteristics of axially loaded Timoshenko and Euler-Bernoulli beams with arbitrary number of cracks. The local compliance induced by a crack was described by a massless rotational spring and a set of boundary conditions were used as initial parameters to define the mode shapes of the segment of the beam before the first crack. Yang *et al.* [2008] by employing the modal series expansion technique presented an analytical method to investigate the free and forced vibration of cracked inhomogeneous Euler-Bernoulli beams under an axial force and a moving load.

Yang and Chen [2008] investigated free vibration analysis of beams made of functionally graded materials (FGM) containing open edge cracks by using Bernoulli-Euler beam theory and the rotational spring model for different boundary conditions. Analytical solutions of the natural frequencies and the corresponding mode shapes are obtained for cracked beams of FGM for different boundary conditions. A parametric study is conducted to show the influences of the location and total number of cracks, material properties, slenderness ratio and end supports on the flexural vibration of cracked FGM beams. Ke *et al*. [2009] studied free vibration and elastic buckling of Timoshenko beams of different boundary conditions made of functionally

graded materials containing open edge cracks. They conducted a parametric study on the influence crack parameters analytically.

Caddemi and Calio [2009] presented the closed-form expressions for the vibration modes of the Euler–Bernoulli beam in the presence of multiple concentrated cracks modelled as a sequence of Dirac's delta generalised functions in the flexural stiffness. They conducted a parametric analysis for different boundary conditions in order to investigate the influence of the number, position, and intensity of the cracks on the dynamical properties of the Euler–Bernoulli beam. Mazanoglu *et al*. [2010] investigated bending vibration of non-uniform rectangular beam with multiple edge cracks along the beam's height analytically and compared their results with FEM softwares. Multi-cracked beams are also analysed by using approach based strain disturbance variation along the beam. They also presented the effects of taper factors, boundaries and positions of cracks on the natural frequency ratios graphically. Rezaee and Hassannejad [2011] used a new analytical approach to free vibration analysis of beam with a breathing crack based on mechanical energy balance method. They also compared their findings with experimental results. Shafiei and Khaji [2011] developed an analytical approach for evaluating the forced vibration response of uniform beams with an arbitrary number of open edge cracks excited by a concentrated moving load.

Yan and Yang [2011] presented an analytical study on the forced flexural vibration of functionally graded beams with open edge cracks under combined action of an axial compressive force and a concentrated transverse load moving along the longitudinal direction. They used analytical method to obtain forced vibration response for beams of different boundary conditions. A parametric study was also conducted to examine the effect of cracks, material property gradient, axial compression and speed of the moving load.

Caddemi and Calio [2012] proposed an exact closed-form solution for the vibration modes and the eigen-value equation of the Euler-Bernoulli beam-column in the presence of an arbitrary number of concentrated open cracks. Agarwalla and Parhi [2013] investigated the effect of an open crack on the modal parameters of the cantilever beam. Results of finite element method (FEM) and the experimental method are compared. Khan and Parhi [2013] estimated the effects of crack depth on natural frequency and mode shape of Cantilever and Fixed-Fixed beams subjected to two transverse open cracks using ANSYS. Experiments were also conducted to validate the results.

2.2.2 Vibration of cracked stepped beams

Balasubramanian and Subramanian [1985] studied the performance of four degrees of freedom per node of an element in vibration analysis of uniform and stepped beam. They considered deflection, slope, bending moment and shearing force as the four degrees of freedom per node instead of conventional displacement and its three derivatives. Jang and Bert [1989] presented an exact and a numerical solution of free vibration analysis of a cracked stepped beam using both analytical and finite element method using non-integer polynomial shape functions and a commercial code MSC/pal. Chaudhary and Maiti [1999] carried out modelling of transverse vibration of a beam of linearly variable depth and constant thickness in the presence of an open edge crack normal to its axis. They proposed the concept of a rotational spring to represent the crack section and the Frobenius method to enable possible detection of the location of the crack based on the measurement of natural frequencies. Zheng and Fan [2001] developed a kind of modified Fourier series method to compute the natural frequencies of a non-uniform beam with an arbitrary number of transverse open cracks. They claimed their method to tackle the beam with arbitrary number of cracks and can handle internal geometrical discontinuities. Li [2002] proposed an exact approach for free vibration analysis of a non-uniform beam with arbitrary number of cracks and concentrated masses. The study assumed a model of massless rotational springs to describe the local flexibility induced by cracks in the beam. Kisa and Gurel [2007] suggested a novel numerical technique combining the finite element and component mode synthesis methods to analyze the free vibration analysis of uniform and stepped cracked beams of circular cross section. Ranjbaran *et al*. [2008] presented mathematical formulation for buckling analysis of a column and vibration analysis of a beam. Mazanoglu *et al*. [2009] presented an energy based analytical method for vibration identification of non-uniform Euler-Bernoulli beam having multiple open cracks. Kukla [2009] proposed a numerical solution to the free vibration, static stability problem of a stepped column with cracks. They investigated the effect of position and size of the cracks on the above parameters. Mazanoglu and Sabuncu [2010] investigated bending vibration of non-uniform rectangular beams with multiple edge cracks along the beam's height based on analytical approach. In the same year the above authors again presented flexural vibrations of non-uniform Rayleigh beams having single-edge and double-edge cracks. Torabi *et al*. [2014] proposed differential quadrature element method (DQEM) for free transverse vibration analysis of multiple cracked non-uniform Timoshenko beams with general boundary conditions. Zhang *et al*. [2014] used a general analytical solution

to study free vibration of non-uniform Timoshenko beams coupled with flexible attachments and multiple discontinuities in engineering applications.

2.3 Buckling of Cracked Beams

The static stability or buckling of beam with transverse cracks under compressive in-plane forces has always been an important field of research with the introduction of steel. More recently there is a renewed interest with development of aviation and aerospace programs which is expanding to off shore and nuclear engineering.

2.3.1 Buckling of cracked uniform beams

The previous studies on buckling/static stability behavior of beam with cracks are reviewed by Dimarogonas [1996] through 1996. Liebowitz *et al.* [1967] conducted experiments to study effect of cracks on maximum load carrying capacity of long and short, notched and un-notched columns. Okamura *et al.* [1969] studied the effect of reduced rigidity on the load carrying capacity, deflection and the fracture load of a slender column with a single-edge crack based on column theory together with the relationship between the compliance and stress intensity factor of a cracked beam. Nikpour [1990] investigated buckling of an edge-notched beam for isotropic and anisotropic composites by an analytical method. The study indicated that the instability increases with the beam slenderness and the crack length. In addition, the material anisotropy conspicuously reduces the load-carrying capacity of an externally cracked member.

Liu and Wang [2000] suggested a finite element procedure to analyze a cracked beam-column on an elastic foundation. Their stability analysis suggested that the buckling loads are hardly influenced by crack location or length. Wang *et al.* [2002] presented exact stability criteria and buckling loads of Timoshenko columns under intermediate and end concentrated loads using an analytical method. They also investigated the effect of transverse shear and end conditions of the beam on buckling load. Fan and Zheng [2003] using modified Fourier series computed the buckling load reduction of a Timoshenko beam column with an arbitrary number of transverse open cracks. Zheng and Fan [2003] investigated on the vibration and stability of cracked hollow-sectional beams from the flexibility coefficients induced due to crack with in solid region and crack extending to hollow region. Wang [2004] presented a comprehensive analysis of the stability of a cracked beam subjected to a follower compressive load and obtained buckling load of the cracked beam through dynamic analysis of the beam. Gurel and

Kisa [2005] investigated the buckling of slender prismatic columns with a single non-propagating edge crack subjected to concentrated vertical loads. They combined transfer matrix method and fundamental solutions of intact columns for determining the buckling loads of cracked columns.

Skrinar [2007] discussed the implementation of a simplified computational model that is widely used for computation of transverse displacement in transversely cracked slender beams into Euler's elastic flexural buckling theory. He also compared these results with the results obtained from FEM analysis. Jiki [2007] presented an analytical method to study the interaction between reduced axial and torsional buckling strengths of thin-beam columns of doubly symmetric sections with an edge crack at the middle. Yang and Chen [2008] investigated buckling of beams made of functionally graded materials containing open edge cracks by using Euler-Bernoulli beam theory and the rotational spring model. Analytical solutions of the critical buckling load and the corresponding mode shapes for different boundary conditions are obtained. A detailed parametric study for the influences of the location and total number of cracks, material properties, slenderness ratio and end supports on buckling characteristics of cracked FGM beams is studied. Karaagac *et al*. [2009] investigated the effects of crack ratios and locations on the fundamental frequencies and buckling loads of slender cantilever Euler beams with a single-edge crack both experimentally and numerically using finite element method.

2.3.2 Buckling of cracked stepped beams

Iremonger [1980] computed buckling loads for tapered and stepped columns by a finite difference method. Li [2000, 2001 and 2003] presented an analytical approach to study the buckling of non-uniform columns under combined concentrated and distributed loads subjected to single and multiple cracks with various end conditions, with or without shear deformation. Arboleda-Monsalve *et al*. [2007] presented the stability and free vibration analyses of a Timoshenko beam-column with generalized end conditions subjected to constant axial load (tension or compression), and weakened by a cracked section along its span. Rahai and Kazemi [2008] formulated a new analytical procedure for buckling analysis of tapered column members without crack or damage. Vadillo *et al.* [2012] presented closed form expressions for the buckling loads of weakened Timoshenko columns with different boundary conditions.

2.4 Dynamic Stability of Cracked Beams

Structural components are often subjected to in-plane harmonic loads which may lead to dynamic instability, due to certain combinations of the applied in-plane forcing parameters and the natural frequency of transverse vibration. Discovery of parametric resonance dates back to 1831. Faraday was the first to observe the phenomenon of parametric excitation, when he noticed that when a fluid filled container vibrates vertically, fluid surface oscillates at half the frequency of the container.

2.4.1 Dynamic stability of cracked uniform beams

The first mathematical expression of the phenomenon is given by Raleigh in 1883. As per Bolotin [1964], the first analysis of parametric resonance of a pinned perfect column is presented by Beliav. The general theory of dynamic stability of elastic system of deriving the coupled second order differential equation of the Mathew-Hill type and the determination of the regions of instability by seeking periodic solution using Fourier series expansion is explained by Bolotin [1964]. The distinction between 'good' and 'bad' vibration regimes of cracked beam subjected to in-plane periodic loading can be distinguished through calculation of dynamic instability regions (DIR). Anifantis and Dimarogonas [1983], studied stability of Beck columns with single crack subjected to follower and vertical loads analytically. They found that cracks in these columns can make this system have flutter type instability which was reported divergent type in earlier works. Chen and Chen [1995] investigated the stability of a rotating cracked shaft subjected to the end load and an axial compressive force by finite element method. They also discussed the influences of open cracks on the natural whirling speeds. Chen and Shen [1997] developed a finite element model to study the dynamic stability aspects of a cracked rotating beam of general orthotropy. They considered the effect of both the transverse shear deformation effect and the rotary inertia effect on buckling load. Briseghella *et al.* [1998] used finite element method to find the regions of dynamic stability of beams and frames without cracks. Brandon and Sudraud [1998] found experimentally that vibrating polymeric cracked cantilever beams exhibiting two distinct non-linear behavior patterns. They found switching between these behavior patterns could be initiated due to change in position of the crack, change in amplitude of excitation, and change in the crack depth ratio or by changing the frequency of excitation. Sekhar [1999] presented finite element analysis of a rotor with two transverse open cracks for flexural vibrations. The eigen value analysis and stability study were carried out and the influence of one crack over the other for eigen frequencies, mode

shapes and threshold speed limits were observed. Kim and Kim [2000] investigated the effect of crack location and depth on the dynamic stability of a free-free Timoshenko beam subjected to a constant follower force using Finite element method. Murphy and Zhang [2000] studied the vibration and stability characteristics of a cracked beam translating between two fixed supports using an analytical method. Javidruzi *et al.* [2004] did a finite element study on the vibration, buckling and dynamic stability behavior of a cracked cylindrical shell with fixed supports and subject to an in plane periodic tensile or compressive periodic edge load. They analyzed the effect of crack length and orientation of vibration parameters using an analytical method. Viola and Marzani [2004] investigated the dynamic stability of beams containing a single crack subjected to conservative and non-conservative forces by analytical method. They found cracked beams becoming unstable in the form of flutter type or divergence depending upon crack parameters. Wu and Shih [2005] analyzed the dynamic instability and non-linear response of the cracked plates subjected to periodic in-plane load theoretically. They applied Galerkin's method to the dynamic analog of the von Karman's plate equations to reduce the governing equation to a time dependent Mathieu equation. They studied plates of various aspect ratios and for different crack ratio.

Huang and Kuang [2006] investigated the effect of a near root local blade crack on the stability of a grouped blade disk following an analytical method. They modeled the blade crack using local flexibility with coupling terms. Kisa [2011] developed a novel technique for the vibration and stability analyses of axially loaded beams with multi-cracks. The model combined the finite element and component mode synthesis methods. Ranjbaran *et al*. [2013] studied dynamic stability of cracked columns by stiffness reduction method using analytical approach.

2.4.2 Dynamic stability of cracked stepped beams

Lee and Kuo [1991, 1992] derived the exact characteristic equations for the non-conservative elastic stability of non-uniform columns using analytical method. Takahasi [1999] presented vibration and stability of a non-uniform Timoshenko beam subjected to a tangential follower force distributed over the center line by use of the transfer matrix approach. Sabuncu and Evran [2006] presented a finite element model to study the static and dynamic stability of pre-twisted Timoshenko beam having asymmetric aero foil cross-section subjected to an axial periodic force.

2.5 Crack Detection in Beams

Structural components are often subjected to damage which can potentially reduce their safety. In recent years, significant efforts have been devoted to develop non-destructive techniques for damage identification in structures. The importance of early detection of cracks appears to be crucial for both safety and economic reasons because fatigue cracks are potential source of catastrophic structural failure. An early crack warning can considerably extend the durability of the expensive machines and important structures, increasing their reliability at the same time. The analysis of the variations in the vibration response signal can identify the element with the damage and quantify its extent. Currently research is going on to develop vibration based new techniques for wide range of applications to structural members like beams, blades and shafts etc.

2.5.1 Detection of crack in uniform beams

Recently, a comprehensive review on modal parameter based damage identification methods for beam and plate type structures is presented by Fan and Qiao [2011] through 2011. Adams *et al.* [1978] found that damage in specimens fabricated from fiber reinforced plastics could be detected by a reduction in stiffness, natural frequency and an increase in damping. Haisty and Springer [1988] developed a beam finite element for use in damage assessment for complex structures which contains a symmetric double-sided open transverse cracks. Qian *et al.*, [1990], discussed about a finite element model to detect an edge crack in a cantilever beam from its dynamic behavior. They also validated their model by comparing the results with experimental data. Shen and Taylor [1991], proposed an analytical method for crack identification procedure to determine the crack characteristics like location and its size from dynamic measurements. The same method was tested for simulated damage for a simply supported Bernoulli-Euler beam. Shekhar and Prabhu [1992] investigated vibration characteristics of cracked shafts and also detected the position of crack by FEM approach.

Bamnios and Trochides [1995] proposed an improved analytical method to estimate location and size of cracks in simple beams based on dynamic behaviors like change in natural frequencies and mechanical impedance. Ruotolo and Surace [1997] employed finite element procedure and genetic algorithm to present a non-destructive method of detecting crack and its size. Leonard *et al.* [2001] experimentally studied free vibration behavior of metallic beams subjected to crack obtained under controlled fatigue crack propagation. Viola *et al.* [2001] developed a special finite element for the FEM analysis of a cracked Timoshenko beam and

proposed a procedure for identifying cracks in structures using modal test data. Saavedra and Cuitino [2001] presented theoretical and experimental dynamic behavior of different multi-beams systems containing transverse cracks and drew some useful conclusions for diagnosing cracked beam systems. Yang *et al.* [2001] developed an energy based numerical model to investigate the influence of open cracks on structural dynamic characteristics during vibration of a beam. Chinchalkar [2001] described a numerical method for determining the location of a crack in a beam of varying depth from the three lowest natural frequencies of the beam. Sinha *et al.* [2002] discussed simplified models for the location of cracks in Euler-Bernoulli beams by minimizing the difference between the measured and predicted natural frequency based on experimental and finite element analysis. Dilena and Morassi [2002] studied identification of crack location of a thin beam subjected to bending vibration by an analytical and experimental investigation.

Dado and Shpli [2003] studied the problem of linear crack quantification, crack depth estimation and crack localization in beam, truss and two dimensional frame structures using finite element method. Patil and Maiti [2003] presented an analytical method for detection of multiple open cracks in a slender Euler-Bernoulli beam based on frequency measurements. They found the method suitable for beams with two simultaneous cracks of depth 10% or more of section depth. Khiem and Lien [2004] formulated a model for detection of multiple cracks in a beam from natural frequencies in the form of a non-linear optimization problem. They also found crack position, depth and crack numbers using their formulation.

Lin [2004] solved direct and inverse problem of simply supported beams with an open crack by an analytical transfer matrix method. He used Timoshenko beam theory and compatibility requirements to obtain characteristic equation from which the crack parameters are obtained. Kishen and Kumar [2004] studied fracture behavior of cracked beam-columns with different eccentricities of load. They determined failure load of cracked columns for different crack depth and slenderness ratio. Dilena and Morassi [2004] presented identification of a single open crack in a vibrating beam, either under axial or bending vibration based on damage induced shifts in natural frequencies and antiresonant frequencies. Loutridis *et al*. [2004] presented a finite element method for crack identification in double-cracked beams based on wavelet analysis. They validated their result both analytically and experimentally for a doubly cracked cantilever beam for cracks of varying depth at different positions.

Hadjileontiadis *et al.* [2005] developed a new technique for crack detection in beam structures based on kurtosis. The location and depth of the crack was predicted by abrupt change in spatial

variation of the response and estimation by kurtosis respectively. Nahvi and Jabbari [2005] described an analytical as well as experimental approach for crack detection in cantilever beams by vibration analysis. Skrinar and Plibersek [2007] described a new finite element method to solve the inverse problem of the beam to find crack presence, location and the depth from the dynamic responses of the transversely cracked slender beam.

Orhan [2007] performed free and forced vibration analysis of a cracked beam to identify the crack in a cantilever beam analytically. Lee [2009] presented a simple method to identify multiple cracks in a beam. Cracks were modeled as rotational springs and FEM was used to solve the direct problem. The inverse problem was solved iteratively for the locations and sizes of the cracks. Xiaoqing *et al.* [2010] presented a method to detect multiple cracks in a beam based on bending vibration of Euler-Bernoulli beam and cracks treated as mass less rotational springs. Bilgehan [2011] presented an adaptive neuro fuzzy inference system (ANFIS) and artificial neural network (ANN) model and successfully applied for the analysis of slender prismatic columns with a single non-propagating open edge crack subjected to axial loads.

2.5.2 Detection of crack in stepped beams

Tsai and Wang [1996] proposed an analytical method to determine the position and size of a transverse open crack on a stationary shaft. They analyzed the dynamic characteristics of a stepped shaft and a multi disc shaft using the transfer matrix method on the basis of Timoshenko beam theory which they verified with some already existing published experimental data. Nandwana and Maiti [1997] suggested a semi graphical method based on measurement of natural frequencies for detection of the location and size of a crack in a stepped cantilever beam. Zhang *et al.* [2009] illustrated an analytical method combining wavelet analysis with transform matrix to identify the location and depth of cracks in a stepped cantilever beam. Attar [2012] explained an analytical approach to investigate natural frequencies and mode shapes of a stepped beam with an arbitrary number of transverse cracks and general form of boundary conditions. Maghsoodi *et al.* [2013] presented a simple analytical method for detecting, localizing, and quantifying multiple cracks in Euler-Bernoulli multi-stepped beams, using the measurement of natural frequencies and estimating the un-cracked mode shapes.

2.6 Critical Discussion

A good amount of literature is available on vibration of beam with transverse cracks using various analytical methods [Papadopoulos and Dimarogonas, 1987, Ostachowicz and Krawczuk, 1991, Shifrin and Ruotolo, 1999, Carneiro and Inman, 2002, Binici, 2005, Yang *et al.*, 2008, Caddemi and Calio, 2012] and numerical methods [Gounaris and Dimarogonas, 1988, Ostachowicz, 1993, Corn *et al.*, 1997, Dado and Abuzeid, 2003, Kisa and Gurel, 2006, Mazanoglu *et al.*, 2010, Agarwalla and Parhi, 2013]. On the whole, the focus of the research is changing from vibration [Papadopoulos and Dimarogonas, 1987, Ostachowicz and Krawczuk, 1990, Ruotolo *et al.*, 1996, Zheng and Fan, 2001, Behera *et al.*, 2006, Kukla, 2009, Attar, 2012] to static stability (buckling) [Liebowitz, 1967, Dimarogonas, 1996, Liu and Wang, 2000, Zheng and Fan, 2003, Skrinar, 2007, Karaagac *et al.*, 2009] and then to the dynamic stability [Kim and Kim, 2000, Javidruzi *et al.*, 2004, Huang and Kuang, 2006, Kisa, 2011] of cracked beams. Recently more studies are conducted on crack detection [Qian *et al.*, 1990, Bamnios and Trochides, 1995, Leonard *et al.*, 2001, Dado and Shpli, 2003, Hadjileontiadis *et al.*, 2005, Orhan, 2007, Lee, 2009, Bilgehan, 2011, Maghsoodi *et al.*, 2013] techniques which have tremendous application to industry. As regards to methodology, the focus is shifted from initial experiments [Liebowitz *et al.* 1967, Qian *et al.* 1991, Brandon and Sudraud, 1998, Dilena and Morassi, 2002, Loutridis *et al*., 2004, Dowell, 2008] to analytical methods. With the advent of high speed computers more studies are carried out using numerical methods like finite element [Qian *et al*, 1991, Shen and Pierre, 1994, Ruotolo, *et al*., 1996, Dado and Abuzeid, 2003, Kisa and Gurel, 2006]. There are number of approaches to the modeling of cracks in beam structures that fall into three main categories, local stiffness reduction [Liebowitz and co-workers, 1967, 1968 and 1969, Adams *et al.*, 1978, Chinchalkar, 2001, Zheng and Kessissoglou, 2004, Viola *et al.*, 2007, Caddemi and Calio, 2009] discrete spring models [Yokoyama and Chen, 1998, Khiem and Lien, 2001, Li, 2002, Viola *et al.*, 2007, Aydin, 2008, Lee, 2009, Xiaoqing *et al.*, 2010] and complex methods in two or three dimensions [Al-Said *et al.*, 2006].

2.7 Objective and Scope of the Present Investigation

As per review of previous literature, a good number of studies are available on vibration of cracked uniform and non-uniform beams by various methods. However buckling (static stability) and dynamic stability studies on stepped beam with transverse cracks are scarce in

literature. Similarly the free vibration study on stepped beams is far from complete. The present research is mainly focused on vibration, static and dynamic stability behavior of stepped Timoshenko beams with multiple cracks. Besides this, the crack detection techniques using Artificial Neural Network (ANN) is studied here for completeness. The influence of various parameters including the position and location of cracks, the boundary conditions and the slenderness ratio of beams on the instability behavior of beam is discussed. The various problems identified for the present investigation are presented below.

- Vibration of cracked uniform and stepped beams
- Buckling of cracked uniform and stepped beams
- Parametric instability behavior of cracked uniform and stepped beams
- Crack detection using ANN

2.8 Summary

As per literature review, the study of parametric resonance characteristics of beams with multiple transverse open cracks is scarce in literature and far from complte. Besides this, the study of buckling and dynamic stability of is not available in literature. Based on these lacunae of existing literature, the scope of the present study is described in detail.

Chapter 3

MATHEMATICAL FORMULATION

3.1 Introduction

Structures are weakened by cracks. When the crack size increases in course of time, the structure becomes weaker than its original configuration. Finally, the structure may collapse under service loads. Hence knowledge of dynamic behavior of cracked members are very important for a safe and reliable structure.

3.2 The Basic Problem

This chapter presents the mathematical formulation for vibration, static and dynamic stability analysis of the cracked beams for uniform and non-uniform sections. The basic configuration of the problem considered here is a stepped cantilever beam with multiple transverse cracks subjected to harmonic in plane load as shown in Fig. 3.1. The choice of a stepped cantilever beam of uniform width as a basic configuration has been made so that depending upon the depth of the beam segments the uniform beam can be considered as special case. As regards to analysis, different load conditions such as free vibration (vibration without load), behavior under static load (buckling) and parametric resonance characteristics of cracked beams are studied. The boundary conditions are incorporated in the most general manner to cater to the need of the different beams.

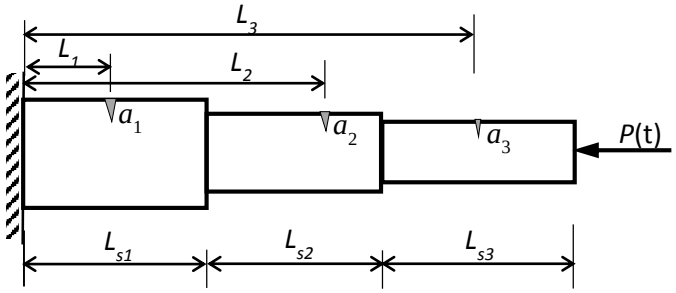

Figure 3.1 Schematic diagram of a cantilever stepped beam with multiple cracks subjected to harmonic in-plane load

3.3 Proposed Analysis

The governing equation for the dynamic stability of cracked stepped Timoshenko beam subjected to in-plane harmonic loading is developed. The equation of motion represents a system of second order differential equation with periodic coefficients of the Mathieu Hill type. The development of regions of instability arises from Floquet's theory and the solution is obtained using Bolotin's approach using finite element method (FEM). The element stiffness matrices, element mass matrices and element geometric stiffness matrices in the equation of motion are found as per standard procedure in case of intact beam elements and following an inverse approach for cracked beam element using fracture mechanics principle. The presence of crack on a beam induces additional flexibility at the crack location. Total flexibility matrix of the cracked beam element is computed by adding flexibility matrix of intact element with additional overall flexibility matrix due to presence of crack. Total flexibility matrix is inverted to obtain the element stiffness matrix of the cracked element. The assumptions made in this analysis are summarized as follows.

3.3.1 Assumptions of the analysis

The assumptions made in the analysis are:

i) Damping effects are neglected.

ii) The analysis is linear. This implies both linear constitutive relations (generalized Hooke's law for the material and linear kinematics) and small displacements to accommodate small deformation theory.

iii) The loading on the beam is considered as axial with a simple harmonic fluctuation with respect to time.

3.4 Governing Equations

Considering a cracked Timoshenko beam of area of cross section *A*, moment of inertia *I*, mass density ρ, the coupled equations for free vibrations of beam are given by Timoshenko (1937).

$$\begin{aligned} \rho A \frac{\partial^2 q_1(x,t)}{\partial t^2} &= \kappa CA\left(\frac{\partial^2 q_1(x,t)}{\partial x^2} - \frac{\partial q_2(x,t)}{\partial x} \right) \\ \rho I \frac{\partial^2 q_2(x,t)}{\partial t^2} &= \kappa CA\left(\frac{\partial q_1(x,t)}{\partial x} - q_2(x,t) \right) + EI \frac{\partial^2 q_2(x,t)}{\partial x^2} \end{aligned} \tag{1}$$

Where, $q_1$and q_2 represent the transverse deflection and rotation of the beam respectively. *E* and *C* are the Young's modulus and Shear modulus respectively and κ is the shear correction

factor. The general governing equation is derived by substituting the beam's kinematic and potential energies in Lagrange's equation:

$$\frac{d}{dt}\left(\frac{\partial T}{\partial \dot{q}}\right)-\frac{\partial T}{\partial q}+\frac{\partial U}{\partial q}=0 \tag{2}$$

The Kinetic energy:

$$T=\frac{1}{2}\int_0^L \rho A\left(\frac{\partial q_1(x,t)}{\partial t}\right)^2 dx+\frac{1}{2}\int_0^L J\left(\frac{\partial q_2(x,t)}{\partial t}\right)^2 dx \tag{3}$$

The potential energy 'U' of the beam due to elastic bending with shear deformation and axial in plane force is given by,

$$U=U_1+U_2$$

Where, U_1 = Strain energy associated due to bending with transverse shear

U_2 = Work done by the initial in-plane stresses and the nonlinear strain

The expression of strain energy 'U' becomes

$$U=\frac{1}{2}\int_0^L EI\left(\frac{\partial q_2(x,t)}{\partial x}\right)^2 dx+\frac{1}{2}\int_0^L \kappa CA\left(\frac{\partial q_1(x,t)}{\partial x}-q_2\right)^2 dx+\frac{1}{2}\int_0^L P(t)\left(\frac{\partial q_1(x,t)}{\partial x}\right)^2 dx \tag{4}$$

The additional strain energy due to the existence of crack is considered according to Zheng and Kessissoglou (2004) and the bending stiffness is modified later.

The energies for the beam with cracks can be written in matrix form as

$$U_1=\frac{1}{2}\{q\}^T[K_e]\{q\} \tag{5}$$

$$U_2=\frac{1}{2}\{q\}^T[K_g]\{q\} \tag{6}$$

$$T=\frac{1}{2}\{\dot{q}\}^T[M]\{\dot{q}\} \tag{7}$$

Where, $[K_e]$ = Bending stiffness matrix with shear deformation of the beam

$[K_g]$ = Geometric stiffness or stress stiffness matrix of the beam

$[M]$ = Consistent mass matrix of the beam

Substituting in the Lagrange's equation and on simplification the equation of motion for vibration of cracked beam subjected to in plane load $P(t)$ reduces to matrix form as:

$$[M]\{\ddot{q}\}+[[K_e]-P(t)[K_g]]\{q\}=0 \tag{8}$$

'q' is the vector of degrees of freedoms. The in-plane load $P(t)$ may be harmonic and can be expressed in terms of static component of load P_s and dynamic component of load P_t, where P_s is the static portion of load $P(t)$, P_t the amplitude of the dynamic portion of $P(t)$. Considering the static and dynamic component of load as a function of the critical load P_{cr},

$$P_s=\alpha P_{cr}\ ,\ \ P_t=\beta P_{cr} \tag{9}$$

Where, α and β are the static and dynamic load factors respectively.

$$\text{Therefore } P(t)=P_s+P_t\cos\Omega t \tag{10}$$

Where, Ω = frequency of the excitation

The stress distribution in the beam may be periodic. Substituting Eq.(9) and (10), in Eq. 8, the equation of motion for a beam with cracks under periodic loads may be reduced to:

$$[M]\{\ddot{q}\}+[[K_e]-\alpha P_{cr}[K_g]-\beta P_{cr}[K_g]\cos\Omega t]\{q\}=0 \tag{11}$$

The equation (11) represents a system of differential equations with periodic coefficients of the Mathieu-Hill type. The development of regions of instability arises from Floquet's theory which establishes the existence of periodic solutions of periods T and $2T$. The boundaries of the primary instability regions with period $2T$, where, $T = 2\pi/\Omega$ are of practical importance and the solution can be achieved in the form of the trigonometric series as suggested by Bolotin (1964)

$$q(t)=\sum_{k=1,3,5,..}^{\infty}[\{a_k\}\sin(k\Omega t/2)+\{b_k\}\cos(k\Omega t/2)] \tag{12}$$

Substituting the value of 'q', Eq.(11) reduces to

$$\begin{aligned}&[M]\sum_{k=1,3,5}^{\infty}-\left(\frac{k\Omega}{2}\right)^2\left(\{a\}_k\sin(k\Omega t/2)+\{b\}_k\cos(k\Omega t/2)\right)\\&+\left[[K_e]-\alpha P_{cr}[K_g]-\beta P_{cr}[K_g]\cos\Omega t\right]\left(\sum_{k=1,3,5...}^{\infty}\left[\{a\}_k\sin(k\Omega t/2)+\{b\}_k\cos(k\Omega t/2)\right]\right)=0\end{aligned}\tag{13}$$

Equating the coefficients of sine and cosine terms leads to a series of algebraic equations for the vectors $\{a\}_k$ and $\{b\}_k$ for determination of instability regions. For nontrivial solutions, the infinite determinants of the coefficients of the groups of homogenous equations are set equal to zero. Approximate solutions are obtained by truncating the determinants. Principal instability region, which is of practical interest corresponds to k = 1 and for this, the instability condition leads to in line with Bolotin (1964) as

$$[[K_e]-\alpha P_{cr}[K_g]\pm\frac{1}{2}\beta P_{cr}[K_g]-\frac{\Omega^2}{4}[M]]\{q\}=0\tag{14}$$

Equation (14) represents an eigenvalue problem for known values of α, β and P_{cr}. The two conditions under the plus and minus sign correspond to two boundaries of the dynamic instability region. The eigenvalues are Ω, which give the boundary frequencies of the instability regions for given values of α and β. In this analysis, the computed static buckling load of the beam with cracks is considered as the reference load.

This equation represents the solution to the following related problems.

(1) Free vibration with $\alpha=0, \beta=0$ and $\frac{\Omega}{2}=\omega$

$$[[K_e]-\omega^2[M]]\{q\}=0\tag{15}$$

(2) Static stability with α =1 , β = 0, Ω = 0 :

$$[[K_e]-P_{cr}[K_g]]\{q\}=0\tag{16}$$

3.5 Finite Element Analysis

In the present analysis the stepped beam is discretized into finite elements as shown in figure 3.2. Each element is considered to be having two degrees of freedoms (transverse deflection

and slope) per node. The elastic stiffness matrix, mass matrix and geometric stiffness matrix of the elements are found separately for intact elements and cracked elements.

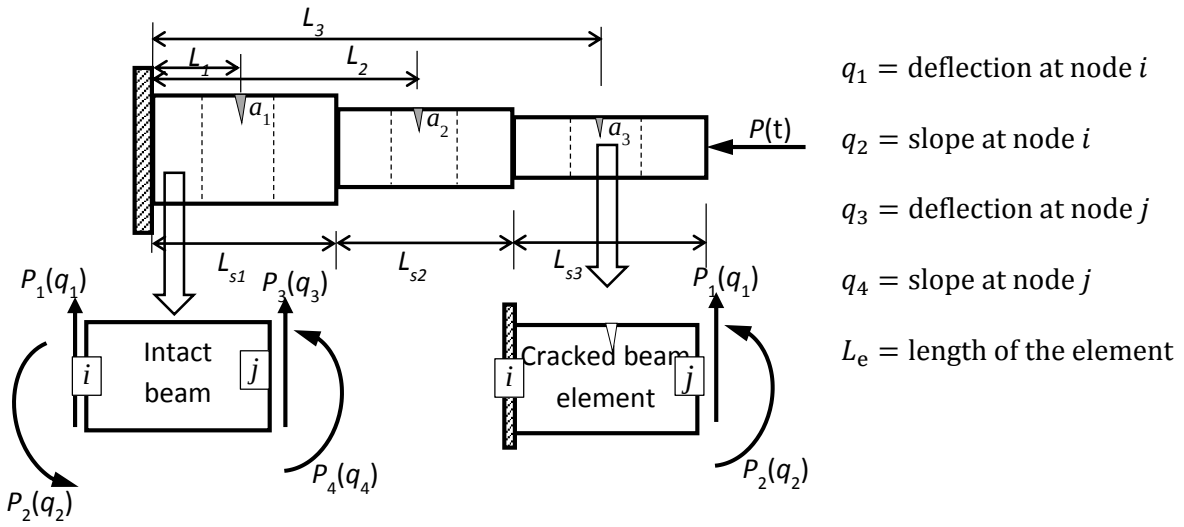

Figure 3.2 Stepped beam discretized into elements and free body diagrams of intact and cracked beam element with 2 degrees of freedom per node

3.5.1 Intact beam element

Element stiffness matrix

The stiffness matrix for 2 degree of freedom *(v,θ)* for bending in the *xy*-plane for a two-noded Timoshenko beam finite element with shear deformation in line with Gounaris and Papazoglou (1992) is given by,

$$[k_e] = \frac{EI}{L_e\left(L_e^2 + 12\mu\right)} \begin{bmatrix} 12 & 6L_e & -12 & 6L_e \\ 6L_e & 4L_e^2 + 12\mu & -6L_e & 2L_e^2 - 12\mu \\ -12 & -6L_e & 12 & -6L_e \\ 6L_e & 2L_e^2 - 12\mu & -6L_e & 4L_e^2 + 12\mu \end{bmatrix} \tag{17}$$

Where, $[k_e]$ = Elemental bending stiffness matrix

L_e = Length of the element

E = Young's modulus of elasticity

I = Moment of inertia of the section with respect to *z*-axis, and

$\mu = \frac{EI}{\kappa CA}$,

Where κ = Shear correction factor

C = Shear modulus

A = Area of cross-section of the element

Element mass matrix

Element mass matrix for a two noded Timoshenko beam element of 2 degree of freedom per node in line with Cook (2003) is given by,

$$[m_e] = \frac{\rho A L_e}{420}\begin{bmatrix} 156 & 22L_e & 54 & -13L_e \\ 22L_e & 4L_e^2 & 13L_e & -3L_e^2 \\ 54 & 13L_e & 156 & -22L_e \\ -13L_e & -3L_e^2 & -22L_e & 4L_e^2 \end{bmatrix} \tag{18}$$

Where, $[m_e]$ = Elemental mass matrix

ρ = Mass density of the beam material

L_e = Length of the element

A = Cross-sectional area of the beam element

Element geometric stiffness matrix

Element geometric stiffness matrix for a two noded Timoshenko beam element of 2 degree of freedom per node in line with Cook (2003) is given by,

$$[k_g] = \frac{1}{30L_e}\begin{bmatrix} 36 & 3L_e & -36 & 3L_e \\ 3L_e & 4L_e^2 & -3L_e & L_e^2 \\ -36 & -3L_e & 36 & -3L_e \\ 3L_e & -L_e^2 & -3L_e & 3L_e^2 \end{bmatrix} \tag{19}$$

Where, $[k_g]$ = Elemental geometric stiffness matrix

A = Cross-sectional area of the element

L_e = Length of the element

ρ = Mass density of the beam material

3.5.2 Cracked beam element

The key problem in using FEM is how to appropriately obtain the stiffness matrix for the cracked beam element. The most convenient method is to obtain the total flexibility matrix first and then take inverse of it. The total flexibility matrix of the cracked beam element includes two parts. The first part is original flexibility matrix of the intact beam. The second part is the additional flexibility matrix due to the existence of the crack, which leads to energy release and additional deformation of the structure.

Elements of the overall additional flexibility matrix [C_{ovl}]

The fig. 3.2 shows a typical cracked beam element with a rectangular cross section. The left hand side end node ***i*** is assumed to be fixed, while the right hand side end node ***j*** is subjected to shearing force P_1 and bending moment P_2. The corresponding generalized displacements are denoted as q_1 and q_2.

Let, b = Breadth of the beam

h = Depth of the beam

a = crack depth

L_c = Distance between the right hand side end node j and the crack location

Le = Length of the beam element

A = Cross-sectional area of the beam

I = Moment of inertia

According to Dimarogonas *et al.* (1983) and Tada *et al.* (2000) the additional strain energy due to existence of crack can be expressed as

$$\Pi_C = \int_A G dA_C \tag{20}$$

Where, G = the strain energy release rate and

A_C = the effective cracked area.

$$G = \frac{1}{E'}\left[\left(\sum_{n=1}^{2} K_{In}\right)^2 + \left(\sum_{n=1}^{2} K_{IIn}\right)^2 + k\left(\sum_{n=1}^{2} K_{IIIn}\right)^2\right] \tag{21}$$

Where, $E' = E$ for plane stress

$= E/1\text{-}\upsilon^2$ for plane strain

and, $k = 1 + \upsilon$

K_I, K_{II} *and* K_{III} = stress intensity factors for opening, sliding and tearing type cracks respectively

Neglecting effect of axial force and for open cracks, Eq.21 can be written as

$$G = \frac{I}{E'}\left[\left(K_{I1} + K_{I2}\right)^2 + K_{II1}^2\right] \tag{22}$$

The expressions for stress intensity factors from earlier studies are given by,

$$K_{I1} = \frac{6P_1 L_c}{bh^2}\sqrt{\pi\xi}\,F_1\left(\frac{\xi}{h}\right)$$
$$K_{I2} = \frac{6P_2}{bh^2}\sqrt{\pi\xi}\,F_1\left(\frac{\xi}{h}\right) \quad (23)$$
$$K_{II1} = \frac{P_2}{bh}\sqrt{\pi\xi}\,F_{II}\left(\frac{\xi}{h}\right)$$

Where,

$$F_I(s) = \sqrt{\frac{\tan\left(\pi s/2\right)}{\left(\pi s/2\right)}}\left[\frac{0.923 + 0.199\left(1-\sin\left(\pi s/2\right)\right)^4}{\cos\left(\pi s/2\right)}\right] \quad (24)$$

$$F_{II}(s) = \frac{1.122 - 0.561s + 0.085s^2 + 0.180s^3}{\sqrt{1-s}} \quad (25)$$

Here, $s = \frac{\xi}{h}$ is the crack depth during the process of penetration of the crack 0 to h

$F_I(s)$ and $F_{II}(s)$ are the correction factors for stress intensity factors

From definition, the elements of the overall additional flexibility matrix C_{ij} can be expressed as

$$C_{ij} = \frac{\partial \delta_i}{\partial P_j} = \frac{\partial^2 \prod_c}{\partial P_i \partial P_j} \quad (i,j = 1, 2,) \quad (26)$$

Substituting Eq. 21 in Eq. 20 and subsequently in Eq. 26 we get,

$$C_{ij} = \frac{b}{E'}\frac{\partial^2}{\partial P_i \partial P_j}\int\left[\begin{array}{l}\left\{\frac{6P_1 L_c}{bh^2}\sqrt{\pi\xi}\,F_1\left(\frac{\xi}{h}\right) + \frac{6P_2}{bh^2}\sqrt{\pi\xi}\,F_1\left(\frac{\xi}{h}\right)\right\}^2 + \\ \left\{\frac{P_1}{bh}\sqrt{\pi\xi}\,F_{II}\left(\frac{\xi}{h}\right)\right\}^2\end{array}\right]d\xi \quad (27)$$

Substituting i, j (1, 2) values, we get

$$C_{11} = \frac{2\pi}{E'b}\left[\frac{36L_c^2}{h^2}\int_0^{\frac{a}{h}} xF_1^2(x)dx + \int_0^{\frac{a}{h}} xF_{II}^2(x)dx\right] \quad (28)$$

$$C_{12} = \frac{72\pi L_c}{E'bh^2}\int_0^{\frac{a}{h}} xF_1^{\,2}(x)dx = C_{21} \tag{29}$$

$$C_{22} = \frac{72\pi}{E'bh^2}\int_0^{\frac{a}{h}} xF_1^{\,2}(x)dx \tag{30}$$

Now, the overall flexibility matrix C_{ovl} is given by,

$$[C_{ovl}] = \begin{bmatrix} C_{11} & C_{12} \\ C_{21} & C_{22} \end{bmatrix} \tag{31}$$

Flexibility matrix of the intact beam element [C_{intact}]

$$[C_{\text{int}act}] = \begin{bmatrix} \frac{L_e^3}{3EI} & \frac{L_e^2}{2EI} \\ \frac{L_e^2}{2EI} & \frac{L_e}{EI} \end{bmatrix} \tag{32}$$

Total flexibility matrix C_{tot} of the cracked beam element

$$[C_{total}] = [C_{intact}] + [C_{ovl}]$$

$$[C_{total}] = \begin{bmatrix} \frac{L_e^3}{3EI} + C_{11} & \frac{L_e^2}{2EI} + C_{12} \\ \frac{L_e^2}{2EI} + C_{21} & \frac{L_e}{EI} + C_{22} \end{bmatrix} \tag{33}$$

Stiffness matrix $[k_c]$ of a cracked beam element

From the equilibrium conditions, the stiffness matrix K_c of a cracked beam element can be obtained as

$$[k_c] = \{L\}\left[C_{tot}^{-1}\right]\{L\}^T \tag{34}$$

Where L is the transformation matrix for equilibrium condition

$$\{L\} = \begin{Bmatrix} -1 & 0 \\ -L_e & -1 \\ 1 & 0 \\ 0 & 1 \end{Bmatrix} \tag{35}$$

Boundary Conditions

The boundary conditions are

- Fixed end: $v = 0$, $\theta = 0$
- Simply supported end: $v = 0$

The element mass matrix and element geometric stiffness matrix of the cracked beam elements are calculated according to Eq. 18 and Eq. 19 respectively similar to that of intact beam elements.

3.6 Computational Procedure

A computer program is developed as per the flow chart in Fig. 3.3 in MATLAB R2012b environment to perform all the necessary computations. In the initialization phase, material properties (Young's modulus, Poisson's ratio and mass density) and geometric properties (dimensions of the beam) are specified. The crack location and depth are supplied as input data to the computer program. The beam is divided in to '*n'* number of elements and *n+1* number of nodes. The elements of the element mass matrices, elastic stiffness matrices and geometric stiffness matrices are formulated as shown in flow chart in Fig. 3.3. The program uses the built in MATLAB R2012b functions. Element matrices are assembled to obtain the global matrices. Boundary conditions are imposed by elimination method. For Timoshenko beam with Fixed-Free end conditions the first two rows and columns of the global matrices are eliminated to obtain the reduced matrices. Similarly matrices are modified for other boundary conditions. The natural frequencies and buckling loads are calculated solving the Eigen value problems in Eq. 15 and Eq. 16 respectively. The built in MATLAB R2012b function 'eig' is used to calculate the Eigen values and eigenvectors. The static load factor 'α' is set to the required value. The dynamic load factor 'β' is increased in steps from zero and for each set of values of α, β and P_{cr} the excitation frequencies at the stability boundaries are obtained by solving for the Eigen values of Eq. 14. The plot of excitation frequency, Ω_1 versus 'β' gives the lower boundary of the instability region, whereas plot of other excitation frequency, Ω_2 versus 'β' gives the upper boundary of the instability regions.

3.7 Numerical Simulation Using ANSYS

For the verification of the present work theoretical simulations was done using ANSYS 10 for completeness. Six noded triangular solid elements is considered for simplicity in meshing particularly for cracked specimens. The finite element meshing was done for the whole specimen with finer meshes near the cracked zones. Fig.3.4 shows the finite element discretization of specimens with crack location. Three degrees of freedom (translation along X, Y and Z axes) are available at each node. Computation is carried out for natural frequencies of free vibration and mode shapes. The difference in mode shapes (and also post processed modal curvatures) between cracked and corresponding intact model can only be appropriately obtained by carrying such careful meshing.

3.8 Summary

A general formulation involving vibration, buckling and dynamic stability of uniform and stepped beams with single and multiple cracks are presented. The displacement based boundary conditions is treated in a generalized manner to consider free-free, cantilever, simply supported and fixed-fixed conditions. A flow chart is developed a code in MATLAB environment is developed for vibration, buckling and parametric instability analysis of uniform and stepped beams subjected to transverse open cracks.

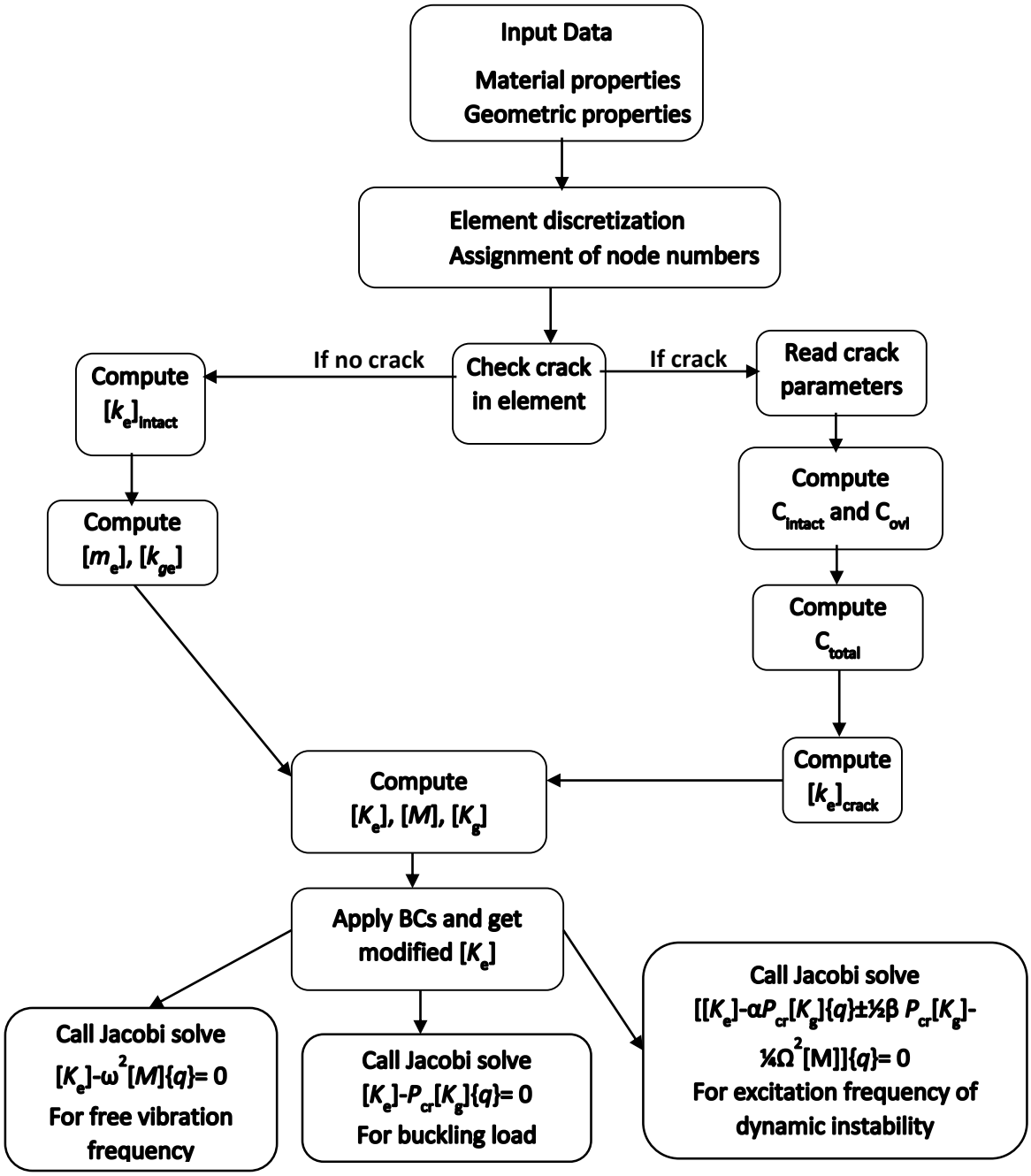

Figure 3.3 Flow Chart of the present Finite Element Formulation

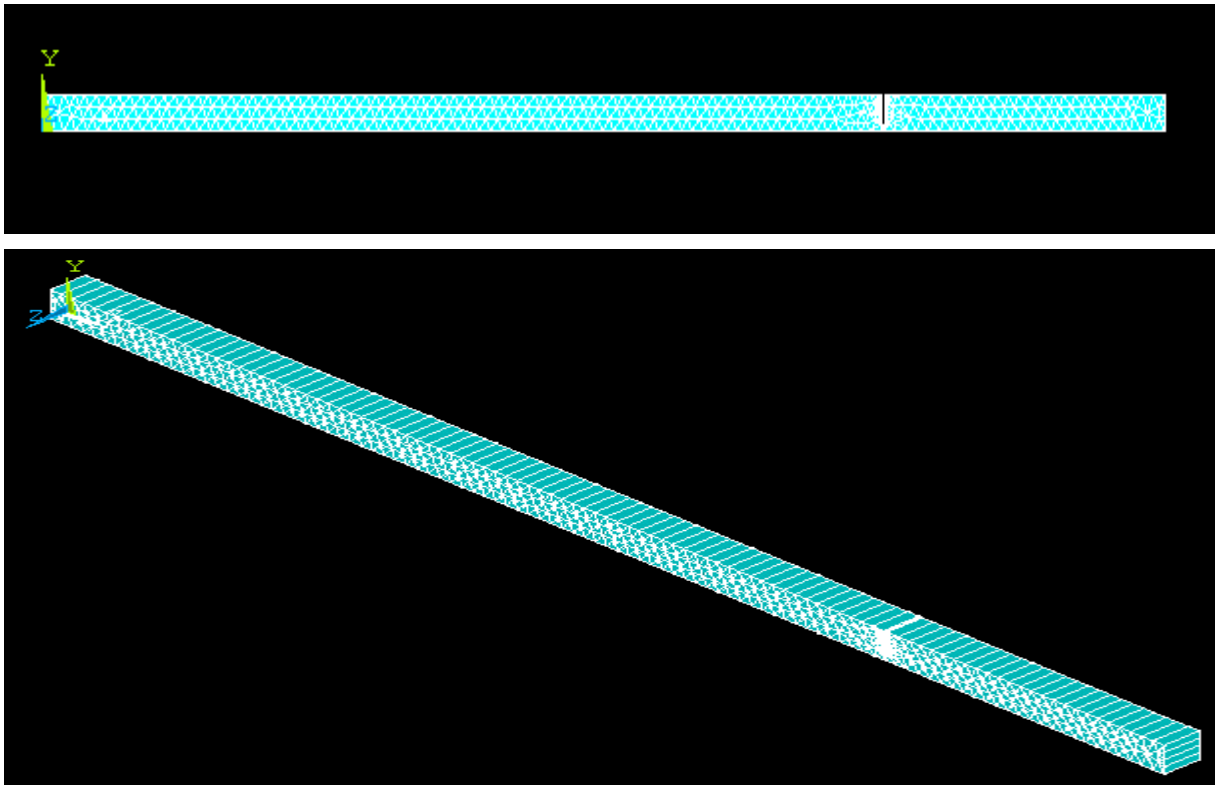

Figure 3.4 Modeling of a cracked beam with six-nodded triangular elements

Chapter 4

EXPERIMENTAL PROGRAMME

4.1 Introduction

Modal testing of beam with single as well as multiple transverse open cracks is carried out to validate the results based on FEM. The natural frequencies of the cracked beam along with modal shapes are interpreted to know the effects of different parameters.

4.2 Specimen Details

Aluminum and steel beam specimens of rectangular section, 300 mm × 10 mm × 10 mm were prepared. Artificial transverse single cracks/notches were introduced at 0.25*L*, 0.33*L* and at the center (i.e. 0.5*L*) separately by cutting across the width with the help of a cutting tool. Frequencies of vibration are measured for the beam with single crack introduced at position 0.25*L*, 0.33*L* and 0.5*L* separately. The depths of the cracks introduced at the said locations of the aluminum specimens were 2 mm, 4 mm and 6 mm and for steel specimens were 2mm, 5mm and 7mm. Three specimens for each location and depth were prepared. For multiple cracked aluminum and steel beams, cracks were introduced at 0.25*L* and 0.33*L* from each ends of same depth.

4.3 Equipment Required for Vibration Test

The equipment used in the vibration measuring test set up, made by Bruel & Kjaer, Denmark comprises of the following.

- Modal hammer
- Accelerometer
- FFT Analyzer
- Display unit

4.3.1 Modal hammer

The modal hammer excites the structure with a constant force over a frequency range of interest. Three interchangeable tips are provided with impact hammer for giving impact to different types specimens and its load measurement. For present experiment, modal hammer type B&K 2302-5 was used, which is shown in Fig. 4.1.

Figure 4.1 Modal Impact Hammer (B&K type 2302-5)

4.3.2 Accelerometer

Miniature Delta Tron accelerometers is specifically designed to withstand the robust environment of the industry. A combination of high sensitivity, low mass and small physical dimensions make the accelerometer ideal for modal measurements, such as on aircraft, automotive and satellites. It can be easily fitted to different test objects using a selection of mounting clips. For the present experiment accelerometer (B&K 4507) was used and was fixed on plates by using bee wax. The accelerometer for free vibration test is shown in Fig. 2.

Figure 4.2 Accelerometer (B&K 4507)

Figure 4.3 FFT Analyzer (B&K3560 B)

4.3.3 Portable FFT analyzer (Type 3560B)

Four channels Bruel & Kjaer pulse analyzer system of type 3560 B as shown in Fig.4.3, was used to measure the frequency for any structure. It can be used for both free vibration as well as forced vibration study. The system has four channels to connect the cables for analyzing both input and output signals.

4.3.4 Display unit

This is mainly in the form of PC (Laptop) as shown in Fig. 4.4. When the specimen was excited in a selected point by means of Impact hammer (B&K 2302-5), the signal of resulting vibrations of the specimens were received to the FFT Analyzer by an accelerometer (B&K 4507) mounted on the specimen by means of bees wax. The output from the analyzer was displayed on the display unit in the graphical form which includes graph of force amplitude spectrum, response amplitude spectrum, and coherence and frequency response functions. A typical auto spectrum window of a vibration test is shown in Fig. 4.5.

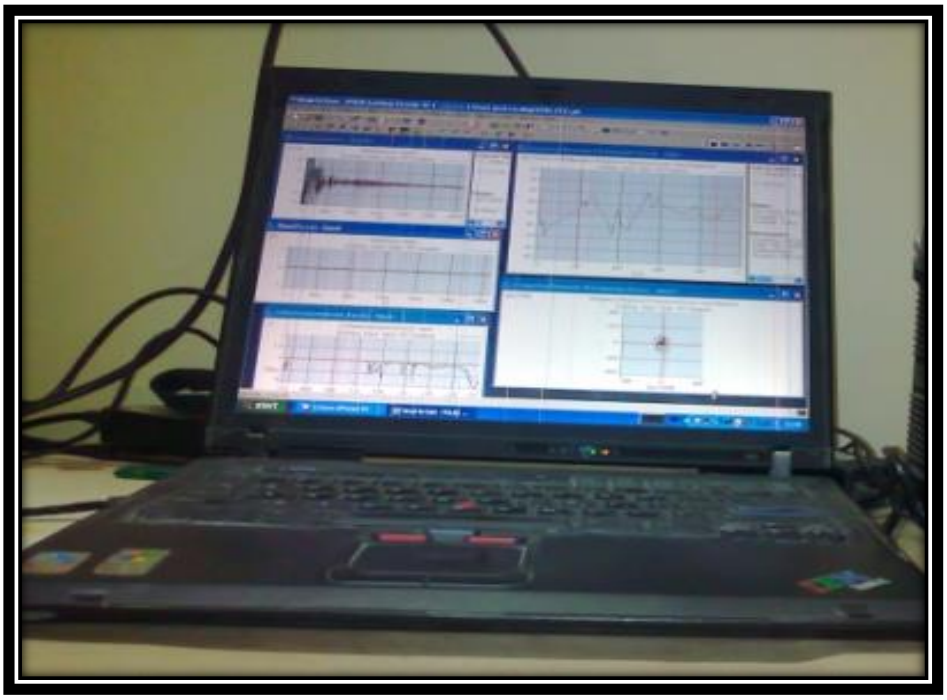

Figure 4.4 Display unit (Laptop)

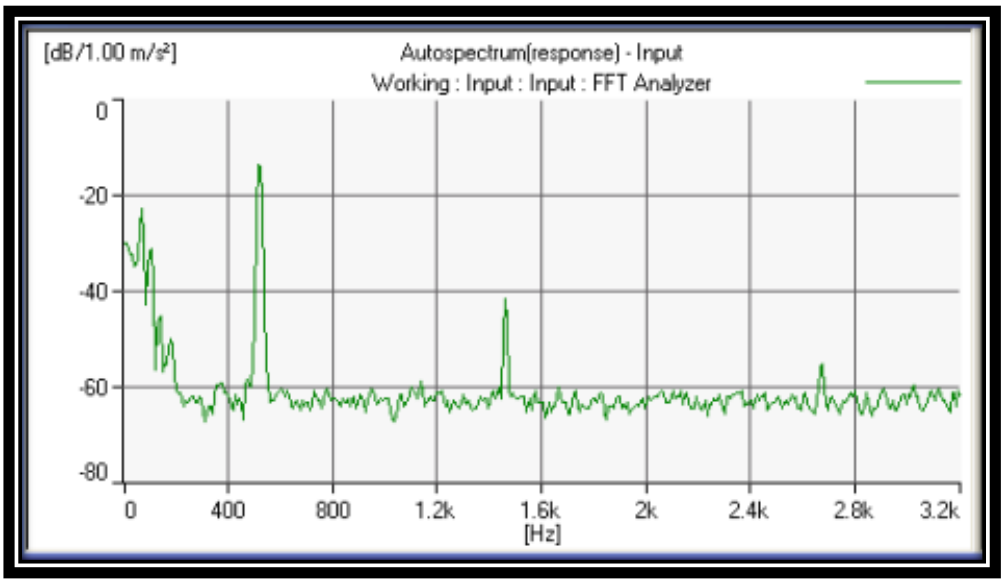

Figure 4.5 Typical Auto spectrum window of a vibration test

4.4 Setup and Test Procedure for Free Vibration Test

The support conditions are very important that leads to the mode of vibration. It was proposed to allow the specimen to vibrate in flexural mode of vibration. The frame was fabricated to provide free support to the specimens by hanging the beam with the help of two threads as shown in the Fig 4.6. The connections of FFT analyzer, laptop, transducers, modal hammer and cables to the system were made. The pulse lab shop version 10.0 software key was inserted to the port of laptop. The accelerometer was placed on the bottom of the beam at the central point of the specimen to get the bending response of the beam. The force was applied gently by using an impact hammer away from the accelerometer. The resulting vibrations of the specimens were measured by the accelerometer.

Both input and output signals are investigated by means of FFT Analyzer and resulting Frequency Response Functions (FRF) are transmitted to a computer for modal parameter extraction. The output from the analyzer was displayed on the analyzer screen by using pulse software. Various forms of FRFs are directly measured. The peaks give the FRF of average of five numbers of loading and the coherence checks the accuracy of the peaks obtained by FRF. When the coherence is straight and equals to one it indicates better FRF and if coherence is not straight the corresponding FRF is not accurate.

The vibration test setup is shown in Fig. 4.6. The test frame was fabricated for conducting vibration tests for beams under different boundary conditions (B.C) i.e. free-free and Fixed-Free.

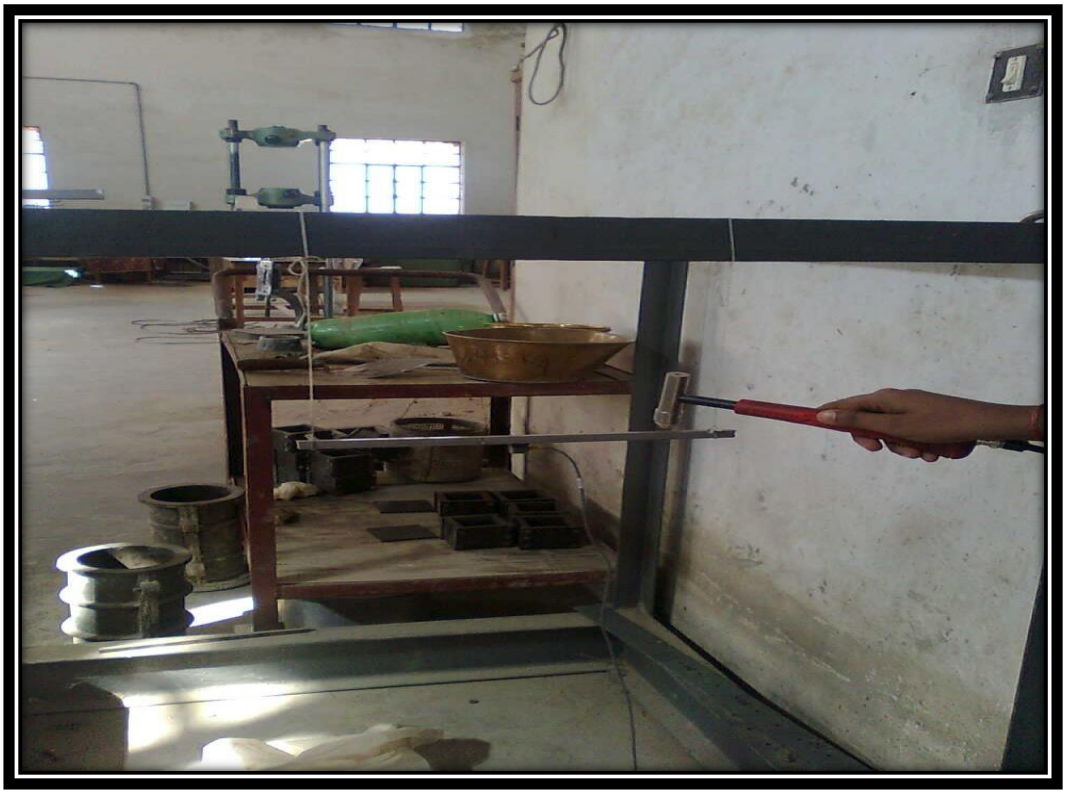

Figure 4.6 Vibration test setup, beam suspended by two strings like free-free beam, accelerometer and modal hammer in position

4.5 Summary

A test set up is fabricated for vibration measurement of steel and aluminum cracked beams of different boundary conditions with the state of the art vibration FFT analyzer and pulse software. Auto spectrum and FRF mode observations along with coherence are carried out to study the effects of different parameters.

Chapter 5

DAMAGE DETECTION BY ANN

5.1 Introduction

Neural Networks which are simplified models of biological neuron system, is a massively parallel distributed processing system made up of highly interconnected processing elements called neurons which have the ability to learn and thereby acquire knowledge and make it available for use. In the present study, artificial neural network (ANN) models are developed for crack detection in beam using data available in literature and experimental data generated as a part of this research. The methodology adopted for artificial neural network model and generation of experimental data is presented briefly as follows.

5.2 Biological Model of a Neuron

The neuron (cell) is the fundamental unit of the biological nervous system. It is the simple processing unit which receives and processes the signal (input) from other neurons through its input path called dendrites. An activity of a neuron is an all or non-process. If the combined signal is strong enough, it generates the output signal to its output path (called axon) which splits up and connects to other neuron's input paths through a junction referred to as synapses shown in fig. 5.1. The amount of signal transferred depends on the synaptic strength of the junction which is chemical in nature. This synaptic strength is found to be modified during the learning process of the brain; therefore it can be considered as a memory unit of each interconnection as discussed by Das (2005).

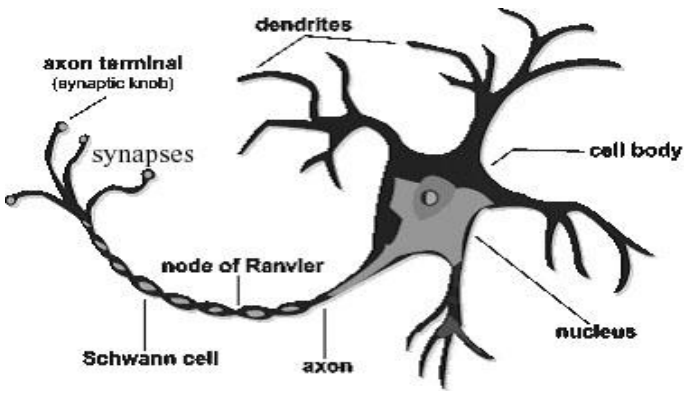

Figure 5.1 Simplified configuration of an organic neuron

5.3 Model of an Artificial Neuron

The simple model of an artificial neuron is shown in Fig. 5.2. In the figure O_1, O_2....O_n are the inputs to the artificial neuron. W_{1B}, W_{2B}, W_{nB} are the weights attached to the input links. The weights are multiplicative factors of the inputs to account for the strength of the synapse. Hence the total input I_B received by the soma of the artificial neuron is

$$\begin{aligned} I_B &= W_{1B}O_1 + W_{2B}O_2 + ... + W_{nB}O_n \\ &= \sum_{i=1}^{n} W_{iB}O_i \end{aligned} \tag{36}$$

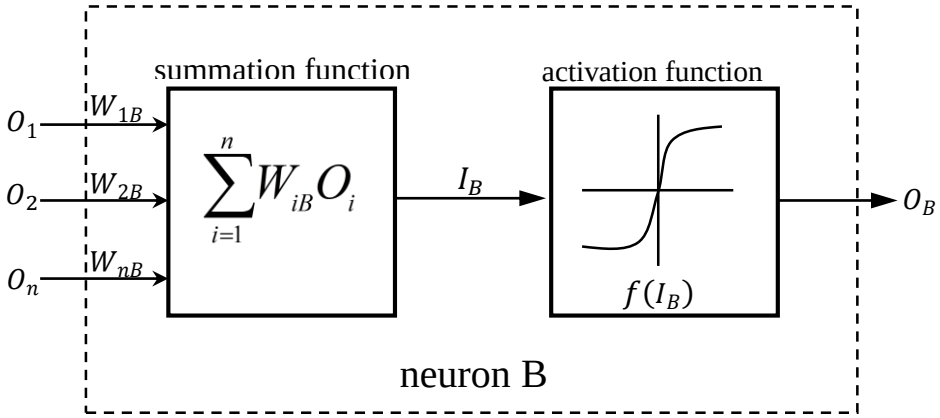

Figure 5.2 Artificial (Mathematical) model of a neuron

To generate the final output O_B, the sum is passed to a non-linear filter '*f*' called Activation function or Transfer function or Squash function which releases the output.

i.e. $O_B = f(I_B)$

5.4 Architecture of an Artificial Neural Network

The neurons are described as processing elements or nodes in mathematical model of the ANN. A typical architecture of artificial neural network showing neurons at different layers is shown in Fig. 5.3. A network with an input vector of elements $x_l \ (l = 1, 2 ....N_i)$ is transmitted through a connection that is multiplied by weight w_{jl} to give the hidden unit $x_j \ (j = 1, 2 ....N_h)$

$$z_j = \sum_{l=1}^{N_i} w_{jl}x_l + b_{j0} \tag{37}$$

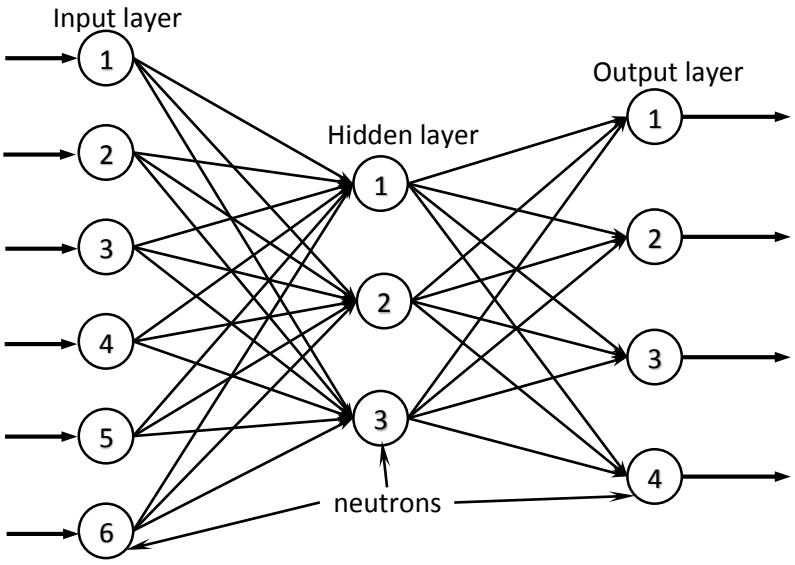

Figure 5.3 Typical architecture of a neural network

Where N_h is the number of hidden units and N_i is the number of input units. The hidden units consist of the weighted input and a bias b_{j0}. A bias is simply a weight with constant input of 1 that serves as a constant added to the weight. These inputs are passed through a layer of transfer function/activation function '*f*' which produces

$$r_j = f(z_j) = f\left(\sum_{l=1}^{N_i} w_{jl} x_l + b_{j0}\right) \tag{38}$$

The activation functions are designed to accommodate the nonlinearity in the input output relationships. Some common activation functions used in ANN are shown in Fig. 5.4.

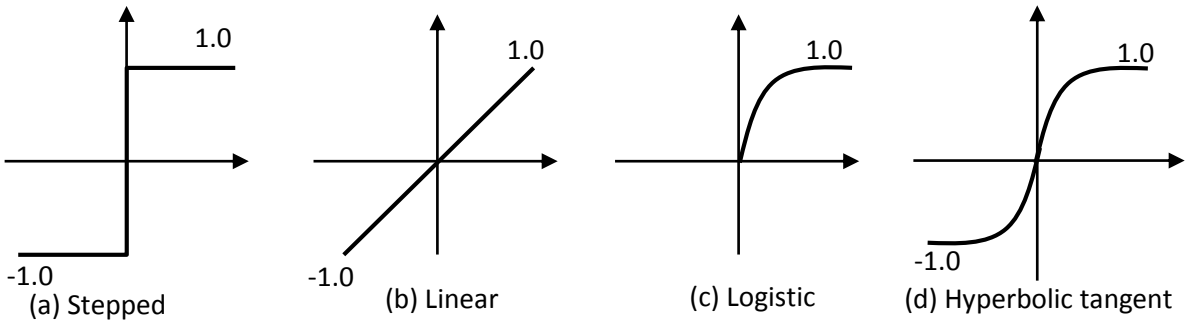

Figure 5.4 Different transfer functions (a) stepped (b) linear (c) logistic sigmoid and (d) hyperbolic tangent sigmoid

The most commonly used activation functions are sigmoid functions, i.e. logistic sigmoid function and hyperbolic tangent sigmoid function as given below. The sigmoid functions are continuous, differentiable and bounded.

$$f(z) = \frac{1}{1+e^{-z}} \tag{39}$$

$$f(z) = \frac{e^{z} - e^{-z}}{e^{z} + e^{-z}} \tag{40}$$

$$v_k = \sum_{j=1}^{N_h} w_{kj} r_j + b_{k0} = \sum_{j=1}^{N_h} w_{kj} f\left(\sum_{l=1}^{N_i} w_{jl} x_l + b_{j0} \right) + b_{k0} \tag{41}$$

The outputs from hidden units pass another layer of filters and are fed into another activation function F to produce output y ($k = 1, \ldots, N_0$)

$$y_k = F(v_k) = F\left[\sum_{j=1}^{N_h} w_{ki} f\left(\sum_{l=1}^{N_l} w_{jl} x_l + b_{j0} \right) + b_{k0} \right] \tag{42}$$

This way it continues depending upon the number of hidden layers and finally the output layer. This multilayer (hidden layer and output layer) with the nonlinear transfer function gives rise to a highly nonlinear function with a number of unknown parameters in terms of weights.

5.5 Learning / Training Process

The learning process in ANN is referred to the ability of the network to learn from their environment and improve the performances. The weights are adjustable parameters of the network and are determined from a set of data through the process of learning or training. The learning techniques may be divided into two main categories.

1) Supervised Learning

2) Unsupervised Learning

In Supervised Learning every input pattern used to train the network is associated with an output pattern, which is the target or desired output. A teacher is assumed to be present during the learning process, when a comparison is made between the networks computed output and the correct expected output to determine the error (Rajsekaran and Vijayalakshmi, 2008). The network parameters such as the weights and the thresholds are updated during the training procedure to minimize the sum of squares of the residuals between the measured and predicted

output. In unsupervised learning target output is not presented to the network. The weights are adjusted based on other criteria known as Kohonen learning rule.

So in case of supervised learning, the objective is to minimize the sum of squares of the residuals between the measured and predicted output given by

$$E(W,U)=\sum_{l=1}^{N_s}\sum_{k=l}^{N_0}\left[y_{lk}(x_l)-y_{lk}\right]^2 \tag{43}$$

Where,

N_s is the number of samples,

N_o is the number of outputs,

W and U are the weights of the hidden and output layer respectively, and

y (x) is the predicted output from inputs x.

The most commonly used neural network is feed forward back-propagation neural network which follows the supervised learning process. It is mainly suited for prediction type problem. Fig. 5.5 shows typical architecture of a back propagation algorithm. Here the computations are passed forward from input to output layer following which calculated errors are propagated back in other direction to change the weights to obtain better performance. In back propagation algorithm based learning; the weights of connection are randomly chosen. Based on the initial weight values, the algorithm tries to minimize the square root of the above mean square error expressed by Eq. 44.

In each subsequent training step, the initial set of weight vectors are adjusted towards the direction of maximum decrease of E which is scaled by a learning rate lambda (λ). Mathematically a weight is updated to its new value as below

$$w_{new}=w_{old}-\lambda\nabla E, \text{ Where, } \nabla E=\left(\frac{dE}{dw_1},\frac{dE}{dw_2},.....,\frac{dE}{dw_n}\right) \tag{44}$$

One useful property of sigmoid function is that

$$\frac{d\,f(x)}{dx}=f(x)(1-f(x)) \tag{45}$$

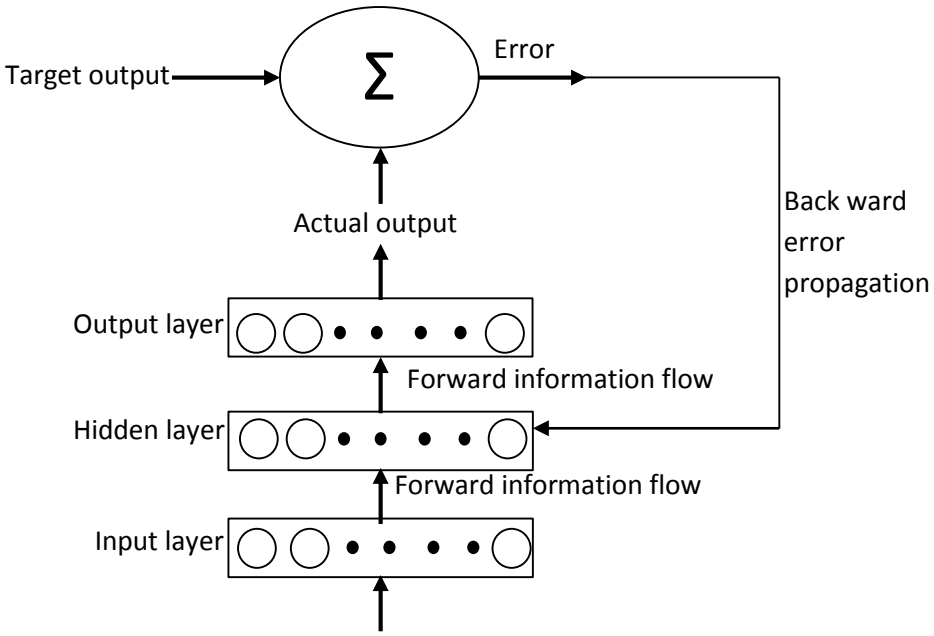

Figure 5.5 Typical back propagation neural network

This means that the derivative (gradient) of the sigmoid function can be calculated by applying a simple multiplication and subtraction operator itself. This property simplifies the computation of new weights from initial random values. Most supervised learning applications use back-propagation. However, when the number of layers and the number of variables and data point increases, the learning time tends to slow during neural network training and learning time increases with size of the problem. Again as it is a gradient based algorithm it may reach a local minimum in weight space. The above problems in back propagation have been taken care of by increasing the step size (learning rate) to increase the speed of the algorithm, and using a momentum factor to avoid the local minima.

5.6 Testing of Network

At the end of the training phase, the associated trained weights of the neurons are stored in the ANN memory. In the next phase, testing phase, the trained network is fed a new set of data. The ANN predictions (using the trained weight) are compared to the target output values to assess the ability of the network to produce (generalize) correct response for the testing patterns that only broadly resembles the data in the training phase. Once the training and testing phases are found to be successful, the corresponding NN can be put to use in practical application. [Das 2013].

5.7 Selection of Model Inputs

The ANNs belong to data driven approach i.e. the model type and the model parameters are developed based on input and output data and the model is suitable for that particular problem. The data driven approaches have the ability to determine which model inputs are critical. Thus, in ANNs little attention is given to the selection of proper input variables. However, presenting a large number of inputs to ANNs usually increases the network size and the amount of data required to estimate the connection weights efficiently and thereby causing a decrease in the processing speed. Hence, there is a need in using analytical technique to determine suitable inputs for the ANN models [Guyon and Elisseeff, 2003, Olden *et al*., 2004].

The choice of input variable is based on a prior knowledge of causal variables in conjunction with inspection of plots of potential inputs and outputs. If the relationship to be modeled is less understood, analytical techniques such as cross-correlation analysis or principal component analysis can be used. A stepwise approach can also be used in which separate networks are trained for each variable. The network performing best is then retained and the effect of adding each of the remaining input in turn is assessed. This is continued until the addition of extra variable does not result in a significant improvement in model performance. However, this approach is computationally intensive and has the disadvantages of being unable to capture the importance of certain combinations of variables that might be insignificant on their own [Guyon and Elisseeff, 2003].

5.8 Division of Data and Preprocessing

To study the generalization in applicability of the neural network models, it is common practice to divide the data into two sub-sets: a training set and an independent testing set. However, depending upon the number of data points a set of data may be used as validation set to avoid over-fitting .It is also essential that the training, testing and validation sets are representative of the same population (data set). The ANNs are generally not used to extrapolate i.e. is not used to find the correlations for data value, outside the range of values for which it was trained.

Once the data have been divided into training, testing and/or validation set it is important to preprocess the data to a suitable form before applying ANNs. The preprocessing helps in avoiding the dimensional dissimilarities of different input parameters. The variables have to be scaled in such a way as to be commensurate with the limits of the activation function used in

the output layer. For example, if the outputs of the logistic functions are between 0 and 1, the data are generally scaled in the range 0.1-0.9 [Maity and Saha, 2004] or 0.2-0. If hyperbolic tangent sigmoid function is used then the data need to be scaled in the range [-1, 1]. The scaling is not strictly required, if the transfer function in the output layer is unbounded (linear). However, scaling to uniform range is recommended for the efficient application of ANNs.

5.9 Generalization

The aim of the training is to minimize the error function to get the optimized weight vectors. However, when dealing with noisy data, reducing it beyond a certain point might lead to overtraining. The overtraining is referred to as the large error in the network when new data is presented to the trained network. The over fitting generally occurs when numbers of data points in training set are scanty, but the error in network is driven to a very small value. [Das 2013]

The network needs to be equally efficient for new data during testing or validation, which is called as generalization. The generalization is the most important aspect for successful implementation of ANN. There are different methods for generalization like early stopping or cross validation and Bayesian regularization. In case of early stopping criteria the error on the validation/testing set is monitored during the training process. The validation error will normally decrease during the initial phase of training, as does the training set error. However, when the network begins to over fit the data, the error on the validation set will typically begin to rise. When the validation error increases for a specified number of iterations, the training is stopped, and the weights and biases at the minimum of the validation error are returned. In cross validation an independent test set is used to assess the performance of the model at various stages of learning. The available data needs to be divided into three subsets; a training set, a testing set and a validation set, which is very data intensive. Early stopping is not suitable when the size of data set is small and also the response obtained in early stopping is not extremely smooth as compared to Bayesian regularization. Because Bayesian regularization does not require a validation data set which to be separated out of the training data set. It uses all of the data.

5.10 Artificial Neural Network Model

In the present study, the results of ANN model trained with Differential Evolution Neural Network (DENN) and Bayesian Regularization Method Neural Network (BRNN) are compared

with the commonly used Levenberg-Marquardt trained Neural Networks (LMNN) to discuss the prediction efficiency of the networks. The above neural network models have been developed using MATLAB R12b tool boxes. A brief description about the LMNN, BRNN and DENN is presented here for completeness.

5.10.1 Levenberg-Marquardt Neural Network (LMNN)

It provides a numerical solution to the problem of minimizing a function. The Levenberg-Marquardt algorithm (LMA) interpolates between the Gauss-Newton algorithms (GNA) and method of Gradient descent. In LMA method, the change in weights (∇w_j) is obtained by solving the following equation.

$$\sum_{j=1}^{n} \alpha_{ij} \nabla w_j = -\frac{1}{2} \frac{dE}{dw_i} \tag{46}$$

Where,

n = Number of adoptive weights of the network, and

E = Mean squared error

Elements of the α matrix are given by

$$\alpha_{ij} = \left(1 + \lambda \nabla w_{ij}\right) \sum_{k=1}^{N} \frac{dy(x_k)}{dw_i} \cdot \frac{dy(x_k)}{dw_j} \tag{47}$$

Where,

N = Number of examples and

$y(x_k)$ = Network output corresponding to the example x_k

λ = A variable which is an adjustable parameter.

If λ is very small, the α matrix becomes the Hessian and same as Newton's method if λ greater than or equal to 1, the method is analogues to Steepest Descent [Deb, 2005].

5.10.2 Bayesian Regularization Neural Network (BRNN)

The most commonly used error function is the mean squared error (MSE) function. In back propagation neural network (BPNN), over-fitting is due to unbounded values of weights (parameters) during minimization of the error function, mean square error (MSE)**.** The training function used BPNN updates the weight and bias values according to Levenberg-Marquardt

optimization. It minimizes a combination of squared errors and weights by modifying the performance function, and then determines the correct combination so as to produce a network that generalizes well. The process is called Bayesian regularization.

$$MSEREG = \gamma MSE + (1-\gamma)MSW \tag{48}$$

Where,

MSE = Mean square error of the network, and

γ = Performance ratio and

$$MSW = \frac{1}{n}\sum_{j=1}^{n} w_j^{\,2} \tag{49}$$

This performance function will cause the network to have smaller weights and biases there by forcing networks less likely to be over fit. The above combination works best when the inputs and targets area scaled in the range [-1, 1] [Demuth and Beale 2000].

5.10.3 Differential Evolution Neural Network (DENN)

The DE optimization is a population-based heuristic global optimization method. Unlike other evolutionary optimization, in DE the vectors in current populations are randomly sampled and combined to create vectors for next generation. The convergence of the search process is achieved by the real-valued crossover and mutation factor governs. A brief discussion about the Differential Evolution technique is presented in this section.

The population size NP is kept constant during the minimization process. Each individual X_i of the population is a vector that contains a set of D optimization parameters as the problem decision variables and can be expressed as

$$\mathrm{X}_{\mathrm{i,G}} = \left\{\mathrm{x}^{1}_{\mathrm{i,G}}, \ldots\ldots\ldots, \mathrm{x}^{\mathrm{D}}_{\mathrm{i,G}}\right\}$$

In this problem the search space is bounded by the parameters such as crack location and depth both for the cantilever and fixed-fixed beam. The minimum and maximum parameter are bounded as, $X_{\min} = \left\{x^{1}_{\min}, \ldots\ldots, x^{D}_{\min}\right\}$ and $X_{\max} = \left\{x^{1}_{\max}, \ldots\ldots, x^{D}_{\max}\right\}$, respectively. The initial value of the *j*th parameter in the *i*th individual at the iteration $G = 0$ can be expressed as

$$x^{j}_{i,0} = x^{j}_{\min} + rand\left(x^{j}_{\max} - x^{j}_{\min}\right)$$

Where, rand represents a uniformly distributed random variable within the range [0, 1].

Mutation Operation

For each target vector $X_{i,G,} i = 1,2,.....,NP$, a mutant vector is generated according to the following mutation strategy as

$$V_{i,G+1} = X_{i,G} + F.(X_{best,G} - X_{i,G}) + F.(X_{r1,G} - X_{r2,G})$$

Where r_1, $r_2 \in \{1, 2\ldots NP\}$ are mutually different integer numbers and are also different from the index i.

The indices $r_1^i, r_2^i, r_3^i, r_4^i, r_5^i$ are mutually exclusive integers randomly generated within the range [1, NP], which are also different from the index *i*. These indices are randomly generated once for each mutant vector. The scaling factor F is a positive control parameter for scaling the difference vector.

Crossover Operation

The crossover operation is introduced in the DE algorithm to increase the diversity of the vectors. The crossover operation is carried out by randomly exchanging the data between the original vectors of the population $X_{i,G}$ and those of the mutant population $V_{i,G+1,}$ to obtain the trial vectors $Z_{i,G+1} = (z^1_{i,G+1,}, \ldots\ldots, z^D_{i,G+1})$. The trial vector determined by a parameter called crossover probability (CR $\in$ [0, 1]), as follows:

$$z_{i,G}^j = \begin{cases} v_{i,G}^j, & if\ (rand \le CR) or\ j = j_{rand}, \\ x_{i,G}^j, & otherwise \end{cases}$$

Where, j_{rand} is a randomly chosen integer in the range [1, D].

Selection

In order to decide if a vector Z_i be the element of the new population of generation G+1, each vector $z_{i,G+1}$ is compared to the previous corresponding target vector $x_{i,G}$. If vector $z_{i,G+1}$ yields a smaller objective function value than $x_{i,G}$, then $x_{i,G+1}$ is set to $z_{i,G+1}$; otherwise, the old value $x_{i,G}$ is retained. The selection operation can be expressed as

$$X_{i,G+1} = \begin{cases} Z_{i,G,} \text{ if } f\left(Z_{i,G}\right) \leq f\left(X_{i,G}\right) \\ X_{i,G,\text{otherwise}} \end{cases}$$

With i=1, 2…….NP.

The above steps are repeated until some specific termination criteria are satisfied.

Pseudo Code for DE

a) Generate a population of solution vectors;
b) Evaluation of the best member of the population $X_{best,I;}$
c) Carry out the mutation operation $V_{i,G+1;}$
d) Perform the crossover strategy $Z_{i,G+1;}$
e) Check the bound constraint;
f) Do the selection;
g) Evaluation of the best member of the population after selection $X_{best,I;}$
h) If the stopping criterion is reached, then print the output results and stop;
i) Go to step3.

5.11 Rationale behind the ANN models

The biggest challenge in successful application of ANN is when to stop training. If training is insufficient then the network will not be fully trained, whereas if training is excessive then it will memorize the training pattern or learn noise and known as over-fitting. The network needs to be equally efficient on new data during testing or validation, which is called generalization. This problem also exists in statistics. The different methods adopted to avoid over-fitting are (1) selection of suitable number of inputs, (2) selection of appropriate number of training data, (3) early stopping and cross validation (Basheer 2001; Shahin et al. 2002, Das and Basudhar 2006). In cross validation, an independent test set is used to assess the performance of the model at various stages of learning. However, this method is not suitable when there are limited data points. This depends upon the number of parameters (weights and biases) of the network and the number of data points available. There are certain guidelines to avoid over-fitting like the number of weights should not exceed the number of training samples (Roger and Dowla 1994), and the ratio of number of training samples to the number of connection weights should be 2 to 1 (Masters 1993) or 10 to 1 (Maier and Dandy 2000). Amari et al. (1997) suggest that over-fitting does not occur if the number of training sample is at least 30 times the number of free parameters.

The connection weights and biases of a network is defined as $(I + 1) \times H + (H + 1) \times O$; where, I is the number of inputs, H is the number of hidden layer neuron and O is the number of outputs. Similarly for more than n number of hidden layers, the total number of parameters is defined as $(I + 1) \times H_i + (H_{i+1}) \times (H_i + 1) + \ldots\ldots\ldots + (H_n + 1) \times O$.

As discussed above, the over-fitting occurs due to unbounded values of weights (parameters) during minimization of the error function, the mean square error (MSE). The other method called regularization, in which the performance function is changed by adding a term that consists of mean square error of weights and biases, which is known as Bayesian regularization neural network (Demuth and Beale 2000). This method avoids overfitting by penalizing the mean square error with higher weigh values.

Another aspect of the ANN is the 'learning' or 'training' process which, in general is a nonlinear optimization of an error function. This is equivalent to the parameter estimation phase in conventional statistical models. The error associated with weights and sigmoid function is a highly non-linear optimization problem with many local minima. In ANNs applied to different engineering problems, the steepest descent algorithm and Levenberg–Marquardt (LM) algorithm are commonly used. However, both are gradient search algorithms and are initial point dependent. Hence, the results obtained using back propagation algorithm is sensitive to initial weight vectors (Shahin et al. 2002). The global optimization algorithms like genetic algorithm (GA) and simulated annealing are now being used in other fields of engineering (Morshed and Kaluarachchi 1998) in such cases. However, in structural health monitoring engineering use of GA for training ANN is limited. In recent past another heuristic global optimization called differential evolution (DE), introduced by Storn and Price (1995) has been used successfully in aerodynamics shape optimization and mechanical design. The training of the feed-forward BPNN using DE optimization is known as differential evolution neural network (DENN) (Ilonen et al. 2003).

5.12 Prediction of Damage Extent in Beam Using ANN

ANN models have been developed for damage assessment in cracked beams. Three models are developed using Bayesian regularization, Differential Evolution and Levenberg-Marquardt for training process with the inputs as non-dimensional free vibration frequencies in 1st mode, 2nd mode and 3rd mode. The statistical performance criteria like correlation coefficient (R), coefficient of efficiency (E), over-fitting ratio (OR) and root mean square error (RMSE) are used to evaluate different ANN models.

5.12.1 Data base and preprocessing

In the present investigation available data in literature has been collected. The set of data randomly divided into training and testing set only, without any validation data set. The training data is taken as 70% of the total data i.e. 39 data set and the 16 data are taken as testing data. Once the data have been divided it is important to preprocess the data to a suitable form before applying ANNs .The variables have to be scaled in such a way as to commensurate with the limits of the activation function used in the output layer. So here all the training and testing sets are scaled in the range [-1, 1] as BRNN works better in the range [-1, 1] before training as follows.

$$X_n = 2\frac{(X - X_{\min})}{(X_{\max} - X_{\min})} - 1 \tag{50}$$

$$Y_n = 2\frac{(Y - Y_{\min})}{(Y_{\max} - Y_{\min})} - 1 \tag{51}$$

Where X_n , $X_{\max}$ and $X_{\min}$ are the normalized, maximum and minimum values of inputs and Y_n , $Y_{\max}$ and $Y_{\min}$ are the normalized, maximum and minimum values of outputs respectively.

5.13 Summary

The architecture of ANN with training and testing of network with details of model is discussed. The detection of extent of damage in cracked beams is described using three ANN models and compared among the three models.

Chapter 6

RESULTS AND DISCUSSIONS

6.1 Introduction

Any changes in the mass and stiffness of a member result in alterations in its dynamic and static behaviours. Structural defects are source of local flexibilities and cause deficiencies in structural resistance. Cracks in a structural element modify its stiffness and damping properties. In view of that, the modal data of the structure contain information relating to the position and size of the cracks.

The present chapter deals with the results of the analyses of the vibration, buckling and parametric resonance characteristics of a rectangular uniform and stepped beam for different boundary conditions using the formulation given in the previous chapter. As explained, the beam element is used to develop the finite element procedure. The Timoshenko beam element is used to model the beam considering the effects of transverse shear deformation without considering rotary inertia. The stability characteristics of cracked beams subjected to in-plane loads are studied. The parametric instability studies are carried out for beams with transverse cracks subjected to in-plane periodic loads with static component of load to consider the effect of various parameters. The studies in this chapter are presented as follows:

- Convergence study
- Comparison with previous studies
- New Examples: Quantitative results on the effects of various parameters on vibration, buckling and dynamic stability of single and multiple cracked beams are presented. A shear correction factor of 5/6 is used in line with previous studies by Loya (2006) for all numerical calculations.

6.2 Convergence Study

6.2.1 Vibration of cracked uniform cantilever beam

The convergence study is carried out for four lowest non-dimensional frequencies of free vibration of a cracked cantilever beam of span (L) 300 mm and section 10 mm× 10 mm. The

beam material is aluminum of elastic modulus (E) 68.22 GPa, Poisson's ratio (ν) 0.28 and material density (ρ) 2569 kg/m^3. A single transverse open crack of relative crack depth (rcd) 0.5 is located at 0.1L from fixed end. The beam is discretized into 2, 4, 6, 8, 16 and 32 numbers of finite beam elements with two degrees of freedom at each node. The non-dimensional free vibration frequencies (ω_c/ω_i) obtained by computing the ratio of cracked beam frequencies and intact beam frequencies for above discretization are computed and plotted in Fig. 6.1.

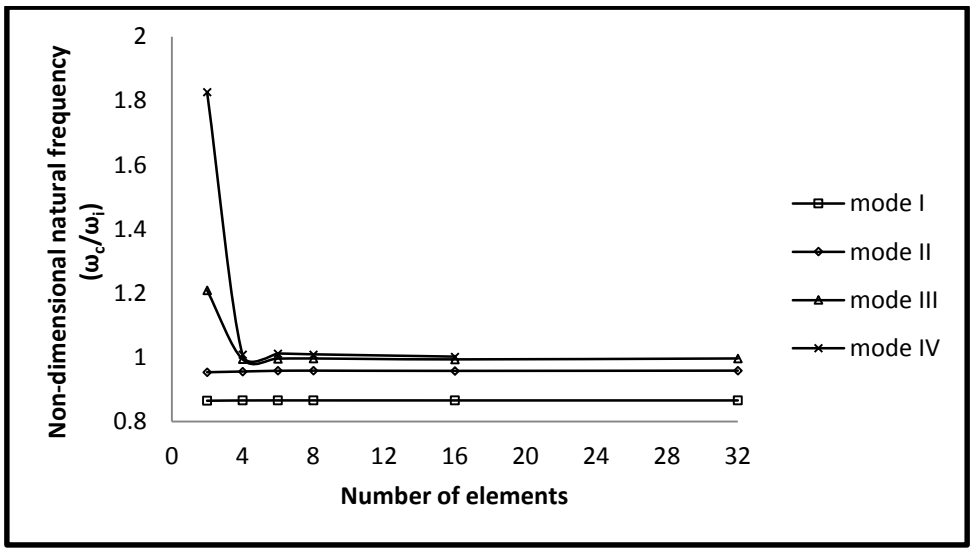

Figure 6.1 Variation of first four modes of non-dimensional free vibration frequencies with no of elements of discretization of the cantilever beam (L = 0.3m, b = h = 0.01m, E = 68.22 GPa, ν = 0.28 and ρ = 2569kg/m^3) with a crack of relative depth 0.5 at 0.1L

It is observed that frequencies of vibration of beam discretized into 4 to 8 elements have yielded good convergence of the numerical solution for free vibration. Though the convergence is achieved in 4 to 8 elements all further computation is carried out using 16 elements for better convergence of solution.

6.2.2 Vibration of cracked stepped cantilever beam

The convergence study is carried out for free vibration of a cracked stepped aluminum beam with three steps (four segments). Length of each segment is L_S = 75 mm, depth of beam is 14 mm, 12 mm, 8 mm and 6 mm for segment 1, 2, 3 and 4 respectively. Breadth of the beam is assumed to be 10 mm for each segment. The material properties of the beam are given by, Elastic modulus E = 68.22 GPa, Mass density ρ = 2569 kg/m^3 and Poisson's ratio ν = 0.28. A single open transverse crack of relative crack depth 0.5 is introduced at 0.05L from the fixed

end. First four modes of non-dimensional natural frequencies are computed and plotted in Fig. 6.2 for 1, 2, 3, 4, 5, 6, 7 and 8 number of element discretization per each segment.

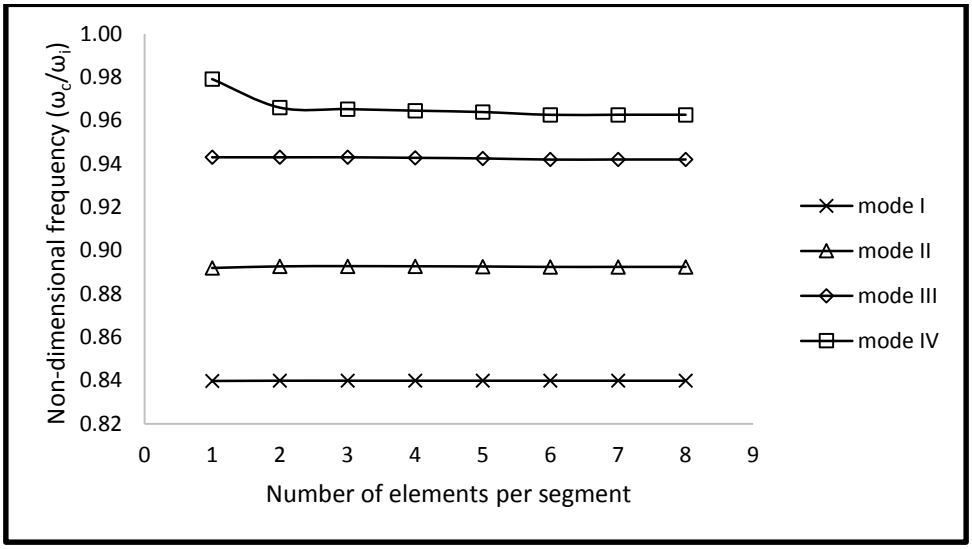

Figure 6.2 Variation of non-dimensional frequencies of a cracked stepped cantilever beam with respect to number of elements per segment for a crack of relative depth 0.5 at 0.05*L* from fixed end ($L_{S1} = L_{S2} = L_{S3} = L_{S4} = 75$ mm, $h_1 = 14$ mm, $h_2 = 12$ mm, $h_3 = 8$ mm, $h_4 = 6$ mm, $b_1 = b_2 = b_3 = b_4 = 10$ mm, $E = 68.22$ GPa, $\rho = 2569$ kg/m^3, $\nu = 0.28$)

Referring to Fig. 6.2, it is observed that 3 to 5 number of elements per segment has yielded good convergence of the numerical solution for free vibration but for all future study on stepped beam a discretization of 6 elements per segment is considered for better convergence of the solution.

6.2.3 Buckling of cracked uniform cantilever beam

The convergence study is carried out for the cracked cantilever aluminum beam of span 300 mm and section 10 mm by 10 mm. The elastic modulus (E) of beam material is considered as 68.22 GPa, Poisson's ratio (ν) 0.28 and density (ρ) 2569 kg/m^3. First mode non-dimensional buckling load (P_c/P_i) is computed for 2, 4, 8, 16 and 32 number of element discretization of the beam by finding the ratio of buckling load of the cracked cantilever beam and intact cantilever beam. The non-dimensional buckling loads obtained from the study are plotted in Fig. 6.3.

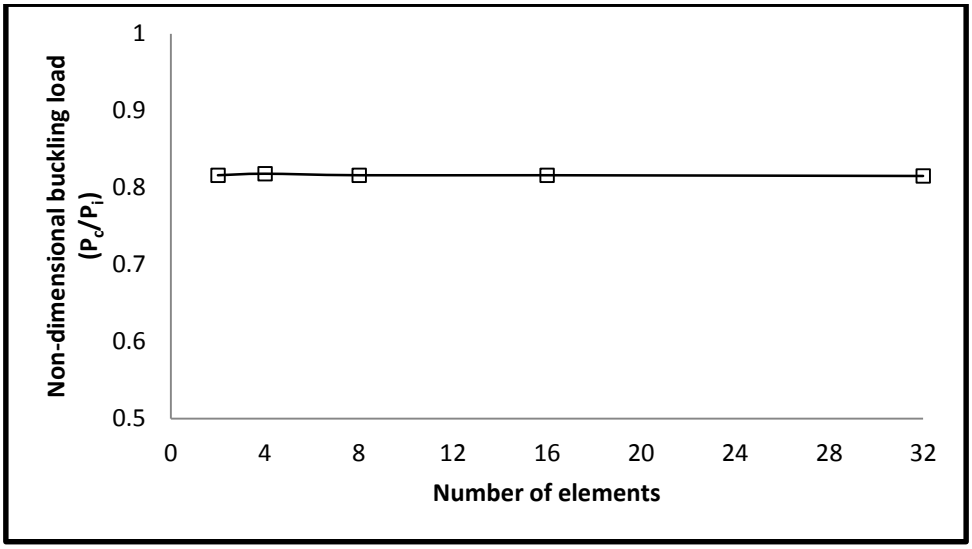

Figure 6.3 Variation of non-dimensional buckling load of a cracked uniform cantilever beam subjected to a crack of relative depth 0.5 at 0.1L from fixed end with no of elements (L = 0.3m, b = h=0.01m, E = 68.22 GPa, ν = 0.28 and ρ = 2569kg/m^3)

Referring to Fig. 6.3, it is observed that non-dimensional buckling load estimation for the beam discretized into 16 elements has yielded good convergence. Hence this discretization is considered in all further calculations.

6.3 Comparison with Previous Studies

6.3.1 Free vibration of cracked uniform cantilever beam

To validate the present finite element formulation for free vibration analysis of cracked beam for various crack positions and crack depths, the example problem solved by Kisa *et al.* (1998) using finite element and component mode synthesis method, is analyzed. The first three modes of natural frequencies of intact and cracked ($L_1 = 0.2L$**)** beam for different relative crack depths along with the results of Kisa *et al.* (1998) and results obtained using ANSYS are tabulated in Table 6.1 and compared. It is observed that there exists an excellent agreement between the present FEM results with the results using ANSYS and previous studies.

Table 6.1 Comparison of free vibration frequencies (rad/sec) of cracked beam (L = 0.2 m, b = 0.025 m, d = 0.0078 m, E = 216 GPa, ν = 0.28 and ρ = 7850 kg/m^3) for a crack at L_1=0.2L for different relative crack depths (a/h)

Relative crack depth (rcd)	Natural frequency (rad/sec)					
	Mode I		Mode II		Mode III	
	Present FEM analysis	Kisa et al. (1998)	Present FEM analysis	Kisa et al. (1998)	Present FEM analysis	Kisa et al. (1998)
0	1037.3	1037.0	6465.8	6458.3	17953.1	17960.5
0.2	1020.5	1020.1	6470.5	6457.4	17880.2	17872.9
0.6	842.4	842.2	6451.4	6448.2	17006.4	16944.6
0.8	551.3	551.0	6397.7	6436.0	15873.4	15512.6

6.3.2 Buckling of cracked uniform beams

To validate the present formulation further, the buckling analysis of a cantilever beam with a crack is carried out for the beam considered by Kisa (2011). The critical buckling load of the cracked beam is determined. The variations of the first non-dimensional buckling load (P_c/P_i) of cracked beam with respect to various crack locations (0.1L to 0.9L) and different relative crack depths (0.2, 0.4, 0.6 and 0.8) is shown in Table 6.2. P_c and P_i represent the critical buckling load of the cracked beam and intact beam respectively. Referring to Table 6.2, there exists an excellent agreement between the present FEM analysis and the analysis of Kisa (2011).

Table 6.2 Comparison of non-dimensional buckling load (P_c/P_i) of cracked beam (L = 3 m, b = 0.2 m, d = 0.2 m, E = 216 GPa, ν = 0.33, ρ = 7850 kg/m^3)

L_1/L	rcd = 0.2		rcd = 0.4		rcd = 0.6		rcd = 0.8	
	Present FEM	Kisa (2011)	Present FEM	Kisa (2011)	Present FEM	Kisa (2011)	Present FEM	Kisa (2011)
0.1	0.95	0.96	0.80	0.81	0.53	0.53	0.18	0.18
0.3	0.96	0.97	0.83	0.84	0.59	0.59	0.22	0.22
0.5	0.97	0.98	0.89	0.89	0.69	0.69	0.29	0.29
0.7	0.99	1.00	0.95	0.95	0.83	0.84	0.45	0.45
0.9	1.00	1.00	0.99	1.00	0.98	0.98	0.87	0.86

6.4 New Examples

Uniform beam

An aluminum beam as shown in Fig. 6.4 of Span L = 300 mm, rectangular cross-section with width b = 10 mm and height h = 10 mm. Elastic modulus (E) = 68.22 GPa, Poisson's ratio (ν) = 0.28, Mass density (ρ) = 2569 kg/m^3 is considered for the analysis of free vibration, buckling and dynamic stability of all uniform beams in this report. The parametric study is carried out for the dynamic analysis of the beam subjected to harmonic in-plane load for different end conditions, different locations and depth of the crack. The study is also extended for the dynamic behavior of the cantilever beam subjected to multiple cracks.

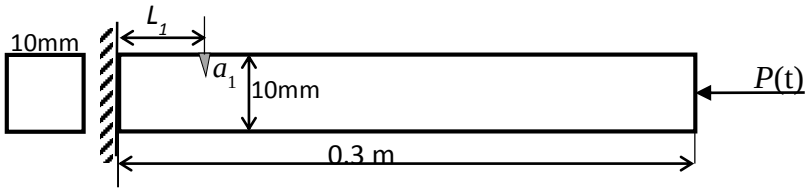

Figure 6.4 Cracked uniform Aluminum cantilever beam, L = 300 mm, b = 10 mm, h = 10 mm, E = 68.22 GPa, ν = 0.28, ρ = 2569 kg/m^3

Stepped beam

A three stepped aluminum cantilever beam of four segments of 75 mm each is considered as shown in the Fig. 6.5 for all analysis of stepped beam in this report. The breadth of the beam is assumed to be 10 mm throughout the span and the depth is considered to be 14 mm, 12 mm, 8 mm and 6 mm respectively for segments 1, 2, 3 and 4 respectively. The material properties of the beam is assumed to be, Elastic modulus E = 68.22 GPa, Poisson's ratio (ν) = 0.28 and Mass density (ρ) = 2569 kg/m^3. The vibration, buckling and parametric instability behavior of the stepped beam with cracks are studied.

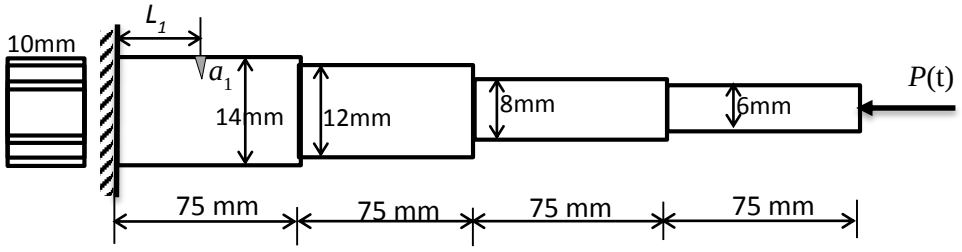

Figure 6.5 Three stepped cracked cantilever beam, L_s = 75 mm, b = 10 mm, h_1 = 14 mm, h_2 = 12 mm, h_3 = 8 mm, h_4 = 6 mm, E = 68.22 GPa, ν = 0.28, ρ = 2569 kg/m^3

6.5 Vibration of Beam Subjected to a Single Crack

The non-dimensional natural frequency (ω_c/ω_i) of aluminum beams with various end conditions are computed for different position and depth of the crack. Here ω_c and ω_i represents natural frequency of cracked beam and intact beam respectively.

6.5.1 Uniform fixed-free beam

Free vibration analysis of the uniform beam shown in Fig. 6.4 is carried out for fixed-free end conditions. The variation of first mode non-dimensional natural frequency with relative location of the crack (L_1/L) for different relative crack depths of the Fixed-Free beam is plotted in Fig. 6.6.

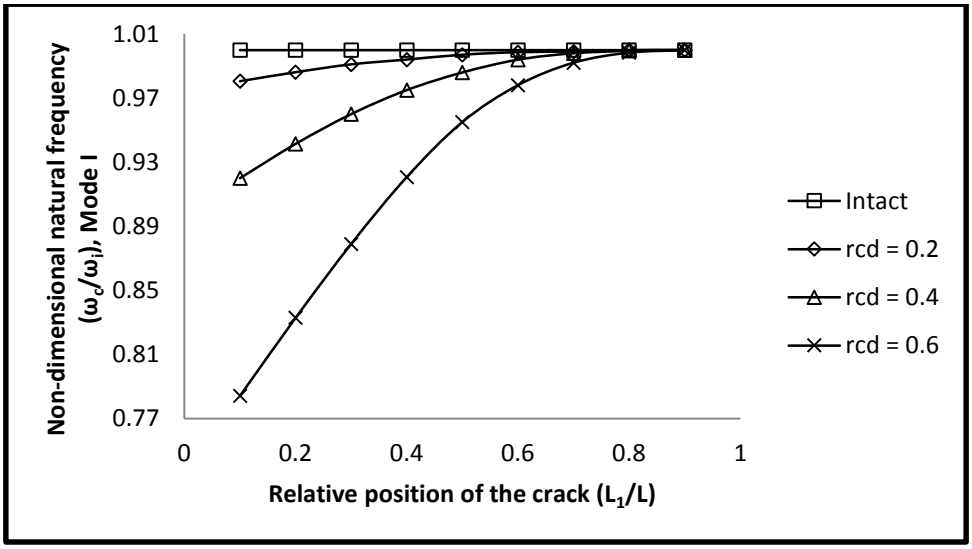

Figure 6.6 Variation of non-dimensional fundamental frequency (ω_c/ω_i) with relative crack location (L_1/L) for different relative crack depths (rcd) of the uniform fixed-free beam

It is observed that for the crack at 0.1L from the fixed end, the non-dimensional natural frequency of first mode reduces by 2.0%, 8.0% and 21.6% than intact beam for relative crack depths of 0.2, 0.4 and 0.6 respectively. It is also observed from the above figure that the non-dimensional natural frequency increases as the crack moves away from the fixed end to free end. As the crack approaches the free end, the non-dimensional free vibration frequencies in first mode are almost same as that of the intact beam. Hence for the first mode of vibration in case of a cantilever beam, crack near the fixed support is more critical than at any other location. Crack near the free end have very little effect on the free vibration frequencies of the

beam. This may be due to the position of maximum bending moment of a cantilever beam near the fixed end and minimum bending moment near free end. The variations of non-dimensional natural frequencies of vibration for the second mode of cracked beam with a single crack are plotted in Fig. 6.7.

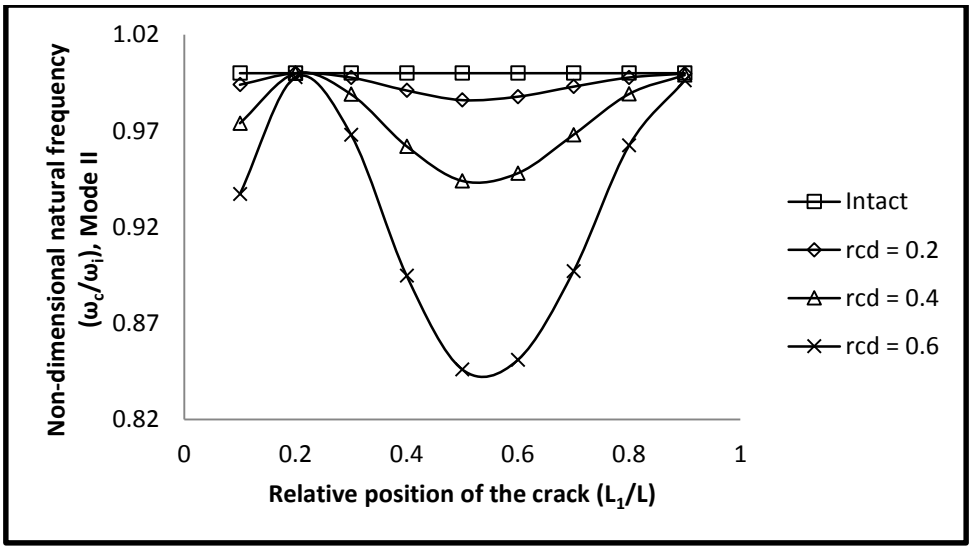

Figure 6.7 Variation of non-dimensional natural frequency (ω_c/ω_i), Mode II, with relative crack location (L_1/L) for different relative crack depths (rcd) of the uniform fixed-free beam

It is observed that the non-dimensional natural frequency of second mode decreased by 0.6%, 2.6% and 6.3% for the crack at 0.1L and the same reduced by 0.0%, 0.0% and 0.2% for the crack at 0.2L for relative depths of crack as 0.2, 0.4 and 0.6 respectively. Similarly crack at 0.5L from fixed end the non-dimensional natural frequency decreased by 1.4%, 5.6% and 15.4% than intact beam for relative crack depths of 0.2, 0.4 and 0.6 respectively and when the crack is near the free end i.e.at 0.9L the non-dimensional free vibration frequencies are almost equal to that of intact beam for all relative depths of the crack. This implies a crack at 0.2L from the fixed end hardly affects the non-dimensional natural frequency for all relative depths of the crack. But, when the crack is situated between 0.5L and 0.6L, the drop in second mode frequencies is maximum. Similarly crack near free end has no effect on the free vibration frequencies as they are same as that of an intact beam. This may be due to the location of node points in second mode at about 0.2L from the fixed end and near the free end. The variations of non-dimensional free vibration frequencies in third mode for various locations and depths of the crack are shown in Fig. 6.8.

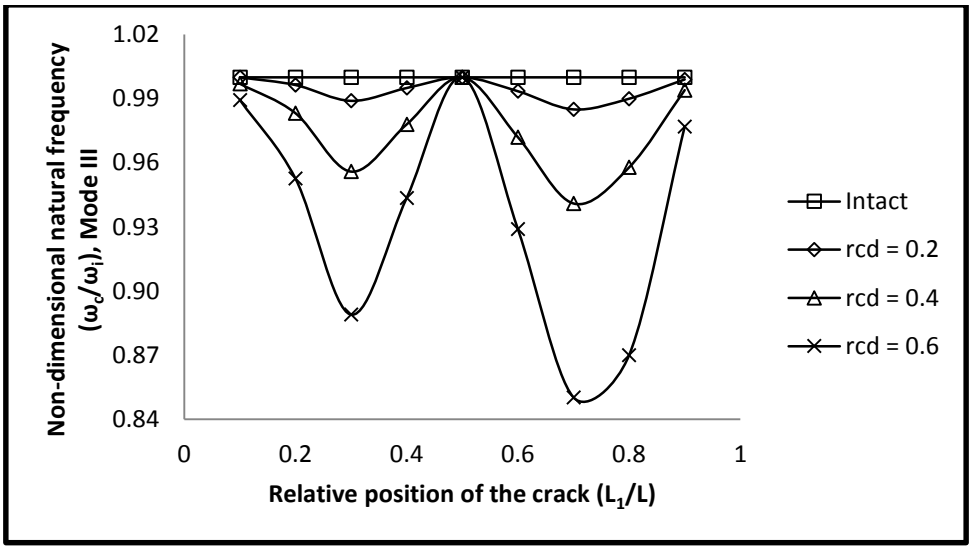

Figure 6.8 Variation of non-dimensional frequency (ω_c/ω_i), Mode III, with relative crack location (L_1/L) for different relative crack depths (rcd) of the uniform fixed-free beam

It is observed that the reduction in non-dimensional free vibration frequencies in third mode for the crack at 0.1L is found to be 0.0%, 0.3% and 1.1% for relative depths of crack as 0.2, 0.4 and 0.6 respectively which shows very little effect as far as reduction in natural frequency is concerned. But when the crack is at 0.3L the reductions in non-dimensional frequencies in third mode are found to be 1.1%, 4.4% and 11.1% and for the crack at 0.5L there is no reduction in frequencies. This may be due to the existence of node points at center and at both ends of beam. But for the crack at 0.7L the non-dimensional frequencies reduce by 1.5%, 5.9% and 15.0% and when the crack is at 0.9L the same reduced by 0.1%, 0.6% and 2.3% for relative crack depths of 0.2, 0.4 and 0.6 respectively. This implies the crack near fixed end or free end has little effect in reducing the non-dimensional natural frequency in third mode than intact beam. But the crack at 0.5L has no effect at all on free vibration frequencies in third mode. But the crack at 0.3L or 0.7L reduces the free vibration frequencies in third mode considerably. The fourth mode non-dimensional free vibration frequencies for fixed-free beam are plotted in Fig. 6.9.

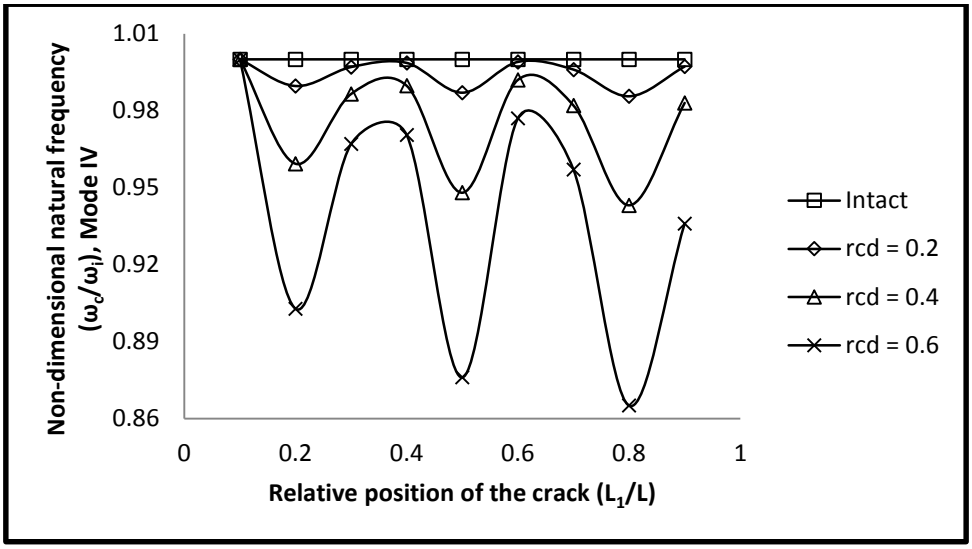

Figure 6.9 Variation of non-dimensional frequency (ω_c/ω_i), Mode IV, with relative crack location (L_1/L) for different relative crack depths (rcd) of the uniform fixed-free beam

It is observed that the fourth non-dimensional natural frequency is not affected by the crack at 0.1L from fixed end. Similarly the effect of crack between 0.3L to 0.4L and between 0.6L to 0.7L has very little effect on free vibration frequencies in fourth mode due to the existence of nodal points. But the decrease in free vibration frequencies in fourth mode is 1.0%, 4.1% and 9.7% for crack at 0.2L, 1.3%, 5.2% and 12.4% for crack at 0.5L and 1.4%, 5.7% and 13.5% for crack at 0.7L for relative crack depths of 0.2, 0.4 and 0.6 respectively. Similarly when the crack is at 0.9L the reduction in frequencies in fourth mode are found to be 0.3%, 1.7% and 6.4% than intact beam for relative crack depths of 0.2, 0.4 and 0.6 respectively.

The variation of the first four fundamental mode shapes of the fixed-free beam with respect to different crack locations (L_1 = 0.1*L*, 0.3L, 0.5*L*, 0.7*L*, 0.9*L*) for relative crack depth of 0.5 are illustrated in Fig. 6.10 to 6.13. Similarly the first bending mode shapes for relative crack depths of 0.0 (intact), 0.2, 0.4 and 0.6 of the cantilever beam is plotted in Fig. 6.14.

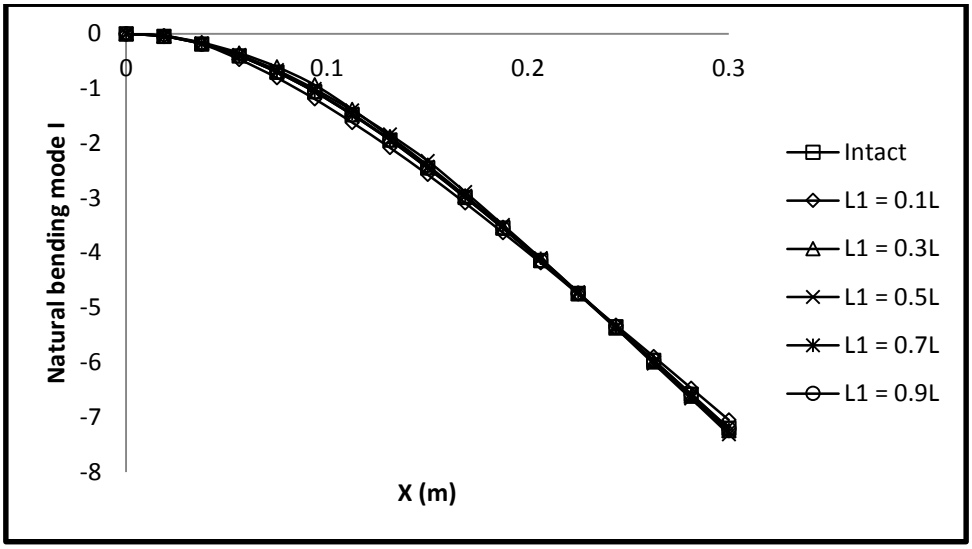

Figure 6.10 Fundamental mode shape of free vibration for different location of a crack of relative depth 0.5 of the uniform fixed-free beam

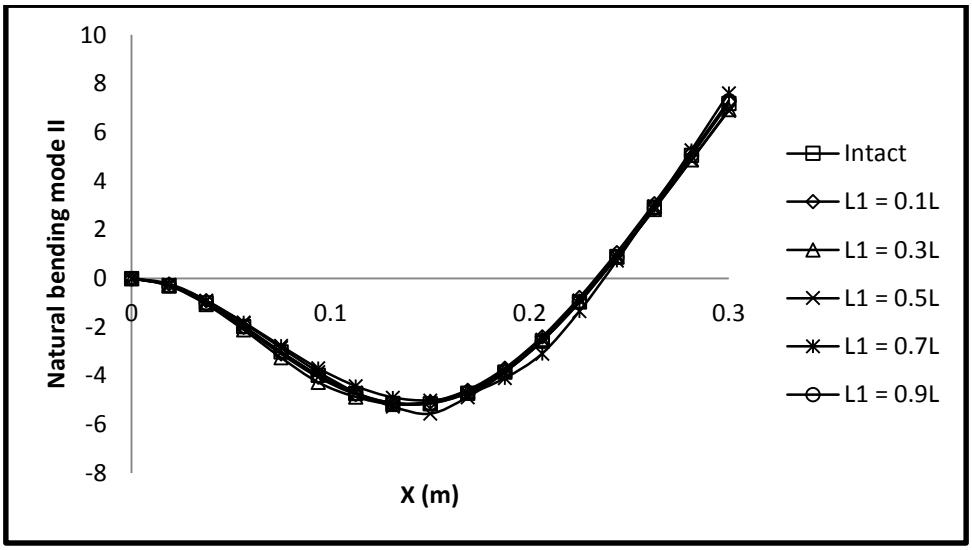

Figure 6.11 Second mode shape of free vibration for different location of a crack of relative depth 0.5 of the uniform fixed-free beam

From these figures it is observed that crack locations and depths play important role on the variation of mode shapes. For most of the cases considered, as the crack grows, the mode shapes undergo a highly noticeable change close to the crack location area. In some cases, as the crack grows deeper (when the crack depth was equal to or greater than 0.5), there were shifts in the position of the nodes for the second and third modes. The changes in the natural

frequency and mode shape depended on how close the crack was to nodes of mode shapes for higher modes.

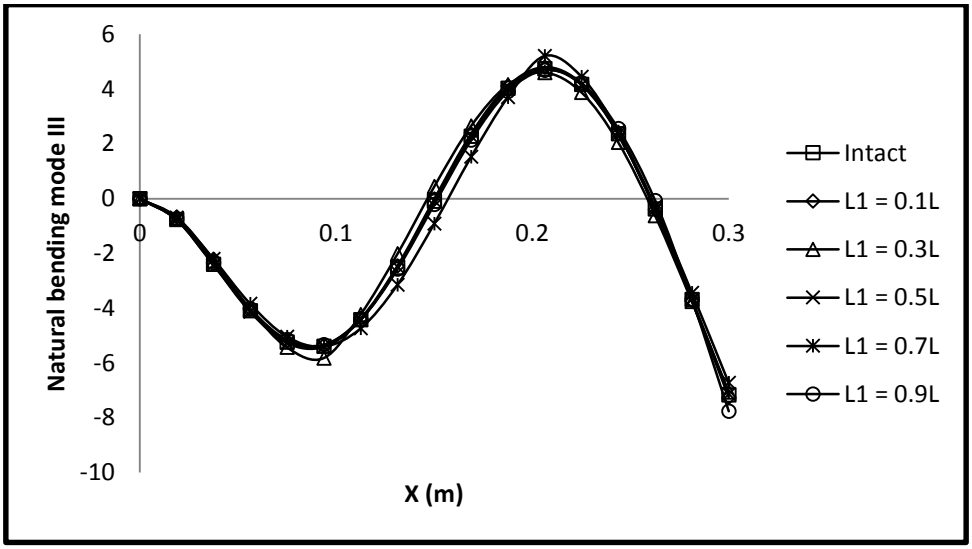

Figure 6.12 Third mode shape of free vibration for different location of a crack of relative depth 0.5 of the uniform fixed-free beam

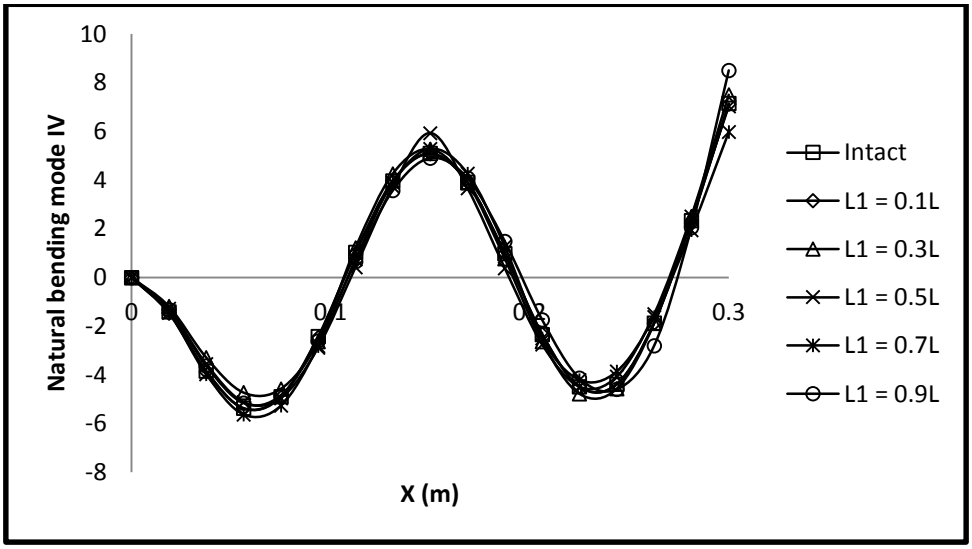

Figure 6.13 Fourth mode shape of free vibration for different location of a crack of relative depth 0.5 of the uniform fixed-free beam

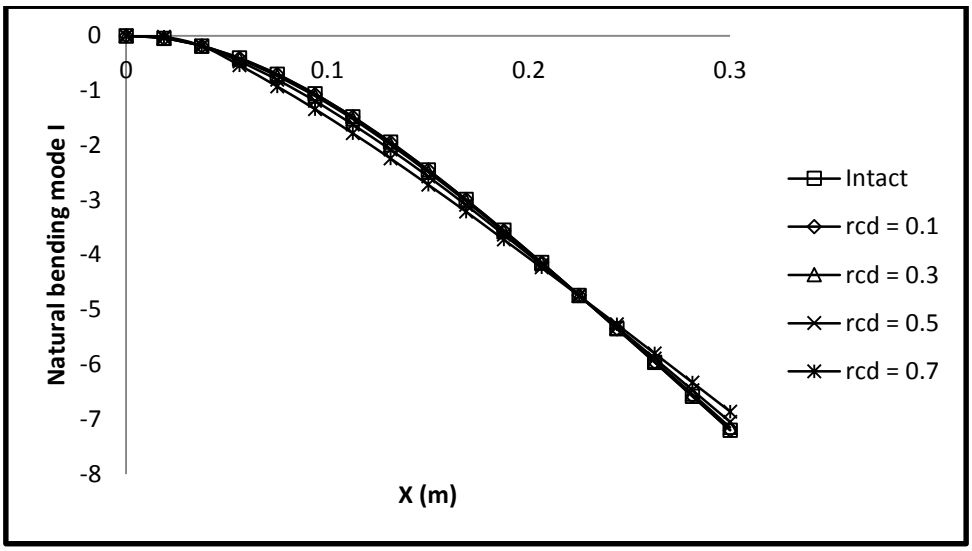

Figure 6.14 Fundamental mode shape of free vibration for different depth of a crack at 0.05L from fixed end of the uniform fixed-free beam

Thus, based on the observed changes in the natural frequencies and mode shapes, the crack position, and crack depth can be estimated. While the cracks located at certain locations have little effects in a particular mode shape and are very difficult to be recognised. It is apparent from these figures that same cracks may have bigger effects on the other mode shapes and can be detected easily. As a consequence, all mode shapes should be checked for the crack detection process. This outcome is significant from the point of damage detection by means of mode shapes. Similarly effect of single crack on free vibration frequencies of the uniform beam for other end conditions is studied.

6.5.2 Uniform hinged-hinged beam

Free vibration analysis of the uniform beam shown in Fig. 6.4 is carried out for hinged-hinged end conditions. The effect of crack depth on non-dimensional natural frequency for hinged-hinged beam in first mode is plotted in Fig. 6.15.

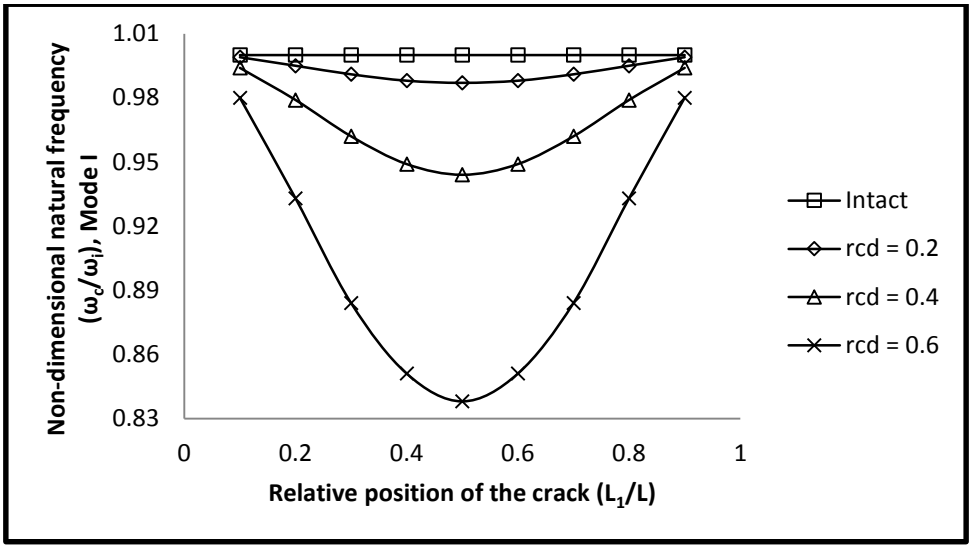

Figure 6.15 Variation of non-dimensional fundamental frequency (ω_c/ω_i) with relative crack location (L_1/L) for different relative crack depths (rcd) of the uniform hinged-hinged beam

It is observed that the non-dimensional frequencies in first mode for the crack at 0.1L or 0.9L, the non-dimensional free vibration frequencies in first mode decrease by 0.1%, 0.6% and 2.0% for relative crack depths of 0.2, 0.4 and 0.6 respectively. Whereas the non-dimensional frequencies in first mode decrease by 1.3%, 5.6% and 16.2% for the crack at 0.5L for relative crack depths of 0.2, 0.4 and 0.6 respectively. This implies the free vibration non-dimensional frequencies are least affected for the crack near the hinged supports but as the crack moves close to the mid-span the reduction in frequencies is considerable and it increases with the relative crack depth. This is due to the fact that the bending moment of a hinged-hinged beam near the supports is lesser in comparison to the bending moment at mid span. The variation of non-dimensional natural frequency in second and third mode with relative crack location is shown in Fig. 6.16 and 6.17 respectively for different relative crack depths.

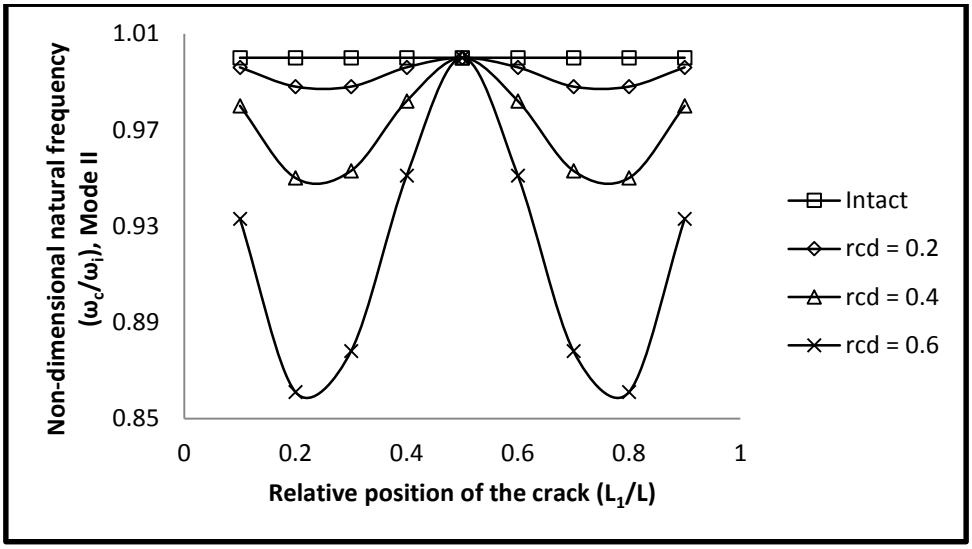

Figure 6.16 Variation of non-dimensional frequency (ω_c/ω_i), Mode II, with relative crack location (L_1/L) for different relative crack depths (rcd) of the uniform hinged-hinged beam

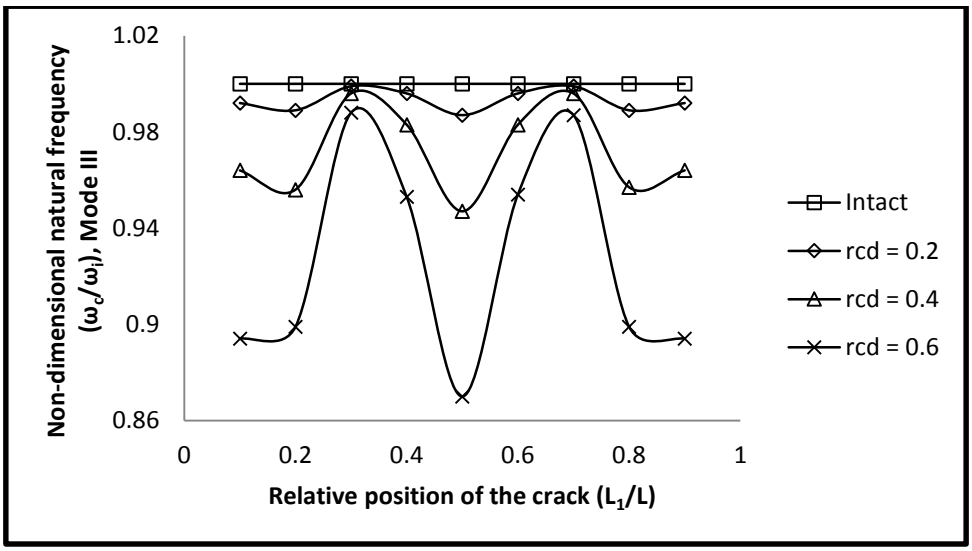

Figure 6.17 Variation of non-dimensional frequency (ω_c/ω_i), Mode III, with relative crack location (L_1/L) for different relative crack depths (rcd) of the uniform hinged-hinged beam

It is observed from Fig. 6.16 that the non-dimensional natural frequency in second mode for a hinged-hinged beam is not at all affected by the crack at 0.5L from the left support i.e. at mid span. Similarly the effect of the crack in reducing the non-dimensional natural frequency decreases as the crack approaches the supports. Hence it can be concluded that the non-dimensional free vibration frequencies are not affected at all when the crack is positioned at the supports or at mid-span due to the presence of node points of the vibration mode.

Referring to Fig. 6.17, it can be concluded that the non-dimensional free vibration frequencies decrease by 0.8%, 3.6% and 10.6% than intact beam for crack at 0.1L or 0.9L from fixed end and by 1.3%, 5.3% and 13.0% than intact beam for crack at 0.5L from the fixed end for relative crack depth of 0.2, 0.4 and 0.6 respectively. This implies the non-dimensional free vibration frequencies in third mode are severely affected by the crack positioned at mid span or at supports. But when the crack is positioned at 0.3L or 0.7L the non-dimensional frequencies in third mode are least affected. The effect of the crack on non-dimensional natural frequency in fourth mode is plotted in Fig. 6.18.

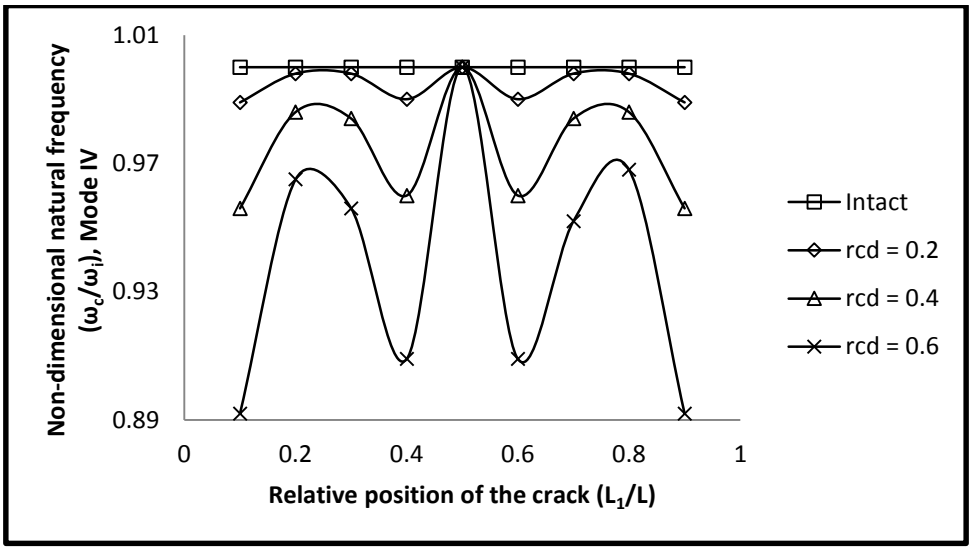

Figure 6.18 Variation of non-dimensional frequency (ω_c/ω_i), Mode IV, with relative crack location (L_1/L) for different relative crack depths (rcd) of the uniform hinged-hinged beam

It is observed that the non-dimensional free vibration frequencies in fourth mode decreases with increase in crack depth for any location of the crack. It is also observed that the non-dimensional free vibration frequencies decrease by 1.1%, 4.4% and 10.8% with respect to intact beam for the crack at 0.1L from the supports for relative crack depth of 0.2, 0.4 and 0.6 respectively. Similarly for the crack at 0.4L from supports the non-dimensional free vibration frequencies in fourth mode decrease by 1.0%, 4.0% and 9.1% and for crack near 0.2L from the supports the same decrease by 0.2%, 1.4% and 3.5% than that of intact beam for relative crack depth of 0.2, 0.4 and 0.6 respectively.

This suggests the presence of a crack near supports severely affects the fourth mode free vibration frequencies and the crack at mid-span does not affect free vibration frequencies in

fourth mode at all. But the crack at 0.4L from each support moderately reduces the free vibration frequencies in fourth mode whereas crack near 0.2L from supports reduces fourth mode free vibration frequencies by a little margin.

6.5.3 Uniform fixed-hinged beam

Free vibration analysis of the uniform beam shown in Fig. 6.4 is carried out for fixed-hinged end conditions. The effect crack on non-dimensional natural frequencies in first mode for different location and depth of crack is shown in Fig. 6.19.

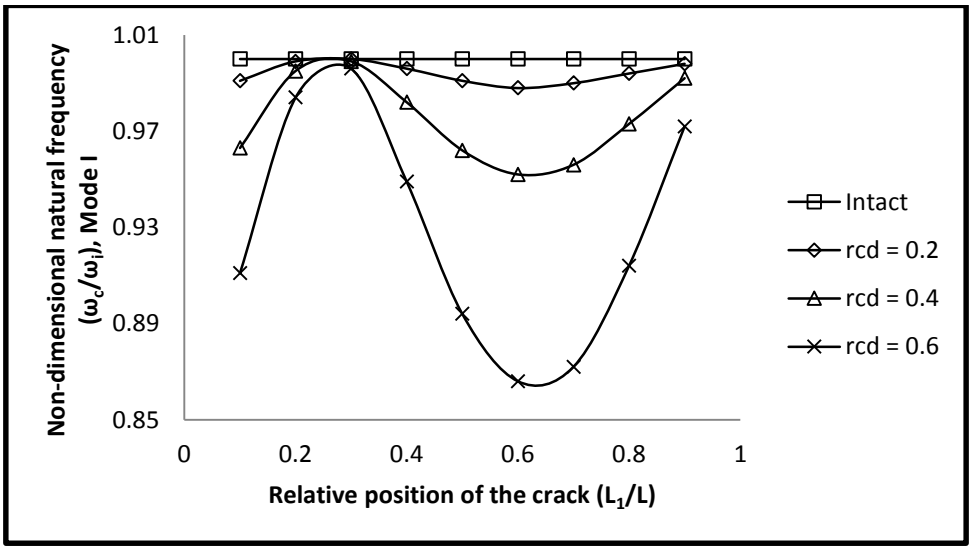

Figure 6.19 Variation of non-dimensional fundamental frequency (ω_c/ω_i) with relative crack location (L_1/L) for different relative crack depths (rcd) of the uniform fixed-hinged beam

It is observed that the first non-dimensional free vibration frequencies decrease by 0.9%, 3.7% and 8.9% for relative crack depth of 0.2, 0.4 and 0.6 respectively due to the crack at 0.1L from left fixed support as shown in Fig. 6.19. For the crack at 0.3L from fixed support, the frequencies in first mode decrease by 0.0%, 0.1% and 0.4% for relative crack depths of 0.2, 0.4 and 0.6 respectively. Similarly crack at 0.6L reduces the free vibration in first mode by 1.2%, 4.8% and 13.4% and crack at 0.9L from fixed end reduces the same by 0.2%, 0.8% and 2.8% than intact beam for relative crack depths of 0.2, 0.4and 0.6 respectively. This implies crack near 0.6L from fixed end is more vulnerable in terms of reducing natural frequency in first mode than anywhere else. The crack near the fixed support moderately reduces the natural frequency in first mode than the crack near the simple support, where the reduction is marginal.

The variation of non-dimensional natural frequency in second mode with location of the crack from fixed end for different relative crack depths are shown in Fig. 6.20.

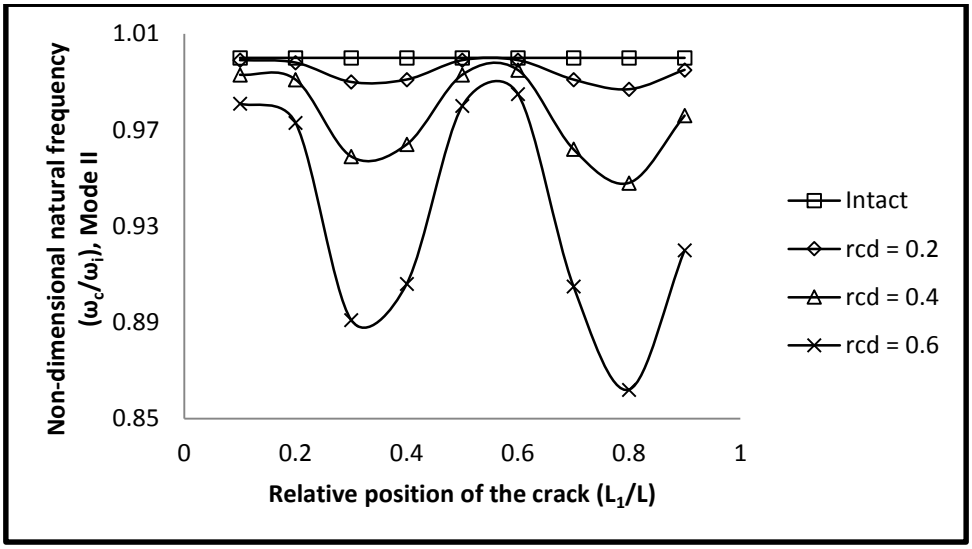

Figure 6.20 Variation of non-dimensional frequency (ω_c/ω_i), Mode II, with relative crack location (L_1/L) for different relative crack depths (rcd) of the uniform fixed-hinged beam

It is observed that the free vibration frequencies in second mode decrease by 0.1%, 0.7% and 1.9% for the crack at 0.1L and by 0.5%, 2.4% and 8.0% for the crack at 0.9L from fixed end for relative crack depths of 0.2, 0.4 and 0.6 respectively. Similarly the crack at 0.3Lfrom fixed end reduces the free vibration frequencies in second mode by 1.0%, 4.1% and 10.9% whereas the crack at 0.8L reduces the same by 1.3%, 5.2% and 13.8% than intact beam for relative crack depths of 0.2, 0.4 and 0.6 respectively. But the crack in between 0.5L and 0.6L from fixed end marginally reduces the natural frequency in second mode. Hence it can be concluded that the presence of a crack near hinged end reduces the free vibration frequencies in second mode more than the same crack near the fixed end. It can also be concluded that the crack at 0.8L from the fixed end which is near the hinged end is more vulnerable than the crack at 0.3L from fixed end. The variation of non-dimensional free vibration frequencies for third and fourth mode of a fixed-hinged beam for different location and depth of the crack from fixed end is plotted in Fig. 6.21 and 6.22 respectively.

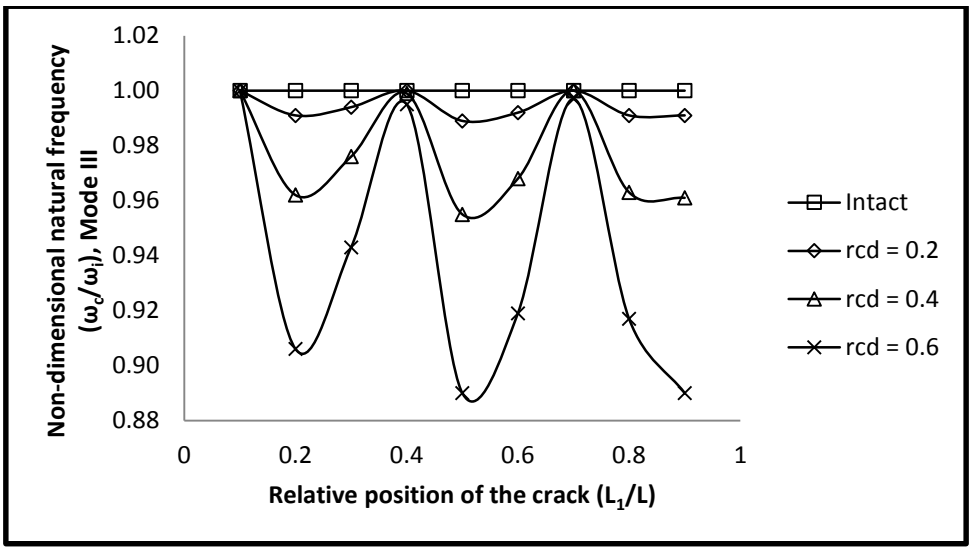

Figure 6.21 Variation of non-dimensional frequency (ω_c/ω_i), Mode III, with relative crack location (L_1/L) for different relative crack depths (rcd) of the uniform fixed-hinged beam

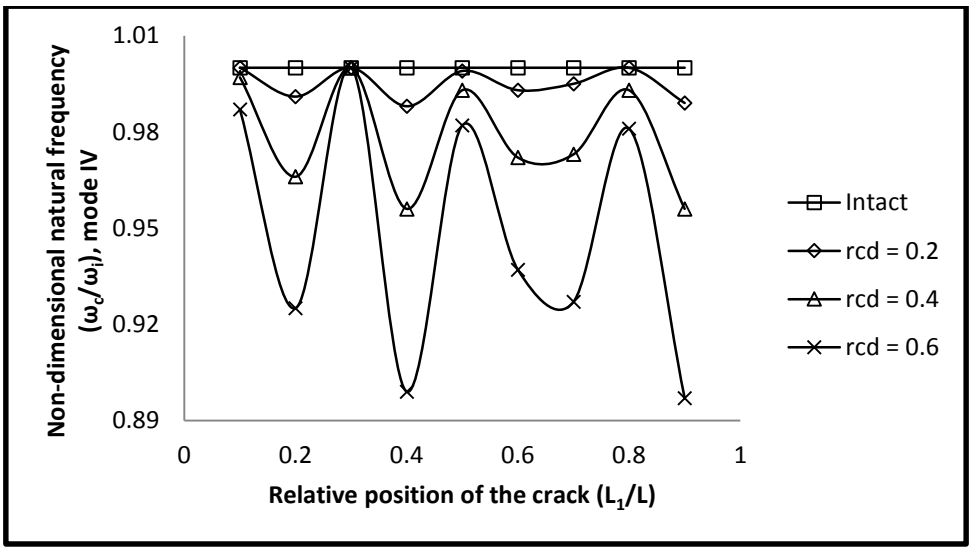

Figure 6.22 Variation of non-dimensional frequency (ω_c/ω_i), Mode IV, with relative crack location (L_1/L) for different relative crack depths (rcd) of the uniform fixed-hinged beam

It is observed from Fig. 6.21 that the free vibration frequencies in third mode are hardly affected by the crack positioned at 0.1L, 0.4L or 0.7L from fixed end. On the other hand for the crack positioned at 0.2L from fixed end the third mode free vibration frequencies decrease by 0.9%, 3.8% and 9.4% and for crack at 0.5L the same decrease by 1.1%, 4.5% and 11.0% than intact beam for relative crack depths of 0.2, 0.4 and 0.6 respectively. Similarly crack near the hinged support i.e. at 0.9L from fixed end reduces the free vibration frequencies in third mode by

0.9%, 3.9% and 11.0% than intact beam for relative crack depths of 0.2, 0.4 and 0.6 respectively. This suggests the presence of the crack near 0.2L, 0.4L or hinged support is more vulnerable than at any other location with regard to free vibration frequencies of third mode.

It is observed from Fig. 6.22 that the free vibration frequencies in fourth mode is not affected at all by the presence of the crack at 0.3L from fixed end for any depth of the crack. But when the crack is at 0.5L and 0.8L from the fixed end the free vibration frequencies in fourth mode decrease marginally by 1.8% and 1.9% for relative crack depth of 0.6. Similarly when the crack is at 0.1L, i.e. near the fixed support, the non-dimensional frequencies in fourth mode decrease marginally by 1.3% for relative crack depth of 0.6, but when the crack is near the hinged support i.e. 0.9L from fixed end the fourth mode free vibration frequencies decrease by 1.1%, 4.4% and 10.3% than intact beam for relative crack depths of 0.2, 0.4 and 0.6 respectively. The non-dimensional free vibration frequencies decrease by 0.9%, 3.4% and 7.5% for the crack at 0.2L from fixed end and the frequencies decrease by 1.2%, 4.4% and 10.1% when the crack is at 0.4L from fixed end for the relative crack depths of 0.2, 0.4 and 0.6 respectively. Again the crack at 0.7L reduces the non-dimensional natural frequency in fourth mode by 0.5%, 2.7% and 7.3% than intact beam for relative crack depths of 0.2, 0.4 and 0.6 respectively. Hence the locations like 0.2L, 0.4L, 0.7L and hinged support are vulnerable in terms of fourth mode natural frequency than the crack at any other location.

6.5.4 Uniform fixed-fixed beam

Free vibration analysis of the uniform beam shown in Fig. 6.4 is carried out for fixed-fixed end conditions. The variation of first and second mode natural frequencies with crack location for different relative depths of the crack for a beam with fixed-fixed end conditions is plotted in Fig. 6.23 and 6.24 respectively.

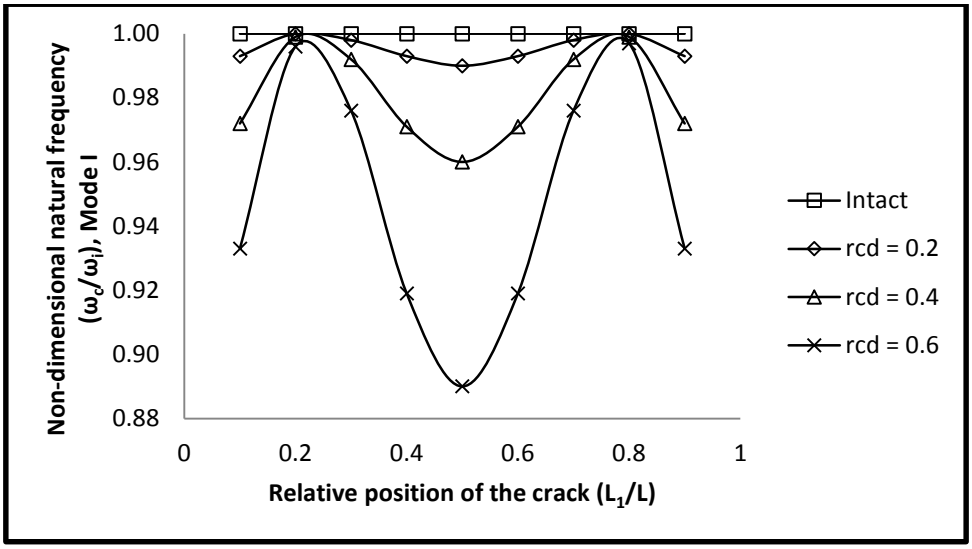

Figure 6.23 Variation of non-dimensional fundamental frequency (ω_c/ω_i) with relative crack location (L_1/L) for different relative crack depths (rcd) of the uniform fixed-fixed beam

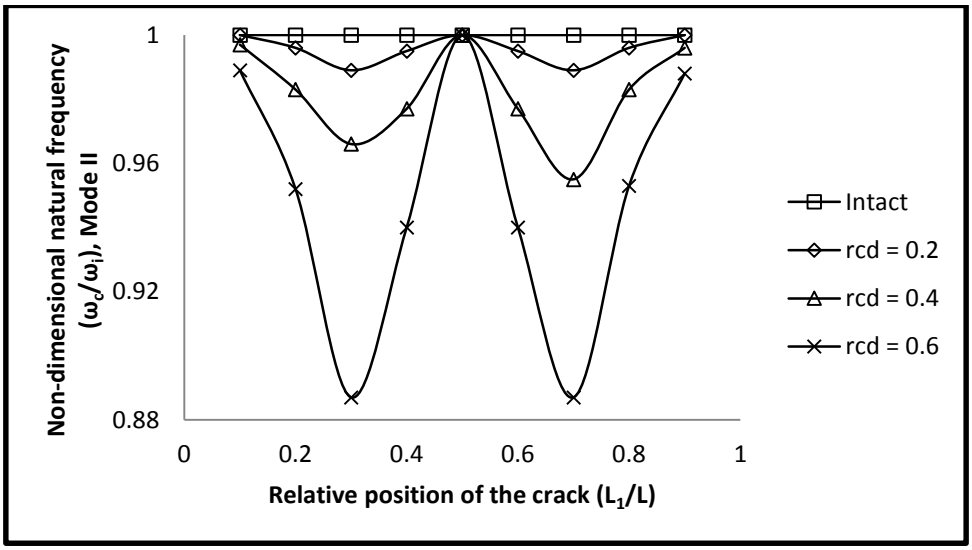

Figure 6.24 Variation of non-dimensional frequency (ω_c/ω_i), Mode II with relative crack location (L_1/L) for different relative crack depths (rcd) of the uniform fixed-fixed beam

Referring to Fig. 6.23, it is observed that the non-dimensional natural frequencies in first mode are not affected by the presence of the crack near 0.2L from either support for any depth of the crack for fixed-fixed end conditions. Crack near the supports i.e. at 0.1L from either supports reduces the free vibration frequencies in first mode by 0.7%, 2.8% and 6.7% than intact beam for relative crack depths of 0.2, 0.4 and 0.6 respectively. Similarly crack at mid-span reduces

the non-dimensional free vibration frequencies in first mode by 1.0%, 4.0% and 11.0% than intact beam for relative crack depths of 0.2, 0.4 and 0.6 respectively. Hence a fixed-fixed beam is more affected by the presence of the crack near supports or mid-span when the beam vibrates in first mode natural frequency than the crack at any other location.

Similarly in Fig. 6.24, it is observed that the second mode natural frequencies are least affected by the presence of the crack near supports or at mid-span for any depth of the crack. On the other hand crack at 0.3L from either supports very much affects natural frequency of second mode, where the reduction in frequencies are found to be 1.1%, 4.5% and 11.3% than intact beam for relative crack depths of 0.2, 0.4 and 0.6 respectively. Similarly variation of non-dimensional natural frequency for third mode with respect to different crack location and depth is plotted in Fig. 6.25.

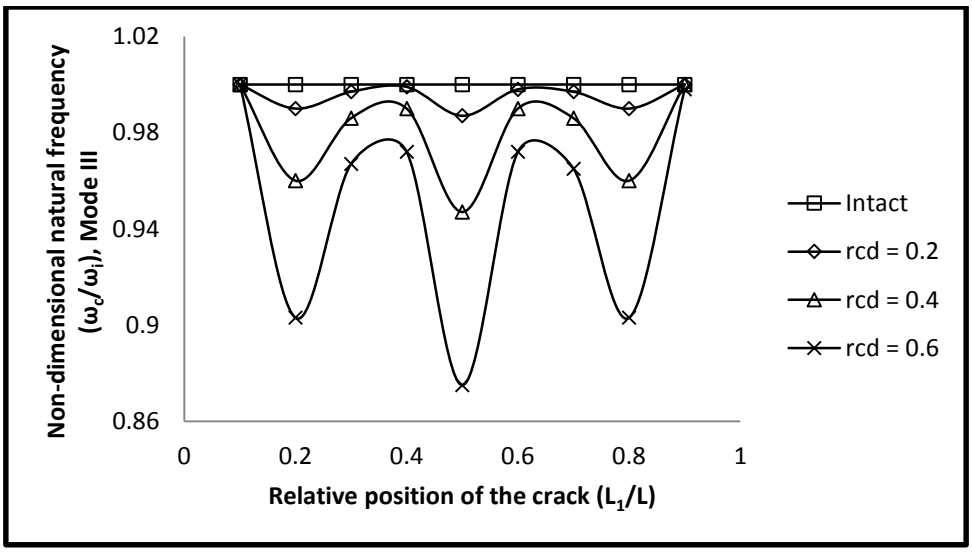

Figure 6.25 Variation of non-dimensional frequency (ω_c/ω_i), Mode III, with relative crack location (L_1/L) for different relative crack depths (rcd) of the uniform fixed-fixed beam

It is observed that the non-dimension free vibration frequencies for the crack at 0.1L or 0.9L are not affected at all for any depth of crack. Similarly presence of crack between 0.3L and 0.4L from either support marginally affects the third mode free vibration frequencies. But the free vibration frequencies in third mode decrease by 1.0%, 4.0% and 9.7% than intact beam for relative crack depths of 0.2, 0.4 and 0.6 respectively, when the crack is at 0.2L from either support. On the other hand crack at mid-span reduces free vibration frequencies in third mode by 1.3%, 5.3% and 12.5% than intact beam for relative crack depth of 0.2, 0.4 and 0.6 respectively. This suggests the presence of crack near 0.2L from either supports or at mid-span

is very vulnerable as far as natural frequency in third mode is concerned. The variation of non-dimensional natural frequencies in fourth mode with location of crack for different depths of crack are plotted in Fig. 6.26.

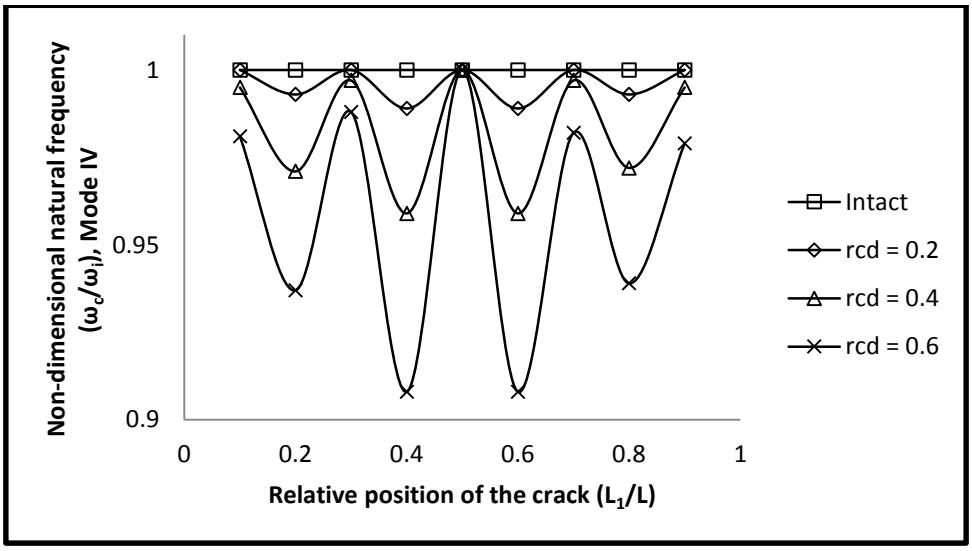

Figure 6.26 Variation of non-dimensional frequency (ω_c/ω_i), Mode IV, with relative crack location (L_1/L) for different relative crack depths (rcd) of the uniform fixed-fixed beam

Referring to the Fig. 6.26, it is observed that the free vibration frequencies in fourth mode are not at all affected by the presence of crack at mid-span. Similarly the crack at 0.3L from either support reduces the fourth mode free vibration frequencies marginally. But crack at 0.4L from each support brings down the free vibration frequencies in fourth mode by 1.1%, 4.1% and 9.2% than intact beam for relative crack depths of 0.2, 0.4 and 0.6 respectively. Crack at 0.2L from the supports also moderately affects in bringing down the non-dimensional natural frequency in fourth mode.

6.5.5 Stepped fixed-free beam

Free vibration analysis is carried out for the stepped beam shown in Fig. 6.5 for different relative crack depths (rcd) and relative location (L_1/L) of the crack from fixed end. The variation of non-dimensional natural frequencies in first mode with relative position of the crack for different relative crack depths are shown in Fig. 6.27.

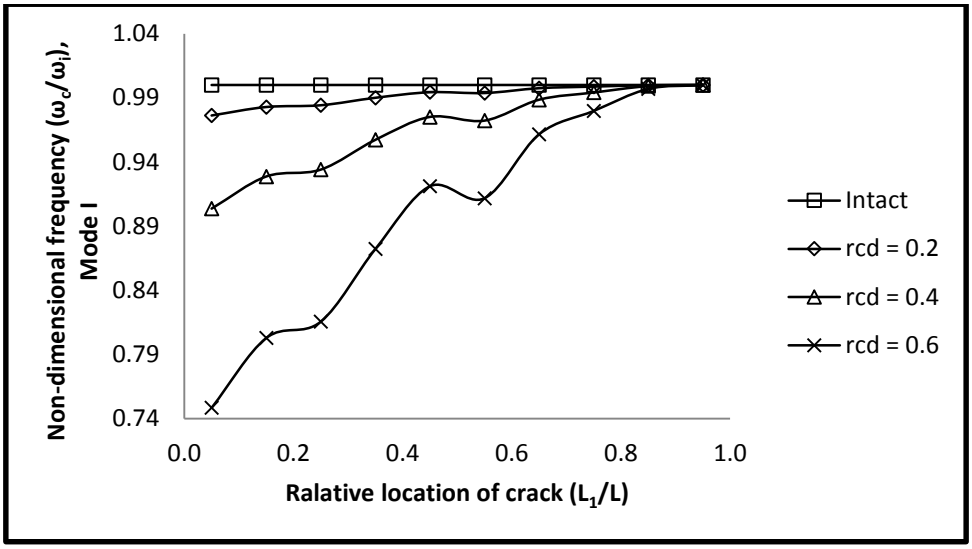

Figure 6.27 Variation of non-dimensional fundamental frequency (ω_c/ω_i) with relative crack location (L_1/L) for different relative crack depths (rcd) of the stepped fixed-free beam

It is observed that the non-dimensional natural frequency in first mode decrease with increase in relative depth of the crack for any location of the crack. It also observed that the non-dimensional free vibration frequencies increase with the crack moving away from the fixed end for all depths of the crack. The crack near the fixed end i.e. crack at 0.05*L* from the fixed end reduces the non-dimensional free vibration frequencies by 2.4%, 9.6% and 25.2% than intact beam for relative crack depth of 0.2, 0.4 and 0.6 respectively. When the crack is at 0.95*L* i.e. near free end, the frequencies are same as that of intact beam. It is also observed the non-dimensional free vibration frequencies decrease by 19.7% and 18.5% for the crack at 0.15*L* and 0.25*L* from fixed end respectively for relative crack depth of 0.6. This implies there is a marginal gain in natural frequency in first mode as the crack shifts from 0.15*L* to 0.25*L* from the fixed end. This is due to the fact that the depth of the beam at 0.25*L* from fixed end suddenly decreases from 14 mm to 12 mm (14.3%). Similarly the non-dimensional free vibration frequencies decrease by 7.9% for the crack at 0.45L and by 8.8% for the crack at 0.55*L* from the fixed end for relative depth of 0.6 of the crack. The reduction in first mode frequency of the beam between the cracks at 0.45*L* and 0.55*L* from the fixed end is due to the fact that there is a great loss of stiffness of the beam at 0.5*L* as the depth of the stepped beam decreases from 12 mm to 8 mm (33.33%) at the section. More over the relative crack depth of 0.6 for the first segment results in a crack depth of 8.4 mm in a depth of 14 mm and that in second segment is 7.2 mm in a depth of 12 mm and 4.8 mm in a depth of 8 mm in third segment. According to

the Fig. 6.27 it can be concluded that the variation of the non-dimensional free vibration frequencies with relative position of the crack for different relative crack depths does not change uniformly as the section is not uniform throughout. It decreases abruptly at the steps which is due to sudden decrease in stiffness of the section. The variation of second mode non-dimensional natural frequencies with different crack location from fixed end for various relative crack depths are shown in Fig. 6.28.

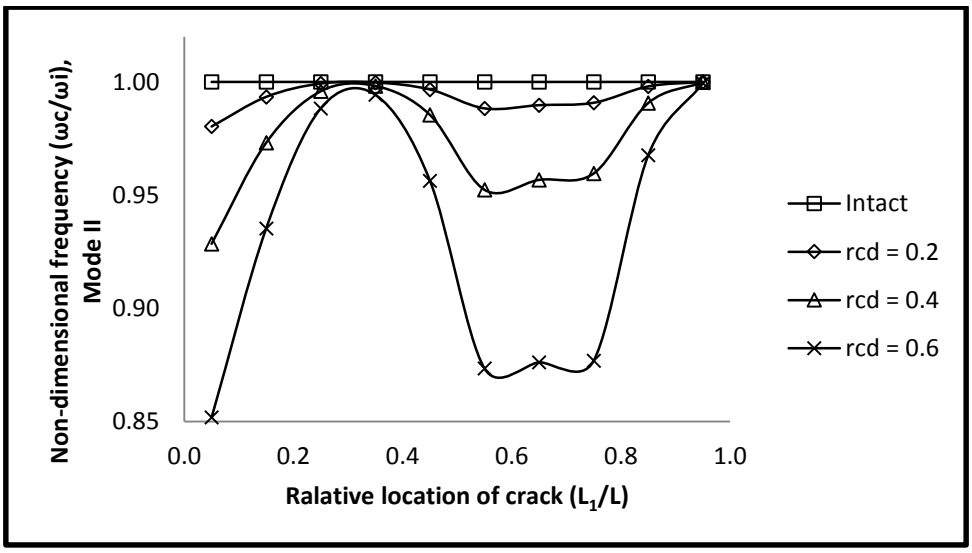

Figure 6.28 Variation of non-dimensional frequency (ω_c/ω_i), Mode II, with relative crack location (L_1/L) for different relative crack depths (rcd) of the stepped fixed-free beam

It is observed that free vibration frequencies in second mode decrease by 2.0%, 7.1% and 14.8% than intact beam frequencies for the crack near fixed end i.e. 0.05*L* for relative depths of 0.2, 0.4 and 0.6 respectively. Whereas the natural frequency in second mode decrease by 1.2%, 4.8% and 12.7% for the crack at 0.55*L*; 1.0%, 4.3% and 12.4% for the crack at 0.65L and 0.9%, 4.0% and 12.3% for the crack at 0.75L from fixed end for relative crack depths of 0.2, 0.4 and 0.6 respectively. Similarly the second mode non-dimensional free vibration frequencies are negligibly affected for the crack between 0.25L to 0.35L from fixed end for all crack depths. The variation of free vibration non-dimensional frequency in third mode for different location and depth of the crack for the stepped beam is plotted in Fig. 6.29.

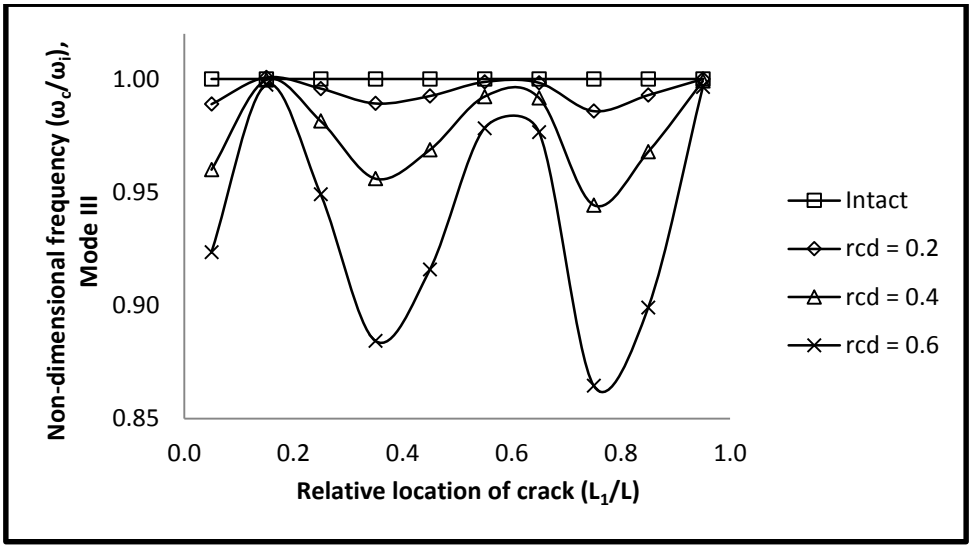

Figure 6.29 Variation of non-dimensional frequency (ω_c/ω_i), Mode III, with relative crack location (L_1/L) for different relative crack depths (rcd) of the stepped fixed-free beam

It is observed that the crack near the fixed end has moderate impact in reducing the frequencies than intact beam. But the crack at 0.15L or at 0.95L doesn't seem to affect the natural frequency in third mode. From the above figure it is observed that presence of crack near 0.35*L* reduce the non-dimensional free vibration frequencies in third mode by 1.1%, 4.4% and 11.6% than intact beam for relative crack depth of 0.2, 0.4 and 0.6 respectively. Similarly presence of crack at 0.75*L* reduce the third mode frequencies by 1.4%, 5.6% and 13.5% and the crack at 0.85*L* reduce the frequencies by 0.7%, 3.2% and 10.1% than intact beam for relative crack depths of 0.2, 0.4 and 0.6 respectively. This implies the crack at 0.75*L* from the fixed end is critical when the relative crack depth is up to 0.6 and the crack at 0.85*L* is critical for relative crack depth of 0.8. This shows the crack at 0.75*L* or 0.85*L* is critical for the beam freely vibrating in third mode depends upon the depth of the crack. It is also observed that the presence of the crack between 0.5*L* and 0.6*L* has moderate effect in reducing natural frequency in third mode. The variation of non-dimensional natural frequency in fourth mode with different location of crack from the fixed end is plotted in Fig. 6.30 for different relative crack depths.

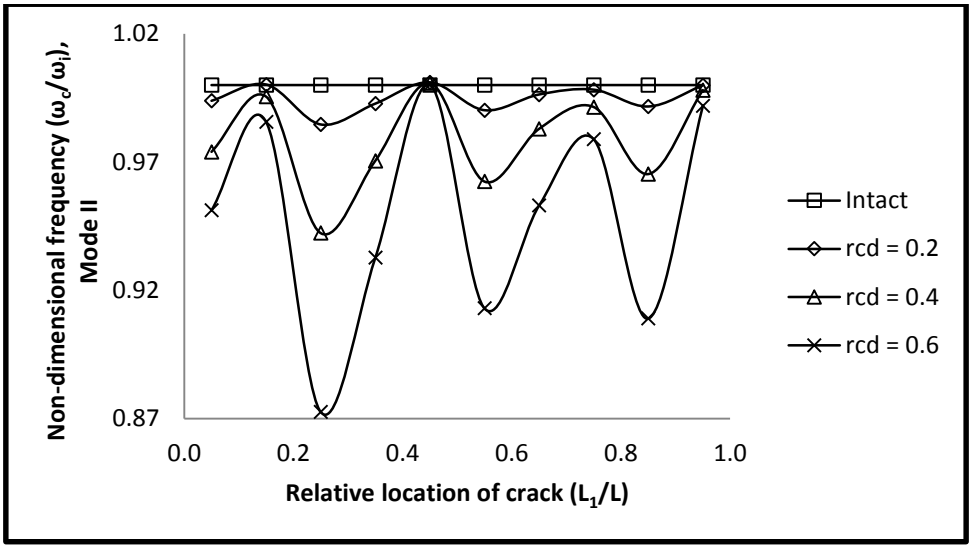

Figure 6.30 Variation of non-dimensional frequency (ω_c/ω_i), Mode IV, with relative crack location (L_1/L) for different relative crack depths (rcd) of the stepped fixed-free beam

According to the figure, the crack near support (0.05*L*) or free end (0.95*L*) has moderate effect in reducing natural frequency in fourth mode, but the crack at 0.45L does not affect the frequencies at all. It is also observed that the cracks near 0.15L and 0.75L have little effect in reducing the natural frequency in fourth mode whereas the cracks at 0.25L, 0.55L and 0.75L have considerable effect. Among the three locations where the effect of crack is predominant, the crack at 0.25L is the most critical. Here the presence of the crack reduces the free vibration frequencies in fourth mode by 1.5%, 5.8%, 12.7% and 20.3% than intact beam for relative crack depths of 0.2, 0.4, 0.6 and 0.8 respectively.

6.6 Vibration of Beam Subjected to Multiple Cracks

6.6.1 Uniform fixed-free beam

Effects of multiple cracks on free vibration frequencies are studied for the beam shown in Fig. 6.4. Beams with two and three cracks are considered. For a beam with two cracks, first crack is considered at 0.1L from left support of relative crack depth 0.3 while the second crack is located between 0.05L to 0.9L from left support of different depths. Similarly in the beam with three cracks, the first crack is considered at 0.1L of relative depth 0.3, second crack is considered at 0.2L of relative depth 0.2 and the third crack is considered between 0.05L to 0.95L of different depths. Non-dimensional free vibration frequencies for four modes are computed for beams with two and three cracks for different locations and depths for Fixed-

Free end conditions. The variation of non-dimensional free vibration frequencies in first mode are computed and plotted in Fig. 6.31 for the Fixed-Free beam with two cracks.

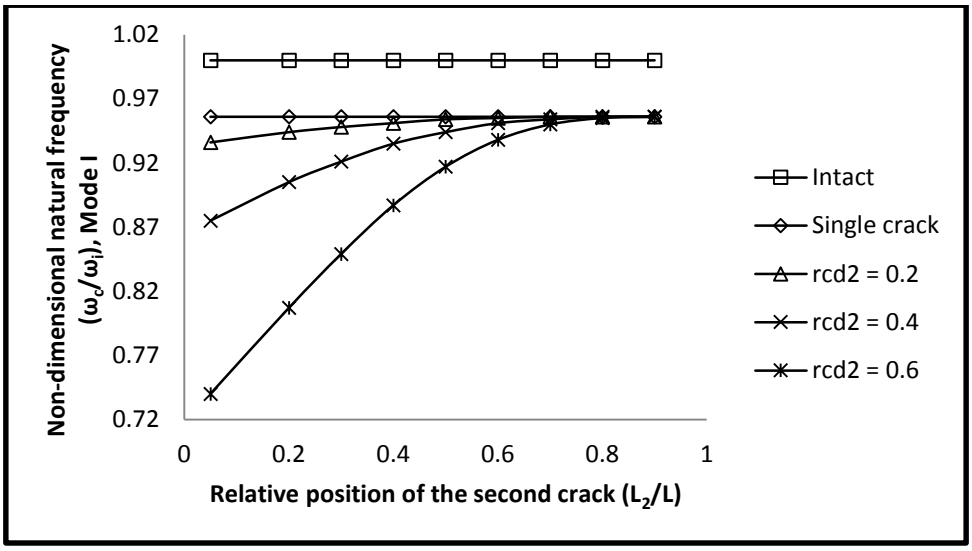

Figure 6.31: Variation of non-dimensional fundamental frequency (ω_c/ω_i) with relative location of the second crack (L_2/L) for different relative crack depths (rcd) of the fixed-free beam (L_1= 0.1L, rcd_1 = 0.3)

It is observed from Fig. 6.31 that the non-dimensional free vibration frequencies for first mode decrease by 4.3% than intact beam for first crack only at 0.1L from fixed beam of relative crack depth 0.3. But with the introduction of the second crack at 0.05L from fixed support the decrease in the frequencies are found to be 6.4%, 12.5% and 26.0% for relative crack depths of 0.2, 0.4 and 0.6 respectively. When the second crack is nearly at the free end, the non-dimensional frequencies reduce by 4.3% which is also the drop in frequencies due to first crack only. This implies when the second crack happens to be near the free end its effect is negligible. On the other hand maximum drop in non-dimensional frequencies for the crack at 0.05L i.e. near the fixed end suggests the vulnerability of the crack near fixed end. Similarly the variation of non-dimensional free vibration frequencies in first mode are computed and plotted in Fig. 6.32 for the Fixed-Free beam subjected to three cracks.

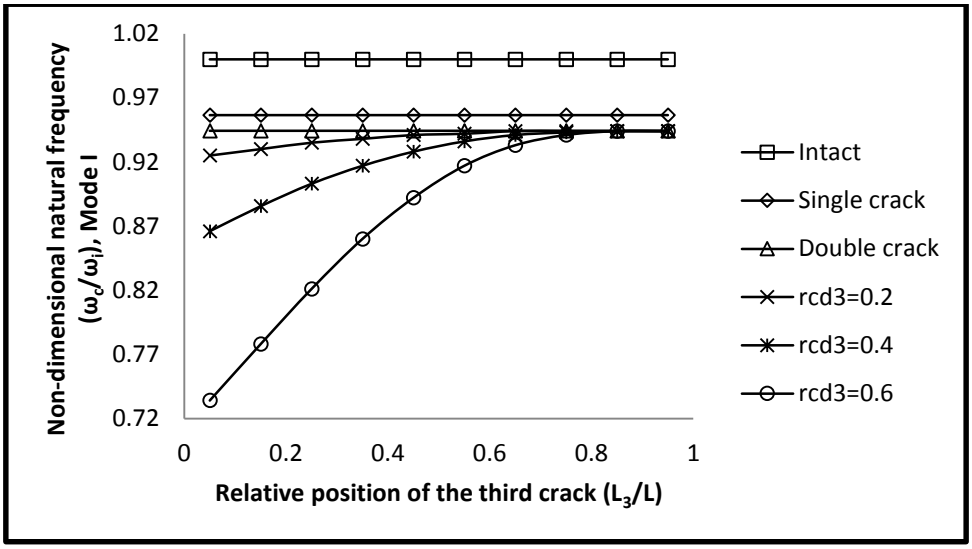

Figure 6.32: Variation of non-dimensional fundamental frequency (ω_c/ω_i) with relative location of the third crack (L_3/L) for different relative crack depths (rcd) of the fixed-free beam (L_1=0.1L, L_2=0.2L, rcd_1=0.3, rcd_2=0.2)

It is observed that the drop in non-dimensional free vibration frequencies in first mode compared to intact beam is 4.3% for first crack only at 0.1L of relative crack depth 0.3. The drop natural frequencies in first mode is 5.6% with the introduction of second crack at 0.2L of relative crack depth 0.2. This implies the effect of second crack reduce the frequency additionally by 1.3% over the first crack. But when third crack is introduced at 0.05L (very close to fixed support) the non-dimensional free vibration frequencies decreased further to 7.5%, 13.4% and 26.6% than intact beam for relative crack depths of 0.2, 0.4 and 0.6 respectively. Similarly for the third crack at 0.95L i.e. very close to free end, the non-dimensional free vibration frequencies are found to be lesser by 5.6% than intact beam. This again suggests crack near free end of a cantilever beam has no effect on free vibration frequencies. Variation of non-dimensional natural frequencies in second mode for different location and depth of second crack are shown in Fig. 6.33.

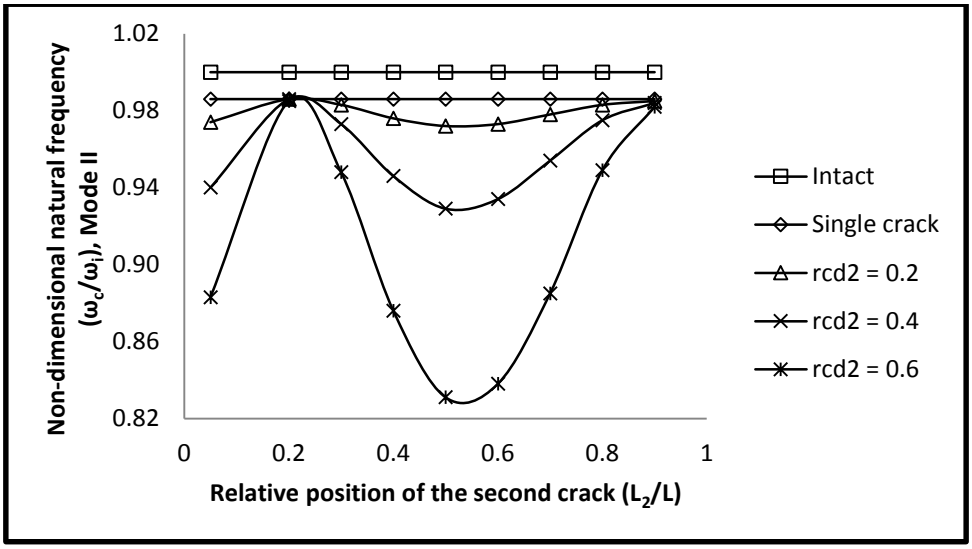

Figure 6.33: Variation of non-dimensional frequency (ω_c/ω_i), Mode II, with relative location of the second crack (L_2/L) for different relative crack depths (rcd) of the fixed-free beam (L_1= 0.1L, rcd_1 = 0.3)

It is observed that the non-dimensional free vibration frequencies in second mode decrease by 1.4% for the beam with first crack only at 0.1L of relative depth 0.3. The addition of the second crack at 0.05L brings down the same frequencies by 2.6%, 6.0% and 11.7% for relative crack depths of 0.2, 0.4 and 0.6 respectively. But when the second crack is placed at 0.2L the decrease in non-dimensional free vibration frequencies in second mode is 1.4%, 1.4% and 1.5% for relative crack depths of 0.2, 0.4 and 0.6 respectively. This implies the second crack at 0.2L hardly affects the natural frequency in second mode. But as the second crack moves further away from the fixed end, frequencies in second mode decrease. When the second crack is positioned at mid-span the drop is found to be 2.8%, 7.1% and 16.9% for relative crack depths of 0.2, 0.4 and 0.6 respectively than intact beam. Similarly as the second crack shifts further towards free end of the fixed-free beam the non-dimensional free vibration frequencies get closure to that of beam with single crack only at 0.1L of relative crack depth 0.3. This implies the second mode frequencies are severely affected by the crack at mid-span than anywhere else. Variation of non-dimensional natural frequencies in second mode for different location and depth of third crack is shown in Fig. 6.34.

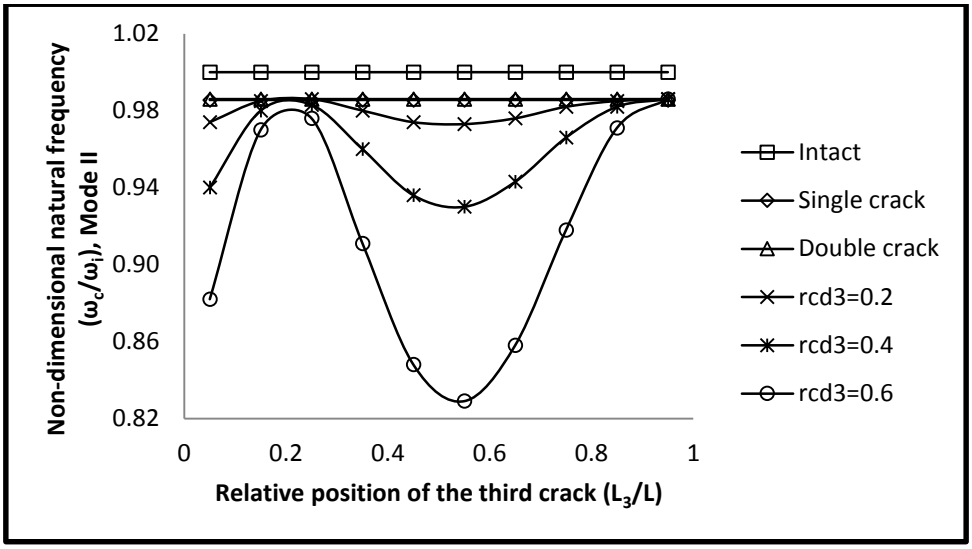

Figure 6.34: Variation of non-dimensional frequency (ω_c/ω_i), Mode II, with relative location of the third crack (L_3/L) for different relative crack depths (rcd) of the fixed-free beam (L_1=0.1L, L_2=0.2L, rcd_1=0.3, rcd_2=0.2)

It is observed that the first crack alone reduce the non-dimensional frequencies in second mode by 1.4% than intact beam. Similarly the first two cracks alone reduce the non-dimensional free vibration frequencies in second mode by 1.4% as the second crack at 0.2L has no effect in frequencies of second mode. But with the inclusion of the third crack at 0.05L the same frequencies decrease by 2.6%, 6.0% and 11.8% for relative crack depths of 0.2, 0.4 and 0.6 respectively. When the third crack is between 0.15L and 0.25L, the non-dimensional free vibration frequencies in second mode are marginally affected by the third crack. This is because the second mode frequencies are not affected by the presence of crack near 0.2L for a Fixed-Free beam and with the inclusion of the third crack the nodal point of second mode frequency shifts a little towards free end. As the third crack moves further away from the fixed end the non-dimensional frequencies in second mode decrease rapidly till the third crack is at mid-span. The non-dimensional free vibration frequencies in second mode decrease by 2.7%, 7.0% and 17.1% than intact beam for relative crack depths of 0.2, 0.4 and 0.6 respectively for the third crack at 0.55L. Similarly the effect of third crack vanishes when its position is at 0.95L i.e. the reduction in free vibration frequencies are 1.4% for all relative crack depths which is also the reduction in frequencies due to first two cracks only. The variations of non-dimensional natural frequencies in third mode for different location and depth of second crack are shown in Fig. 6.35 for beams with fixed-free end conditions.

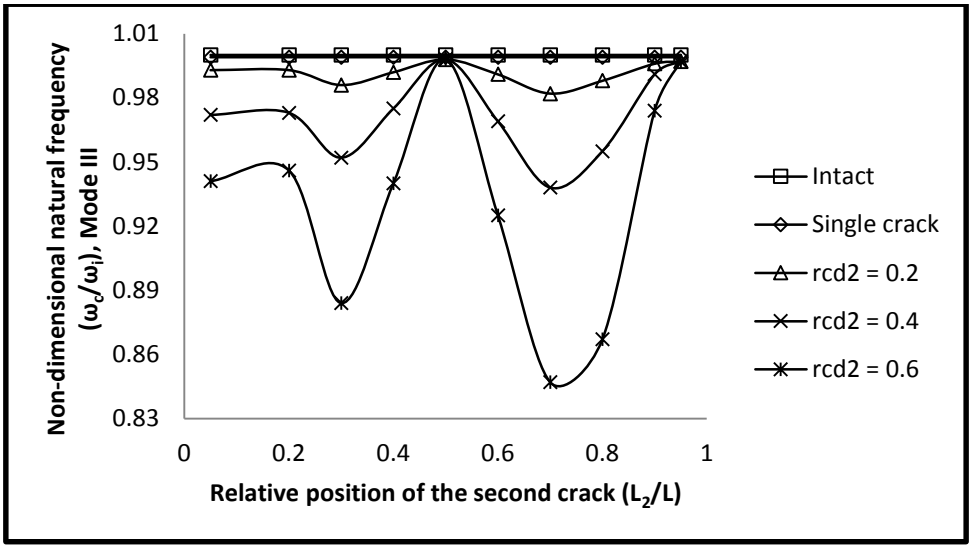

Figure 6.35: Variation of non-dimensional frequency (ω_c/ω_i), Mode III, with relative location of the second crack (L_2/L) for different relative crack depths (rcd) of the fixed-free beam (L_1= 0.1L, rcd_1 = 0.3)

It is observed that the presence of first crack alone at 0.1L of relative depth 0.3 brings down the free vibration frequencies by only 0.1%. When the second crack is introduced at 0.05L, the third mode natural frequencies decreases by 0.7%, 2.8% and 5.9% for relative crack depths of 0.2, 0.4 and 0.6 respectively. This implies the third mode frequencies are moderately affected by the cracks near the fixed end. As the second crack shifts away from the fixed end, the free vibrational frequencies in third mode decrease by 0.7%, 2.7% and 5.4% than intact beam for the second crack at 0.2L and the same reduces by 1.4%, 4.8% and 11.6% than intact beam when the crack is at 0.3L from fixed end for relative crack depths of 0.2, 0.4 and 0.6 respectively. Similarly the non-dimensional free vibration frequencies in third mode decrease marginally for all relative crack depths of second crack at 0.5L from fixed end. This shows that the second crack at 0.5L has no effect on natural frequencies of third mode for a Fixed-Free beam. The non-dimensional free vibration frequencies in third mode decrease by 1.8%, 6.2% and 15.3% for relative depths of 0.2, 0.4 and 0.6 for the second crack positioned near 0.7L resulting in maximum influence of the crack. Similarly there is approximately a reduction of 0.3% in non-dimensional free vibration frequencies in third mode when the crack is at 0.95L. This implies the crack near the free end of a cantilever beam has no effect in reducing free vibration frequencies in third mode. The variation of non-dimensional natural frequencies in third mode for three cracks are shown for different location of third crack in Fig. 6.36.

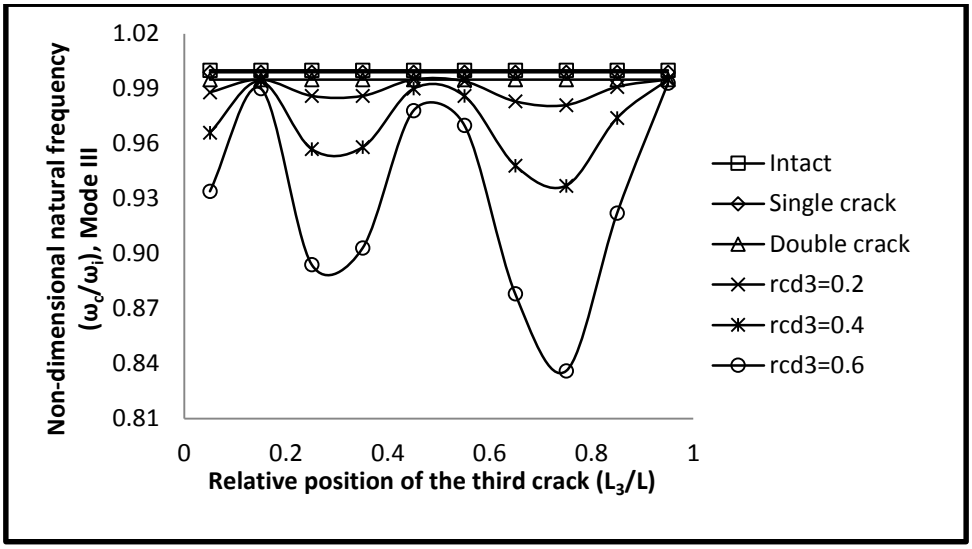

Figure 6.36: Variation of non-dimensional frequency (ω_c/ω_i), Mode III, with relative location of the third crack (L_3/L) for different relative crack depths (rcd) of the fixed-free beam (L_1=0.1L, L_2=0.2L, rcd_1=0.3, rcd_2=0.2)

It is observed that the non-dimensional natural frequencies in third mode decrease by 0.5% for first crack at 0.1L of relative depth 0.3 and the second crack at 0.2L of relative depth 0.2. This implies inclusion of the second crack at 0.2L brings down the non-dimensional frequencies in third mode by 0.4% more than the beam with the first crack only. Third crack at 0.15L or 0.95L does not affect the free vibration frequencies in third mode for any depth of the crack. Similarly the third crack near mid-span has very little or no effect on reducing the free vibration frequencies in third mode. Presence of the third crack near mid-span brings down the free vibration frequencies in third mode by 0.5%, 0.5% and 1.0% which is almost the same as the free vibration of the beam with first two cracks only. The reductions in free vibration frequencies of third mode for the crack near 0.25L is 1.4%, 4.3% and 10.6%, for the crack at 0.75L from fixed end the same reduce by 1.9%, 6.3% and 16.4% than intact beam for relative crack depths of 0.2, 0.4 and 0.6 respectively. This implies crack at 0.75L has a bigger reducing effect of frequencies than the crack at 0.25L for third mode of free vibration. The variation of non-dimensional frequencies in fourth mode for two cracks are plotted for different location and depth of the second crack for a doubly cracked beam in Fig. 6.37.

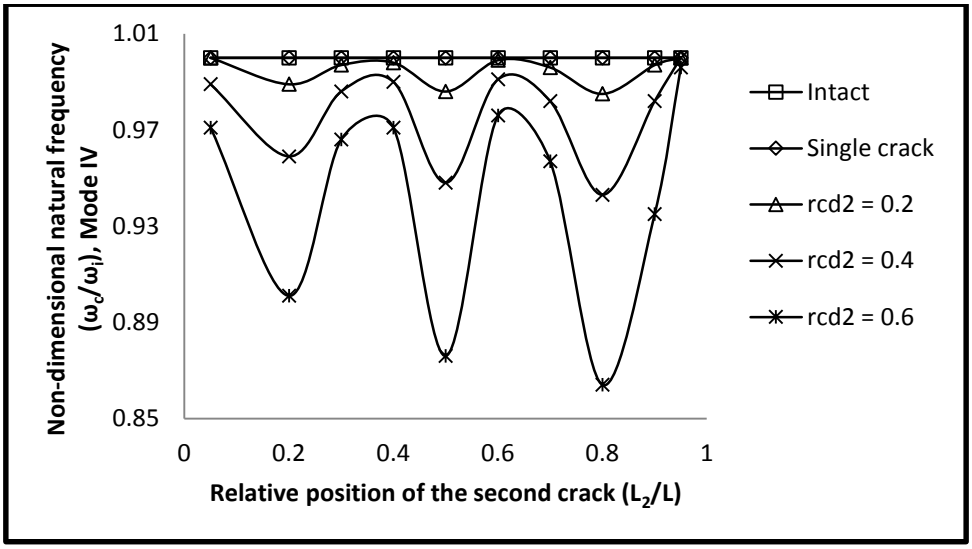

Figure 6.37: Variation of non-dimensional frequency (ω_c/ω_i), Mode IV, with relative location of the second crack (L_2/L) for different relative crack depths (rcd) of the fixed-free beam (L_1= 0.1L, rcd_1 = 0.3)

According to the above figure the non-dimensional frequencies in fourth mode are not affected by the presence of only the first crack at 0.1L of relative crack depth 0.3. That is because the presence of crack near the fixed end i.e. at 0.1L does not much affect the free vibration frequencies in fourth mode. From Fig. 6.37, it can be concluded that the position of the second crack near fixed end (0.05L) or free end (0.95L) does not affect the free vibration frequencies in fourth mode as the drop in frequencies for those two locations are very small. Similarly the effect of second crack near L/3 or 2L/3 is very little. But the non-dimensional free vibration frequencies in fourth mode reduce by 1.1%, 4.1% and 9.9% for the presence of the second crack at 0.2L, the reduction in same frequencies were 1.4%, 5.2% and 12.4% for the second crack at 0.5L and the reduction in same frequencies for the second crack at 0.8L are given by 1.5%, 5.7% and 13.6% than intact beam for relative crack depth of 0.2, 0.4 and 0.6 respectively. This implies the reduction in non-dimensional free vibration frequencies in fourth mode decrease increasingly for the second crack location moving away from fixed end. The variations of non-dimensional natural frequencies in fourth mode for three cracks are shown for different location and depth of third crack Fig. 6.38.

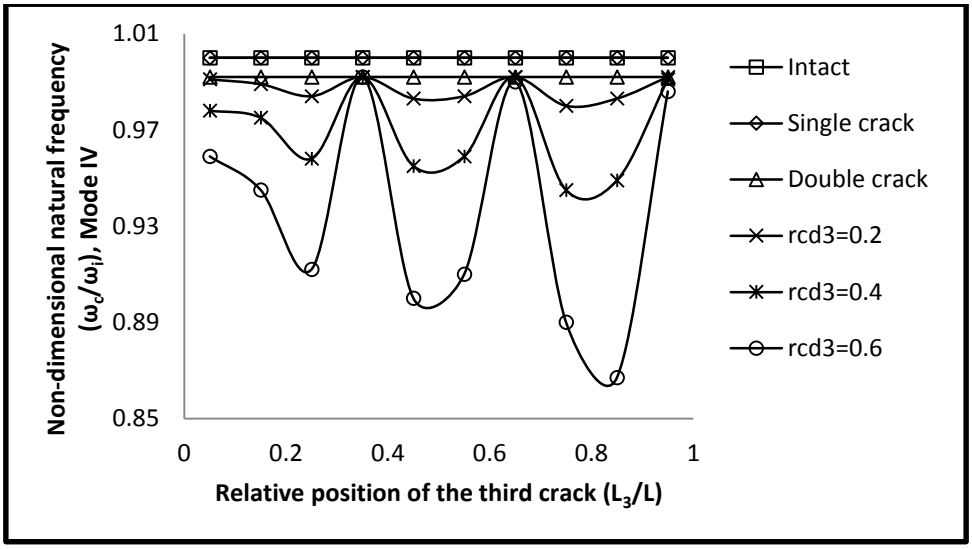

Figure 6.38: Variation of non-dimensional frequency (ω_c/ω_i), Mode IV, with relative location of the third crack (L_3/L) for different relative crack depths (rcd) of the fixed-free beam (L_1=0.1L, L_2=0.2L, rcd_1=0.3, rcd_2=0.2)

It is observed that the variation of the non-dimensional free vibration frequencies in fourth mode for different locations and depths of the third crack. From the Fig. 6.38 it is found that the non-dimensional free vibration frequencies in fourth mode do not change due to first crack only at 0.1L of relative depth 0.3 and the same dropped by 0.8% for inclusion of the second crack at 0.2L of relative crack depth 0.2. The third crack at 0.05L decreased the above frequencies by 0.9%, 2.2% and 4.1% for relative crack depths of 0.2, 0.4 and 0.6 respectively. This shows when the cracks are near the fixed end of the cantilever beam the fourth mode frequencies are not very much affected by their position. Similar to the variation of non-dimensional free vibration frequencies in fourth mode for different position of second crack in a doubly cracked beam in Fig. 6.37, a beam with three cracks has similar trend of variation of frequencies in fourth mode in Fig. 6.38. There is very little or no decrease in frequencies for the third crack near 0.35L or 0.65L for all relative depths of the cracks. It is also observed that the decrease in non-dimensional frequencies in fourth mode decrease by 1.6%, 4.2% and 8.8% for third crack at 0.25L, decrease by 1.7%, 4.5% and 10.0% for third crack at 0.45L and decrease by 1.7%, 5.1% and 13.3% for third crack at 0.85L than intact beam for relative depths of 0.2, 0.4 and 0.6 of the cracks respectively.

6.6.2 Stepped fixed-free beam

The three stepped cantilever beam shown in Fig. 6.5 subjected to multiple cracks is considered for free vibration study. Multiple cracks at different locations are considered of same relative depth (*a/h*). The variation of first mode non-dimensional natural frequency with relative crack depths for various location of two and three cracks are studied and plotted in Fig. 6.39 and 6.40 respectively.

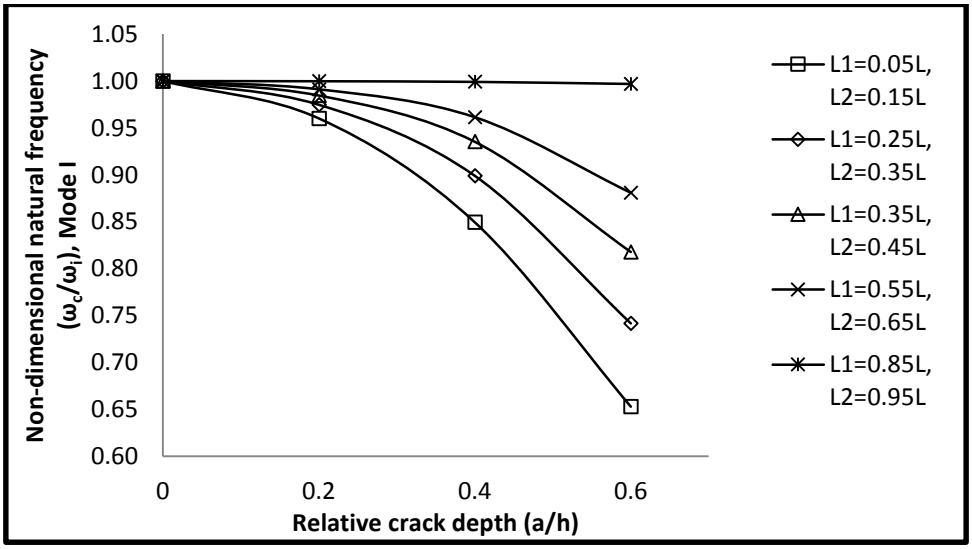

Figure 6.39 Variation of non-dimensional fundamental frequency (ω_c/ω_i) with relative crack depth (*a*/*h*) for different relative crack locations of two cracks the stepped fixed-free beam

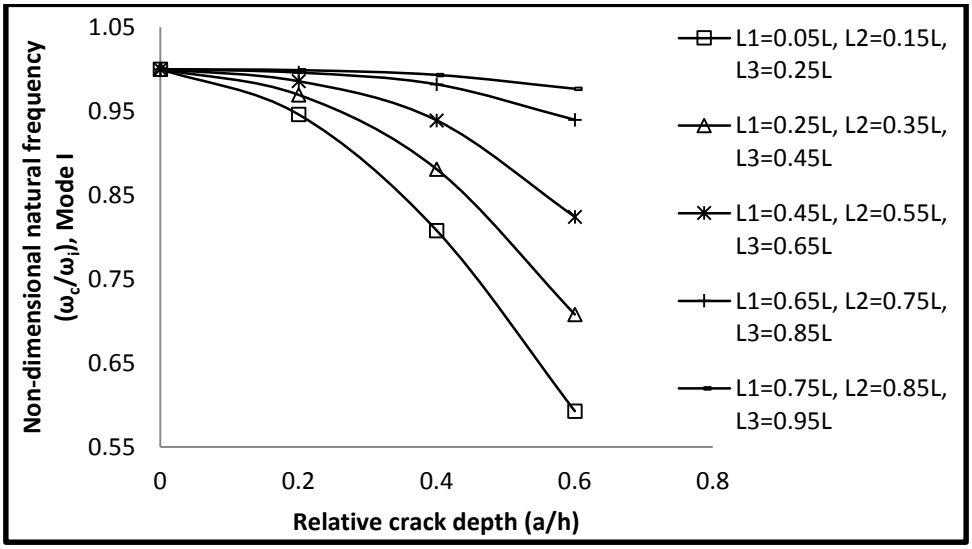

Figure 6.40 Variation of non-dimensional frequency (ω_c/ω_i), Mode I, with relative crack depth (*a*/*h*) for different relative locations of three cracks in the stepped fixed-free beam

Referring to Fig. 6.39 and 6.40, it is observed that the first mode non-dimensional natural frequencies decreases with increase in relative crack depth for all locations of cracks. However the cracks near to fixed end affects the first mode non-dimensional frequency more than the cracks at any other location. As the position of cracks shifts away from the fixed end, their effect gradually decreases. In Fig. 6.39, the non-dimensional natural frequencies in first mode for the cracks to be at 0.05L and 0.15L decrease by 4.0%, 15.1% and 34.7% than the intact beam frequencies for relative crack depths of 0.2, 0.4 and 0.6 respectively. In Fig. 6.40, the non-dimensional natural frequencies in first mode decrease by 5.4%, 19.2% and 40.7% than the intact beam frequencies for relative crack depths of 0.2, 0.4 and 0.6 respectively for the cracks to be at 0.05L, 0.15L and 0.25L from fixed end. Referring to Fig. 6.27, the reduction in first mode frequency for single crack of relative depth 0.6 considered separately at 0.05L, 0.15L and 0.25L are 25.2%, 19.7% and 18.5% respectively than intact beam. But when multiple cracks happen to be in the beam simultaneously the net decrease in frequency is found to be lesser than their individual effects taken together on the beam. Similarly as the cracks shifts towards the free end the first mode non-dimensional frequencies almost coincides with those of intact beam suggesting very little or no effect of the cracks. The variation of second mode non-dimensional natural frequency for two and three cracks are shown in Fig. 6.41 and 6.42 respectively.

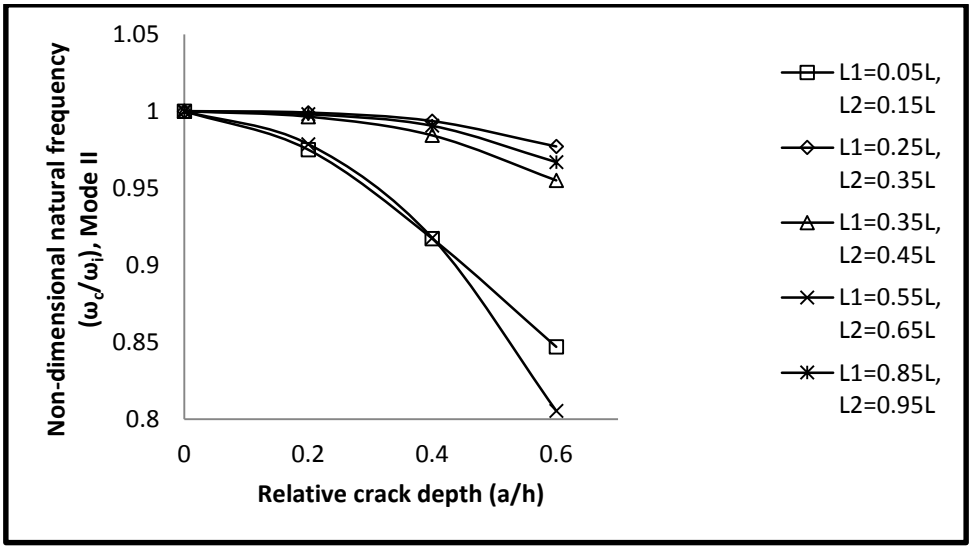

Figure 6.41 Variation of non-dimensional frequency (ω_c/ω_i), Mode II, with relative crack depth (a/h) for different relative crack locations of two cracks the stepped fixed-free beam

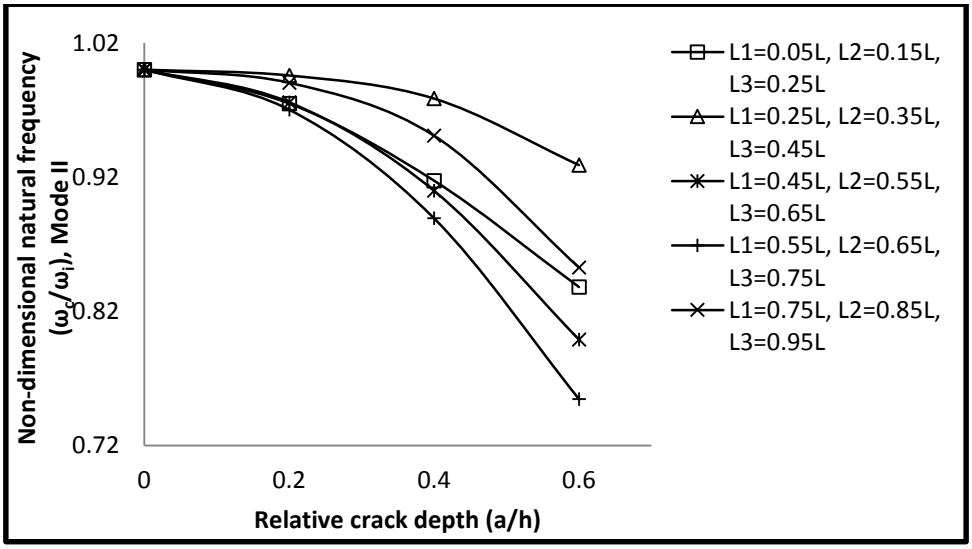

Figure 6.42 Variation of non-dimensional frequency (ω_c/ω_i), Mode II, with relative crack depth (a/h) for different relative locations of three cracks in the stepped fixed-free beam

Referring to Fig. 6.41, the second mode non-dimensional natural frequencies decrease by 2.5%, 8.3% and 15.3% than intact beam for relative crack depths of 0.2, 0.4 and 0.6 respectively when the cracks are at 0.05L and 0.15L (near fixed end). Similarly the cracks at 0.25L and 0.35L reduce the second mode non-dimensional natural frequencies decrease by 0.1%, 0.6% and 2.3% and the cracks at 0.55L and 0.65L reduces the same frequencies by 2.1%, 8.2% and 19.5% for relative crack depths of 0.2, 0.4 and 0.6 respectively. But the cracks at 0.85L and 0.95L (i.e. near free end) reduce the second mode non-dimensional frequencies by 0.2%, 0.9% and 3.3% for relative crack depths of 0.2, 0.4 and 0.6 respectively. Hence the second mode natural frequencies are most affected when the cracks are near 0.55L to 0.65L from fixed end. When the cracks are near fixed end the second mode frequencies are considerably affected. But, there is very little effect of the cracks near free end or near 0.25L to 0.35L from fixed end even if the crack at 0.25L is on the step where the depth of the beam changes from 14 mm to 12 mm. This may be due to the fact that the nodal point of second mode free vibration be in that region. It is also observed that for lower depth of the cracks (rcd = 0.2 and 0.4) the crack near the fixed end was more critical than other locations, but for higher depths (rcd = 0.6) the cracks at 0.55L and 0.65L become critical. This may be due to the fact that a relative crack depth of 0.6 is 8.4 mm deep crack in first segment and 4.8 mm deep in third segment. So, a 6.4 mm deep crack in a depth of 8 mm beam segment is resulting in severe release in strain energy in addition to loss of energy at the step at 0.5L where the depth of the segment changes from 12 mm to 8 mm.

Referring to Fig. 6.42, the beam is least affected by the cracks at 0.25L, 0.35L and 0.45L but are severely affected by the cracks at 0.55L, 0.65L and 0.75L for all depths of the cracks. Cracks at 0.05L, 0.15L and 0.25L brings down the second mode non-dimensional frequencies by 2.5%, 8.3% and 16.2% and cracks at 0.55L, 0.65L and 0.75L brings down the same by 3.0%, 11.1% and 24.5% than intact beam for relative crack depths of 0.2, 0.4 and 0.6 respectively. Similarly the cracks at 0.25L, 0.35L and 0.45L reduce the second mode frequencies by 0.4%, 2.1% and 7.1% and cracks near free end i.e. at 0.75L, 0.85L and 0.95L reduce the same frequencies by 1.0%, 4.9% and 14.7% than intact beam for relative crack depths of 0.2, 0.4 and 0.6 respectively. This implies the multiple cracks present between 0.45L to 0.85L becomes more vulnerable in second mode vibration and the multiple cracks present near fixed end also have considerable impact on second mode frequencies. The variation of non-dimensional natural frequencies in third mode with relative crack depths for different positions of two cracks are shown in Fig. 6.43.

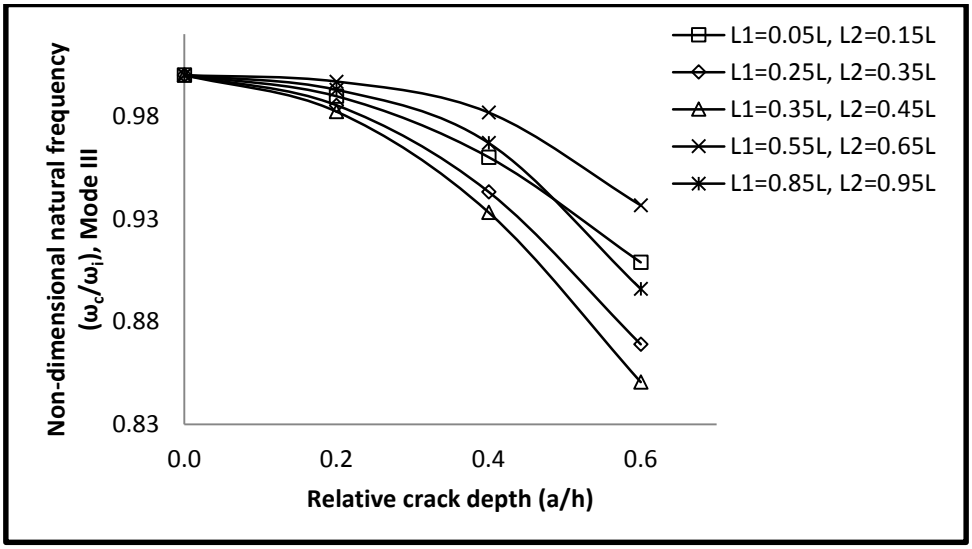

Figure 6.43 Variation of non-dimensional frequency (ω_c/ω_i), Mode III, with relative crack depth (a/h) for different relative crack locations of two cracks the stepped fixed-free beam

It is observed that the cracks near fixed end i.e. at 0.05L and 0.15L decrease third mode natural frequencies by 1.0%, 4.0% and 9.1%, cracks near free end i.e. at 0.85L and 0.95L decrease the same frequencies by 0.7%, 3.3% and 10.4% than intact beam for relative crack depths of 0.2, 0.4 and 0.6 respectively. Similarly the cracks at 0.55L and 0.65L reduce the second mode frequencies by 0.3%, 1.8% and 6.3%, on the other hand the reduction in frequencies for cracks at 0.35L and 0.45L is found to be 1.8%, 6.7% and 15.0% than intact beam for relative crack depths of 0.2, 0.4 and 0.6 respectively. Hence presence of two cracks between 0.35L to 0.45L

is vulnerable in third mode natural frequency but cracks between 0.55L and 0.65L are less effective. Cracks near the fixed end and free end have moderate impact on third mode frequencies. The variation of non-dimensional natural frequencies in third mode with relative crack depths for different positions of three cracks are shown in Fig. 6.44.

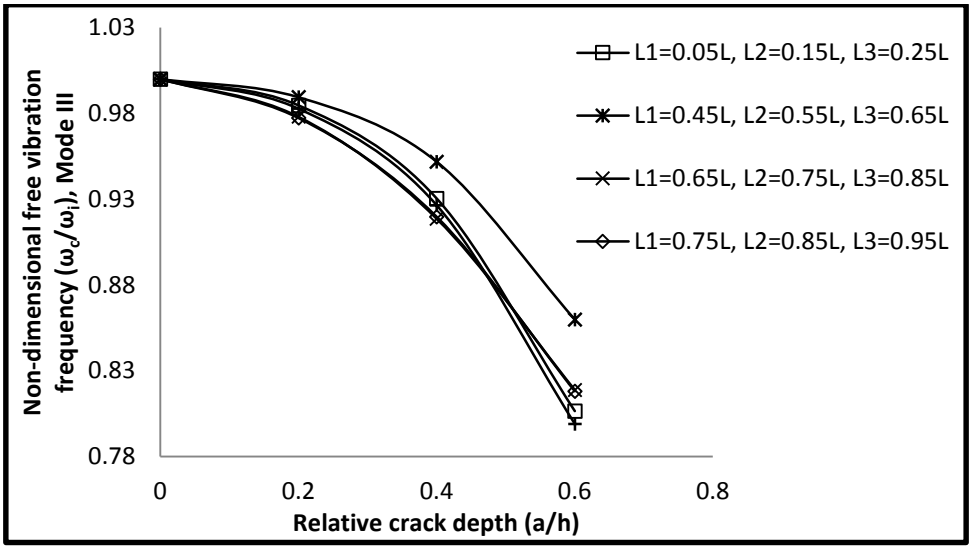

Figure 6.44 Variation of non-dimensional frequency (ω_c/ω_i), Mode III, with relative crack depth (a/h) for different relative locations of three cracks in the stepped fixed-free beam

It is observed from Fig. 6.44 that reduction in third mode natural frequency of the beam due to cracks near fixed end i.e. at 0.05L, 0.15L and 0.25L is given by 1.5%, 7.0% and 19.4% and due to cracks near free end i.e. at 0.75L, 0.85L and 0.95L it is 2.3%, 8.0% and 18.2% than intact beam for relative crack depths of 0.2, 0.4 and 0.6 respectively. It is observed that the cracks near midspan i.e. at 0.45L, 0.55L and 0.65L brings down the third mode frequencies by 1.1%, 4.8% and 14.0% than intact beam for relative crack depths of 0.2, 0.4 and 0.6 respectively. The effect of three cracks at 0.65L, 0.75L and 0.85L and at 0.75L, 0.85L and 0.95L are found to be almost similar. It is observed that the third mode non-dimensional natural frequency is found to be minimum when the three cracks are at 0.75L, 0.85L and 0.95L for relative crack depth of 0.2, at 0.65L, 0.75L and 0.85L for relative crack depth of 0.4 and at 0.55L, 0.65L and 0.75L for relative crack depth of 0.6. This is due to the fact that in third mode free vibration of a single cracked beam the lowest frequency is observed for the crack to be at 0.75, for the double cracked beam the same frequency occurs for the cracks to be between 0.75L and 0.85L. Hence for beams subjected to multiple cracks the cracks near 0.75L brings down the frequency in third mode more than any other location. The variation of non-

dimensional natural frequencies in fourth mode with relative crack depths for different positions of two cracks are shown in Fig. 6.45.

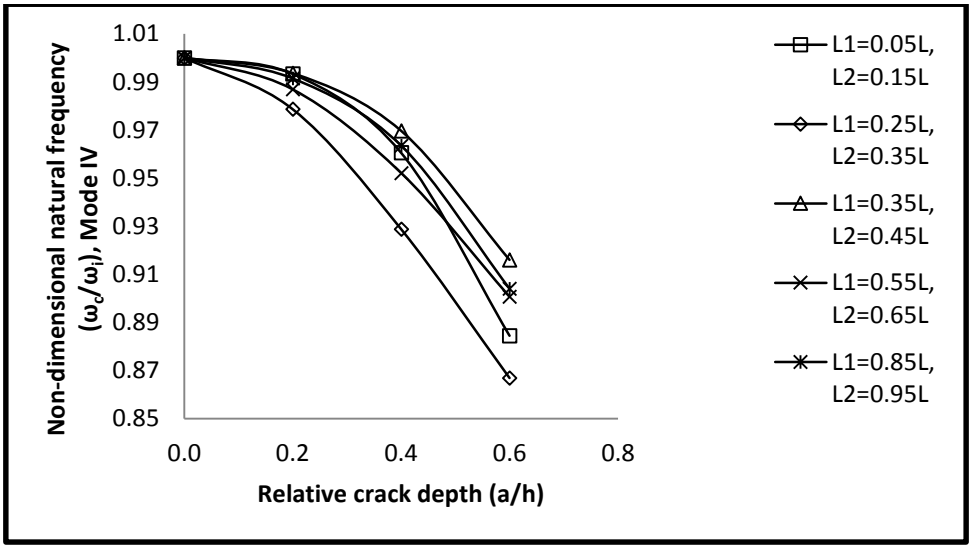

Figure 6.45 Variation of non-dimensional frequency (ω_c/ω_i), Mode IV, with relative crack depth (a/h) for different relative crack locations of two cracks the stepped fixed-free beam

In Fig. 6.45, the maximum drop of natural frequencies is observed when two cracks are placed at 0.25L and 0.35L from fixed end and minimum drop in frequencies occurs when the cracks are at 0.35L and 0.45L from the fixed end. The non-dimensional natural frequencies in fourth mode decrease by 2.1%, 7.1% and 13.3% for cracks to be at 0.25L and 0.35L from fixed end, and by 0.6%, 3.0% and 8.4% for cracks to be at 0.35L and 0.45L from the fixed end than intact beam for relative crack depths 0.2, 0.4 and 0.6 respectively. It is observed that the cracks at 0.05L and 0.15L (near fixed end) records a drop in fourth mode non-dimensional natural frequency by 0.7%, 3.9% and 11.5% and the cracks at 0.85L and 0.95L (near free end) reduce the same frequencies by 0.9%, 3.7% and 9.6% than intact beam frequencies for relative crack depths of 0.2, 0.4 and 0.6 respectively. The variation of fourth mode non-dimensional natural frequency in a beam subjected to three cracks is shown in Fig. 6.46.

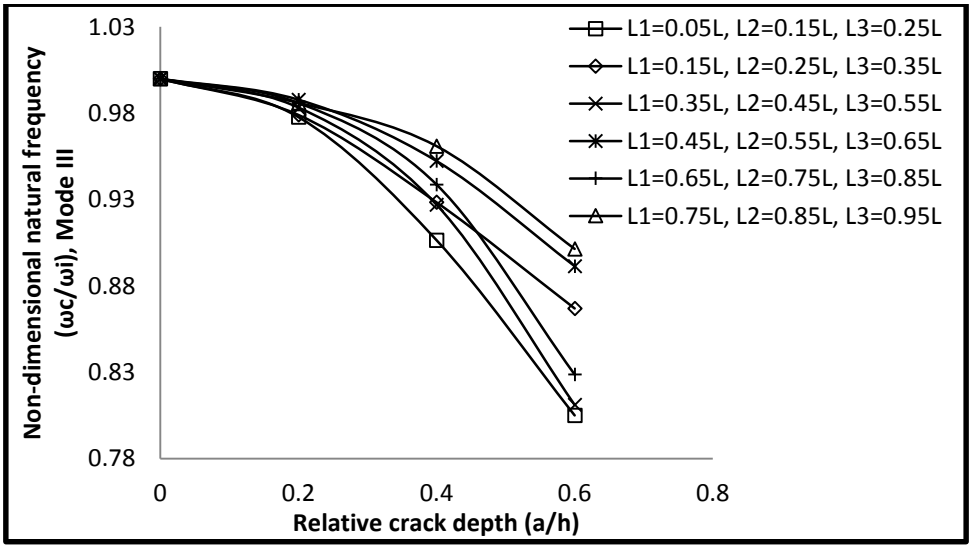

Figure 6.46 Variation of non-dimensional frequency (ω_c/ω_i), Mode IV, with relative crack depth (a/h) for different relative locations of three cracks in the stepped fixed-free beam

Referring to Fig. 6.46, it is observed that the three cracks at 0.05L, 0.15L and 0.25L, near fixed end brings down the non-dimensional natural frequencies in fourth mode by 2.2%, 9.3% and 19.5% for relative crack depth of 0.2, 0.4 and 0.6 respectively. Similarly the cracks near free end given by 0.75L, 0.85L and 0.95L reduce the same frequencies by 1.4%, 3.9% and 9.8% than intact beam frequencies for relative crack depth of 0.2, 0.4 and 0.6 respectively. Among all the locations shown in Fig. 6.46 the cracks near the fixed end suffers the maximum drop in frequencies for all depths of the crack and the cracks near free end gets the minimum. It is also observed that the effect of the cracks affects the beam in a fluctuating manner in a sense that the odd groups of cracks affect the frequencies considerably but the even groups are not similar.

6.7 ANSYS and Experimental Results

Aluminum beam of geometric and material properties; L = 0.3 m, b = h = 0.01 m, E = 68.22 GPa, ρ = 2569 kg/m^3 and v = 0.28 and steel beam of properties; L = 0.3 m, b = h = 0.01 m, E = 200 GPa, ρ = 7660 kg/m^3 and v = 0.3 subjected to open transverse cracks are considered for numerical analysis using ANSYS 10.0. Modal parameters like frequency, displacement, mode shapes for first four modes of the intact beam, single cracked and double cracked beam for different crack location and depth are computed using ANSYS. The free vibration frequencies for first four modes are considered for the present study.

6.7.1 Single cracked uniform beam

The natural frequencies of the cracked aluminum and steel beam for a single crack at different location and depth are tabulated in Table 6.3 and 6.4 respectively.

Table 6.3 Free vibration frequencies of single cracked free-free Aluminum beam by ANSYS (L = 0.3 m, b = 0.01 m, d = 0.01 m, E = 68.22 GPa, ν = 0.28, ρ = 2569 kgm^{-3})

Crack location	Crack depth (mm)	Natural Frequency (Hz)			
		1st mode	2ndmode	3rd mode	4th mode
Intact	Nil	547.0	1500.0	2913.2	4757.4
0.25L	2	544.3	1474.5	2889.9	4743.1
	4	531.7	1393.5	2811.2	4709.8
	6	491.8	1212.0	2651.0	4657.5
0.33L	2	540.4	1482.0	2910.3	4724.1
	4	517.5	1425.0	2895.7	4624.2
	6	452.4	1264.5	2875.3	4414.9
0.50L	2	536.1	1498.5	2869.5	4752.6
	4	500.5	1499.4	2741.3	4752.6
	6	415.2	1498.8	2508.3	4747.9

Table 6.4 Free vibration frequencies of single cracked free-free Steel beam by ANSYS (L = 0.3 m, b = h = 0.01 m, E = 200 GPa, ρ = 7660 kg/m^3 and ν = 0.3)

Crack location	Crack depth (mm)	Natural Frequency (Hz)			
		1st mode	2nd mode	3rd mode	4th mode
Intact	0	536.1	1494.6	2849.3	4654.5
0.25L	2	531.8	1466.2	2803.7	4635.9
	5	503.9	1301.8	2604.3	4575.4
	7	408.0	1038.7	2416.2	4505.6
0.33L	2	528.6	1467.7	2840.8	4617.3
	5	478.2	1327.2	2815.1	4421.8
	7	350.1	1147.9	2780.9	4123.9
0.5L	2	523.8	1493.1	2800.9	4649.8
	5	450.9	1491.6	2564.4	4645.2
	7	306.6	1491.6	2268.0	4635.9

From Table 6.3 and 6.4 it is observed that the free vibration frequencies as obtained from numerical analysis using ANSYS 10.0 decrease with the introduction of crack at any location in comparison to intact beams. It is observed from Table 6.3 that the reduction in frequencies for a 2 mm depth crack is found to be 0.1%, 1.2% and 2.0% than intact beam for relative position of the crack to be at 0.25, 0.33 and 0.5 respectively from either end of the free-free

aluminum beam in first mode. But a 6 mm crack at the same locations reduce the free vibration frequencies in first mode by 10.1%, 17.3% and 24.1% respectively than the intact aluminum beam. Similar observations are found from Table 6.4 in case of a steel free-free beam. This suggests that for lower depth of the crack the effect of the crack on natural frequencies is very marginal. But as the depth of the crack increases the effect is significant. It is observed that the crack at 0.25*L* in free-free aluminum beam reduces the free vibration frequencies in first mode by 0.5%, 2.8% and 10.1% than intact beam for crack depths of 2 mm, 4 mm and 6 mm respectively. But the crack at 0.5*L* reduces the free vibration frequencies by 2.0%, 8.5% and 24.1% than the intact beam for crack depths of 2 mm, 4 mm and 6 mm respectively. This suggests the crack at 0.5*L* affects the free-free aluminum beam more than any other location of the crack in first mode.

Similar observations are found from Table 6.4 for free-free steel beam. It is observed from the Table 6.3 that the crack at 0.25*L* of free-free aluminum beam brings down the free-vibration frequencies in second mode by 1.7%, 7.1% and 19.2% than intact beam for crack depths of 2 mm, 4 mm and 6 mm respectively. But the same cracks at 0.5*L* reduce the free vibration frequencies by 0.0%, 0.0% and 0.1% than intact beam. This implies the crack at 0.5*L* does not affect the free vibration frequencies in second mode but the effect of the same cracks at 0.25*L* is maximum. Similar results are also observed from the Table 6.4 for the free-free steel beam. From Table 6.3 it is observed that the crack at 0.33*L* reduces the free vibration frequencies in third mode by 0.1%, 0.6% and 1.3% than intact beam for crack depth of 2 mm, 4 mm and 6 mm respectively. Whereas the same cracks at 0.5*L* bring down the free vibration frequencies in third mode by 1.5%, 5.9% and 13.9% than intact beam for crack depth of 2 mm, 4 mm and 6 mm respectively. This suggests the presence of crack at 0.33*L* marginally affects the beam in third mode but the crack at 0.5*L* affects the beam considerably. The free-free steel beam also shows similar results in Table 6.4. For fourth mode of free vibration of free-free aluminum beam in Table 6.3, it is observed that a crack at 0.33*L* of depth 2 mm, 4 mm and 6 mm bring down the frequencies by 0.7%, 2.8% and 7.2% respectively than intact beam. The same cracks at 0.5*L* decrease the free vibration frequencies in fourth mode by 0.0%, 0.1% and 0.2% respectively than intact beam. Hence a free-free aluminum is more affected by the crack at 0.33*L* but the crack at 0.5*L* has very little effect. Same results are also observed in Table 6.4 for free-free steel beam.

Free vibration mode shapes with maximum displacement corresponding to mode of vibration for free-free cracked aluminum subjected to a crack of 8 mm deep at 0.25*L* and steel beam subjected to a crack of 7 mm deep at 0.5*L* are shown in Fig. 6.47 and 6.48 respectively.

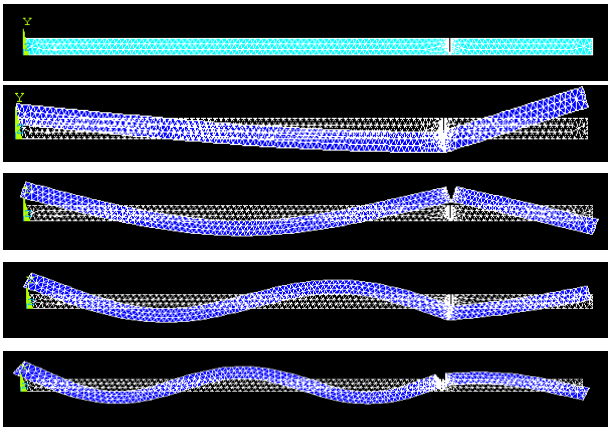

Figure 6.47 Mode shapes of single cracked free-free Aluminum beam for a 8 mm depth crack at 0. 25*L* from right end

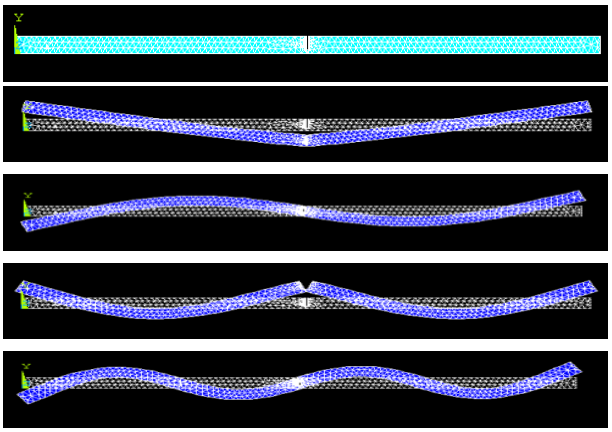

Figure 6.48 Mode shapes of single cracked Steel free-free beam with a 7 mm deep crack at 0.5*L* from either end

From Fig. 6.47 it is observed that the maximum displacement in the beam happens to be 10.585 mm, 7.987 mm, 8.360 mm and 8.291 mm for first, second, third and fourth mode of free vibration respectively due to the crack at 0.25L from free end. Similarly from Fig. 6.48 for steel beam subjected to a 7 mm deep crack at 0.5*L* (mid-span) it is observed that the maximum deflection during vibration is 4.141 mm, 4.532 mm, 4.491 mm and 4.528 mm for first, second, third and fourth modes respectively.

6.7.2 Double cracked uniform beam

Free vibration frequencies of double cracked free-free aluminum and steel beam are tabulated in Table 6.5 and 6.6.

Table 6.5 Free vibration frequencies of double cracked free-free Aluminum beam by ANSYS (L = 0.3 m, b = 0.01 m, d = 0.01 m, E = 68.22 GPa, ν = 0.28, ρ = 2569 kgm^{-3})

Crack location	Crack depth (mm)	Natural Frequency (Hz)			
		1st mode	2nd mode	3rd mode	4th mode
Intact	Nil	547.0	1500.0	2913.2	4757.4
0.25L	2	540.4	1449.0	2828.7	4733.6
	4	518.0	1303.5	2595.7	4662.3
	6	454.6	1003.5	2182.0	4533.8
0.33L	2	533.9	1450.5	2904.5	4695.6
	4	492.8	1303.5	2875.3	4533.8
	6	398.8	1002.0	2805.4	4286.4

From Table 6.5 it is observed that the presence of two cracks at 0.33L from free ends affects the beam more than the two cracks at 0.25L from each end. Referring to Table 6.3, it was observed that the free vibration frequencies in first mode were most affected by the crack at 0.5L than other locations. This suggests in first mode of free vibration the cracks present near to mid-span will affect the beam more than the cracks away from mid-span. It is also observed from Table 6.5 that the free vibration frequencies in first mode of the double cracked free-free aluminum beam subjected to cracks at 0.33L reduces the frequencies by 2.4%, 9.9% and 27.1% for crack depths of 2 mm, 4 mm and 6 mm respectively. Whereas the decrease due to a single crack at 0.33L from either ends is 1.2%, 5.4% and 17.3% than intact beam for crack depths of 2 mm, 4 mm and 6 mm respectively. This suggests introduction of a similar crack from the other free end decreases the free vibration frequencies further by 1.2%, 4.5% and 9.8% for crack depths of 2 mm, 4 mm and 6 mm respectively. Hence the decrease in natural frequency due to presence of two symmetric cracks of same depth is not equal to the sum of their individual effects. It is also observed in Table 6.5 that the free vibration frequencies in second mode of the free-free aluminum beam subjected to two cracks at 0.25L or 0.35L from each end are equally affected by the cracks as the decrease in natural frequency for the two locations are nearly same.

Table 6.6 Free vibration frequencies of double cracked free-free Steel beam by ANSYS (L = 0.3 m, b = h = 0.01 m, E = 200 GPa, ρ = 7660 kg/m^3 and v = 0.3)

Crack location	Crack depth	Frequency (Hz)			
		1st mode	2nd mode	3rd mode	4th mode
Intact	0	535.8	1467.9	2852.2	4660.7
0.25L	2	528.1	1415.4	2763.1	4630.3
	5	479.2	1133.0	2332.6	4500.5
	7	358.1	700.0	1839.7	4336.0
0.33L	2	521.8	1416.7	2841.0	4595.1
	5	439.6	1133.6	2784.1	4315.5
	7	291.0	705.7	2676.3	4039.9

It is observed that the natural frequency in third mode of the free-free aluminum beam decrease by 2.9%, 10.9% and 25.1% due to double cracks at 0.25L from each end for 2 mm, 4 mm and 6 mm respectively. It is observed that in third mode of free vibration of the beam subjected to two cracks, the cracks at 0.25L from each free end affects the beam more than the cracks at 0.33L from each end. Similarly it is observed that the cracks at 0.33L from each free ends reduce free vibration frequencies more than the cracks at 0.25L from each ends. Similar to double cracked aluminum beam steel beam subjected to two cracks also exhibits similar trends as observed in Table 6.6. Free vibration mode shapes of double cracked aluminum beam subjected to 8 mm deep cracks at 0.25L from each end with modal maximum deflection in the beam are shown in Fig. 6.49. It is observed that the double cracked aluminum beam experiences a maximum deflection of 8.487 mm, 7.377 mm, 6.297 mm and 6.288 mm in first, second, third and fourth mode of free vibration respectively. This suggests maximum deflection in a double cracked vibrating beam occurs in first mode of free vibration. Similar results are also observed for double cracked steel beam.

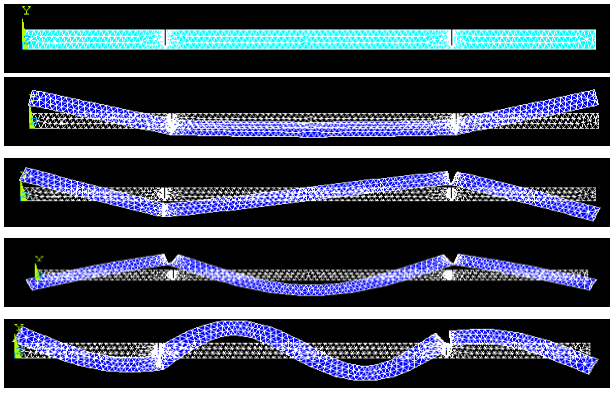

Figure 6.49 Mode shapes of double cracked free-free Aluminum beam subjected to 8 mm deep crack at 0. 25L from each end

6.8 Experimental Results on Cracked Beam

Experimental program was carried out in the same aluminum beam and steel beams of dimensions, L = 0.3 m, $b = h$ = 0.01 m for free-free end conditions. The material properties of aluminum specimens were taken as E = 68.22 GPa, ρ = 2569 kg/m^3, ν = 0.28 and for steel beams E = 200 GPa, ρ = 7660 kg/m^3, ν = 0.3. The natural frequencies of free vibration of aluminum beam specimens and steel beam specimens were found using FFT Analyzer with PULSE set up by both Auto spectrum and Frequency Response Function (FRF) method for the intact, single and double cracked specimens. It was observed that the free vibration frequencies of the beams obtained from autospectrum method was little conservative than the FRF method of measurements. Hence in all experimental measurements FRF method is adopted. A typical autospectrum of the free-free aluminum beam subjected to a 6 mm deep crack at 0.33L from free end is shown in Fig. 6.50, where the free vibration frequencies are picked at the peaks of the spectrum. Similarly a typical FRF response and coherence of the free-free Aluminum beam subjected to a 2 mm deep crack at 0.33L from the free end is shown in Fig. 6.51.

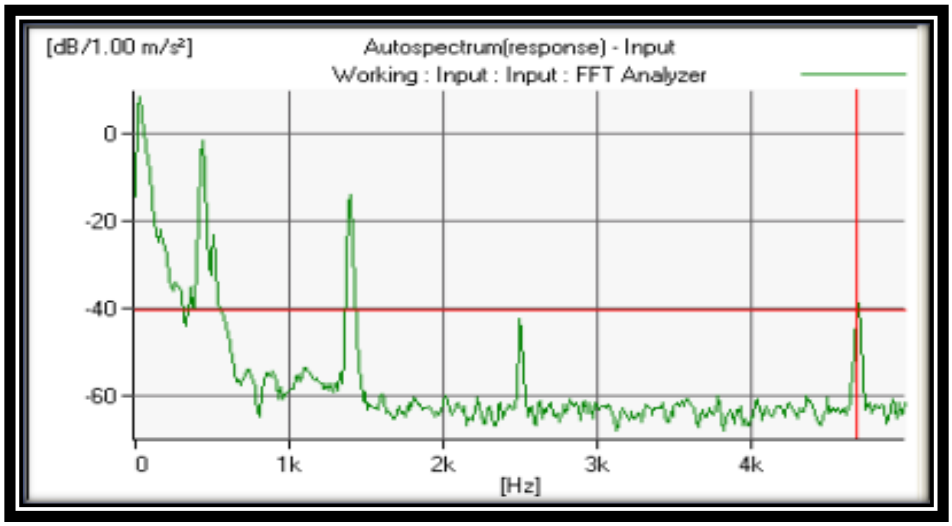

Figure 6.50 Autospectrum of the free-free Aluminum beam subjected to a 6mm deep crack at 0.33*L*

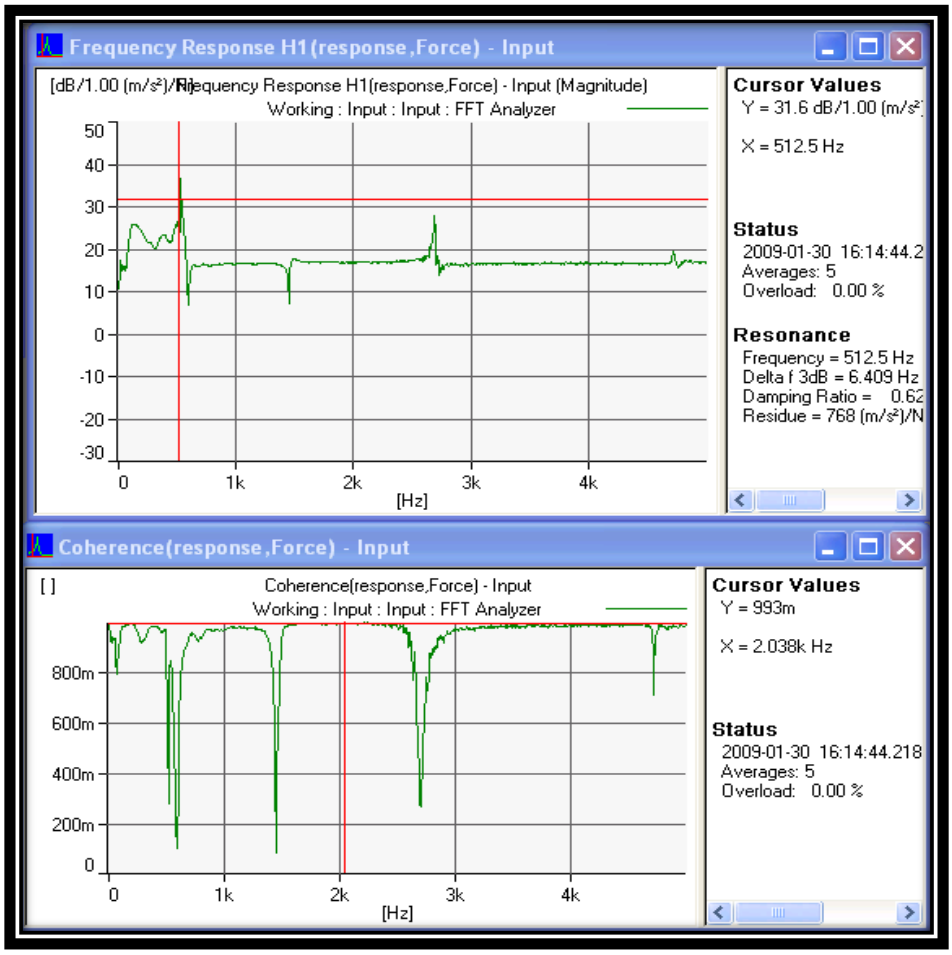

Figure 6.51 FRF response and Coherence of the free-free Aluminum beam with a 2 mm deep single crack at 0.33*L*

The frequency response function and the coherence obtained from pulse software which takes the average of five number of loads with better coherence as shown in Fig. 6.52. The peaks give the FRF of average of five numbers of loading and the coherence checks the accuracy of the peaks obtained by FRF. When the coherence is straight it indicates better FRF and if coherence is not straight the corresponding FRF is assumed to be not accurate and the test is to be repeated.

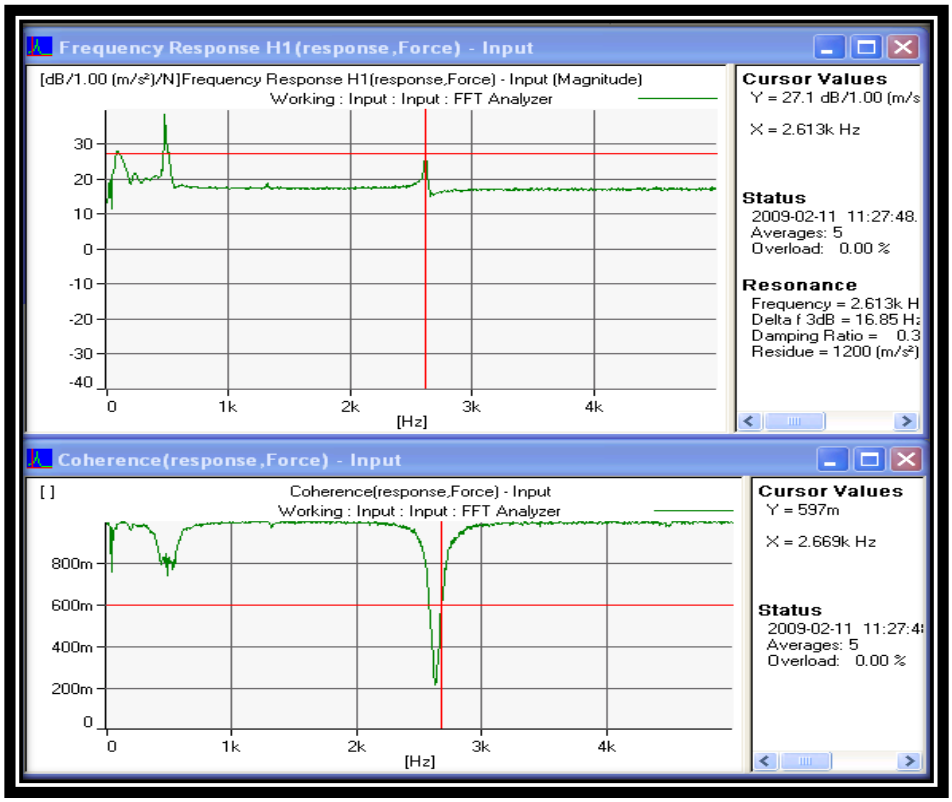

Figure 6.52 FRF response and Coherence of the double cracked free-free Aluminum beam with a 4 mm deep crack at 0.33*L* from both ends

6.8.1 Single cracked beam

First mode non-dimensional free vibration frequencies of the aluminium and steel beam subjected to a single crack at different locations of different depths are obtained from numerical (ANSYS) analysis and experimental analysis are shown in Fig. 6.53 and 6.54 respectively.

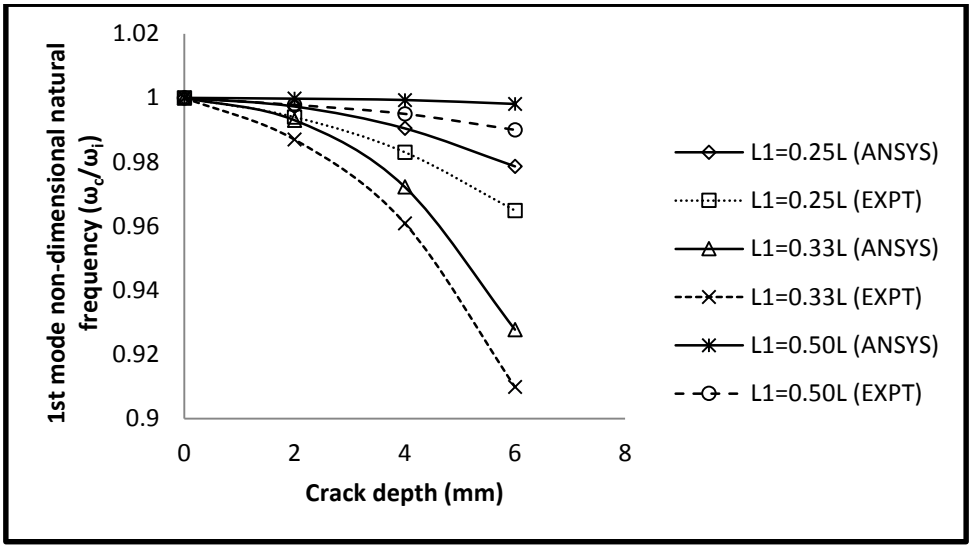

Figure 6.53 Variation of non-dimensional fundamental frequency (ω_c/ω_i) of single cracked free-free Aluminum beam for different location and depth of the crack in numerical and experimental method of analysis

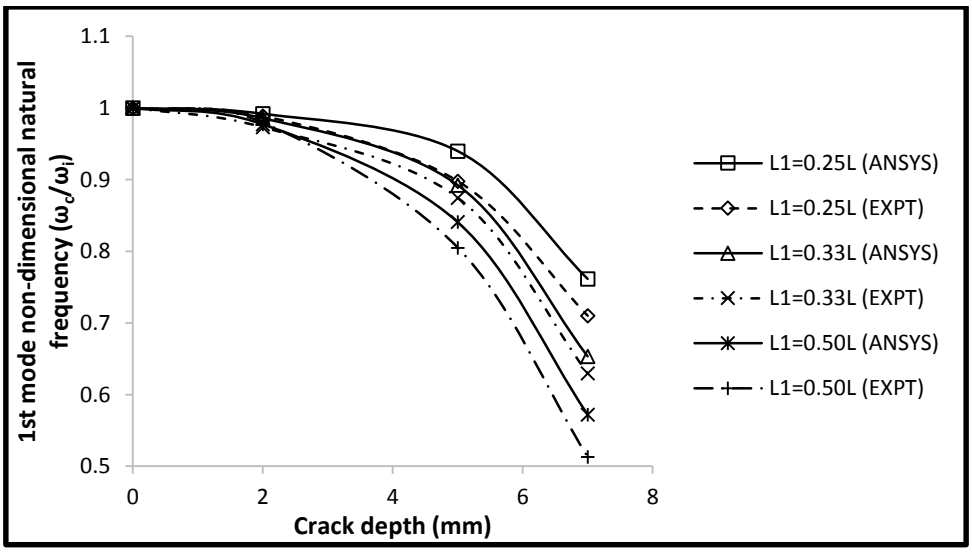

Figure 6.54 Variation of non-dimensional fundamental frequency (ω_c/ω_i) of single cracked free-free Steel beam for different location and depth of the crack in numerical and experimental method of analysis

It is observed from Fig. 6.53 and 6.54 that the experimental results and numerical results follow the similar trend. However the values of experimental results are little lower than the numerical results. As observed, in Fig. 6.53 for aluminum beam, the non-dimensional free vibration frequencies in first mode is worst affected by the crack at 0.5*L* from free end. The experimental frequencies are found to be 1.4%, 1.7% and 3.1% lower than the numerical values for a 6 mm deep crack located at 0.25*L*, 0.33*L* and 0.50*L* from free end respectively. It is also observed

that the crack at 0.5*L* from free end reduces the free vibration frequencies in first mode by 0.0%, 1.5% and 3.1% than numerical analysis for 2 mm, 4 mm and 6 mm deep cracks respectively. This suggests that the measured free vibration frequencies are nearly same as those obtained from numerical analysis for lower depths of the crack. But the difference increases as the depth of the crack increases. Similarly it is observed in Fig. 6.54 for steel beam that non-dimensional free vibration frequencies in first mode for 7 mm deep crack reduce by 5.1%, 2.3% and 5.9% than numerical results for the crack to be at 0.25*L*, 0.33*L* and 0.50*L* respectively from free end. This suggests the crack at 0.50*L* has maximum impact on free vibration frequencies in first mode similar to aluminum beam in Fig. 6.53. It is also observed that the effect of the crack in reducing the free vibration frequencies increases as the crack moves from free end to mid-span. The experimentally measured frequencies happens to be lower than the numerically obtained frequencies. The variation of second mode non-dimensional frequency (ω_c/ω_i) of single cracked free-free aluminum beam for different location and depth of the crack from numerical and experimental of analysis are shown in Fig. 6.55.

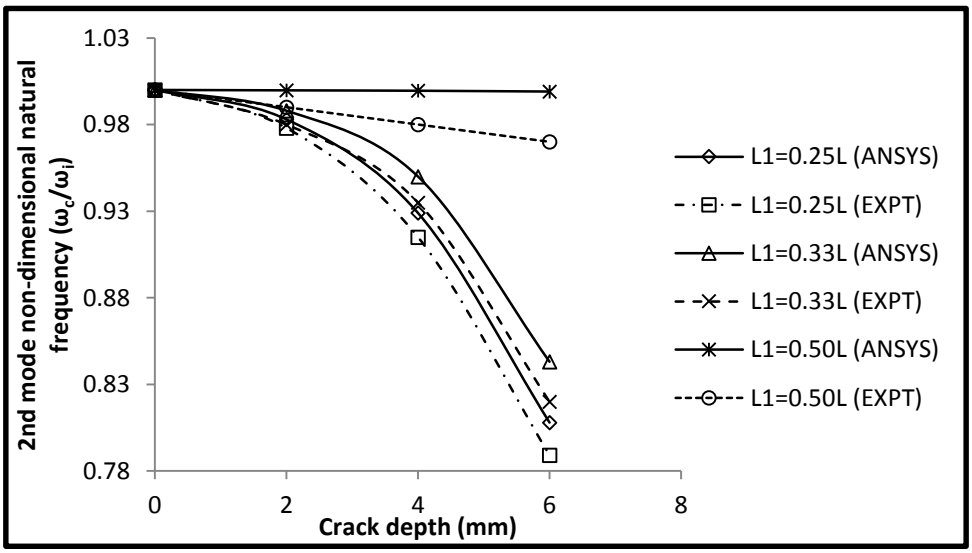

Figure 6.55 Variation of 2nd mode non-dimensional frequency (ω_c/ω_i) of single cracked free-free Aluminum beam for different location and depth of the crack in numerical and experimental method of analysis

It is observed that the free vibration frequencies in second mode are least affected for the crack to be at 0.5*L*. The effect of the crack on free vibration frequencies in second mode increases as the crack moves from mid-span to free end of the free-free beam. For the crack to be at 0.25*L* the decrease in non-dimensional frequencies are found to be 0.5%, 1.4% and 1.9% than

numerically obtained frequencies of the beam for crack depths of 2 mm, 4 mm and 6 mm respectively. It is also observed that the crack at 0.25L affects the beam more in second mode of free vibration. The variation of second mode non-dimensional frequency (ω_c/ω_i) of single cracked free-free steel beam for different location and depth of the crack from numerical and experimental of analysis are shown in Fig. 6.56.

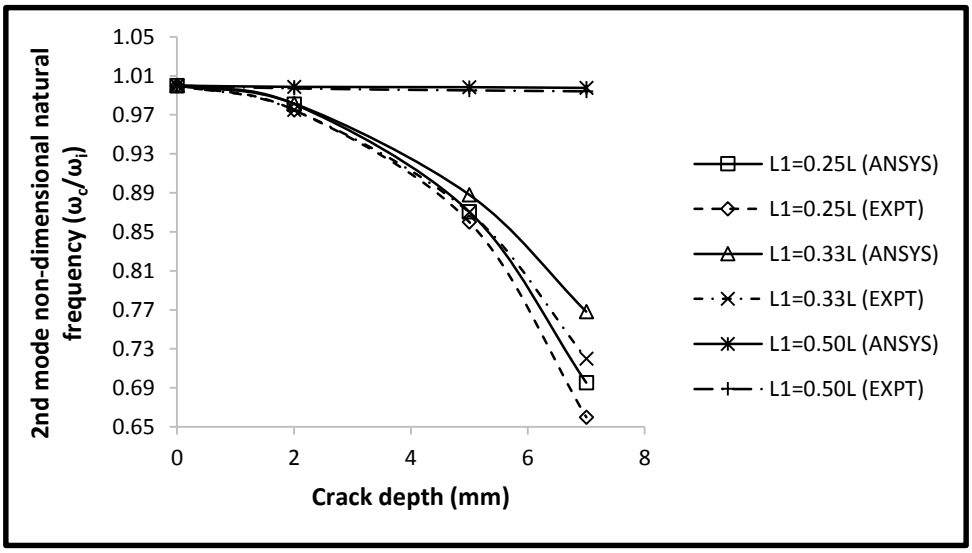

Figure 6.56 Variation of 2nd mode non-dimensional frequency (ω_c/ω_i) of single cracked free-free Steel beam for different location and depth of the crack in numerical and experimental method of analysis

It is observed that steel free-free beam in second mode of free vibration are also least affected by the crack at 0.5*L* similar to aluminum beam in Fig. 6.55 for all depths of the crack. But the influence of the crack on free vibration frequencies increase as the crack moves towards the free end of the beam. Referring to Fig. 6.56, non-dimensional frequencies are in good agreement with the numerical results. The variation of non-dimensional frequencies in third mode for aluminum and steel free-free beams subjected to single crack at different location of different depth is shown in Fig. 6.57 and 6.58 respectively.

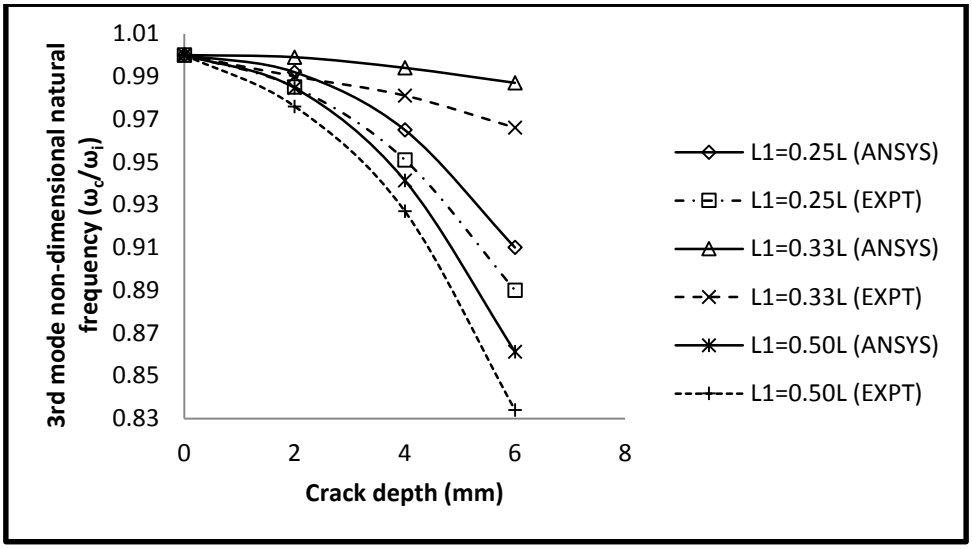

Figure 6.57 Variation of 3rd mode non-dimensional frequency (ω_c/ω_i) of single cracked free-free Aluminum beam for different location and depth of the crack in numerical and experimental method of analysis

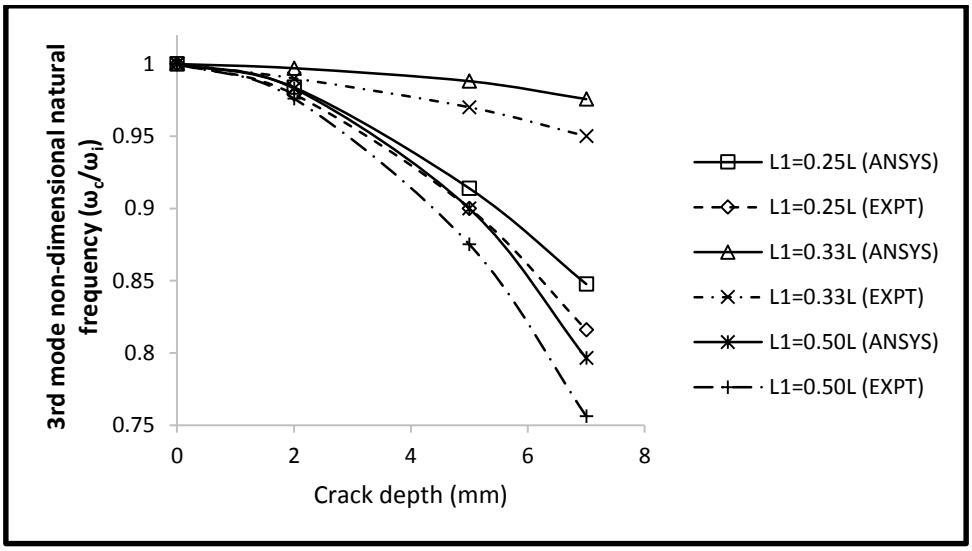

Figure 6.58 Variation of 3rd mode non-dimensional frequency (ω_c/ω_i) of single cracked free-free Steel beam for different location and depth of the crack in numerical and experimental method of analysis

It is observed that presence of the crack at 0.5*L* reduces the non-dimensional free vibration frequencies more than other locations in both beams. It is also observed that the crack at 0.33*L* has least influence on free vibration frequencies in third mode. The experimental result happens to be at lower side than that of numerical results. The difference between experimental analysis and numerical analysis for 6 mm deep crack in free-free aluminum beam is found to be 2.0%,

2.1% and 2.7% and for steel beam, it is 3.2%, 2.6% and 4.0% for crack locations of 0.25*L*, 0.33*L* and 0.50*L* respectively from free end. Variation of non-dimensional frequencies (ω_c/ω_i) in fourth mode of single cracked free-free aluminum and steel beam for different location and depth of the crack from numerical and experimental analysis are shown in Fig. 6.59 and 6.60 respectively.

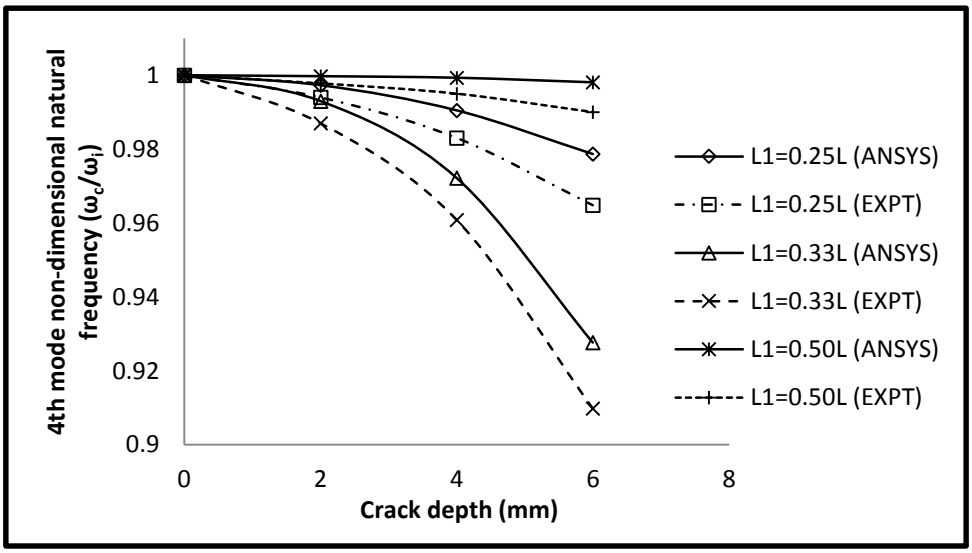

Figure 6.59 Variation of 4th mode non-dimensional frequency (ω_c/ω_i) of single cracked free-free Aluminum beam for different location and depth of the crack in numerical and experimental method of analysis

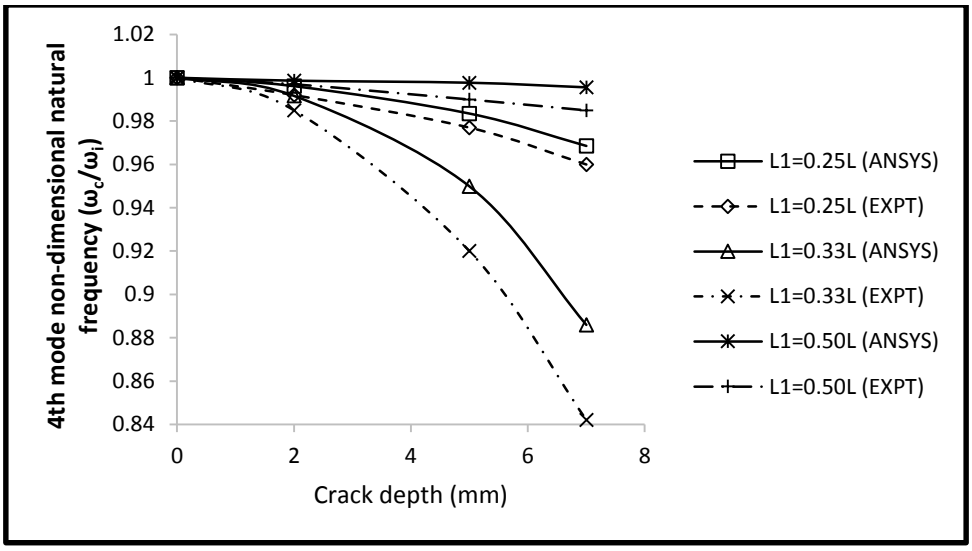

Figure 6.60 Variation of 4th mode non-dimensional frequency (ω_c/ω_i) of single cracked free-free Steel beam for different location and depth of the crack in numerical and experimental method of analysis

It is observed that presence of the crack at 0.33*L* reduces the non-dimensional free vibration frequencies in fourth mode more than other locations in both the beams. It is also observed that the crack at 0.50*L* has least influence on free vibration frequencies in fourth mode. The experimental results happens to be at lower side than that of numerical results. The difference between experimental analysis and numerical analysis for 6 mm deep crack in free-free aluminum beam in Fig. 6.59 is found to be 1.4%, 1.8% and 0.8% and for steel beam in Fig. 6.60, it is 0.8%, 4.4% and 1.1% for crack locations of 0.25*L*, 0.33*L* and 0.50*L* respectively from free end.

6.8.2 Double cracked Beam

Variations of non-dimensional free vibration frequencies of a doubly cracked aluminum and steel free-free beam in different modes are studied between experimental method and numerical method. FRF method is adopted for experimental method of analysis for both beams like that of single cracked beams. Variations of non-dimensional free vibration frequencies in first mode of double cracked aluminum and steel beam for different location and depths of the crack are shown in Fig. 6.61 and 6.62 respectively for free-free end conditions.

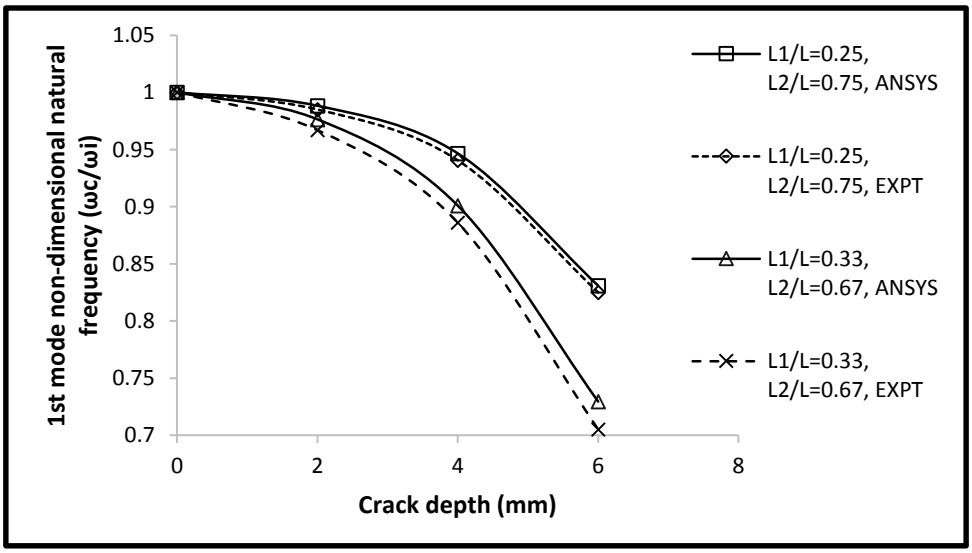

Figure 6.61 Variation of non-dimensional fundamental frequency (ω_c/ω_i) of double cracked free-free Aluminum beam for different location and depth of the crack in numerical and experimental method of analysis

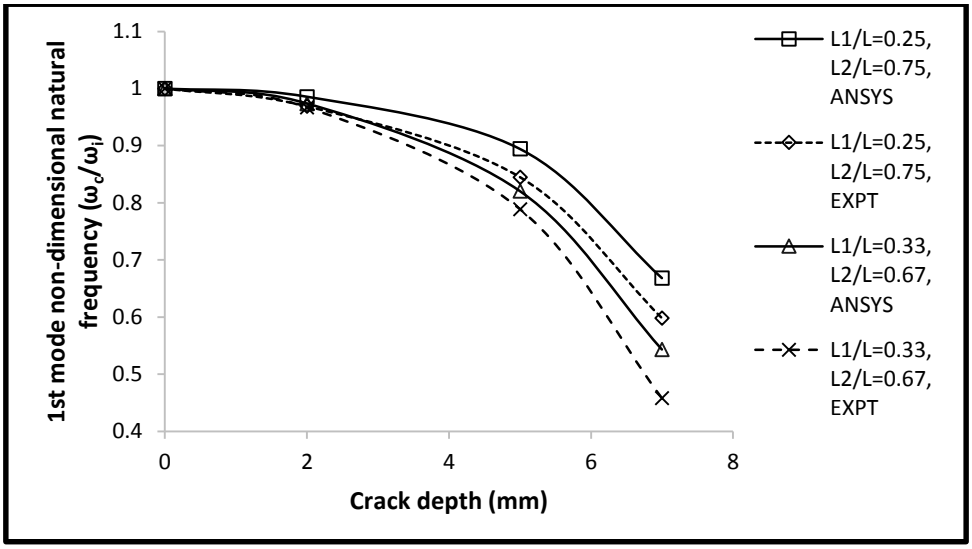

Figure 6.62 Variation of non-dimensional fundamental frequency (ω_c/ω_i) of double cracked free-free Steel beam for different location and depth of the crack in numerical and experimental method of analysis

It is observed that the non-dimensional free vibration frequencies in first mode follow similar trends both in numerical analysis and experimental analysis for both the beams. The experimentally observed frequencies in aluminum beam subjected to two cracks at 0.25*L* from each end differs by 1.7%, 4.9% and 7.0% than numerical results for crack depths of 2 mm, 4 mm and 6 mm respectively. Similarly for cracks at 0.33*L* from both ends in aluminum beam the difference in frequencies obtained from numerical and experimental analysis are found to be 0.7%, 1.5% and 3.4% for 2mm, 4 mm and 6 mm depths of crack respectively. It is also observed that the cracks at 0.33*L* from both ends have greater influence on first mode frequencies than the cracks at 0.25*L* from both ends. Similarly for steel beam in Fig. 6.62, the cracks at 0.33*L* from both ends reduce the non-dimensional free vibration frequencies in first mode more than the cracks at 0.25*L* from both ends for all depths of the crack. Comparing the results from experimental analysis and numerical analysis there exists an excellent agreement in Fig. 6.61 and 6.62. Variations of non-dimensional free vibration frequencies in second mode between experimental analysis and numerical analysis are plotted in Fig. 6.63 and 6.64 respectively for aluminum and steel beams.

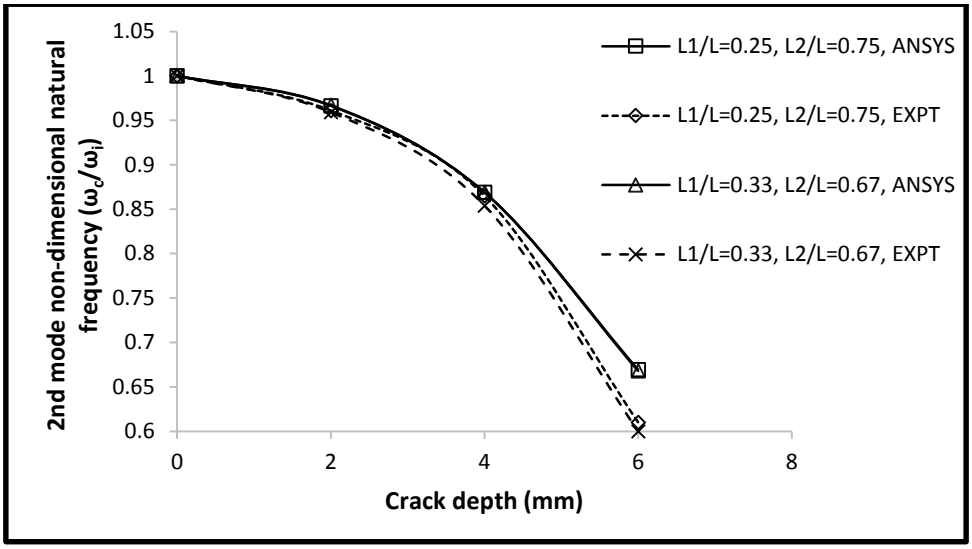

Figure 6.63 Variation of 2nd mode non-dimensional frequency (ω_c/ω_i) of double cracked free-free Aluminum beam for different location and depth of the crack in numerical and experimental method of analysis

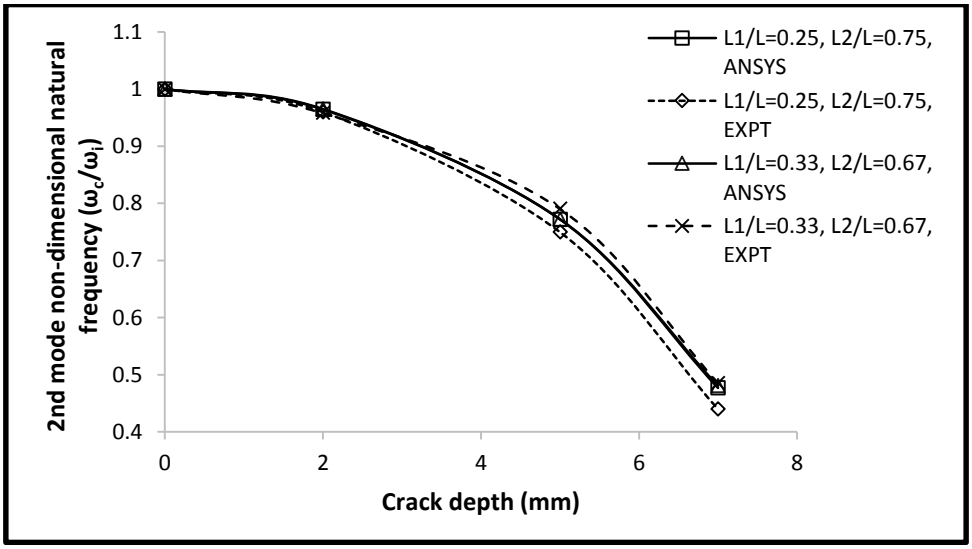

Figure 6.64 Variation of 2nd mode non-dimensional frequency (ω_c/ω_i) of double cracked free-free Steel beam for different location and depth of the crack in numerical and experimental method of analysis

It is observed that the second mode frequencies obtained from both the analysis almost match each other in aluminum and steel beam. It is also observed that the second mode free vibration frequencies are not affected by the position of the crack as they produce similar results. The variation between the non-dimensional free vibration frequencies happens to be 5.9% and 6.8%

than numerical analysis results for cracks to be at 0.25*L* and 0.33*L* from the free end respectively.

Similar results like aluminum beam in Fig. 6.63 are also observed Fig. 6.64 for steel beam. But the difference in frequencies for the cracks to be at 0.25L and 0.33L from free ends happens to be 3.7% and -0.4% than the results of numerical analysis. Though the result from experimental analysis almost matches with the numerical analysis, it shows little higher values for the cracks at 0.33*L* from both ends. Variation of third mode non-dimensional frequencies with various crack depths for different crack locations of double cracked aluminum beam and steel beam are shown in Fig. 6.65 and 6.66 respectively.

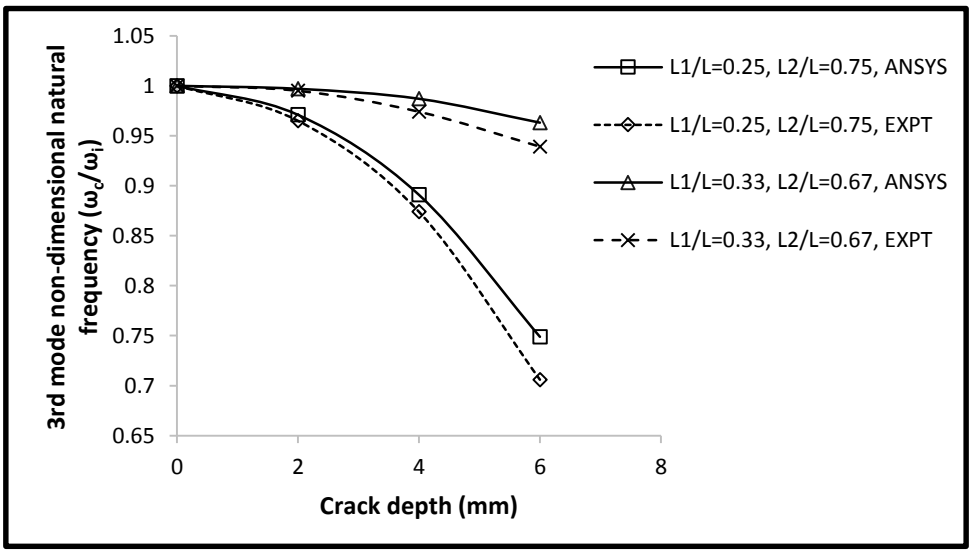

Figure 6.65 Variation of 3rd mode non-dimensional frequency (ω_c/ω_i) of double cracked free-free Aluminum beam for different location and depth of the crack in numerical and experimental method of analysis

It is observed from Fig. 6.65 that presence of cracks at 0.25*L* from each end of the free-free aluminum beam has a more effect in reducing the frequencies in third mode than the cracks at 0.33*L* from each ends. The reduction in frequencies due to cracks at 0.25*L* from each end in third mode is given by 0.6%, 1.7% and 4.3% for crack depths of 2 mm, 4 mm and 6 mm respectively than the frequencies obtained from numerical analysis. Similar trend in reduction of frequency due to double cracks is also observed in steel beam in Fig. 6.66. But the reduction in frequencies due to cracks at 0.25*L* from each end of steel beam is given by 0.9%, 4.2% and 6.4% for crack depths of 2 mm, 5 mm and 7 mm respectively.

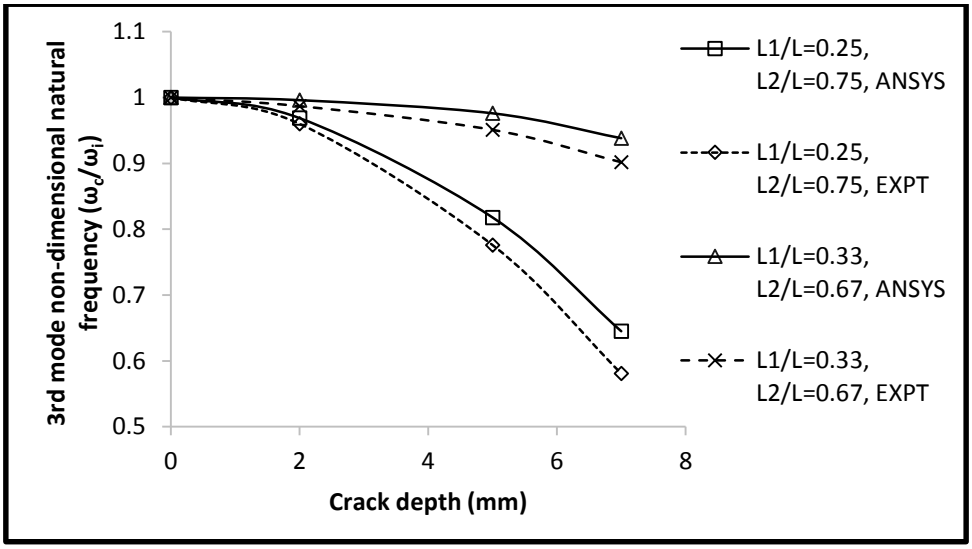

Figure 6.66 Variation of 3rd mode non-dimensional frequency (ω_c/ω_i) of double cracked free-free Steel beam for different location and depth of the crack in numerical and experimental method of analysis

Thus the experimental results are in good agreement with the numerical results of the double cracked free-free steel beam. Variation of fourth mode non-dimensional frequencies with various crack depths for different crack locations of double cracked aluminum beam and steel beam are shown in Fig. 6.67 and 6.68 respectively.

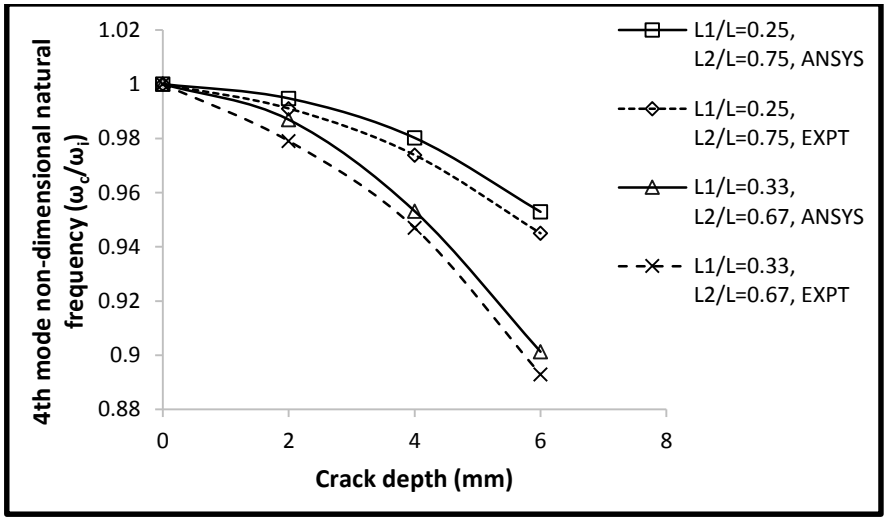

Figure 6.67 Variation of 4th mode non-dimensional frequency (ω_c/ω_i) of double cracked free-free Aluminum beam for different location and depth of the crack in numerical and experimental method of analysis

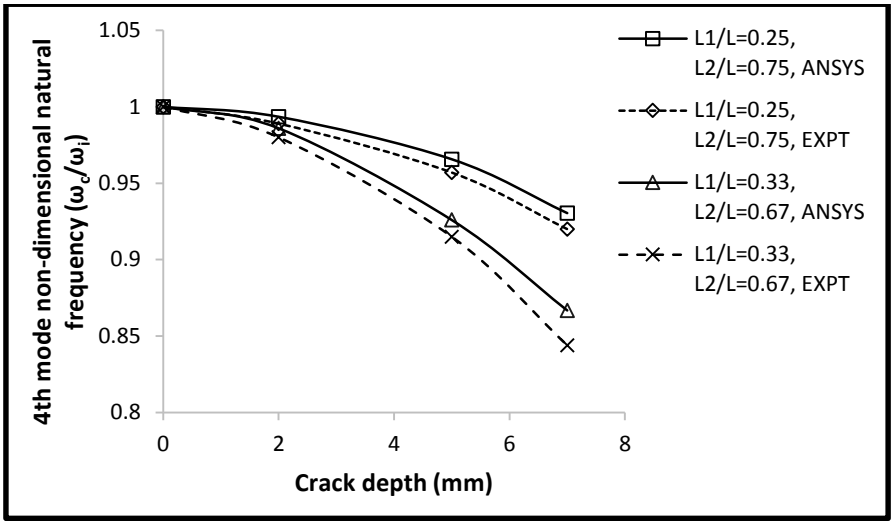

Figure 6.68 Variation of 4th mode non-dimensional frequency (ω_c/ω_i) of double cracked free-free Steel beam for different location and depth of the crack in numerical and experimental method of analysis

It is observed from Fig. 6.67 that presence of cracks at 0.25*L* from each end of the free-free aluminum beam has a lesser effect in reducing the frequencies in fourth mode than the cracks at 0.33*L* from each ends. The reduction in frequencies due to cracks at 0.33*L* from each end in third mode is given by 0.8%, 1.6% and 3.7% for crack depths of 2 mm, 4 mm and 6 mm respectively than the frequencies obtained from numerical analysis. Similar trend in reduction of frequency due to double cracks is also observed in steel beam in Fig. 6.68. But the reduction in frequencies due to cracks at 0.33*L* from each end of steel beam is given by 0.6%, 1.1% and 2.3% for crack depths of 2 mm, 5 mm and 7 mm respectively. Thus the experimental results are in good agreement with the numerical results of the double cracked free-free steel beam.

6.9 Buckling of Beam Subjected to a Single Crack

The non-dimensional buckling loads are computed for the uniform beam in Fig. 6.4 for a crack considered at relative locations (L_1/L) varying from 0.1 to 0.9 with relative crack depths (rcd) 0.1, 0.3, 0.5 and 0.7 for different end conditions.

6.9.1 Uniform fixed-free beam

The variation of non-dimensional buckling loads of the uniform beam for different crack locations and relative crack depths are plotted in Fig. 6.69 for fixed-free end conditions.

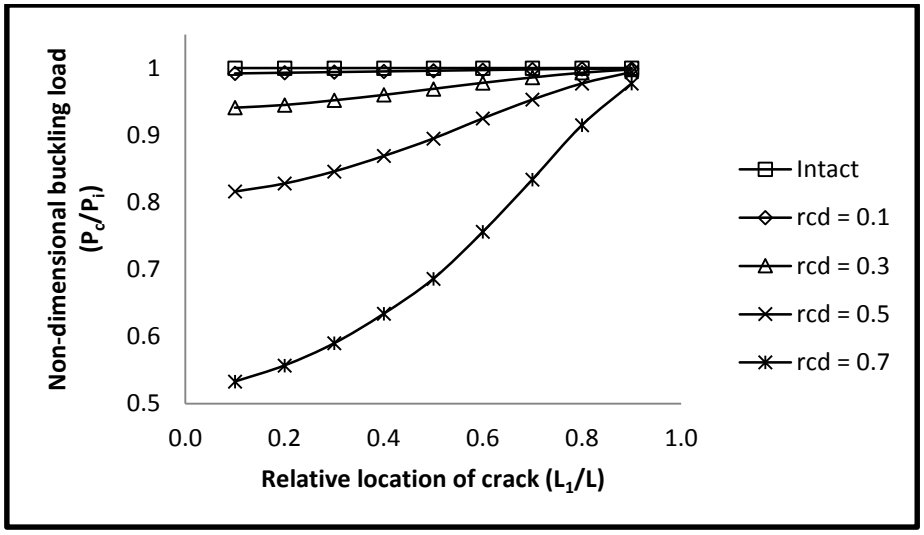

Figure 6.69 Variation of non-dimensional buckling load with respect to relative location of crack (L_1/L) for different relative crack depths for Fixed-Free beam

It is observed that for the crack at 0.1L from the fixed end the buckling loads reduce approximately by 0.8%, 5.9%, 18.4% and 46.7% than the intact beam for relative crack depths of 0.1, 0.3, 0.5 and 0.7 respectively. When the crack is at 0.9L from fixed end the non-dimensional buckling loads are lesser by only 0.1%, 0.2%, 0.6% and 2.3% than intact beam for relative crack depths of 0.1, 0.3, 0.5 and 0.7 respectively. This implies the non-dimensional buckling loads of the fixed-free beam for the crack at 0.1L is minimum compared to other locations for all relative depths. As the crack moves away from the fixed end of the beam the reduction of buckling loads decrease suggesting decrease in influence of crack from fixed end to free end. For the crack at 0.9L there is very little decrease in buckling loads suggests very little or no influence of crack on buckling loads near free end. This is due to the fact that higher bending moment near the fixed end of a fixed-free beam results in larger release in strain energy in the section due to a crack. Due to larger release in strain energy, the beam becomes more flexible; hence there is maximum drop of buckling load. Whereas the release in strain energy of the section due to a crack near the free end is very small due to lesser bending moment. Hence the buckling load of the fixed-free beam is marginally affected by a crack near free end. It is also observed that the rate of decrease of buckling load increases with the relative crack

depth for any location of the crack. A small crack near fixed end has a bigger effect on buckling load than a bigger crack at free end.

6.9.2 Uniform hinged-hinged beam

The variation of non-dimensional buckling load with relative crack locations for various relative crack depths of the beam with hinged-hinged end condition is observed in Fig. 6.70.

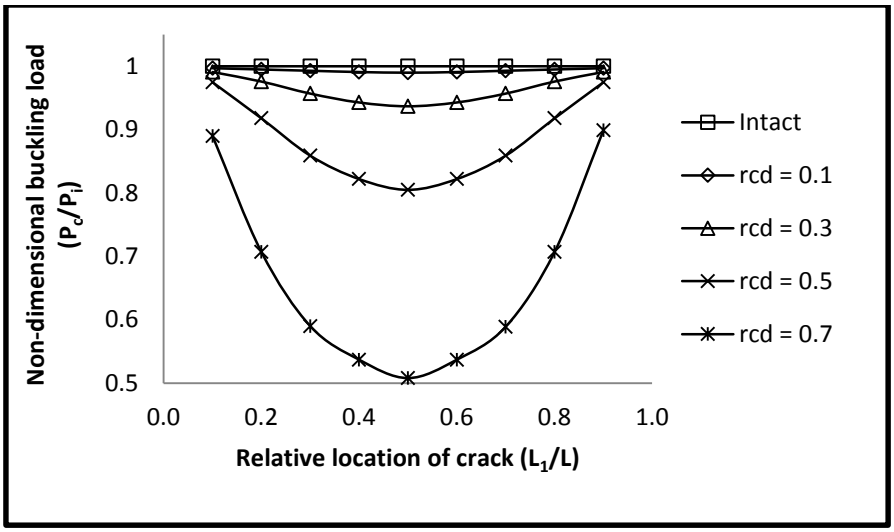

Figure 6.70 Variation of non-dimensional buckling load (P_c/P_i) with respect to relative location of crack (L_1/L) for different relative crack depths for Hinged-Hinged beam

It is observed that the crack at 0.1L from the supports of either end, the non-dimensional buckling load reduce by 0.3%, 0.9%, 2.5% and 11.0% than intact beam for relative crack depths of 0.1, 0.3, 0.5 and 0.7 respectively. The same cracks at mid span of the hinged-hinged beam reduce the buckling loads by 1.0%, 6.3%, 19.5% and 49.2% respectively. It is observed that when the crack happens to be near the support for a beam with hinged-hinged end conditions the effect of a crack is marginal but the same crack at the mid-span reduces the buckling load drastically. This is due to the fact that the bending moment of a beam with hinged-hinged end conditions is subject to lower bending moment near the support and maximum bending moment at mid-span. More bending moment results in more release in strain energy. Hence buckling load due to presence of crack near mid span will be less in comparison to the same crack near supports of the hinged-hinged beam.

6.9.3 Uniform fixed-hinged beam

The variation of non-dimensional buckling load with relative crack locations for various relative crack depths of the beam with fixed-hinged end condition is shown in Fig. 6.71.

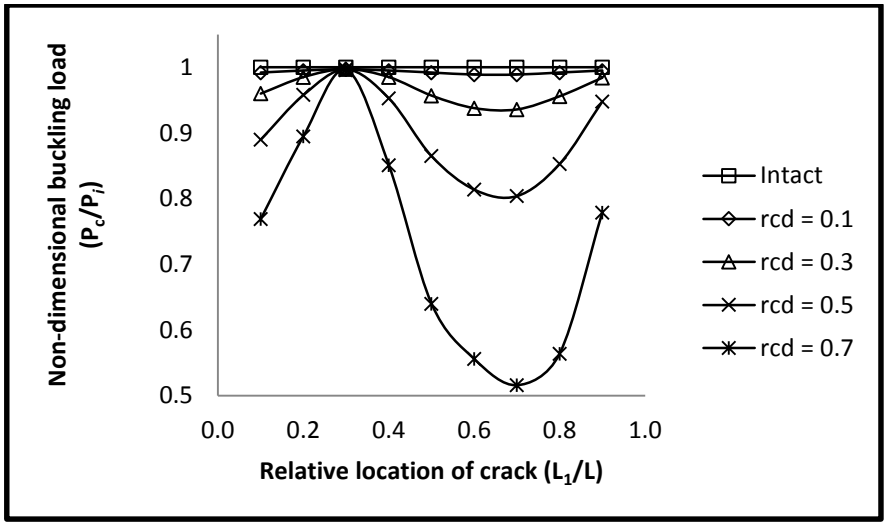

Figure 6.71 Variation of non-dimensional buckling load (P_c/P_i) with respect to relative location of crack (L_1/L) for different relative crack depths for Fixed-Hinged beam

It is observed that the crack near the fixed support of the fixed-hinged beam i.e. at 0.1L from left support reduces the non-dimensional buckling load by 1.5%, 4.7%, 11.3% and 22.4% than intact beam for relative crack depths of 0.1, 0.3, 0.5 and 0.7 respectively. Whereas the same cracks at 0.3L from left fixed end reduce the buckling loads marginally by 0.3%, 0.3%, 0.3% and 0.4% respectively. Hence it can be concluded that with the crack moving from 0.1L to 0.3L from fixed end, the buckling load increases and becomes almost equal to that of intact beam when the crack is at 0.3L. Similarly it is observed that the buckling load decreases as the crack moves further away from fixed end till it appears at 0.7L where the decrease in buckling load is found to be 1.1%, 6.4%, 19.6% and 48.4% for relative crack depths of 0.1, 0.3, 0.5 and 0.7 respectively. As the crack moves further towards the hinged end there is gain in buckling load in comparison to the buckling load for the crack at 0.7L. This suggests effect of crack on buckling load decreasing as the crack approaches hinged end. Finally when the crack is at 0.9L from fixed end i.e. near hinged end the buckling loads decrease by 0.5%, 1.6%, 5.2% and 22.1% than intact beam for relative crack depth of 0.1, 0.3, 0.5 and 0.7 respectively. The trend suggests when the crack will be at the hinged support its effect on buckling load will vanish.

6.9.4 Uniform fixed-fixed beam

The variation of non-dimensional buckling load with relative crack locations for different relative crack depths is shown in Fig. 6.72.

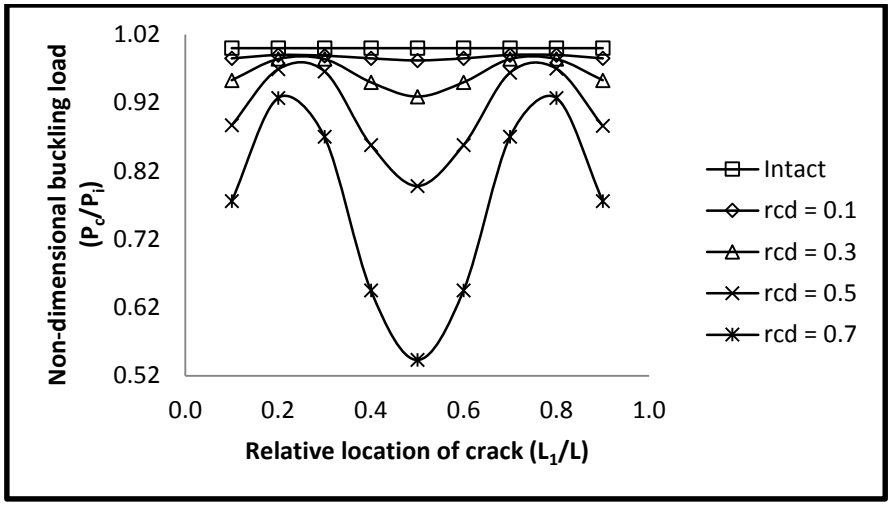

Figure 6.72 Variation of non-dimensional buckling load (P_c/P_i) with respect to relative location of crack (L_1/L) for different relative crack depths for Fixed-Fixed beam

It is observed that for a crack at 0.1L from either fixed end the non-dimensional buckling loads decrease by 1.5%, 4.7%, 11.3% and 22.4% than intact beam for relative crack depths of 0.1, 0.3, 0.5 and 0.7 respectively. The same crack at mid-span decrease the non-dimensional buckling loads by 1.8%, 7.1%, 20.2% and 45.7% respectively than intact beam. It is also observed that when the crack is in between 0.2L to 0.3L from either fixed end the decrease in buckling load is marginal. This suggests when the crack is on the fixed support; its effect is considerable as the fixed end of a fixed beam is subject to adequate amount of bending moment. Since maximum bending moment occurs at mid-span there is maximum drop of buckling load and bending moment between 0.2L to 0.3L is minimum hence there is marginal drop in buckling load.

6.9.5 Stepped fixed-free beam

Buckling analysis of the stepped beam shown in Fig. 6.5 is carried out for the stepped beam for different location and depth of the crack. Non-dimensional buckling load is computed and plotted in Fig. 6.73 with respect to relative crack location for different depths of the crack.

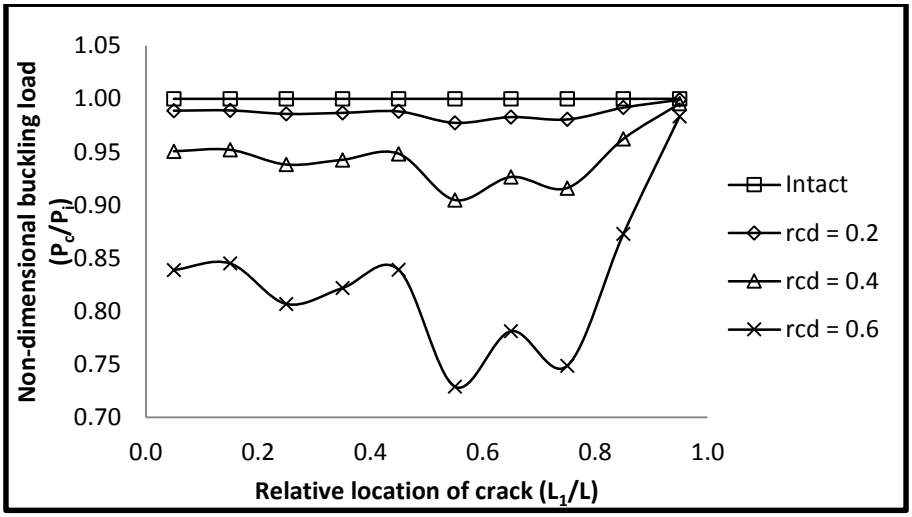

Figure 6.73 Variation of non-dimensional buckling load with relative location of crack for various relative crack depths of a stepped beam

It is observed that the crack at 0.05L from fixed end brings down non-dimensional buckling load by 1.1%, 4.9% and 16.1% for relative crack depth of 0.2, 0.4 and 0.6 respectively. It is observed in Fig. 6.69 that for a beam of uniform section the buckling load approaches the buckling load of intact beam as the crack approaches the free end of the cantilever (fixed-free) beam. But in Fig. 6.73, there is marginal increase in buckling load between the crack at 0.05L and 0.15L from free end. But when the crack happens to be at 0.25L from fixed end there is drop in buckling load by 1.4%, 6.2% and 19.3% than that of intact beam for relative crack depths of 0.2, 0.4 and 0.6 respectively. The buckling load which increases with the crack shifting away from the fixed end as shown in Fig. 6.69 in a uniform beam gets a drop here. This is due to the fact that there is sudden decrease in depth of the beam at the section 0.25L from the fixed end resulting in sudden loss of stiffness. Presence of the crack at the same location decreases the stiffness further which leads to loss in buckling load. The same phenomenon takes place again at 0.5L (i.e. between 0.45L and 0.55L) where the drop in buckling is found to be 2.3%, 9.5% and 27.1% than intact beam for relative crack depth of 0.2, 0.4 and 0.6 respectively. Similarly the drop in buckling load for crack at 0.75L where there is another step is given by 1.9%, 8.4% and 25.1% than intact beam for relative crack depths of 0.2, 0.4 and 0.6 respectively. Like previous cases when the crack is near the free end (i.e. 0.95L) the buckling load of the cracked beam almost coincides with that of intact beam suggesting effect of crack near the free end of a stepped cantilever beam is also negligible.

6.10 Buckling of Beam Subjected to Multiple cracks

6.10.1 Uniform fixed-free beam

Analysis of non-dimensional buckling load for the uniform beam shown in Fig. 6.4 with cantilever end conditions is carried out for two and three cracks. The variation of non-dimensional buckling loads of the uniform cantilever beam subjected to two cracks is shown in Fig. 6.74. The first crack is positioned at 0.1L of relative crack depth 0.3 and the position of the second crack is varied between 0.05L to 0.95L from the fixed support.

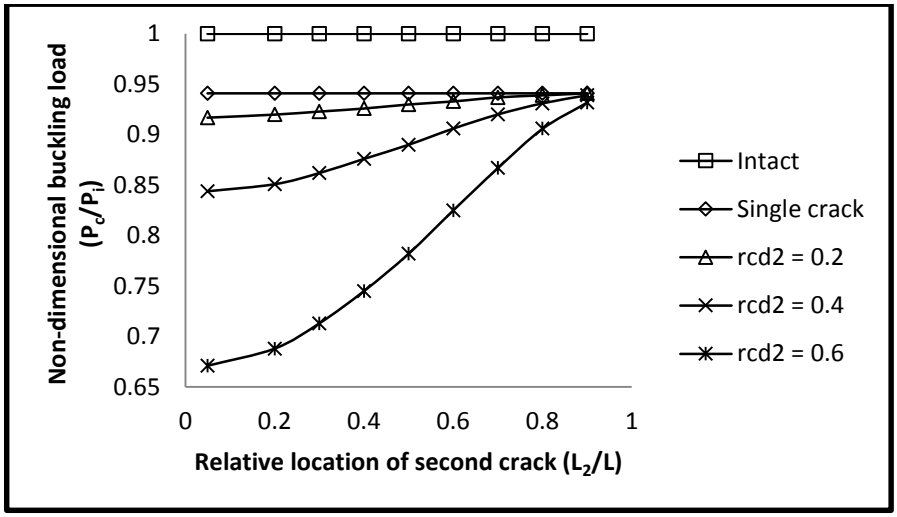

Figure 6.74 Variation of non-dimensional buckling load (P_c/P_i) with relative location of the second crack (L_2/L) for different relative crack depths (rcd) of the Fixed-Free beam (L_1= 0.1L, rcd_1= 0.3)

It can be concluded from Fig. 6.74 that the presence of first crack alone at 0.1L of relative depth 0.3 reduces the buckling load by 5.9% than that of an intact beam. But inclusion of a second crack at 0.05L from the fixed end reduces the non-dimensional buckling load by 6.5%, 11.2% 22.9% and 49.5% than intact beam for relative crack depth of 0.1, 0.3, 0.5 and 0.7 respectively. This implies inclusion of the second crack at 0.05L from fixed end brings down the buckling loads by additional 0.6%, 5.3%, 17% and 43.6% for relative crack depths of 0.1, 0.3, 0.5 and 0.7 respectively. Similarly when the second crack is near the free end i.e. at 0.95L from fixed end, the decrease in buckling loads are 5.9%, 5.9%, 6.0% and 6.4% for relative crack depths of 0.1, 0.3, 0.5 and 0.7 respectively compared to the intact beam. This implies introduction of a second crack in the beam weakens it further in terms of buckling but the severity of its effect depends upon its position from fixed end. Second crack close to fixed end of the beam reduces

buckling loads more than this crack at any other location. Second crack near free end has very little or no effect on buckling loads. Similarly buckling analysis is carried out for the beam subjected to three cracks and variations of non-dimensional buckling load for different relative locations of the third crack for different relative crack depths is plotted in Fig. 6.75.

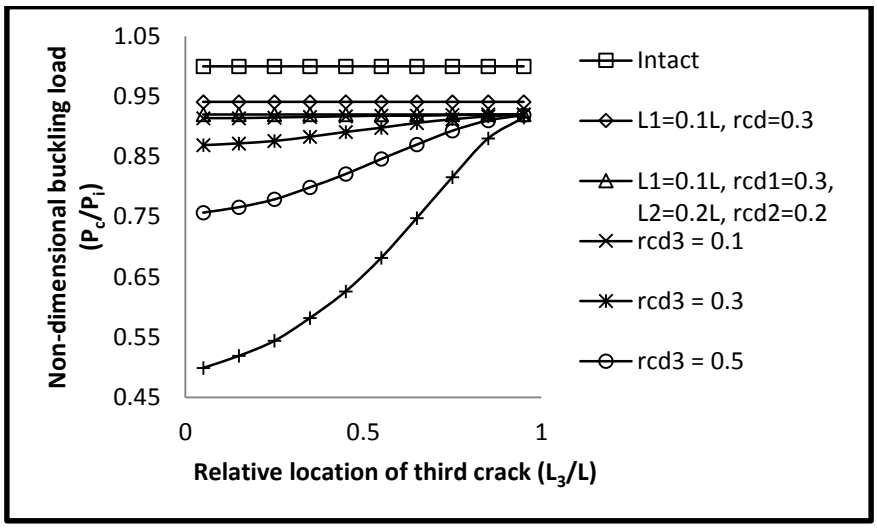

Figure 6.75 Variation of non-dimensional buckling load (P_c/P_i) with relative location of the third crack (L_3/L) for different relative crack depths (rcd) of the Fixed-Free beam (L_1=0.1L, L_2=0.2L, rcd_1=0.3, rcd_2=0.2)

It is observed from the Fig. 6.74 and 6.75 that the non-dimensional buckling loads decrease by 5.9% for first crack only of relative depth 0.3 at 0.1L from fixed end. Similarly introduction of the second crack of relative depth 0.2 at 0.2L from fixed end reduce the buckling load by 8.0% than intact beam. This implies introduction of the second crack brings down the buckling load by additional 2.1%. Now the introduction of the third crack at 0.05L reduces the non-dimensional buckling loads by 8.6%, 13.1%, 24.3% and 50.1% than intact beam for relative crack depths of 0.1, 0.3, 0.5 and 0.7 respectively. It is observed that the non-dimensional buckling loads increase with the third crack moving away from the fixed end. Finally when it is positioned at 0.95L from the fixed end (i.e. close to free end), the non-dimensional buckling loads decrease by 8.0%, 8.0%, 8.1% and 8.5% than intact beam for relative crack depths of 0.1, 0.3, 0.5 and 0.7 respectively. This implies the effect of third crack gradually decreases as it moves towards free end and the beam behaves like a beam of two cracks.

From the Fig. 6.74 and 6.75, it can be concluded that there is decrease in buckling loads due to presence of cracks. However the effect of the crack is more pronounced for those nearer to fixed end than free end. This is due to the fact that the sections nearer to fixed end are subjected

to more bending moment than those nearer to free end. More bending moment in sections result in more release of strain energy due to presence of a crack and vice versa. Release of strain energy at a section makes the beam weaker than intact beam.

6.10.2 Stepped fixed-free beam

Buckling analysis is carried out for the stepped fixed-free beam shown in Fig. 6.5 for multiple cracks. The variation of buckling load of the stepped beam subjected to two cracks at different locations and depths is shown in Fig. 6.76.

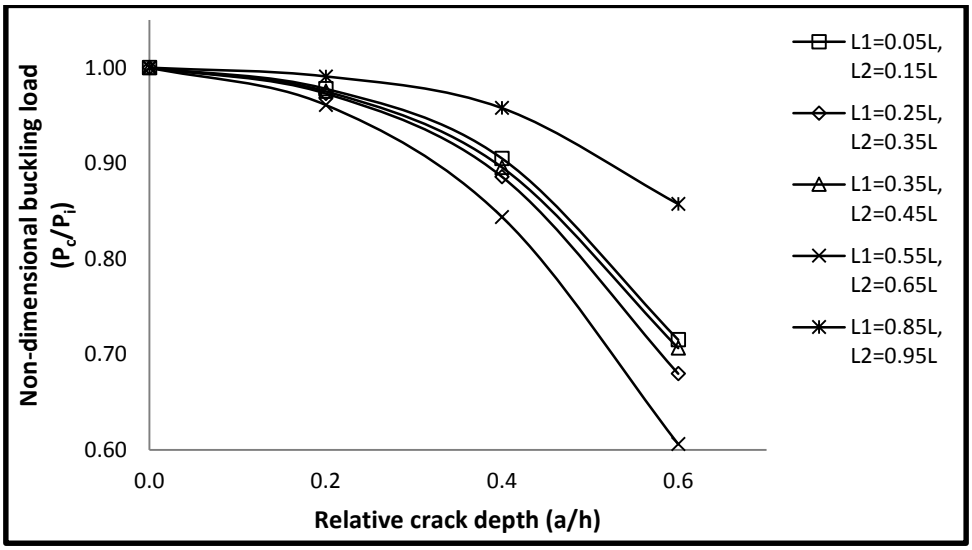

Figure 6.76 Variation of non-dimensional buckling load (P_c/P_i) with relative crack depth for various location of two cracks of the double cracked stepped fixed-free beam

It is observed that the beam suffers a loss of 3.9%, 15.6% and 39.4% in buckling load when two cracks are at 0.55L and 0.65L from fixed end for relative crack depths of 0.2, 0.4 and 0.6 respectively. The loss of buckling load due to cracks at 0.05L and 0.15L from fixed end i.e. near fixed end is 2.2%, 9.5% and 28.5% in comparison to intact beam for relative crack depths of 0.2, 0.4 and 0.6 respectively. Similarly cracks near free end i.e. at 0.85L and 0.95L bring down the buckling load by 0.9%, 4.2% and 14.2% for relative crack depths of 0.2, 0.4 and 0.6 respectively. The cracks in the third segment i.e. at 0.55L and 0.65L reduce the buckling load more than other locations mainly due to the fact that the depth of a step at 0.5L where the depth of the beam changes from 12 mm to 8 mm. Crack in the segment reduces the stiffness further and there is a severe loss of strain energy which brings down the buckling load for all depths of the crack. Cracks near free end affect the buckling loads marginally but in present case the

effect is considerable. This is due to steps in the beam which causes loss of stiffness and cracks near free end add to that. Similarly cracks at other locations considerably affect the buckling load as shown in Fig. 6.76. The variation of non-dimensional buckling load with relative crack depth for different locations of three cracks on stepped beam is shown in Fig. 6.77.

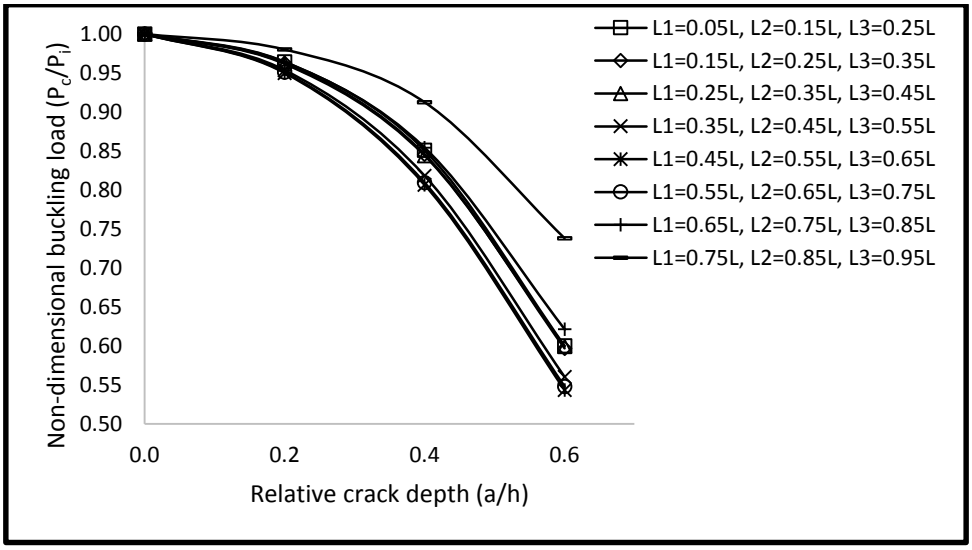

Figure 6.77 Variation of non-dimensional buckling load (P_c/P_i) with relative crack depth for various location of crack of the triple cracked stepped fixed-free beam

It is observed that the buckling load for first three cases of crack positions are almost not affected by crack position. There is decrease of 40.0%, 40.1% and 40.3% of buckling load in first three cases of cracks for a relative crack depth of 0.6. This implies the buckling load which should increase as the cracks move away from fixed end is getting compensated by the steps. It is also observed that as long as the cracks are within the first two segments of the beam the buckling load of the beam almost remains constant for multiple cracks. But as the crack shifts towards third segment there is a big drop in buckling load. Similarly when the cracks moves to fourth segment there is little improvement in buckling load. When the three cracks are at 0.75L, 0.85L and 0.95L from fixed end (near free end) the decrease in buckling load is 2.0%, 8.7% and 26.2% than intact beam for relative crack depth of 0.2, 0.4 and 0.6 respectively. It is also observed that for small depths there is little change in buckling load but as the depth increases the intensity of loss of buckling load increases.

6.11 Parametric Resonance Characteristics for Single Cracked Beams

The study is then extended to find the effect of cracks on regions of dynamic instability. The effect of static and dynamic load factors, location and depth of cracks upon excitation frequencies of dynamic instability are computed and plotted for different end conditions of the beam.

6.11.1 Uniform fixed-free beam

The variation of excitation frequencies with dynamic load factor (β = 0.1 to 1.0) for different static load factor (α = 0.0, 0.2, 0.4 and 0.6) of the beam with a single crack of relative depth 0.4 at 0.1L from fixed end are shown in Fig. 6.78.

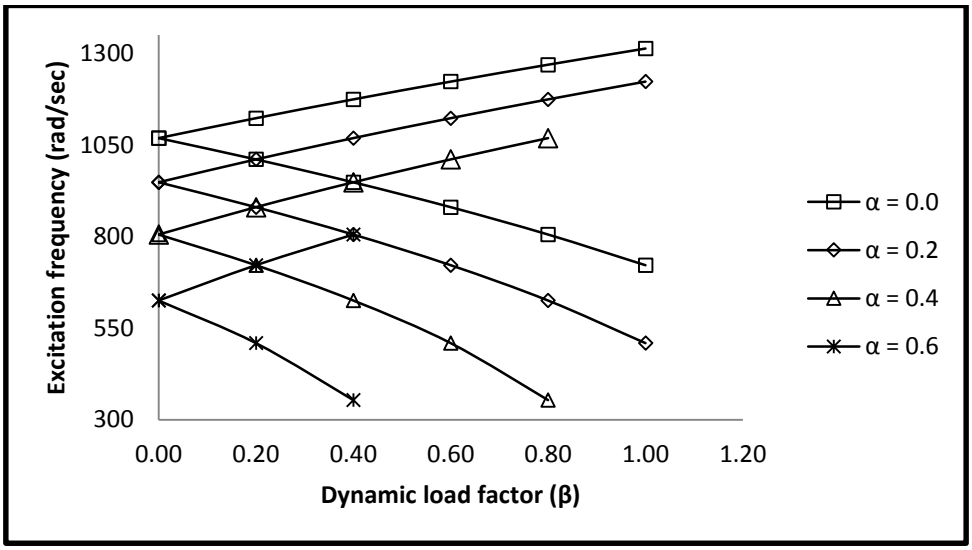

Figure 6.78 Variation of excitation frequencies with dynamic load factors (β) for different values of static load factor (α) of the fixed-free beam subjected to a single crack at L_1 = 0.1*L* of relative crack depth (rcd) = 0.4

It is observed that the onset of dynamic instability occurs earlier by 8.0%, 18.4%, 30.7% and 46.2% than the intact beam for static load factors of 0.0, 0.2, 0.4 and 0.6 respectively. Increase in static load factor increases the width of dynamic instability region (DIR) by 16.3%, 42.6% and 99.7% for static load factor of 0.2, 0.4 and 0.6 respectively than the width of instability region corresponding to α = 0. Thus with increase in static load factors the onset of dynamic instability occurs earlier and the instability region widens. The effect of dynamic load factors on dynamic instability regions of intact beam and the beam with a crack at 0.1L of static load factor 0.2 for relative depth 0.2, 0.4 and 0.6 are shown in Fig. 6.79. Similarly the effect of

dynamic laod factors on dynamic instability regions for different locations of a crack of relative depth of 0.4 and static load factor of 0.4 are shown in the Fig. 6.80.

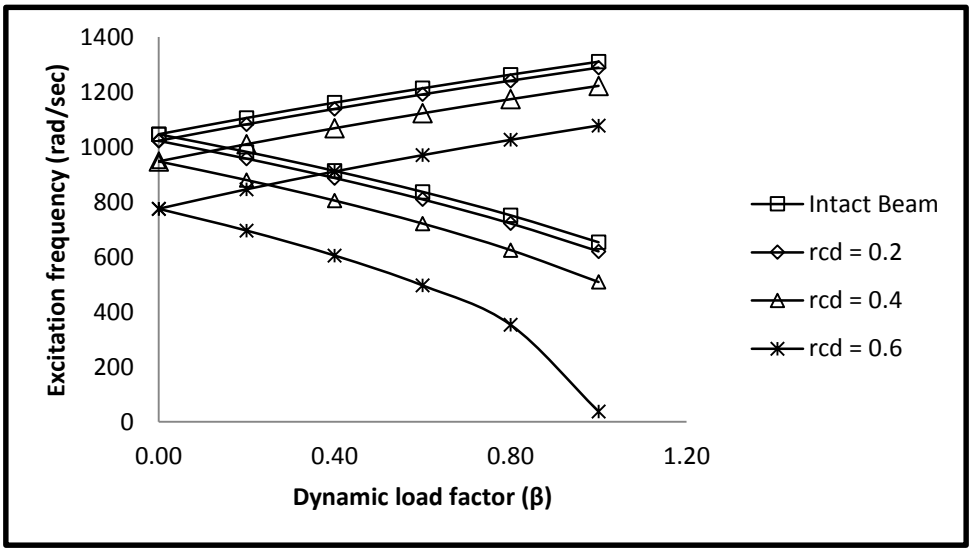

Figure 6.79 Variation of excitation frequencies with dynamic load factors (β) for different values of relative crack depth of the fixed-free beam subjected to a single crack at L_1 = 0.1L and static load factor α = 0.2

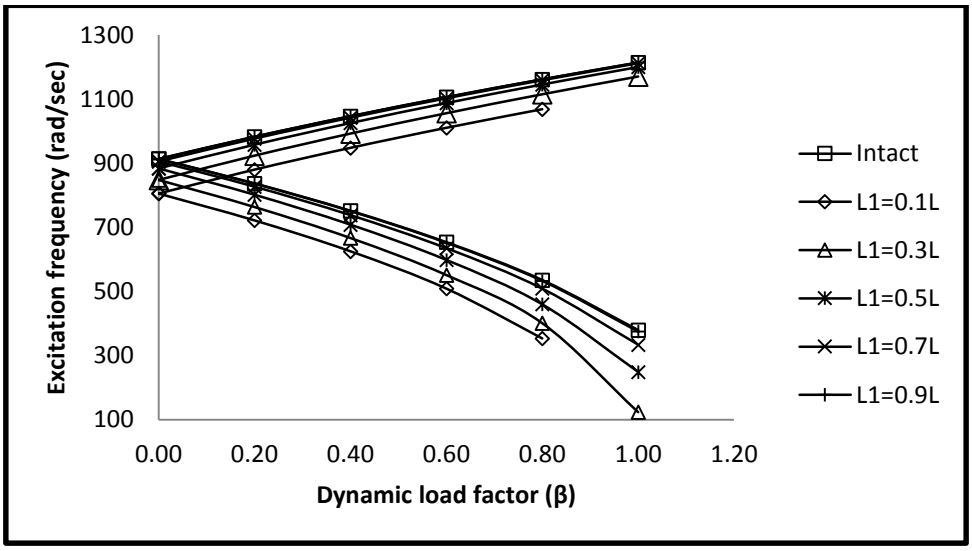

Figure 6.80 Variation of excitation frequencies with dynamic load factor (β) for different relative location of crack of the fixed-free beam subjected to a single crack of relative depth (rcd) = 0.4 and static load factor α = 0.4

It is observed from Fig. 6.79 that the onset of dynamic instability occurs earlier by 2.3%, 9.4% and 25.9% for relative crack depths of 0.2, 0.4 and 0.6 respectively than the corresponding intact beam. There is also increase in width of dynamic instability region by 1.8%, 8.6% and

58.4% for relative crack depth of 0.2, 0.4 and 0.6 respectively than intact beam. This implies the rate of decrease in the excitation frequencies and width of instability region are proportional to the relative crack depth i.e. more the depth of the crack more is the rate of decrease in excitation frequencies and more is the width of dynamic instability region due to reduction of stiffness of the beam.

According to Fig. 6.80, the onset of dynamic instability frequencies decrease by 11.8%, 7.2%, 3.2%, 0.9% and 0.1% for the crack at 0.1L. 0.3L, 0.5L, 0.7L and 0.9L respectively. This implies with the crack moving away from the fixed end the onset of the dynamic instability occurs later and at the same time the width of dynamic instability region gets narrower by 14.3%, 14.1%, 9.6%, 3.9% and 0.4% than intact the corresponding intact beam for crack location of 0.1L, 0.3L, 0.5L, 0.7L and 0.9L respectively and dynamic load factor 0.8.

Thus it is observed that the onset of dynamic instability region occurs earlier as the cracks get closer to fixed end of the fixed-free beam and as the crack moves away from the fixed end the dynamic instability gets delayed. The region of dynamic instability approaches to that of intact beam when the location of the crack approaches the free end suggesting the effect of the crack gradually decreases as the crack moves away from fixed end and its effect near free end is negligible on dynamic instability regions.

6.11.2 Uniform hinged-hinged beam

The variations of dynamic instability regions with dynamic load factors for different static load factors are plotted in Fig. 6.81 for a crack at 0.1L from hinged support of relative depth 0.4. Similarly the variations of dynamic instability regions with dynamic load factors for different relative crack depths are plotted in Fig. 6.82 for the crack at 0.5L from hinged support for static load factor of 0.2.

It is observed from Fig. 6.81 that the onset of dynamic instability regions occurs earlier by 0.6%, 11.2%, 23.3% and 37.8% for static load factors of 0.0, 0.2, 0.4 and 0.6 respectively than intact beam. It is also observed that the width of the dynamic instability region gets wider with increase in static load factors.

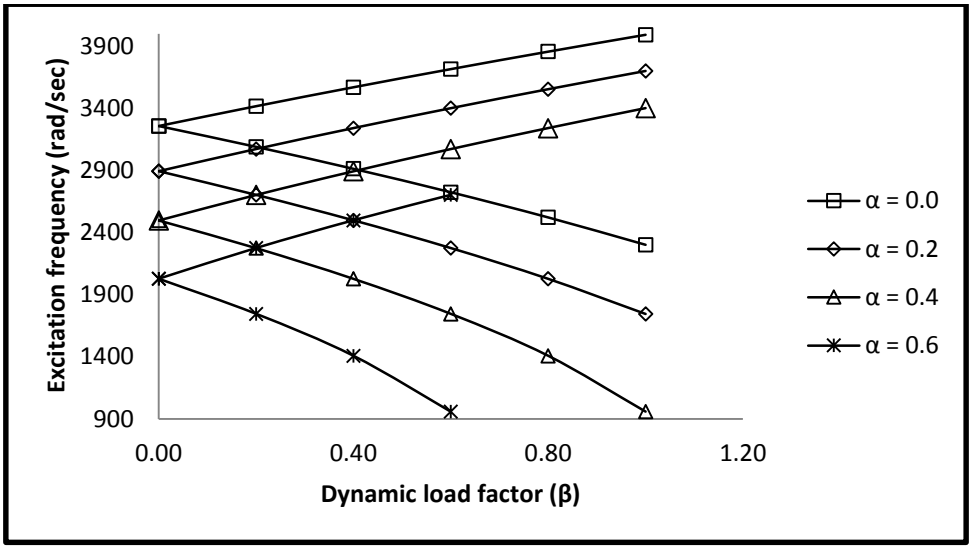

Figure 6.81 Variation of excitation frequencies with dynamic load factor (β) for different values of static load factor (α) of the hinged-hinged beam subjected to a single crack at L_1 = 0.1L of relative crack depth (rcd) = 0.4

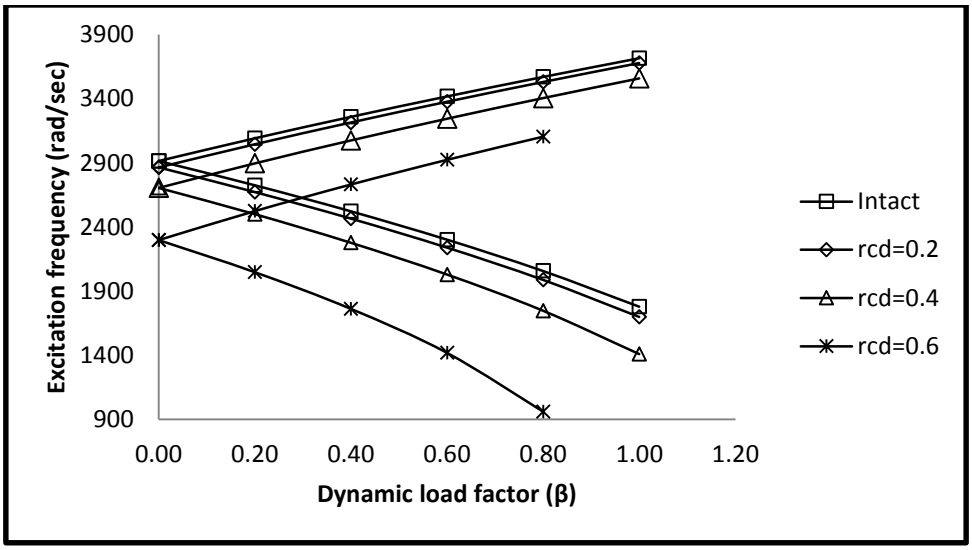

Figure 6.82 Variation of excitation frequencies with dynamic load factor (β) for different values of relative crack depth of the hinged-hinged beam subjected to a single crack at L_1 = 0.5L and static load factor α = 0

Similarly Fig. 6.82 shows that the onset of dynamic instability regions occur earlier by 1.7%, 7.1% and 21.1% for relative crack depths of 0.2, 0.4 and 0.6 respectively when the crack happens to be at 0.5L and static load factor 0.2. When static load factor is 0.2 and dynamic load factor is 0.8, the width of dynamic instability region increases by 2.0%, 9.6% and 41.7% for relative crack depths of 0.2, 0.4 and 0.6 respectively. This implies the increase in crack depth makes the beam dynamically unstable earlier than intact beam and the regions of dynamic

instability gets wider. The variations of dynamic instability regions of the beam with dynamic load factors for various relative location of the crack from a hinged support of relative depth 0.4 are plotted in Fig. 6.83.

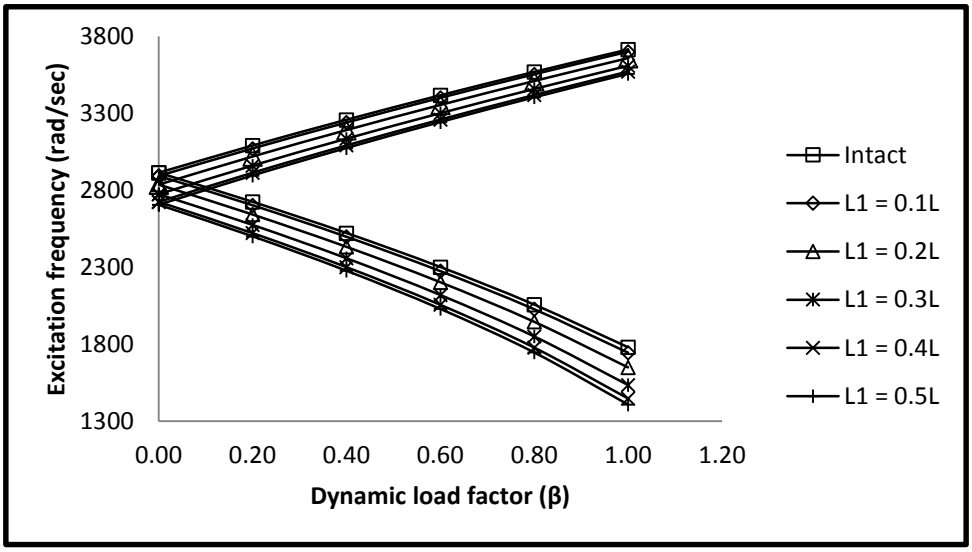

Figure 6.83 Variation of excitation frequencies with dynamic load factor (β) for different relative location of crack of the hinged-hinged beam subjected to a single crack of relative depth (rcd) = 0.4 and static load factor α = 0.2

It is observed from Fig. 6.83 that the onset of dynamic instability occurs earlier as the crack moves towards mid-spam from supports. The decrease in dynamic instability frequency for no dynamic load factor is found to be lesser by 0.7%, 2.6%, 4.8%, 6.4% and 7.1% than the corresponding intact beam when the crack is at 0.1L, 0.2L, 0.3L, 0.4L and 0.5L respectively. Similarly the width of dynamic instability regions expands by 1.0%, 3.7%, 7.1%, 9.8% and 11.0% compared to width of corresponding intact beam for the crack at 0.1L, 0.2L, 0.3L, 0.4L and 0.5L respectively from the support. This implies the effect of the crack increases as the crack moves towards the mid-span from the support. This is due to the fact that the sections near mid-span are subjected to more bending moment than the section near supports. For sections subjected to more bending moment, presence of crack results in more release of strain energy, for which the beam becomes more flexible. So the sections become more vulnerable in dynamic stability than the sections subjected to less bending moment near the supports. Comparing the excitation frequencies of the onset of dynamic instability in fixed-free beam and hinged-hinged beam in Fig. 6.80 and 6.83, the fixed-free beam attains dynamic instability at a frequency much less than that of hinged-hinged beam.

Thus it is observed that the onset of dynamic instability occurs earlier and the dynamic instability region widens as the crack approaches mid-span. Similarly the effect of crack gradually decreases as the crack appears to be near the hinged supports.

6.11.3 Uniform fixed-hinged beam

The variations of dynamic instability regions for the beam with fixed-hinged end conditions for a crack at 0.1L from fixed end of relative depth 0.6 are plotted in Fig. 6.84 for different static load factors. Similarly the variations of excitaing frequencies of dynamic instability regions with dynamic load factor for different relative crack depths of uniform beam with fixed-hinged end conditions are shown in Fig. 6.85.

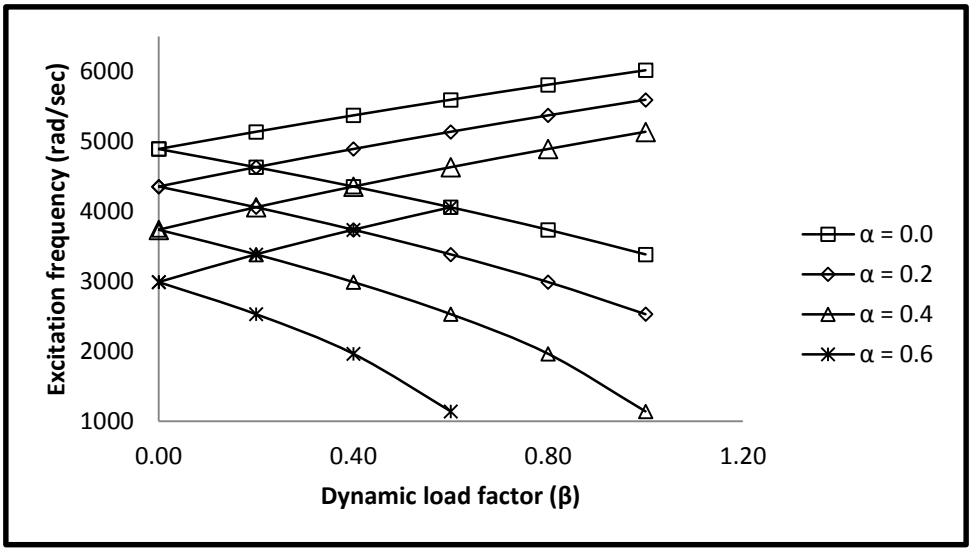

Figure 6.84 Variation of excitation frequencies with dynamic load factor (β) for different values of static load factor (α) of the fixed-hinged beam subjected to a single crack at L_1 = 0.6*L* of relative crack depth (rcd) = 0.6

Referring to Fig. 6.84, it can be concluded that the onset of dynamic instability regions occur earlier by 3.7%, 14.2%, 26.4% and 41.1% for static load factors of 0.0, 0.2, 0.4 and 0.6 respectively for the crack at 0.6L subjected to a static load factor of 0.2. It is also observed that increase in static load factors increases the width of the dynamic instability regions.

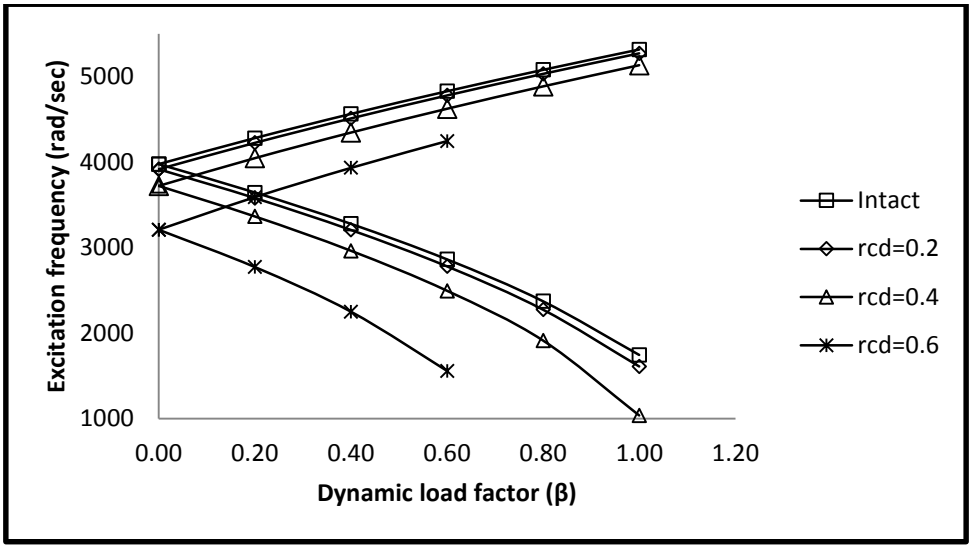

Figure 6.85 Variation of excitation frequencies with dynamic load factor (β) for different values of relative crack depth of the fixed-hinged beam subjected to a single crack at $L_1 = 0.6L$ and static load factor α = 0.2

Similarly from Fig. 6.85, it is observed that onset of dynamic instability regions occur earlier by 1.5%, 6.4% and 19.3% than corresponding intact beam for relative crack depth of 0.2, 0.4 and 0.6 respectively. Similarly the width of dynamic instability regions increase by 1.7%, 8.3% and 36.8% than that of intact beam for static load factor of 0.4 and dynamic load factor of 0.6 when relative crack depths are 0.2 and, 0.4 and 0.6 respectively. Thus it can be concluded that increase in depth of the crack for any particular location increase the rate of decrease in dynamic instability frequency and increase in width of the the dynamic instability region. The variations of dynamic instability regions with dynamic load factors for various locations of crack from fixed end are shown in Fig. 6.86.

It is observed from Fig. 6.86 that presence of crack at 0.1L from fixed end lowers the onset of dynamic instability region by 5.9% and the crack at 0.3L from fixed end lowers the same by 0.1% only. Hence the dynamic instability regions of intact beam and crack at 0.3L of relative depth 0.4 and static load factor 0.4 almost coincides with each other. As the crack moves further away from the fixed end the onset of dynamic instability regions occurs earlier by 6.4% and 8.2% for the crack to be at 0.5L and 0.7L respectively from the fixed end. Finally when the crack is at 0.9L from fixed end i.e. close to hinged end, the dynamic instability commences at frequency lesser by 1.6% than the intact beam brequency. Hence it can be concluded that the

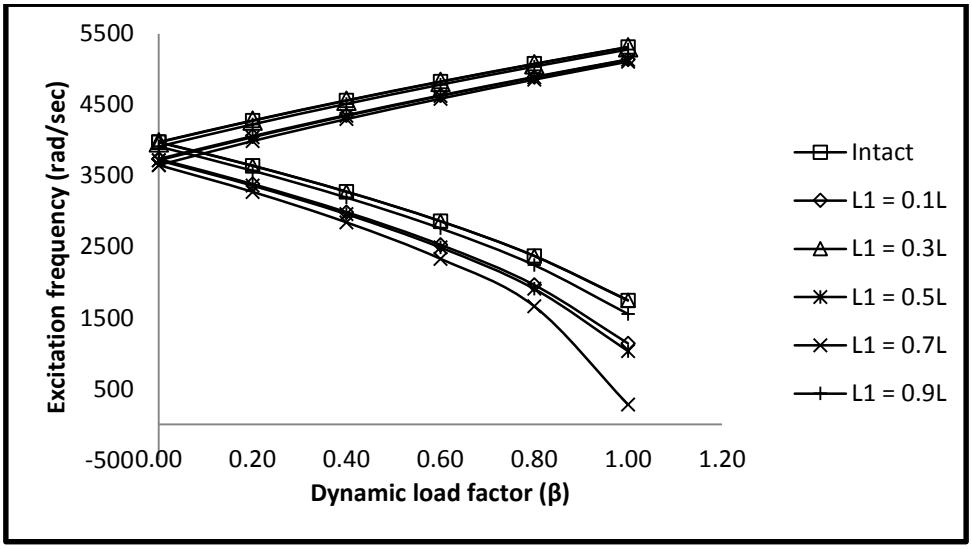

Figure 6.86 Variation of excitation frequencies with dynamic load factor (β) for different relative location of crack of the fixed-hinged beam subjected to a single crack of relative depth (rcd) = 0.6 and static load factor α = 0.4

crack near the fixed end affects more than the crack near the hinged end corresponding to dynamic instability. The crack near 0.3L marginally affects the beam. Comparing the excitation frequencies of the onset of dynamic instability in fixed-hinged beam and fixed-free beam in Fig. 6.86 and 6.80, the fixed-hinged beam attains dynamic instability at a frequency much later than that of fixed-free beam.

Thus it is observed that the dynamic instability region is hardly affected by a crack near 0.3L from fixed end. But for the crack at 0.7L the dynamic instability occurs earlier than any other location. Similarly the crack near fixed support affects the dynamic instability regions more than the crack near hinged support.

6.11.4 Uniform fixed-fixed beam

The variation of dynamic instability frequencies with dynamic load factors for different static load factors for a fixed-fixed beam end conditions are shown in Fig. 6.87.

According to Fig. 6.87, the onset of dynamic instability regions occur earlier by 2.8%, 13.6%, 26.2% and 41.7% than intact beam for static load factors of 0.0, 0.2, 0.4 and 0.6 respectively for a crack present at 0.1L from either end of relative depth 0.4. Similarly the width of the

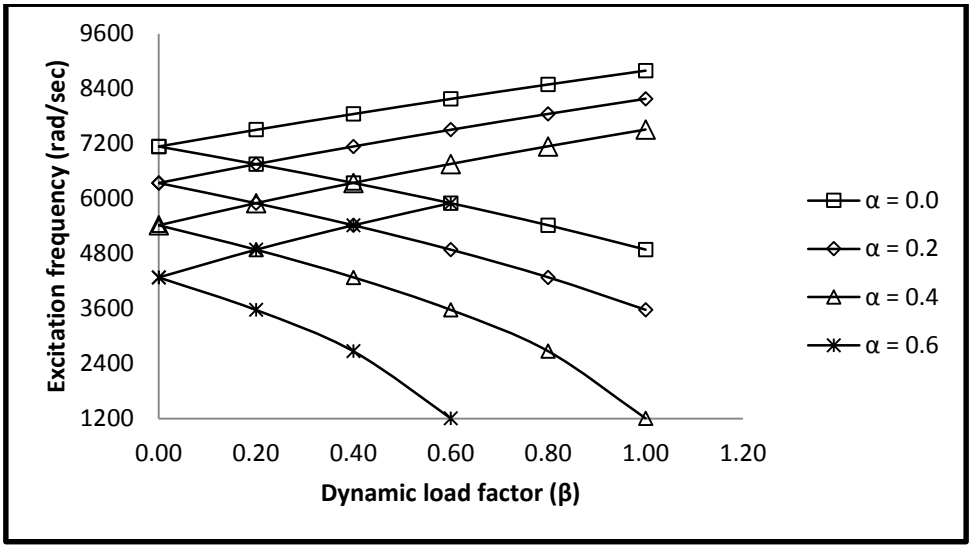

Figure 6.87 Variation of excitation frequencies with dynamic load factor (β) for different values of static load factor (α) of the fixed-fixed beam subjected to a single crack at L_1 = 0.5L of relative crack depth (rcd) = 0.4

dynamic instability region expands by 15.0%, 39.7% and 106.1% than the width corresponding to static load factor of 0.0 for the crack at 0.1L of relative depth 0.4. The variations of dynamic instability regions with dynamic load factors for different depths of a crack at 0.5L and static load factor 0.4 is shown in Fig. 6.88.

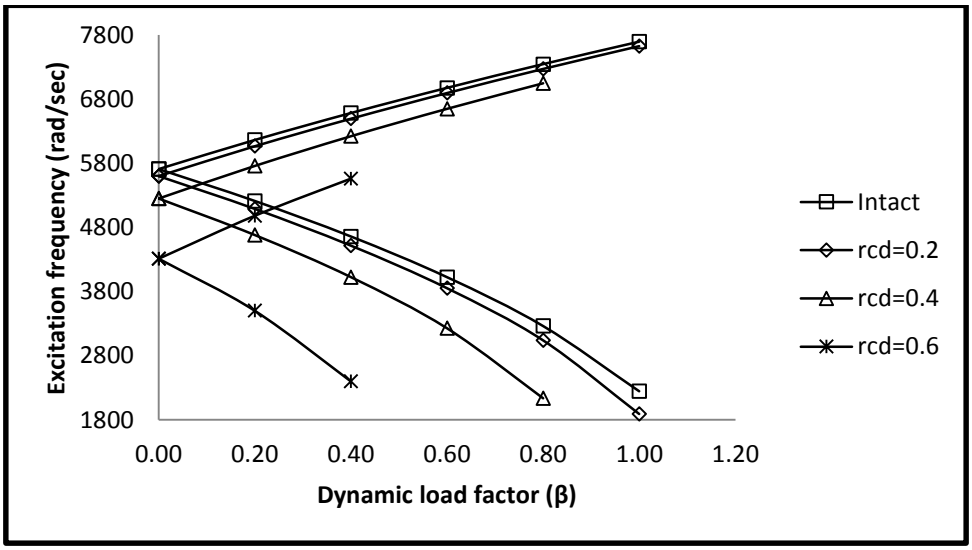

Figure 6.88 Variation of excitation frequencies with dynamic load factors (β) for different values of relative crack depth of the fixed-fixed beam subjected to a single crack at L_1 = 0.5L and static load factor α = 0.4

It is observed from Fig. 6.88 that increase in depth of the crack at 0.5L (mid-span) of the fixed-fixed beam of static load factor 0.4 brings down the commencement of the dynamic instability by 1.9%, 8.0% and 24.4% than intact beam for relative crack depths of 0.2, 0.4 and 0.6 respectively. Correspondingly the increase in dynamic instability region is by 2.9%, 14.2% and 64.1% than intact beam. Similarly variations of dynamic instability regions with different dynamic load factor for various locations of the crack are plotted in Fig. 6.89.

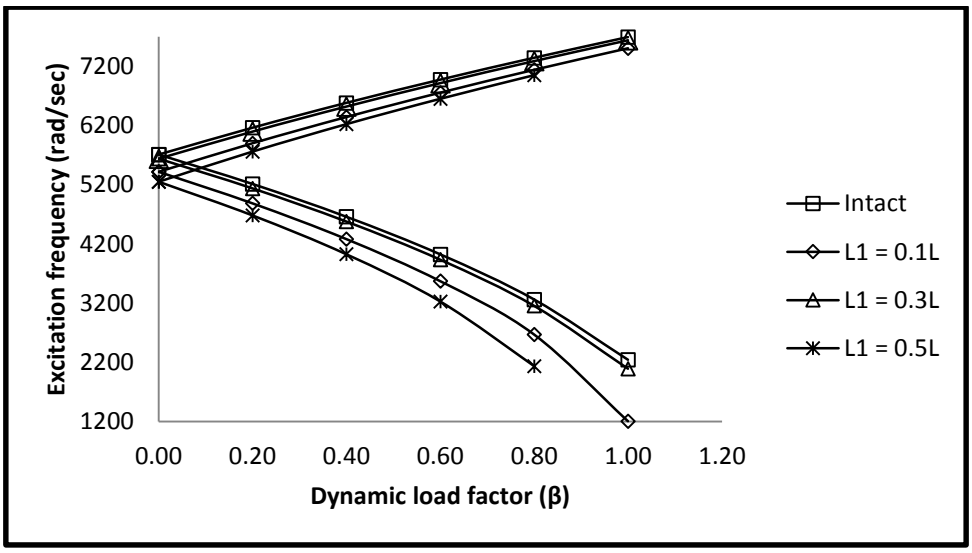

Figure 6.89 Variation of excitation frequencies with dynamic load factor (β) for different relative location of crack of the fixed-free beam subjected to a single crack of relative depth (rcd) = 0.6 and static load factor α = 0.4

It is observed from Fig. 6.89 that the onset of dynamic instability regions occurs earlier by 5.1%, 1.2% and 8.0% than intact beam for crack locations of 0.1L, 0.3L and 0.5L respectively from fixed end when the relative crack depth is 0.4 and static load factor 0.4. This implies the effect of crack gradually decreases as the crack moves from fixed end to 0.3L and its effect is maximum at mid-span. Comparing the excitation frequencies for the onset of dynamic instability in fixed-fixed beam and fixed-free beam in Fig. 6.89 and 6.80, the fixed-fixed beam attains dynamic instability at a frequency 528.98% later than that of fixed-free beam.

The variation of excitation frequencies with dynamic load factor for different end conditions of the beam subjected to a single crack at 0.1L from the left support of relative depth 0.4 and static load factor 0.4 is shown in Fig. 6.90.

It is observed that the excitation frequencies decrease by 9.4% for fixed-free, 0.7% for hinged-hinged, 4.5% for fixed-hinged and 3.6% for fixed-fixed end condition than their corresponding

intact beams for a crack of relative depth 0.4 at 0.1L and static load factor 0.2. The decrease in excitation frequencies for different end conditions is different as the location of crack i.e. 0.1L from left support for fixed-free, fixed-hinged and fixed-fixed end conditions are in different energy zones. The given location of crack for fixed-free, fixed-hinged and fixed-fixed end conditions is in comparatively higher energy zone (due to higher bending moment) than hinged-hinged end condition. Crack in a higher energy zone results in more strain energy release than the same crack in a lower energy zone. More strain energy release results in more effect on the beam in reducing its excitation frequencies and increasing in width of dynamic instability regions.

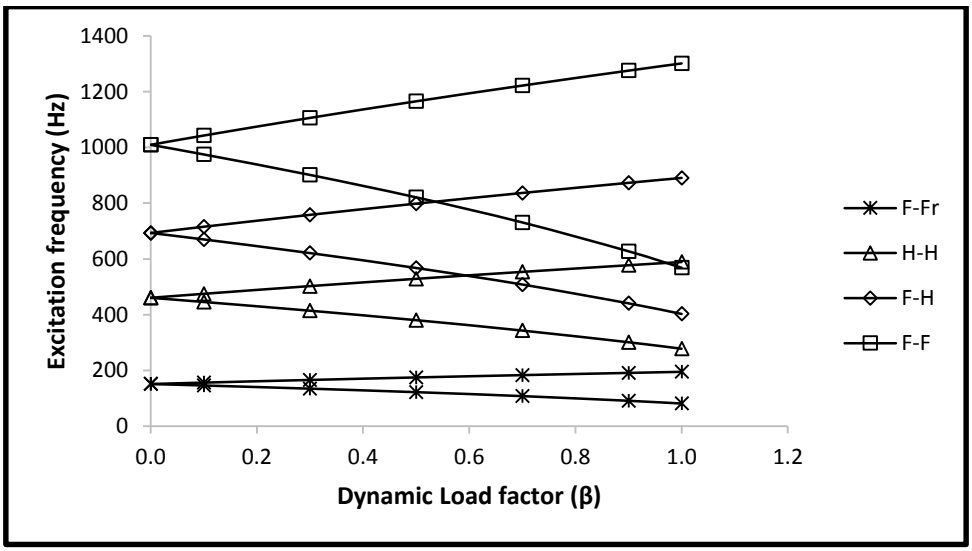

Figure 6.90 Variation of excitation frequencies with dynamic load factor (β) for different end conditions of the beam subjected to a single crack at 0.1L of relative depth (rcd) = 0.4 and static load factor α = 0.2

Variation of excitation frequencies of dynamic instability regions with dynamic load factors of the beams subjected to a single crack of relative depth 0.4 and static load factor 0.2 at their relatively higher bending moment zone for different end conditions is shown in Fig. 6.91.

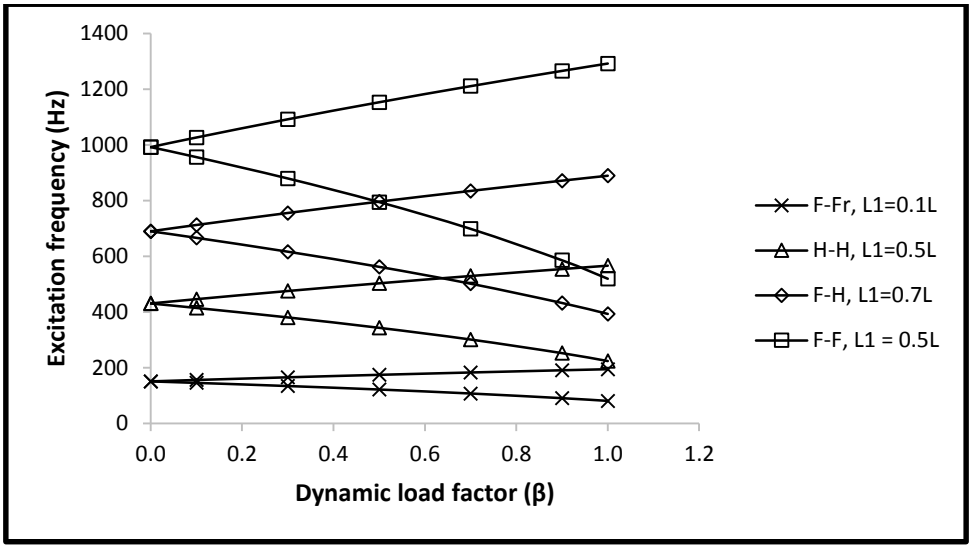

Figure 6.91 Variation of excitation frequencies with dynamic load factor (β) for different end conditions of the beam subjected to a single crack at critical region of the beam of relative depth (rcd) = 0.4 and static load factor α = 0.2

It is observed that the excitation frequencies of dynamic instability decrease by 9.4%, 7.1%, 5.0% and 5.3% than their corresponding intact beam frequencies for fixed-free, hinged-hinged, fixed-hinged and fixed-fixed end conditions respectively. The corresponding increase in dynamic instability region is given by 8.7%, 11.0%, 7.5% and 12.2% than their corresponding intact beam instability region widths.

6.11.5 Stepped fixed-free beam

Parametric resonance characteristics of the stepped beam subjected to a transverse crack is carried out. Effect of static load factor on dynamic instability regions for the stepped beam subjected to a crack at 0.05L from fixed end is shown in Fig. 6.92.

It is observed from Fig. 6.92 that the onset of dynamic instability regions occur earlier by 11.5%, 19.4%, 29.2% and 42.1% for static load factor of 0.0, 0.2, 0.4 and 0.6 than the intact beam when the crack is at 0.05L from fixed end of depth 4 mm.

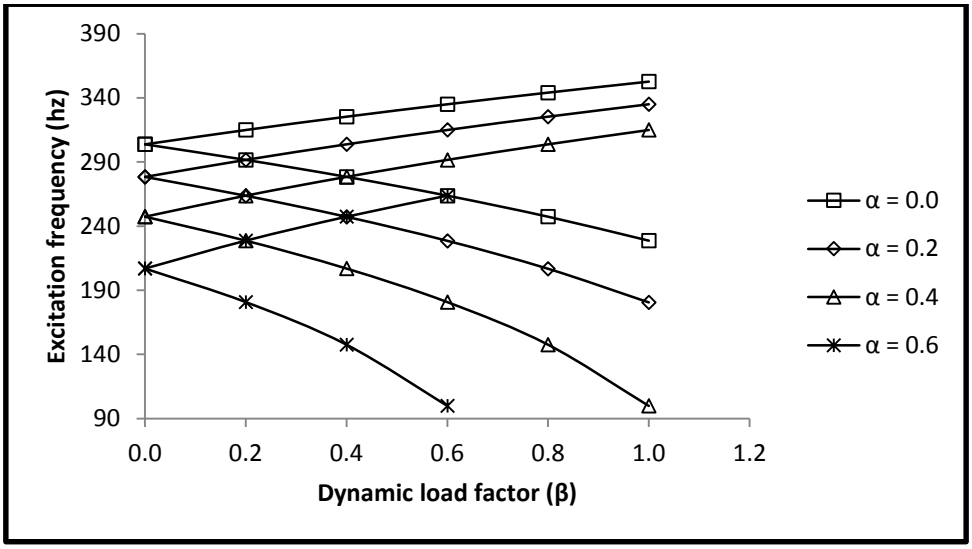

Figure 6.92 Effect of dynamic load factor (β) on dynamic instability regions of the Stepped cantilever beam subjected to a single crack at L_1 = 0.1L from fixed end of 4 mm crack depth for different values of static load factor (α)

It is also observed from Fig. 6.92 that there is increase in width of dynamic instability region by 21.9%, 59.3% and 155.7% over the width of the cracked stepped beam when dynamic load factor is 0.6 and static load factors are 0.2, 0.4 and 0.6 respectively. The variation of dynamic instability regions with dynamic load factor for various depths of the crack are shown in Fig. 6.93.

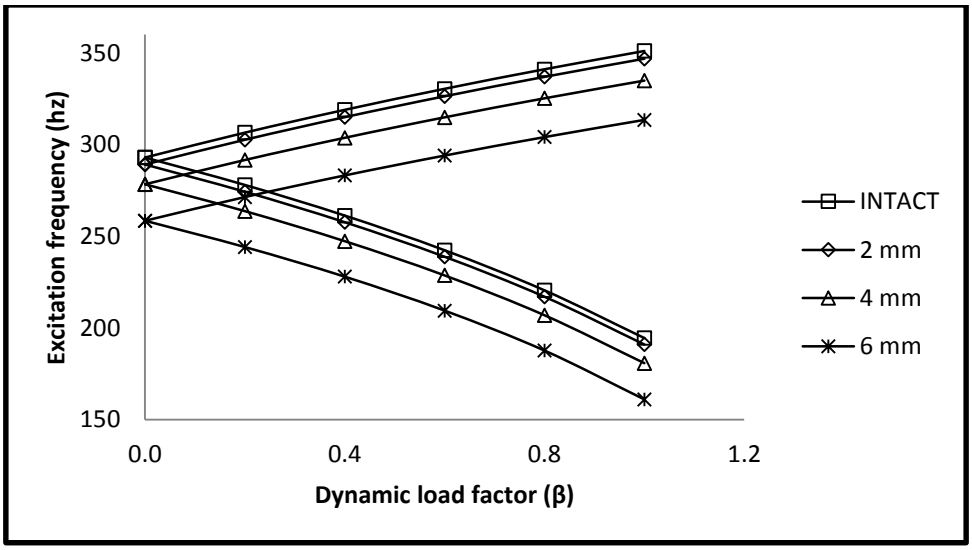

Figure 6.93 Effect of dynamic load factor (β) on dynamic instability regions of the Stepped cantilever beam subjected to a single crack at L_1 = 0.05L from fixed end for different values of crack depths and static load factor α = 0.2

It is observed from Fig. 6.93 that the onset of dynamic instability region occurs earlier by 9.8%, 12.7% and 19.0% than intact beam for relative crack depths of 0.2, 0.4 and 0.6 respectively. But it is observed that with increase in depth of the crack there is decrease in dynamic instability region with for the crack to be at 0.05L from fixed end of static load factor 0.2. The variation of dynamic instability regions for various position from fixed end of the 4 mm deep crack with dynamic load factors are shown in Fig. 6.94.

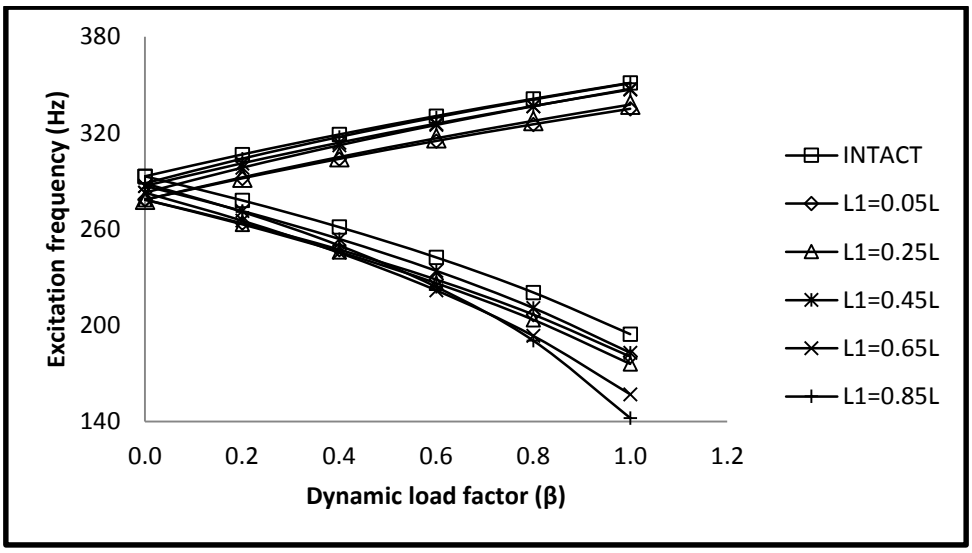

Figure 6.94 Effect of dynamic load factor (β) on dynamic instability regions of the Stepped beam subjected to a 4 mm deep single transverse open crack at different locations from fixed end and static load factor α = 0.4

It is observed that the onset of dynamic instability regions occurs earlier by 12.7%, 12.7%, 10.1%, 11.3% and 9.6% than intact beam for crack at 0.05L, 25L, 0.65L and 0.85L respectively for static load fcator of 0.2 and crack depth of 4 mm. But the width of the dynamic instability regions increase by -1.4%, 3.2%, 4.7%, 21.6% and 33.3% than intact beam for crack location of 0.05L, 0.25L, 0.45L, 0.65L and 0.85L respectively. Here it can be mentioned that for a uniform cantilever beam as the crack approaches free end the instability regions for different crack location approaches to that of intact beam. But in the present case even though the dynamic instability region due crack at 0.05L occurs12.7% earlier than intact beam the width of dynamic instability region decrease by 1.4% instead of increase in beam of uniform section. At the same time the width of the dynamic instability regions for all other locations mentioned increases. This may be due to fact that the effect of change in stiffness due to steps becoming predominant.

6.12 Parametric Resonance Characteristics for Multiple Cracks

6.12.1 Uniform fixed-free beam

Similarly dynamic instability regions for the beam subjected to two cracks are computed. First crack is considered at 0.1L and the second crack is introduced between 0.05L to 0.9L. Dynamic instability regions for different static and dynamic load factors for first crack at 0.1L of relative depth 0.2 and second crack at L_2 = 0.05L of relative depth 0.2 of a doubly cracked beam are shown in Fig. 6.95.

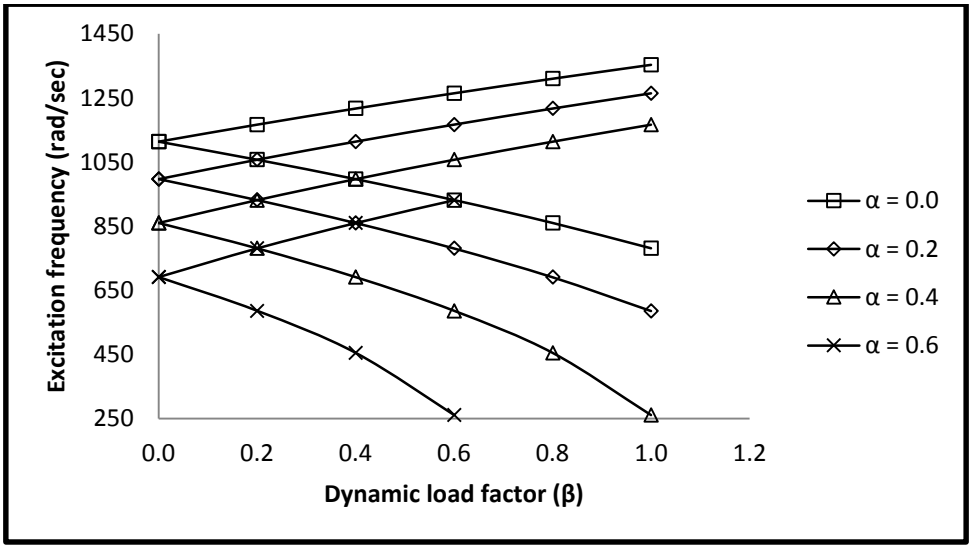

Figure 6.95 Effect of Static load factor (α) on dynamic instability regions of the fixed-free beam subjected to two cracks at $L_1 = 0.1L$, $rcd_1 = 0.2$ and $L_2 = 0.05L$ and $rcd_2 = 0.2$

It is clear from Fig. 6.95 that the dynamic instability frequencies decrease by 4.1%, 4.7%, 5.8% and 8.1% than intact beam for static load factors of 0.0, 0.2, 0.4 and 0.6 respectively. This implies, for a doubly cracked beam the dynamic instability occurs earlier than a beam with single crack. Similarly as in previous cases the frequencies of dynamic instability for a doubly cracked beam decreases by 4.1%, 4.7%, 5.8% and 8.1% with the increase in static load factors of 0.0, 0.2, 0.4 and 0.6. respectively. Again from the Fig. 6.95, it is found that the width of dynamic instability regions increase by 2.0%, 3.3% and 8.7% for static load factors of 0.0, 0.2 and 0.4 respectively. Similarly the variation of dynamic instability regions with dynamic load factors for different depth of second crack and static load factor 0.2 is computed and plotted in Fig. 6.96.

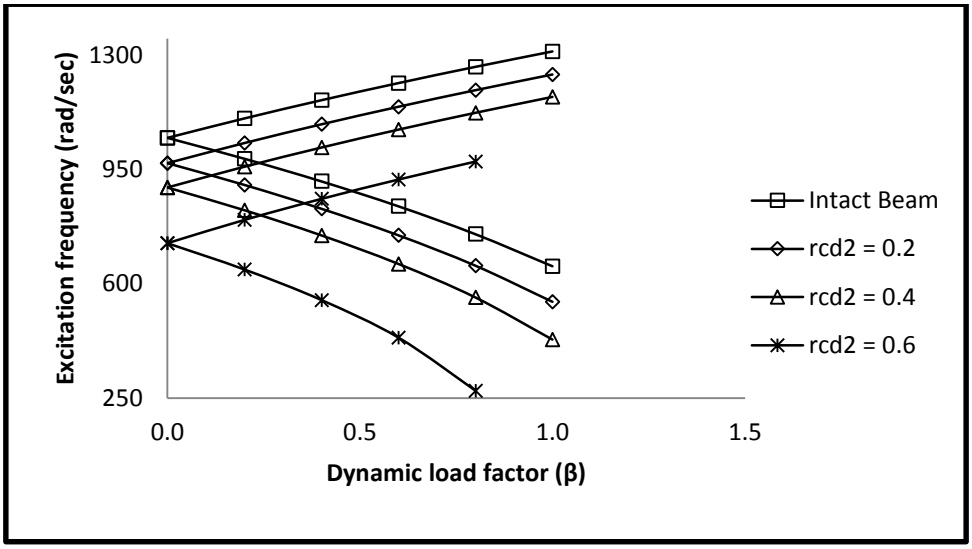

Figure 6.96 Effect of second crack depth on dynamic instability regions of the cantilever beam (*L*= 0.3m, b=*h*= 0.01m, *E*= 68.22GPa, *v*= 0.28 and *ρ*= 2569kg/m^3) with two cracks at L_1 = 0.1L, rcd_1 = 0.2 and L_2 = 0.05L for static load factor, α = 0.2

It is observed that the first crack of relative depth 0.2 is considered at 0.1L from fixed end and the second crack is considered at 0.05L from fixed end of relative depths 0.2, 0.4 and 0.6. According to Fig. 6.96, the onset of dynamic instability frequencies occur earlier by 2.3%, 4.7%, 12.4% and 29.5% than intact beam for relative crack depth of 0.0, 0.2, 0.4 and 0.6 respectively. It is also observed that the width of instability regions increase by 1.8%, 3.3% and 9.9% than the corresponding width of intact beam for relative crack depth of 0.0, 0.2 and 0.4 respectively. This implies with increase in relative depth of the crack the onset of dynamic instability occurs earlier and there is also marginal increase in width of the regions. The variation of dynamic instability regions with dynamic load factor for different locations of second crack for static load factor of 0.4 is computed and plotted in Fig. 6.97.

It is observed from Fig. 6.97 that the onset of dynamic instability occurs at a frequency lesser by 11.8% of intact beam when there is only the first crack at 0.1L of relative depth 0.4 and static load factor of 0.4. as the second crack is introduced at 0.05L of relative depth 0.4 and static load factor 0.4 the onset of dynamic instability occurs at a frequency lesser by 22.7% than intact beam. similarly as the second crack moves away from the fixed end the onset of dynamic instability occurs at frequencies lesser by 17.9%, 14.6%, 12.6% and 11.9% than intact beam for second crack location at 0.3L, 0.5L, 0.7L and 0.9L respectively. It is also observed

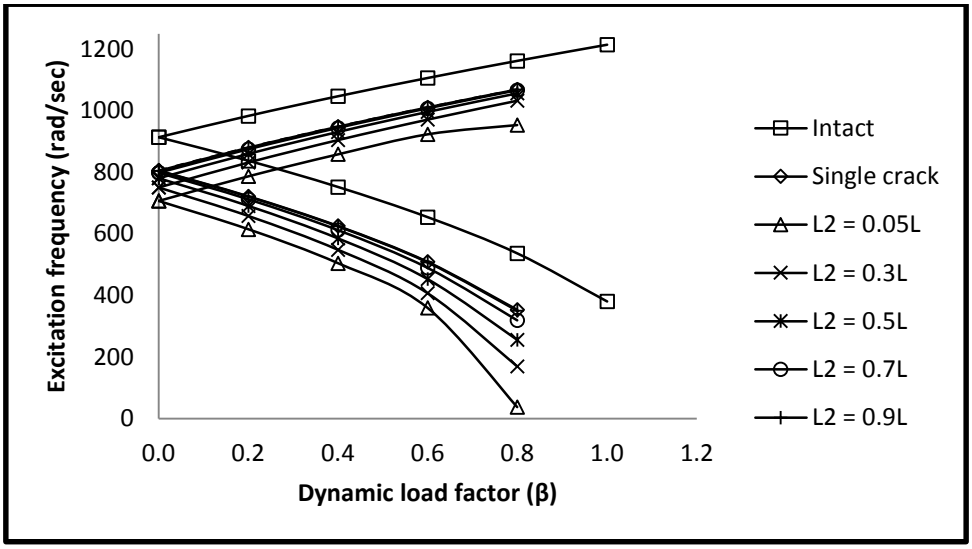

Figure 6.97 Effect of dynamic load factor (β) on dynamic instability regions of a cantilever beam for different locations of the second crack with two cracks, $L_1 = 0.1L$, $rcd_1 = 0.4$, $L_2 = 0.05L$ to $0.9L$, $rcd_2 = 0.4$ for $\alpha = 0.4$

that the width of dynamic instability increase by 14.3% for the first crack only at 0.1L of relative depth 0.4, static load factor 0.4 and dynamic load factor 0.8. But with the introduction of the second crack at 0.05L of relative depth 0.4, static load factor 0.4 and dynamic load factor 0.8, the same increased by 46.6%. Similarly the width of dynamic instability region increased by 38.0%, 27.9%, 19.5% and 14.8% for the second crack locations of 0.3L, 0.5L, 0.7L and 0.9L respectively for relative crack depth of 0.4, static load factor 0.4 and dynamic load factor 0.8. Hence it can be concluded that as the crack moves away from fixed end the onset of dynamic instability gets delayed and the effect of second crack is almost negligible for the second crack near free end. At the same time the width of dynamic instability regions decreased as the second crack moves away from the fixed end and when the second crack is placed near the free end its effect is almost negligible.

Similarly dynamic stability parameters for the cantilever beam subjected to three cracks are studied. The first crack is considered at 0.1L from the fixed end is of relative depth 0.2 and the second crack at 0.2L is of relative depth 0.2. the third crack is introduced between 0.05L to 0.95L of varying relative depth. The variations of dynamic instability regions and onset of dynamic instability frequencies are studied for for different dynamic load factors for different static load factors, location and relative depth of the cracks. The variation of dynamic instability regions with dynamic load factors for different static load factors of the beam with three cracks at $L_1 = 0.1L$ ($rcd_1 = 0.2$), $L_2 = 0.2L$ ($rcd_2 = 0.2$) and $L_3 = 0.05L$ ($rcd_3 = 0.2$**)** are shown in Fig.

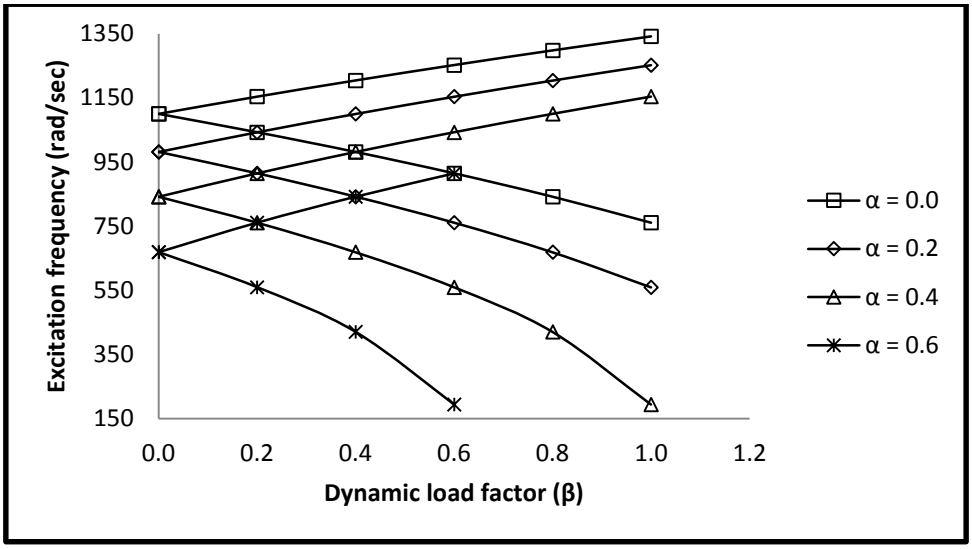

Figure 6.98 Effect of Static load factor (α) on dynamic instability regions of the cantilever beam with three cracks, $L_1 = 0.1L$, $rcd_1 = 0.2$, $L_2 = 0.2L$ and $rcd_2 = 0.2$ and $L_3 = 0.05L$, $rcd_3 = 0.2$

6.98. It is observed that, the onset of dynamic instability frequencies occur earlier by 5.3%, 6.3%, 7.9% and 11.1% than intact beam for static load factor of 0.0, 0.2, 0.4 and 0.6 respectively. At the same time the width of instability regions increase by 3.5%, 5.52% and 15.16% than intact beam for static load factor of 0.0, 0.2 and 0.4 respectively. The variations of dynamic instability regions for different relative depth of third crack with dynamic load factor are computed and plotted in Fig. 6.99.

It is observed from Fig. 6.99 that increase in depth of the third crack reduced the excitation frequencies of dynamic instability by 6.3%, 13.6% and 30.3% than intact beam for relative crack depth of 0.2, 0.4 and 0.6 respectively. It is also observed that presence of one crack alone at 0.1L of relative depth 0.2 made the instability to occur earlier by 2.3% and with the intrusion of the second crack at 0.2L from fixed end of relative depth 0.2 made the instability to occur earlier by 4.7% than intact beam. So intrusion of the second crack is responsible for the additional reduction in the excitation. Similarly intrusion of the third crack at 0.05L from fixed end reduced the excitation frequencies of dynamic instability further by 1.6%, 8.9% and 29.6%

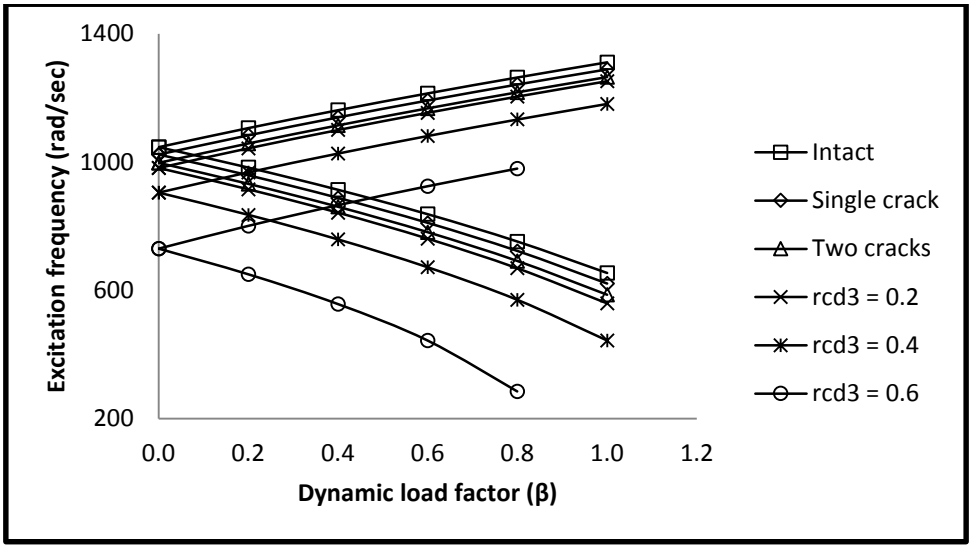

Figure 6.99 Variation of dynamic instability regions of the cantilever beam subjected to three cracks at $L_1 = 0.1L$, $rcd_1 = 0.2$ and $L_2 = 0.2L$, $rcd_2 = 0.2$ and $L_3 = 0.05L$ with dynamic load factors for different relative depths of third crack and static load factor, $\alpha = 0.2$

than intact beam for relative crack depth of 0.2, 0.4 and 0.6 respectively. It is also observed that with the increase in depth of the crack the width of dynamic instability regions increase by 1.5% than intact beamfor one crack alone at 0.1L of relative depth 0.2 when static and dynamic load factors are 0.2 and 0.8 respectively. Similarly inclusion of second crack at 0.2L of relative crack depth 0.2 increased the width of dynamic instability region by 1.3% more than that due to single crack alone. Inclusion of the third crack increased the dynamic instability regions further by 3.2%, 8.5% and 34.3% for relative depths of 0.2, 0.4 and 0.6 respectively when static load factor is 0.2 and dynamic load factor 0.8. The variations of dynamic instability regions of the uniform beam for single, double and triple cracks with different position of third crack of relative depth 0.2 is shown in Fig. 6.100.

It is observed from Fig. 6.100 that when the beam is subjected to a single crack at 0.05L of relative depth 0.4, the dynamic instability commences at excitation frequencies lesser by 10.6% and at the same time the width of the dynamic instability region increases by 7.6% than intact beam. When the beam is subjected to two cracks at 0.05L and 0.1L of relative depth 0.4, the dynamic instability commences at excitation frequency lesser by 18.0% and the width of the region increased by 19.1% with respect to that of intact beam. Similarly when the beam is

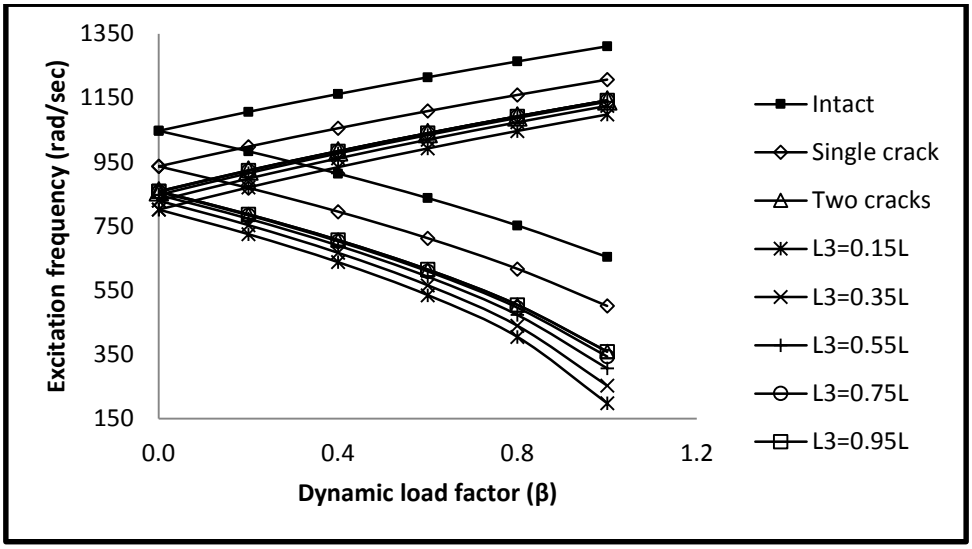

Figure 6.100 Variation of instability regions with dynamic load factor (β) for cantilever intact beam, single cracked beam (L_1 = 0.05L, rcd = 0.4), double cracked beam (L_1 = 0.05L, rcd_1 = 0.4 and L_2 = 0.1L, rcd_2 = 0.4) and triple cracked beam (L_1 = 0.05L, rcd_1 = 0.4, L_2 = 0.1L, rcd$_2$ = 0.4) for different position of third crack of relative depth 0.2

subjected to three cracks at 0.05L, 0.1L and 0.15L of relative depth 0.4, the dynamic instability commences at excitation frequency of lesser by 23.5% and the width of dynamic instability region increases by 37.1%. It is also observed that when the beam is subjected to three cracks at 0.05L, 0.15L and 0.95L of relative crack depth 0.4, the dynamic instability commences at excitation frequency lesser by 18.0% and the increase in width of dynamic instability increases by 37.2% than that of intact beam. This implies when the third crack happens to be at free end its effect is negligible.

6.12.2 Stepped fixed-free beam

Parametric resonance characteristics of the stepped beam subjected to multiple transverse open cracks is carried out. The stepped beam as shown in Fig. 6.5 is anlysed for parametric resonance characteristics for two and three cracks subjected to a harmonic load. The variation of excitation frequencies with dynamic load factors for different depth of crack and static load factor 0.2 is shown in Fig. 6.101.

It is observed from Fig. 6.101 that the excitation frequencies for commencement of dynamic instability decreases by 3.0%, 108% and 22.8% for crack depths of 2 mm, 4 mm and 6 mm

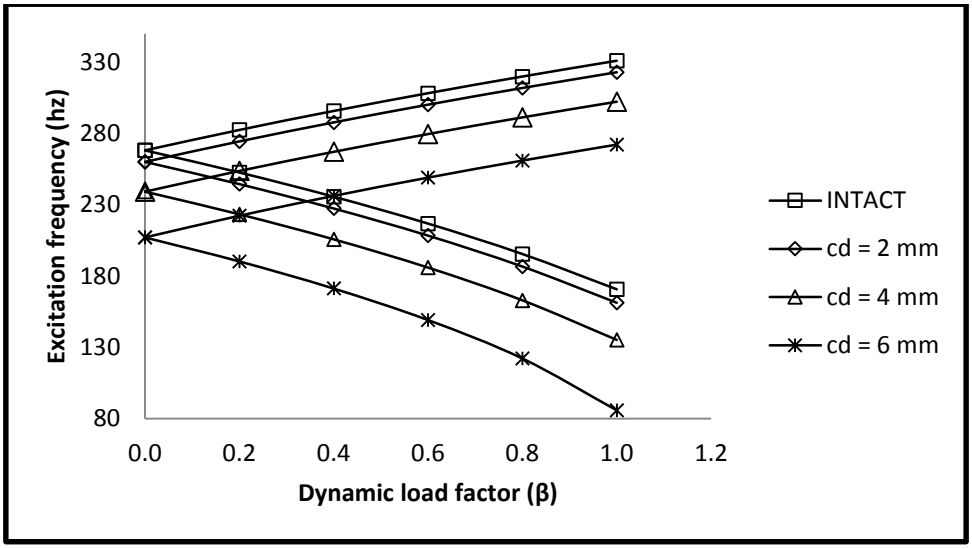

Figure 6.101 Variation of dynamic instability regions with dynamic load factors of the stepped cantilever beam subjected to two cracks at 0.05L and 0.15L of different depths and static load factor, α = 0.2

respectively. Similarly the width of dynamic instability regions increase by 0.8%, 4.3% and 16.3% than that of intact beam for crack depths of 2 mm, 4 mm and 6 mm respectively. The variation of excitation frequencies of dynamic instability regions of the stepped beam for different locations of two cracks is shown in Fig. 6.102.

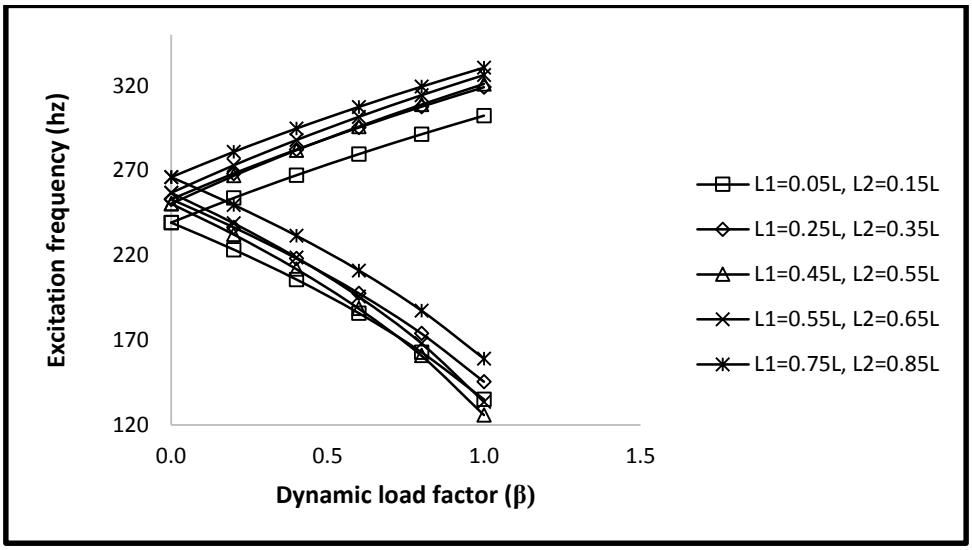

Figure 6.102 Variation of dynamic instability regions with dynamic load factors of the stepped cantilever beam subjected to two cracks at varous locations for static load factor, α = 0.2 and crack depth 4 mm each

It is observed from Fig. 6.102 that the excitation frequencies for commencement of dynamic instability decreases by 10.8%, 5.6%, 6.6%, 4.2% and 0.8% as the two cracks changes their position from fixed end to free end as shown in Fig. 102. Similarly the width of the dynamic instability regions increase by 4.3%, 8.3%, 21.8%, 20.2% and 7.1% than that of intact beam for the crack positions shown in the figure. This implies as the crack moves away from the fixed end, the excitation frequencies which increase in case of a uniform beam decreases here due to presence of steps. At the same time there is increase in width of dynamic instability. The variation of excitation frequencies for dynamic instability regions with dynamic load factors for different depths of crack are shown in Fig. 6.103.

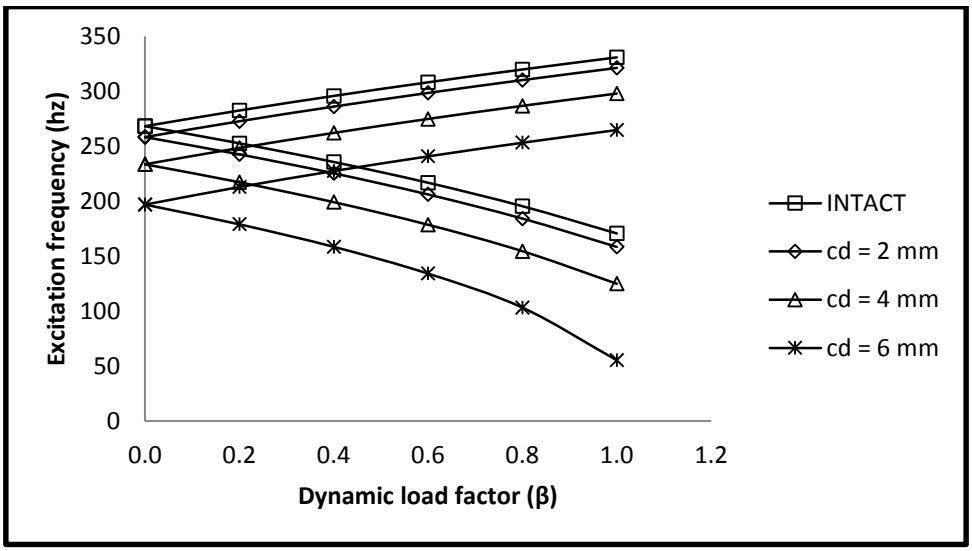

Figure 6.103 Variation of dynamic instability regions with dynamic load factors of the stepped cantilever beam subjected to three cracks at 0.05L, 0.15L and 0.25L of different crack depths for static load factor, α = 0.2

It is observed that the excitation frequencies for the commencement of dynamic instability decrease by 3.7%, 12.9% and 26.6% than that of intact beam for crack depths of 2 mm, 4 mm and 6 mm respectively. At the same time the width of dynamic instability regions increase by 1.6%, 7.8% and 30.7% than that of intact beam for crack depths of 2 mm, 4 mm and 6 mm respectively. The variations of excitation frequencies of dynamic instability regions with different locations of three cracks for a crack depth of 4 mm and static load factor pf 0.2 is shown in Fig. 6.104.

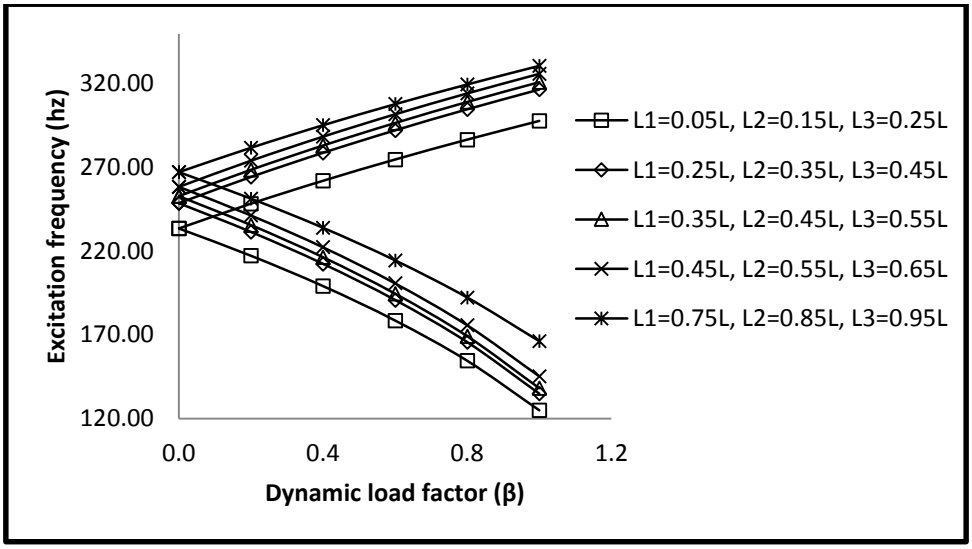

Figure 6.104 Variation of dynamic instability regions with dynamic load factors of the stepped cantilever beam subjected to three cracks at varous locations for static load factor, α = 0.2 and crack depth 4 mm each

It is observed that the excitation frequencies for the commencement of the dynamic instability regions decrease by 10.8%, 5.6%, 6.6%, 4.2% and 0.8% for the crack positions shown in Fig. 6.104. At the same time, the width of dynamic instability regions increase by 4.3%, 8.3%, 21.8%, 20.2% and 7.1% for the same locations of the cracks. The onset of dynamic instability has increased gradually with cracks shifting from fixed end to free end. But the deviations are marked near stepped sections.

6.13 Crack Detection Using ANN

6.13.1Data base and preprocessing

The data on frequencies of vibrations of beams are collected from the literature (Owolabi et al. 2003) shown in Table 6.7**.** The problem involves determination of damage extent for a simply supported aluminum beam using ANN by taking input parameters as changes in natural frequency ratio in 1st mode, 2nd mode and 3rd mode, and relative depth of crack as output parameters. The acceleration frequency responses were found out at seven different points on the beam model experimentally by using a dual channel frequency analyzer**.** The cracks were generated as single open transverse cracks with a thickness of 0.4 mm approximately.

Properties of the beam:

Width of the beam = 25.4 mm Depth of the beam = 25.4 mm

Length of the beam = 650 mm Elastic modulus of the beam = 70 GPa

Poisson's Ratio = 0.35 Density = 2.696 gm/cm^3

Table 6.7 Natural frequencies for simply supported Aluminum beam with or without cracks (L = 650 mm, b = h = 25.4 mm, E = 70 GPa, ρ = 2696 kg/m^3 and ν = 0.35)

INPUTS			OUTPUTS	
Fundamental natural Frequency ratio (ω_c/ω_i)			L_1/L	rcd = a/h
1st mode	2nd mode	3rd mode		
1	1	1	0.0625	0
1	1	1	0.0625	0.1
1	0.9991	0.9915	0.0625	0.2
1	0.9963	0.9915	0.0625	0.3
0.9995	0.9817	0.9829	0.0625	0.4
0.9974	0.9848	0.9658	0.0625	0.5
0.993	0.9714	0.9573	0.0625	0.6
0.9848	0.9544	0.9402	0.0625	0.7
1	1	1	0.1875	0
0.998	0.9962	1	0.1875	0.1
0.9956	0.9889	1	0.1875	0.2
0.9881	0.9712	0.9828	0.1875	0.3
0.9781	0.9481	0.9741	0.1875	0.4
0.9664	0.9232	0.9569	0.1875	0.5
0.9371	0.8818	0.9483	0.1875	0.6
0.8756	0.8175	0.931	0.1875	0.7
1	1	1	0.3125	0
0.9923	0.9967	1	0.3125	0.1
0.9892	0.9903	1	0.3125	0.2
0.9758	0.9767	1	0.3125	0.3
0.9507	0.9524	1	0.3125	0.4
0.868	0.8902	1	0.3125	0.6
0.7896	0.8424	1	0.3125	0.7
1	1	1	0.4375	0
0.996	0.9994	1	0.4375	0.1
0.9849	0.9976	0.9915	0.4375	0.2
0.9686	0.9952	0.9829	0.4375	0.3
0.9418	0.9918	0.9744	0.4375	0.4
0.8961	0.9861	0.9402	0.4375	0.5
0.8318	0.9811	0.8547	0.4375	0.6
0.7065	0.9704	0.8245	0.4375	0.7
1	1	1	0.5	0
0.994	0.9999	1	0.5	0.1

INPUTS			OUTPUTS	
Fundamental natural Frequency ratio (ω_c/ω_i)			L_1/L	rcd = a/h
1st mode	2nd mode	3rd mode		
0.997	0.9998	0.9915	0.5	0.2
0.9535	0.9995	0.9744	0.5	0.3
0.9234	0.9995	0.9573	0.5	0.4
0.8724	0.9995	0.9402	0.5	0.5
0.8119	0.999	0.9145	0.5	0.6
0.7085	0.9986	0.8014	0.5	0.7
1	1	1	0.6875	0
0.998	0.9979	1	0.6875	0.1
0.9968	0.9889	1	0.6875	0.2
0.9797	0.9774	0.9915	0.6875	0.3
0.9617	0.9613	0.9915	0.6875	0.4
0.9225	0.9337	0.9915	0.6875	0.5
0.8546	0.8988	0.9915	0.6875	0.6
0.7713	0.8693	0.9915	0.6875	0.7
1	1	1	0.875	0
0.9994	0.9994	1	0.875	0.1
0.999	0.9975	1	0.875	0.2
0.9978	0.9936	1	0.875	0.3
0.9971	0.9905	0.9914	0.875	0.4
0.9945	0.9824	0.9828	0.875	0.5
0.9893	0.9696	0.9483	0.875	0.6
0.9829	0.9578	0.931	0.875	0.7

6.13.2 Design of ANNs

In order to find the most effective ANN that uses vibration-based analysis data for the severity predictions, a neural network with one hidden layer is designed by using MATLAB R12b neural network toolbox. Successful application of ANN depends upon factors like number of hidden nodes, data division, data normalization, transfer function, learning algorithm etc. The number of hidden layer neurons is determined through a trial- and-error process and the smallest number of neurons that yield satisfactory results (based on performances criteria) is used. ANN models are developed using, Levenberg- Marquardt, Bayesian regularization and DE algorithm for training process. The transfer function which used here is hyperbolic tangent sigmoid function. In the present study the network consists of 3 nodes in the hidden layer and 1 node in the output layer for determination of extent of crack.

6.13.3 ANN results and discussions

The results of ANN model trained with DENN and Bayesian regularization method (BRNN) and commonly used Levenberg-Maqruardt trained neural networks (LMNN) are presented here. The correlation coefficient (R) and root means square errors (RMSE) are mostly used statistical performance criteria for evaluation of ANN models. Based on R values it was observed that there is a strong correlation (R > 0.8) between observed and predicted values (Smith 1986). However, R is a biased parameter and sometimes, higher values of R may not necessarily indicate better performance of the model because of the tendency of the model to be biased towards higher or lower values. So the coefficient of efficiency (E) is also considered. The E is defined as

$$E = \frac{E_X - E_Y}{E_X} \tag{52}$$

$$\begin{aligned} E_X &= \sum_{t=1}^{N} (cd_m - \overline{cd}_m)^2 \\ E_Y &= \sum_{t=1}^{N} \left(cd_p - cd_m\right)^2 \end{aligned} \tag{53}$$

Where cd_m, $\overline{cd}_m$ and cd_p are the measure, average and predicted crack depth ratio respectively. The E value compares the modeled and measured values of the variable and evaluates how far the network is able to explain total variance in the data set. The over-fitting ratio is defined as the ratio of RMSE for testing and training data and it defines the generalization. The condition for best generalization is over-fitting ratio value as 1.0. The over-fitting ratio close to 1.0 shows good generalization. The comparison between measured and predicted values during training and testing using DENN, BRNN and LMNN is presented in Fig. 6.105, 6.106, 6.107, 6.108, 6.109 and 6.110 respectively.

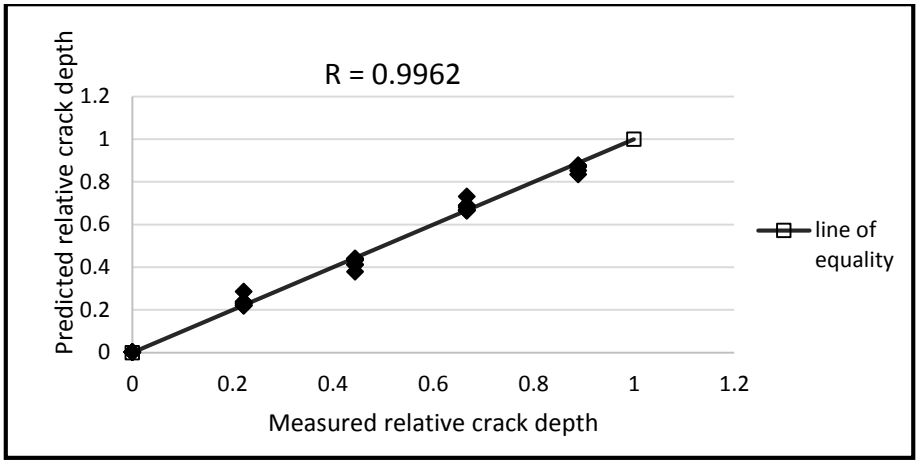

Figure 6.105 Comparison between predicted relative crack depth and measured relative crack depth showing correlation coefficient (R) during training of LMNN model.

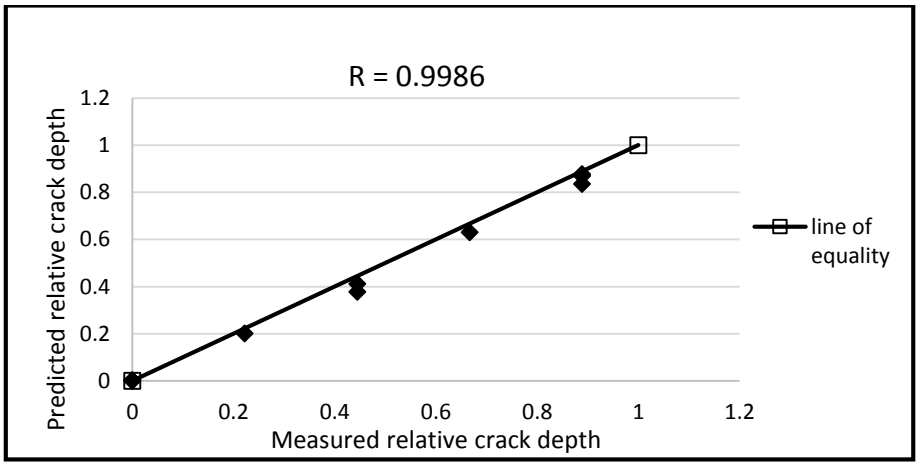

Figure 6.106 Comparison between predicted relative crack depth and measured relative crack depth showing correlation coefficient (R) during testing of LMNN model.

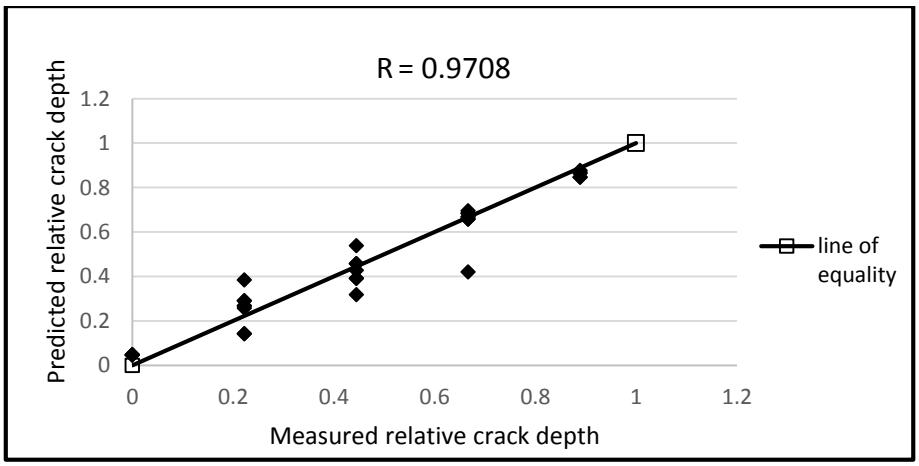

Figure 6.107 Comparison between predicted relative crack depth and measured relative crack depth showing correlation coefficient (R) during training of BRNN model.

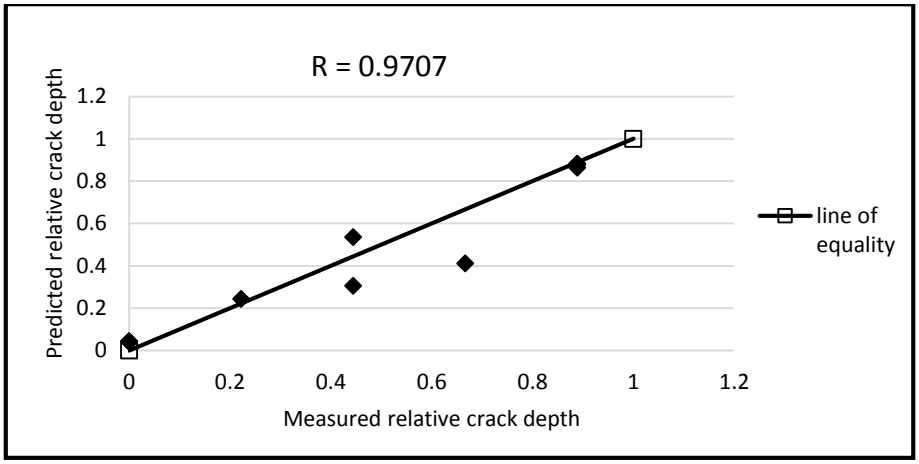

Figure 6.108 Comparison between predicted relative crack depth and measured relative crack depth showing correlation coefficient (R) during testing of BRNN model.

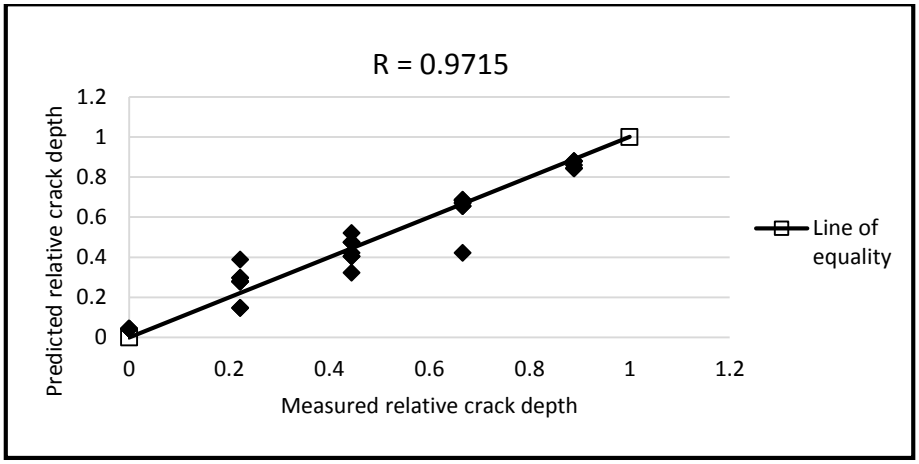

Figure 6.109 Comparison between predicted relative crack depth and measured relative crack depth showing correlation coefficient (R) during training of DENN model.

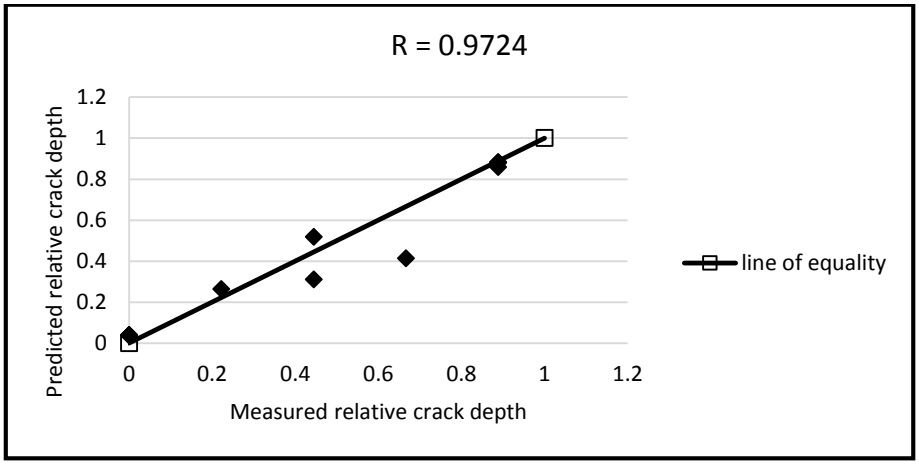

Figure 6.110 Comparison between predicted relative crack depth and measured relative crack depth showing correlation coefficient (R) during testing of DENN model.

It is observed from Fig. 105 to 110 that based on R value during training, LMNN (R = 0.987)

is found to have good predictions. However it shows poor prediction for testing data signified by high over fitting ratio (OR = 2.03). Similarly the DENN (R = 0.964, OR = 0.942) model is found to have good predictions and generalization. It can be seen that during training the R value for BRNN is 0.965 which is almost same as of DENN, but model is having better generalization with an over fitting ratio of 0.982 which is nearly equal to 1. So BRNN model is found to the best model as compared to DENN and LMNN. The performance of different neural network models has been shown in Table 6.8.

Table 6.8 Performance of different neural network models for simply supported Aluminum beam

ANN models	Training data				Testing data				Over-fitting ratio
	R	E	RMSE	Avg % error	R	E	RMSE	Avg % error	
DENN	0.964	0.928	0.063	2.58	0.971	0.927	0.059	-3.24	0.942
BRNN	0.965	0.931	0.061	1.41	0.97	0.924	0.06	-3.72	0.982
LMNN	0.987	0.973	0.038	0.58	0.96	0.875	0.077	-4.06	2.03

From the Table 6.8 it is found that the BRNN (OR = 0.982) model is having good predictions and has better generalization compared to DENN (OR = 0.942) and LMNN (OR = 2.03). Hence following BRNN model crack location and depth can satisfactorily be detected for simply supported beams.

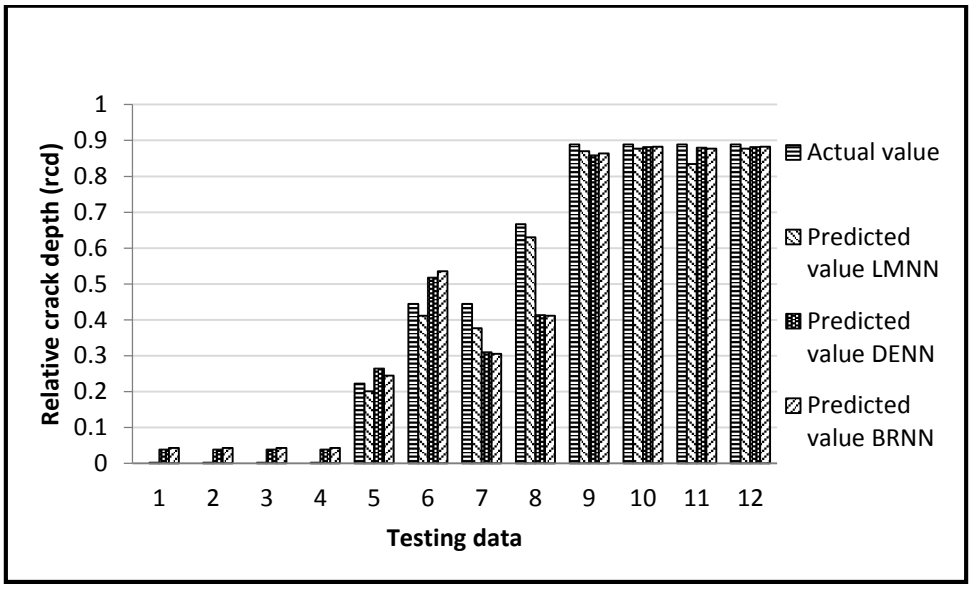

Figure 6.111 Comparison of the three models between measured and predicted value of relative crack depth (rcd) of the beam

6.14 Critical Analysis of Result

Based on the present finite element formulation, study is carried out to decide the discretization of the whole beam into specified number of elements. As per the convergence study, a mesh of 16 elements is considered throughout the analysis in this study except stepped beam. For this 6 elements per stepped segment are considered for all analysis. Comparison of free vibration and buckling of uniform beam are carried out with the studies available in literature. There exists good agreement of the results based on present FEM with the previous studies. From the free vibration studies on uniform and stepped beams, it is observed that presence of crack is more pronounced near fixed support than crack near free or hinged ends. But the stepped beam behave differently than uniform beam. The behaviour of stepped beam due to crack is significantly influenced by the steps. The effect of crack is considerable when it is located near higher bending moment region. The frequencies of vibration of cracked beam are least affected when the crack is near the nodal point of mode of vibration.

Similarly the presence of crack weakens the beam in buckling. The reduction of buckling load due to crack mainly depends upon its location and depth. It is observed that a crack near fixed end of the cantilever beam reduces the buckling load more than the crack at any other location. Buckling load is least affected when the crack is near free end of the cantilever beam or near the hinged end of the simply supported beam. It is also observed that a crack present near the higher bending moment region affects the buckling load more that its presence near lesser bending moment region. Presence of crack near higher bending moment region results in more strain energy release than the crack near lesser bending moment region. More strain energy release due to presence of crack weakens the beam. In stepped beams, presence of crack decreases the buckling load but the steps in the beam plays a vital role. The presence of crack near the steps reduces the buckling load more than that of uniform beam due to steps. As the buckling load is directly proportional to its flexural rigidity, the presence of crack near the step reduces its flexural rigidity to a great extent in comparison to uniform beam. Hence there is a severe drop in buckling load near the steps.

The parametric resonance characteristics of beams which depends upon the onset of dynamic instability and the width of the instability regions is also greatly affected by position and depth of cracks in uniform and stepped beams. The crack present near the higher bending moment region of a beam lowers the onset of dynamic instability more than the same crack near lower

bending moment region. This is also associated with increase in width of dynamic instability region (DIR). But the onset of dynamic instability happens to be at a greater frequency than the crack near lesser bending moment region and the corresponding width of the instability region is smaller than that near higher bending moment area.

6.15 Summary

Results are presented for free vibration, buckling and dynamic stability of uniform and stepped beams with single and multiple transverse open cracks are presented. The convergence studies are carried out to decide the discretization. Comparisons with previous studies are carried out to validate the present finite element formulation. The effects of different parameters on the natural frequencies, buckling load and dynamic instability regions are presented and possible reasons are discussed wherever applicable.

Chapter 7

CONCLUSIONS

7.1 Introduction

Theoretical investigations of the vibration, buckling and dynamic stability behavior of uniform and stepped beam with single to multiple cracks subjected to in-plane loading are carried out using finite element formulation. An experimental programme was conducted on aluminum and steel beams to validate the vibration results using ANSYS. Crack detection techniques are used using ANN for identifying the location and intensity of cracks.

7.2 Conclusions

The results on the studies of the beam for different boundary conditions for various crack locations and depths are summarized as follows:

- A general formulation for vibration, buckling and parametric resonance characteristics of uniform and stepped beam with single and multiple transverse open crack is presented.
- Cracks severely affect the dynamic behaviour of beams. Cracks result in decrease in free vibration frequencies. Location and depth of the crack also affect the free vibration frequencies of the uniform and stepped beams.
- The effect of cracks on beams depends upon the end conditions of the beam. A crack present near fixed support of a cantilever beam or fixed beam makes the beam weaker than a crack near hinged end of a simply supported beam.
- The effect of cracks in beams are significant when they are in the region of higher bending moment. Their effect is negligible or very less when they are in the region of lesser bending moment. That is why a crack near free end of the cantilever beam is less vulnerable than a crack near fixed end. Similarly the crack present near mid span of a fixed beam or simply supported beam are more vulnerable in reducing free vibration frequencies than other locations.

- The frequencies of vibration of beams are more affected by the position of the cracks than depths. A relatively smaller crack near fixed end of a cantilever beam reduces free vibration frequencies more than a relatively bigger crack at free end.
- The effect of the multiple cracks on a beam is the cumulative effect of their position and depth considered individually. Multiple cracks make the beam dynamically weaker.
- Cracks affect the buckling load similar to first mode of free vibration in beams. A crack anywhere on a beam reduces the critical load to some extent. But its position at some locations reduces the buckling load more than some other locations. Similar to a cantilever beam a crack near fixed end reduces buckling load more than a similar crack near free end. Hence similar to vibration results a crack present near high bending moment region in a beam reduces buckling load more than a similar crack present near less bending moment region.
- Buckling loads of cracked beams decrease with increase of crack depth for a crack at any particular location.
- When the crack is located nearer to the free end the instability regions almost coincide with the instability region for the intact beam.
- For a given crack location from fixed end the instability region for maximum relative crack depth occurs at lower excitation frequency compared to other relative crack depths.
- For a given relative crack depth the instability region for the crack location nearer to fixed end occurs at lower frequency and it increases as the crack position shifts towards free end.
- The static load component has a destabilizing effect in terms of shifting of instability regions towards lower frequencies of excitation and increases the area of instability.
- It can be observed that the damage extent can be found out using ANN models trained with only natural frequencies with reasonable accuracy.
- The proposed BRNN and DENN model is found to be efficient for simply supported beam in predicting damage extent with high R value 0.965 and 0.964 respectively and showing good generalization as compared to LMNN (high OR-2.03).
- The OR value for BRNN and DENN model is obtained 0.982 and 0.942 respectively. So BRNN is found as the best model compared DENN model for simply supported beam.

- For free-free beam case, LMNN is obtained as the best model for detecting damage extent having high values of R for training (0.996) and testing (0.999) with minimum RMSE value (0.033) for testing data.

From the above studies, it can be concluded that the natural frequency and buckling behaviour of uniform and stepped beams are greatly affected by the location, depth and number of cracks. The instability behaviour is significantly affected by the static, dynamic load factors, besides the position and intensity of cracks. So the designer has to be cautious while dealing with beams with cracks subjected to harmonic in-plane loading. The vibration data can be used as a non-destructive tool for crack identification using ANN technique. These can be used as a tool for structural health monitoring and structural integrity.

7.3 Novelty of the present study

Good number of studies on vibration of cracked beams is available in literature but stability investigations especially parametric resonance studies on beams subjected to transverse open cracks are very scarce. More over the stability problem on stepped beams are not available in open literature. In the present study, vibration, buckling and dynamic stability of beams, subjected to single and multiple transverse open cracks are presented. Besides this, vibration and stability of stepped beams of steel and aluminium are investigated for the first time as new examples for the benefit of future researchers in this area. These results can be used as design-aids for prediction of dynamic behaviour of beams with transverse cracks. A single formulation is presented from the basics of Hamilton's principle to solution of vibration, buckling and parametric resonance of uniform and stepped beams with single and multiple transverse cracks. Experimental results on free vibration of steel and aluminium beams are presented for validation of investigation. The vibration and stability results can be used as a tool for structural health monitoring for identification, location and extent of damage in cracked beams. This can also help in assessment of integrity of structural members. The artificial neural network approach is also presented in this study for structural health monitoring.

Scope of Future Work

The future scope of work may be

- Vibration and stability of Isotropic beam considering non-linearity
- Vibration and stability of Laminated composite cracked beams
- Vibration of beam by introducing slant cracks in place of transverse crack
- Vibration Reinforced concrete beam with cracks

REFERENCES

Adams, R.D., Cawley, P., Pye, C.J. and Stone, B.J., (1978), "A vibration technique for non-destructively assessing the integrity of structures", *Journal of Mechanical Engineering Science*, 20, 93–100.

Agarwalla, D. K., and Parhi, D. R., (2013), "Effect of Crack on Modal Parameters of a Cantilever Beam subjected to Vibration", *Procedia Engineering*, 51, 665-669.

Al-Said, S. M., Naji, M. and Al-Shukry, A. A. (2006), "Flexural vibration of rotating cracked Timoshenko beam", *Journal of V ibrat ion and Control*, 12(11), 1271-1287.

Anifantis, N. and Dimarogonas, A. (1983), "Stability of columns with a single crack subjected to follower and vertical loads", *International Journal of Solids Structures*, 19, 281-291.

Arboleda-Monsalvea, L. G., Zapata-Medina, D. G. and Aristizabal-Ochoa, J. D., (2007), "Stability and natural frequency of a weakened Timoshenko beam-column with generalized end conditions under constant axial load", *Journal of Sound and Vibration*, 307, 89-112.

Attar, M., (2012), "A transfer matrix method for free vibration analysis and crack identification of stepped beams with multiple edge cracks and different boundary conditions", *International Journal of Mechanical Sciences*, 57, 19-33.

Aydin, K. (2008), "Vibratory characteristics of Euler-Bernoulli beams with an arbitrary number of cracks subjected to axial load." *Journal of Vibration and Control*, 14(4), 485-510.

Balasubramanian, T. S. and Subramanian, G. (1985), "On the performance of a four degree of freedom per node element for stepped beam analysis and higher frequency estimation", *Journal of Sound and Vibration*, 99(4), 563-567.

Bamnios, G. and Trochides, A. (1995), "Dynamic behavior of a cracked cantilever beam." *Applied Acoustics*, 45, 97-112.

Bayat, M., Pakar I. and Bayat Mahdi, (2011), "Analytical study on the vibration frequencies of tapered beams", *Latin American Journal of Solids and Structures*, 8, 149-162.

Behera, R. K., Parhi, D. R. K. and Sahu, S. K., (2006), "Dynamic Characteristics of a Cantilever Beam with transverse cracks." *International Journal of Acoustics and Vibration,* 11(1), 3-18.

Bilgehan, Mahmut, (2011), "Comparison of ANFIS and NN models – with a study in critical buckling load estimation",*Applied Soft Computing*, 11, 3779-3791.

Binici, B. (2005), "Vibration of beams with multiple open cracks subjected to axial force", *Journal of Sound and Vibration,* 287, 277-295.

Bolotin, V. V., (1964), "*The Dynamic Stability of Elastic Systems*", Holden-Day, San Fransisco

Brandon, J. A. and Sudraud, C. (1998), "An experimental investigation into the topological stability of a cracked cantilever beam." *Journal of Sound and Vibration,* 211(4), 555-569.

Briseghella, L., Majorana, C.E. and Pellegrino, C. (1998), "Dynamic stability of elastic structures: a finite element approach." *Computers and Structures,* 69, 11-25.

Bueckner, H. F., (1958), "The propagation of cracks and the energy of elastic deformation", *Transactions of the American Society of Mechanical Engineers*, 80, 1225-1230.

Caddemi, S. and Calio, I. (2009), "Exact closed-form solution for the vibration modes of the Euler–Bernoulli beam with multiple open cracks" *Journal of Sound and Vibration,* 327, 473-489.

Caddemi, S. and Calio, I. (2012), "The influence of the axial force on the vibration of the Euler-Bernoulli beam with an arbitrary number of cracks." *Archive of Applied Mechanics*, 82, 827-839.

Carneiro, S. H. S. and Inman, D. J. (2001), "Letters to the editor – Comments on the free vibrations of beams with single- edge crack." *Journal of Vibration and Acoustics*, 244(4), 729-737.

Carneiro, S. H. S. and Inman, D. J. (2002), "Continuous Model for the Transverse Vibration of Cracked Timoshenko Beams." *Journal of Vibration and Acoustics,* 124, 310-320.

Cawley, P. and Adams, R. D., (1979), "A vibration technique for non-destructive testing of fibre composite structures", *Journal of Composite Materials*, 13, 161-175.

Chati, M., Rand, R. and Mukherjee S. (1997), "Modal analysis of a cracked beam." *Journal of Sound and Vibration*, 207(2), 249-270.

Chaudhury, T. D. and Maiti, S. K., (1999), "Modelling of transverse vibration of beam of linearly variable depth with edge crack", Engineering Fracture Mechanics, 63, 425-445

Chen, L.-W. and Chen, H.-K. (1995), "Stability analyses of a cracked shaft subjected to the end load." *Journal of Sound and Vibration,* 188(4), 497-513.

Chen, L.-W. and Shen, G. S. (1997), "Dynamic stability of cracked rotating beams of general orthotropy." *Composite Structures*, 37, 165-172.

Chen, W. H. and Wang, H. L., (1986), "Finite element analysis of axisymmetric cracked solid subjected to torsional-loadings", *Engineering Fracture Mechanics*, 23, 705-717.

Chinchalkar, S. (2001), "Determination of crack location in beams using natural frequencies." *Journal of Sound and Vibration*, 247(3), 417-429.

Chondros T. G., Dimarogonas A. D. and Yao J., (2001), "Vibration of a beam with a breathing crack", *Journal of Sound and Vibration*, 239(1), 57-67.

Chondros, T. G. and Dimarogonas, A. D. (1998), "A continuous beam vibration theory." *Journal of Sound and Vibration*, 215(1), 17-34.

Cook, R. D., Malkus, D. S., Plesha, M. E. and Witt, R. J. (2003, 4e), "Concept and Applications of Finite Element Analysis." *John Wiley & Sons, INC*."

Corn, S., Bouhaddi, N. and Piranda, J. (1997), "Transverse vibrations of short beams: Finite element models obtained by a condensation method." *Journal of Sound and Vibration,* 201(3), 353-363.

Dado, M.H.F. and Abuzeid, O. (2003), "Coupled transverse and axial vibratory behavior of cracked beam with end mass and rotary inertia." *Journal of Sound and Vibration,* 261, 675-696.

Dado, M.H.F. and Shpli, O. A. (2003), "Crack parameter estimation in structures using finite element modeling." *International Journal of Solids and Structures*, 40, 5389-5406.

Das, S.K. (2005). "Applications of genetic algorithm and artificial neural network to some geotechnical engineering problems." *Ph.D. Thesis*, Indian Institute of Technology Kanpur, Kanpur, India.

Das, S.K. (2013), Ärtificial Neural Networks in Geotechnical Engineering: Modelling and Application Issues", Metaheuristics in Water, Geotechnical and Transport Engineering, 231-270.

Demuth, H., and Beale, M. (2000). *Neural Network Toolbox*. The MathWorks Inc.USA.

Dharmaraju, N., Tiwari, R. and Talukdar, S. (2004). "Identification of an open crack model in a beam based on force–response measurements". *Computers and Structures*, Vol. 82, pp.167–179.

Dilena, M. and Morassi, A. (2002), "Identification of crack location in vibrating beams from changes in node positions," *Journal of Sound and Vibration*, 255(5), 915-930.

Dilena, M. and Morassi, A. (2004), "The use of antiresonances for crack detection in beams," *Journal of Sound and Vibration*, 276, 195-214.

Dimarogonas, A. D., (1981), "Buckling of rings and tubes with longitudinal cracks", *Mechanics Research Communications*, 8, 179-186.

Dimarogonas, A. D., (1996), "Vibration of Cracked Structures: A state of the art review", *Engineering Fracture Mechanics*, 55(5), 831-857.

Fan, S. C. and Zheng, D. Y. (2003), "Letter to the Editor - Stability of a cracked Timoshenko beam column by modified Fourier series." Journal of Sound and Vibration, 264, 475-484.

Fan, W. and Qiao, P., (2011), "Vibration-based Damage Identification Methods: A Review and Comparative Study", *Tructural Health Monitoring*, 10(1), 83-111.

Fang, X., Tang, J., Jordan, E. and Murphy, K. D. (2006), "Crack induced vibration localization in simplified bladed-disk structures." *Journal of Sound and Vibration*, 291, 395-418.

Fang,X., Luo, H. and Tang, J. (2005).”Structural damage detection using neural network with learning rate improvement”. *Computers and Structures*, Vol.83, pp.2150-2161.

Fernandez-Saez, J. and Navarro, C. (2002), “Fundamental frequency of cracked beams in bending vibrations: an analytical approach.” 256(1), 17-31.

Gounaris, G. and Dimarogonas, A., (1988), “A finite element of a cracked prismatic beam for structural analysis”, *Computers & Structures*, 28, 309-313.

Gounaris, G. and Papazoglou, V. J., (1992), “Three-dimensional effects on the natural vibrations of cracked Timoshenko beams in water”, *Computers & Structures*, 42(5), 769-779.

Gudmundson, P., (1983), “The dynamic behavior of slender structures with cross-sectional cracks”, *Journal of the Mechanics and Physics of Solids*, 31(4), 329-345.

Gurel, M. A., and Kisa, M., (2005), “Buckling of Slender Prismatic Columns with a Single Edge Crack under Concentric Vertical Loads”, *Turkish Journal of Engineering and Environmental Science*, 29, 185-193.

Gurel, M.A. and KisaM., (2005), “Buckling of slender prismatic columns with a single edge crack under concentric vertical loads”, *Turkish Journal of Environmental Science*, 29, 185-193.

Guyon, I., and Elisseeff, A. (2003). “An Introduction to variable and feature selection.”, *Journal of Machine learning Research*, Vol. 3, pp. 1157-1182.

Guyon, I., Elisseeff, A., (2003), An introduction to variable and feature section”, Journal of Machine Learning Research, 3, 1157-1182.

Hadjileontiadis, L. J., Douka, E. and Trochidis, A. (2005), “Crack detection in beams using kurtosis.” *Computers & Structures*, 83, 909-919.

Haisty, B. S. and Springer, W. T., (1988), “A general beam element for use in damage assessment of complex structures”, *Journal of Vibration, Acoustics Stress and Reliability in Design*, 110(3), 389-394.

Haryanto, I., Setiawan, J.D. and Budiyono, A. (2007), "Structural Damage Detection Using Randomized Trained Neural Networks". *International Conference on Intelligent Unmanned System*, Bali, Indonesia, pp.439-443.

Hsu, M.-H., (2005), "Vibration analysis of edge-cracked beam on elastic foundation with axial loading using the differential quadrature method", *Computer methods in applied mechanics and engineering*, 194, 1-17.

Huang, B.-W. and Kuang, J.-H. (2006), "Variation in the stability of a rotating blade disk with a local crack defect." *Journal of Sound and Vibration*, 294, 486-502.

Ilonen, J., Kamarainen J.K., and Lampinen J. (2003). "Differential Evolution training algorithm for feed-forward neural network." *Neural Processing Letters*, 17, 93-105.

Iremonger, M. J., (1980), "Finite difference buckling analysis of non-uniform columns", *Computers & Structures*, 12, 741-748.

Irwin, G. R., (1957), "Analysis of stresses and strains near the end of a crack traversing a plate", Journal of Applied Mechanics, 24, 361-364.

Irwin, G. R., (1957), "Relation of stresses near a crack to the crack extension force", 9th Congress of Applied Mechanics, Brussels.

Jang, S. K. and Bert, C. W., (1989), "Free vibration of stepped beams: exact and numerical solutions", Journal of Sound and Vibration, 130(2), 342-346

Jassim, Z.A., Ali, N.N., Mustapha, F. and Abdul Jalil, N.A., (2013), "A review on the vibration analysis for a damage occurrence of a cantilever beam", *Engineering Failure Analysis*, 31, 442–461.

Javidruzi, M., Vafai, A., Chen, J. F. and Chilton, J. C. (2004), "Vibration, buckling and dynamic stability of cracked cylindrical shells." *Thin-walled Structures*, 42, 79-99

Jaworski, J. W. and Dowell, E. H, (2008), "Free vibration of a cantilevered beam with multiple steps: Comparison of several theoretical methods with experiment", *Journal of Sound and Vibration*, 312, 713-725.

Jeyasehar, C. and Sumangala, K. (2006). "Nondestructive Evaluation of Pre-stressed concrete Beams using an Artificial Neural Network (ANN) Approach". *Structural Health monitoring,* Vol.5, pp.313-323.

Jiki P. N. (2007), "Buckling Analysis of pre-cracked beam-columns by Liapunov's second method, *European Journal of Mechanics A/Solids*, 26, 503-518.

Kao, C.Y. and Hung, S.L. (2003)."Detection of structural damage via free vibration responses generated by approximating artificial neural network". *Computers and Structures,* Vol.81, pp.2631-2644.

Karaagac, C., Ozturk, H. and Sabuncu, M. (2009), "Free vibration and lateral buckling of a cantilever slender beam with an edge crack: Experimental and numerical studies." *Journal of Sound and Vibration,* 326, 235-250.

Ke, L.-L. Yang, J. and Kitipornchai, S., (2009), "Postbuckling analysis of edge cracked functionally graded Timoshenko beams under end shortening", *Composite Structures*, 90, 152-160.

Khan, A. I., Parhi, D. R., (2013), "Finite Element Analysis of Double Cracked beam and its Experimental Validation", *Procedia Engineering*, 51, 703-708.

Khiem, N. T. and Lien, T. V. (2001), "A simplified method for natural frequency analysis of a multiple cracked beam." *Journal of Sound and Vibration,* 245 (4), 737-751.

Khiem, N. T. and Lien, T. V. (2002), "The dynamic stiffness matrix method in forced vibration analysis of multiple-cracked beam." *Journal of Sound and Vibration,* 254(3), 541-555.

Khiem, N. T. and Lien, T. V. (2004), "Multi-crack detection for beam by the natural frequencies." *Journal of Sound and Vibration*, 273, 175-184.

Kikidis, M.L. and Papadopoulos, C.A. (1992), "Slenderness ratio effect on cracked beam." *Journal of Sound and Vibration,* 155(1), 1-11.

Kim, K.-H. and Kim, J. –H. (2000), "Effect of a crack on the Dynamic stability of a free-free beam subjected to follower force." *Journal of Sound and Vibration*, 233(1), 119-135.

Kirmsher, P. G., (1944), "The effect of discontinuities on the natural frequency of the beam", *Proceedings of American Society of Testing and Materials*, 44, 897-904.

Kisa, M. (2004), "Free vibration analysis of a cantilever composite beam with multiple cracks." *Composites Science and Technology*, 64, 1391-1402.

Kisa, M. and Gurel, M. A. (2006), "Modal analysis of multi-cracked beams with circular cross section." *Engineering Fracture* Mechanics, 73, 963-977.

Kisa, M. and Gurel, M. A. (2007), "Free vibration analysis of uniform and stepped cracked beams with circular cross sections." *International Journal of Engineering Science*, 45, 364-380.

Kisa, M., (2011), "Vibration and stability of multi-cracked beams under compressive axial loading", *International Journal of the Physical Sciences*, 6(11), 2681-2696.

Kisa, M., Brandon, J. and Topcu, M. (1998), "Free vibration analysis of cracked beams by a combination of finite elements and component mode synthesis methods, *Computers and Structures*, 67, 215-223.

Kishen, J. M. C. and Kumar, A. (2004), "Finite element analysis for fracture behavior of cracked beam-columns." *Finite Elements in Analysis and Design*, 40, 1773-1789.

Koplow, M. A., Bhattacharyya, A. and Mann, B. P., (2006), "Closed form solutions for the dynamic response of Euler–Bernoulli beams with step changes in cross section", *Journal of Sound and Vibration*, 295, 214–225.

Krawczuk, M. (1994), "A new finite element for the static and dynamic analysis of cracked composite beams." *Computers & Structures*, 52(3), 551-561.

Krawczuk, M. and Ostachowicz, W. M. (1995), "Modelling and vibration analysis of a cantilever composite beam with a transverse open crack." *Journal of Sound and Vibration*, 183(1), 69-89.

Krawczuk, M. and Ostachowicz, W. M., (1992), "Parametric vibrations of beam with crack", *Archive of Applied Mechanics*, 62, 463-473.

Krawczuk, M. and Ostachowicz, W. M., (1993), "Transverse natural vibrations of a cracked beam loaded with a constant axial force", *Journal of Vibration and Acoustics*, 115(4), 524-528.

Krawczuk, M., Ostachowicz, W. M. and Zak, A. (1997), "Dynamics of cracked composite material structures." *Computational Mechanics*, 20, 79-83.

Krawczuk, M., Palacz, M. and Ostachowicz, W. (2003), "The dynamic analysis of a cracked Timoshenko beam by the spectral element method." *Journal of Sound and Vibration*, 264, 1139–1153

Krawwczuk, W., (1994), "A new finite element for the static and Dynamic analysis of cracked composite beams," *Computers and Structures*, 52(3), 551-561

Kukla, S., (2009), "Free vibrations and stability of stepped columns with cracks", *Journal of Sound and Vibration*, 319, 1301–1311.

Lee, J. (2009), "Identification of multiple cracks in a beam using natural frequencies." *Journal of Sound and Vibration*, 320, 482-490.

Lee, S. Y. and Kuo, Y. H., (1991), "Elastic stability of non-uniform columns", Journal of Sound and Vibration, 148(1), 11-24.

Lee, S. Y. and Kuo, Y. H., (1992), "Exact solutions for the non-conservative elastic stability of non-uniform columns", Journal of Sound and Vibration, 155(2), 291-301.

Leonard, F., Lanteigne, J., Lalonde, S. and Turcotte, Y. (2001), "Free vibration behavior of a cracked cantilever beam and crack detection." *Mechanical Systems and Signal Processing*, 15(3), 529-548.

Li, Q. S. (2002), "Free vibration analysis of non-umniform beams with an arbitrary number of cracks and concentrated masses." *Journal of Sound and Vibration*, 252(3), 509-525.

Li, Q. S., (2000), "Buckling of elastically restrained non-uniform columns", *Engineering Structures*, 22, 1231-1243.

Li, Q. S., (2001), "Buckling of multi-step cracked columns with shear deformation", *Engineering Structures*, 23, 356-364.

Li, Q. S., (2003), "Classes of exact solutions for buckling of multi-step non-uniform columns with an arbitrary number of cracks subjected to concentrated and distributed axial loads", *International Journal of Engineering Science*, 41, 569-586.

Liebowitz, H. and Claus, W. D., (1968), "Failure of notched columns", *Engineering Fracture Mechanics*, 1, 379-383.

Liebowitz, H., Vanderveldt, H. and Harris, D. W., (1967), "Carrying capacity of notched column", *International Journal of Solids and Structures*, 3, 489-500.

Lin, H. P., Chang, S. C. and Wu, J. D. (2002), "Beam vibrations with an arbitrary number of cracks." *Journal of Sound and Vibration*, 258 (5), 987-999.

Lin, H.-P., (2004), "Direct and inverse methods on free vibration analysis of simply supported beams with a crack", *Engineering Structures*, 26, 427-436.

Liu, C.H. and Wang, D. M. (2000), "Analysis of a cracked beam-column on an elastic foundation", *International Journal of Computer Applications in Technology*, 13, 273-279.

Loutridis, S., Douka, E. and Trochidis, A. (2004), "Crack identification in double-cracked beams using wavelet analysis." *Journal of Sound and Vibration*, 277, 1025-1039.

Loya, J. A., Rubio, L. and Fernandez-Saez, J. (2006), "Natural frequencies for bending vibrations of Timoshenko cracked beams." *Journal of Sound and Vibration*, 290, 640-653.

Lu, T. T. and Li, Z. C. (2005), "The cracked-beam problem solved by the boundary approximation method." *Applied Mathematics Letters*, 18, 11-16.

Lu, Z.R., Huang, M., Liu, J.K., Chen, W.H. and Liao, W.Y., (2009), "Vibration analysis of multiple-stepped beams with the composite element model", *Journal of Sound and Vibration*, 322, 1070–1080.

Maghsoodi, A., Ghadami, A. and Mirdamadi, H. R., (2013), "Multiple-crack damage detection in multi-step beams by anovel local flexibility-based damage index", *Journal of Sound and Vibration*, 332, 294–305.

Maity, D. and Saha, A. (2004)."Damage assessment in structure from changes in static parameter using neural networks".*Sadhana*, Vol.29 (3), pp.315-327.

Manivasagam, *S.* and Chandrasekaran, K., (1992), "Characterization of damage progression in layered composites", *Journal of Sound and Vibration*, 152, 177-179.

Mao, Q., (2011), "Free vibration analysis of multiple-stepped beams by using Adomian decomposition method", *Mathematical and Computer Modelling*, 54, 756-764.

Mazanoglu, K. and Sabuncu, M. (2010), "Vibration analysis of non-uniform beams having multiple edge cracks along the beam's height." *International Journal of Mechanical Sciences*, 52, 515-522.

Mazanoglu, K., Yesilyurt, I. and Sabuncu, M., (2009), "Vibration analysis of multiple-cracked non-uniform beams", Journal of Sound and Vibration, 320, 977-989

Mei, C., Karpenko, Y., Moody, S. and Allen, D. (2006), "Analytical approach to free and forced vibrations of axially loaded cracked Timoshenko beams." *Journal of Sound and Vibration*, 291, 1041-1060.

Mendelsohn, D. A. (2006), "Free vibration of an edge-cracked beam with a Dugdale-Barenblatt cohesive zone." *Journal of Sound and Vibration*, 292, 59-81

Murphy, K. D. and Zhang, Y. (2000), "Vibration and stability of a cracked translating beam." *Journal of Sound and Vibration*, 237(2), 319-335.

Naguleswaran, S. (2002), "Vibration of an Euler–Bernoulli beam on elastic end supports and with up to three step changes in cross-section", *International Journal of Mechanical Sciences*, 44, 2541-2555.

Naguleswaran, S. (2003), "Vibration and stability of an Euler–Bernoulli beam with up to three-step changes in cross-section and in axial force", *International Journal of Mechanical Sciences*, 45, 1563-1579.

Nahvi H., Jabbari M. (2005), "Crack detection in beams by experimental modal data and finite element model." *International Journal of Mechanical Sciences*, 47, 1477–1497.

Nandwana, B. P. and Maiti, S. K., (1997), "Detection of the location and size of a crack in stepped cantilever beams based on measurements of natural frequencies", *Journal of Sound and Vibration*, 203(3), 435-446.

Nikpour, K. (1990), "Buckling of cracked composite columns." *International Journal of Solids Structures*, 26(12), 1371-1386.

Nikpur, K. and Dimarogonas, A., (1988), "Local compliance of composite cracked bodies", *Composites Science and Technology*, 32, 209-223.

Okamura, H. Liu, H. W., Chu C.-S. and Liebowitz, H., (1969), "A cracked column under compression", *Engineering Fracture Mechanics*, 1, 547-564.

Olden, J. D., Joy, M. K., and Death, R. G. (2004). "An accurate comparison of methods for quantifying variable importance in artificial neural networks using simulated data." *Ecological Modellling*, Vol.178 **(**3), pp. 389-397.

Olden, J. D., Joy, M. K., Death, R. G. (2004), "An accurate comparison of methods for quantifying variable importance in artificial neural networks using simulated data", *Ecological Modelling*, 178(3), 389-397.

Orhan, S. (2007), "Analysis of free and forced vibration of a cracked cantilever beam." *NDT&E International*, 40, 443-450.

Ostachowicz, W. M. and Krawczuk, M., (1990), "Vibration analysis of a cracked beam." *Computers & Structures*, 36(2), 245-250.

Ostachowitz, W. M. and Krawczuk, M. (1991), "Analysis of the effect of cracks on the natural frequencies of a cantilever beam." *Journal of Sound and Vibration*, 150(2), 191-201.

Owolabi, G.M., Swamidas, A.S.J. and Seshadri, R. (2003). "Crack detection in beams using changes in frequencies amplitudes of frequency response functions". *Journal of Sound and Vibration*, 265, 1-22.

Papadopoulos, C. A. and Dimarogonas, A. D., (1987), "Coupled longitudinal and bending vibrations of a rotating shaft with an open crack", *Journal of Sound and Vibration*, 117(1), 81-93.

Patil, D. P. and Maiti, S. K. (2003), "Detection of multiple cracks using frequency measurements." *Engineering Fracture Mechanics*, 70, 1553-1572.

Qian, G.-L., Gu, S.-N. and Jiang, J.-S. (1990), "The dynamic behavior and crack detection of a beam with a crack." *Journal of Sound and Vibration*, 138(2), 233-243

Qian, G.-L., Gu, S.-N. and Jiang, J.-S. (1991), "Finite element model of cracked plates and application to vibration problems." *Composite Structures*, 39(5), 483-487.

R. D., Cawley, P., Pye, C. J. and Stone, B. J., (1978), "A vibration testing for non-destructively assessing the integrity of the structures", *Journal of Mechanical Engineering Science*, 20, 93-100.

Rahai, A. R. and Kazemi, S., (2008), "Buckling analysis of non-prismatic columns based on modified vibration modes", *Communications in Nonlinear Science and Numerical Simulation*, 13, 1721-1735.

Rajasekaran, S. and Pai, G. V. (2008), "Neural Networks, Fuzzy Logic and Genetic Algorithm synthesis and application", *Prentice - Hall of India, Eastern Economy Edition*.

Ranjabaran, A., Hashemi, S. and Ghaffarian, A. R., (2008), "A new approach for buckling and vibration analysis of cracked column", IJE Transactions, 21(3), 225-230

Ranjbaran, A., Rousta, H., Ranjbaran, M. and Ranjbaran M., (2013), "Dynamic stability of cracked columns; the stiffness reduction method", Scientia Iranica, 20(1), 57-64.

Rauch, A., (1985), "Shaft cracking supervision of heavy turbine rotors by FMM-method", *Proceedings of 3rd Modal Analysis Conference, Vol. 2, Orlando, Union College New York, U. S. A.*, 714-722.

Rezaee, M. and Hassannejad, R. (2011), "A new approach to free vibration analysis of a beam with a breathing crack based on mechanical energy balance method." *Acta Mechanica Solida Sinica*, 24(2), 185-194

Ruotolo, R. and Surace, C., (1997), "Damage assessment of multiple cracked beams: Numerical results and Experimental validation", *Journal of Sound and Vibration*, 206(4), 567-588.

Ruotolo, R., Surace, C., Crespo, P. and Storer, D. (1996), "Harmonic analysis of the vibrations of a cantilevered beam with a closing crack." *Computers & structures*, 61(6), 1057-1074.

Saavedra, P. N. and Cuitino, L. A. (2001), "Crack detection and vibration behavior of cracked beams." *Computers & Structures,* 79, 1451-1459.

Sabuncu, M. and Evran K., (2005), "Dynamic stability of a rotating asymmetric cross-section Timoshenko beam subjected to an axial periodic force", Finite Elements in Analysis and Design' 41, 1011-1026.

Sekhar A. S. (1999), "Vibration characteristics of a cracked rotor with two open cracks." *Journal of Sound and Vibration*, 223(4), 497-512.

Sekhar A. S. and Prabhu, B. S. (1992), "Crack detection and vibration characteristics of cracked shafts, *Journal of Sound and Vibration*, 157(2), 375-381.

Shafiei, M. and Khaji, N. (2011), "Analytical solutions for free and forced vibrations of a multiple cracked Timoshenko beam subject to a concentrated moving load." *Acta Mechanica*, 221, 79-97.

Shen, M. H. H. and Taylor, J. E. (1991), "An identification problem for vibrating cracked beams." *Journal of Sound and Vibration*, 150(3), 457-484.

Shen, M.-H. H. and Pierre, C. (1994), "Free vibrations of beams with a single-edge crack." *Journal of Sound and Vibration*, 170(2), 237-259.

Shifrin, E. I. and Ruotolo, R. (1999), "Natural frequencies of a beam with an arbitrary number of cracks." *Journal of Sound and Vibration*, 222(3), 409-423.

Sinha, J. K., Friswell, M. I. and and Edwards, S. (2002), "Simplified models for the location of cracks in beam structures using measured vibration data." *Journal of Sound and Vibration*, 251(1), 13-38.

Skrinar, M. (2007), "On the application of a simple computational model for slender transversely cracked beams in buckling problems." *Computational Materials Science*, 39, 242-249.

Skrinar, M. and Plibersek, T. (2007), "New finite element for transversely cracked slender beams subjected to transverse loads." *Computational Materials Science*, 39, 250-260.

Smith, G.N. (1986). "*Probability and statistics in civil engineering: An Introduction*." Collins, London.

Tada, H., Paris, P. C. and Irwin, G. R., The Stress Analysis of Cracks Handbook. Del Research Corporation, Hellertown, Pennsylvania, U.S.A., 1985.

Takahashi, I. (1999), "Vibration and stability of non-uniform cracked Timoshenko beam subjected to follower force." *Computers & Structures*, 71, 585-591.

Thomson, W. J., (1943), "Vibration of slender bars with discontinuities in stiffness", Journal of Applied Mechanics, 17, 203-207.

Timoshenko, S. P., (1937), "Vibration Problems in Engineering", 2nd Edition, Fifth Printing, D. Van Nostrand Company, Inc, Newyork.

Torabi, K., Afshari, H. and Aboutalebi, F. Haji, (2014), "A DQEM for transverse vibration analysis of multiple cracked non-uniform Timoshenko beams with general boundary conditions", *Computers and Mathematics with Applications*, 67, 527-541

Tsai, T. C. and Wang, Y. Z. (1996), "Vibration analysis and diagnosis of a cracked shaft." *Journal of Sound and Vibration*, 607-620.

Vadillo, G., Loya, J. A. and Fernandez-Saez, J., (2012), "First order solutions for the buckling loads of Weakened Timoshenko columns", Journal of Computers & Mathematics with Applications, 64(8), 2395-2407.

Viola, E. and Marzani A. (2004), "Crack effect on dynamic stability of beams under conservative and non-conservative forces." *Engineering Fracture Mechanics*, 71, 699-718.

Viola, E., Federici, L. and Nobile, L. (2001), "Detection of crack location using cracked beam element method for structural analysis." *theoretical and applied fracture mechanics*, 36, 23-35

Viola, E., Ricci, P. and Aliabadi, M.H. (2007), "Free vibration analysis of axially loaded cracked Timoshenko beam structures using the dynamic stiffness method." *Journal of Sound and Vibration*, 304, 124-153.

Wang Q., (2004), "A comprehensive stability analysis of a cracked beam subjected to follower compression," *International Journal of Solids and Structures*, 41, 4875-4888.

Wang, C. M., Ng, K. H. and Kitipornchai, S., (2002), "Stability criteria for Timoshenko columns with intermediate and end concentrated axial loads", *Journal of Constructional Steel Research*, 58, 1177-1193.

Waur, J., (1991), "Dynamics of cracked rotors: a literature survey", *Journal of Applied Mechanics Reviews*, 17, 1-7

Westmann, R. A. and Yang, W. H., (1967), "Stress analysis of cracked rectangular beams", Journal of Applied Mechanics, 32, 693-701.

Wu, Guan-Yuan and Shih, Yan-Shin (2005), "Dynamic instability of rectangular plate with an edge crack." *Computers & Structures*, 84, 1-10.

Xiaoqing, Z., Qiang, H. and Feng. L, (2010), "Analytical approach for detection of multiple cracks in a beam", *Journal of Engineering Mechanics*, 136, 345-357.

Yan, T. and Yang, J., (2011), "Forced Vibration of Edge-Cracked Functionally Graded Beams Due to a Transverse Moving Load", *Procedia Engineering*, 14, 3293-3300.

Yang, J. and Chen, Y., (2008), "Free vibration and buckling analyses of functionally graded beams with edge cracks", *Composite Structures*, 83, 48–60

Yang, J., Chen, Y., Xiang, Y. and Jia, X.L. (2008), "Free and forced vibration of cracked inhomogeneous beams under an axial force and a moving load." *Journal of Sound and Vibration*, 312, 166-181.

Yang, X. F., Swamidas, A. S. J. and Seshadri, R. (2001), "Crack identification in vibrating beams using the energy method." *Journal of Sound and Vibration*, 244(2), 339-357.

Yokoyama, T. and Chen, M.-C., (1998), "Technical note – Vibration analysis of edge cracked beams using a line-spring model", *Engineering Fracture Mechanics*, 59(3), 403-409.

Zhang, W., Wang, Z. and Ma, H., (2009), "Crack identification in stepped Cantilever beam combining wavelet Analysis with transform matrix", *Acta Mechanica Solida Sinica*, 22(4), 360-368.

Zhang, Z., Chen, F., Zhang Z. and Hua, H., (2014), “Vibration analysis of non-uniform Timoshenko beams coupled with flexible attachments and multiple discontinuities”, *International Journal of Mechanical Sciences*, 80, 131-143

Zheng, D. Y. and Fan S. C., (2001), “Natural frequencies of a non-uniform beam with multiple cracks via modified fourier series”, *Journal of Sound and Vibration,* 242(4), 701-717

Zheng, D. Y. and Fan, S. C., (2001), “Natural frequency changes of a cracked Timoshenko beam by modified fourier series”, *Journal of Sound and Vibration,* 246(2), 297-317.

Zheng, D.Y. and Fan, S.C., (2003), “Vibration and stability of cracked hollow-sectional beams”, *Journal of Sound and Vibration,* 267, 933–954.

Zheng, D.Y. and Kessissoglou, N.J., (2004), “Free vibration analysis of a cracked beam by finite element method”, *Journal of Sound and Vibration,* 273, 457–475.